Supplementary Information

Long-Lived Charge Transfer States of Nickel(II) Aryl Halide Complexes Facilitate Bimolecular Photoinduced Electron Transfer

Benjamin J. Shields, Bryan Kudisch, Gregory D. Scholes, and Abigail G. Doyle

correspondence to: agdoyle@princeton.edu

Table of Contents

I. Materials and Instrumentation

Materials. All reagents were purchased from Sigma Aldrich, Oakwood, Acros, Alfa Aesar, Strem, or TCI, and stored in a N_2-filled glovebox. THF was purchased inhibitor free, dried by passing through activated alumina columns and stored over activated molecular sieves in a N_2-filled glovebox.

General Instrumentation. Proton nuclear magnetic resonance (^{1}H NMR) spectra were recorded on a Bruker 500 AVANCE spectrometer (500 MHz). Carbon nuclear magnetic resonance (^{13}C NMR) spectra were recorded on a Bruker 500 AVANCE spectrometer (126 MHz). High-resolution mass spectra were obtained on an Agilent 6220 LC/MS using electrospray ionization time-of-flight (ESI-TOF). Gas chromatography was performed on an Agilent 7890A series instrument equipped with a split-mode capillary injection system and flame ionization detectors. Fourier transform infrared (FT-IR) spectra were recorded on a Perkin-Elmer Spectrum 100 and are reported in terms of frequency of absorption (cm^{-1}). Linear ultraviolet-visible absorption spectra were collected on an Agilent Cary 60 Spectrophotometer.

Light Sources. Experiments were carried out using 25W blue LED arrays (12-inch Sapphire Flex LED Strips 5050, High Density, 12V DC Power Leads, Waterproof, Black backing) purchased from Creative Lightings (λ_{max} = 467 nm) or 34W blue LED lamps (Kessil H150 LED Grow Lights) purchased from Kessil (λ_{max} = 450 nm flanked by a second peak at λ = 422 nm). Blue LED arrays were assembled in 4×4 plastic blocks, holding 12×35mm ½ dram vials, with 2×3 side lighting strips and 1×2 bottom lighting strip.

X-Ray Crystallography. X-ray intensity data were measured on a Bruker PHOTON 100 CMOS system equipped with a Mo Kα ImuS micro-focus source (λ = 0.71073 Å). Frames were integrated with the Bruker SAINT software package. The structure was solved and refined using Bruker SHELXTL software package.

Transient Absorption Spectroscopy. A 1 kHz regeneratively amplified Ti:Sapphire laser (Coherent Libra, Santa Clara, California) with a commercial optical parametric amplifier (OPerA Solo, Vilnius, Lithuania) and commercial transient absorption spectrometer (Ultrafast Systems Helios, Sarasota, Florida) were used for pump-probe experiments. See section V for details.

II. Synthesis and Characterization Ni Complexes

All Ni(II)(dtbbpy)(*o*-tolyl) halide complexes (dtbbpy = 4,4'-Di-*tert*-butyl-2,2'-bipyridyl) were prepared via oxidative addition of the corresponding *o*-tolyl halide to *in situ* prepared Ni(dtbbpy)(cod). Spectroscopically the halide series can be readily distinguished via ^{1}H NMR by shifts in the 6-pyridyl proton resonances (Figure S1). Note preparation of complex **1–I** required cooling to obviate the formation of paramagnetic impurities. It was found that Ni(dtbbpy)(cod) is soluble in pentane even at -30˚C but Ni(II)(dtbbpy) aryl halide complexes are not. Therefore, a dynamic precipitation of product after the addition of *o*-tolyl iodide enabled the isolation of pure **1–I**.

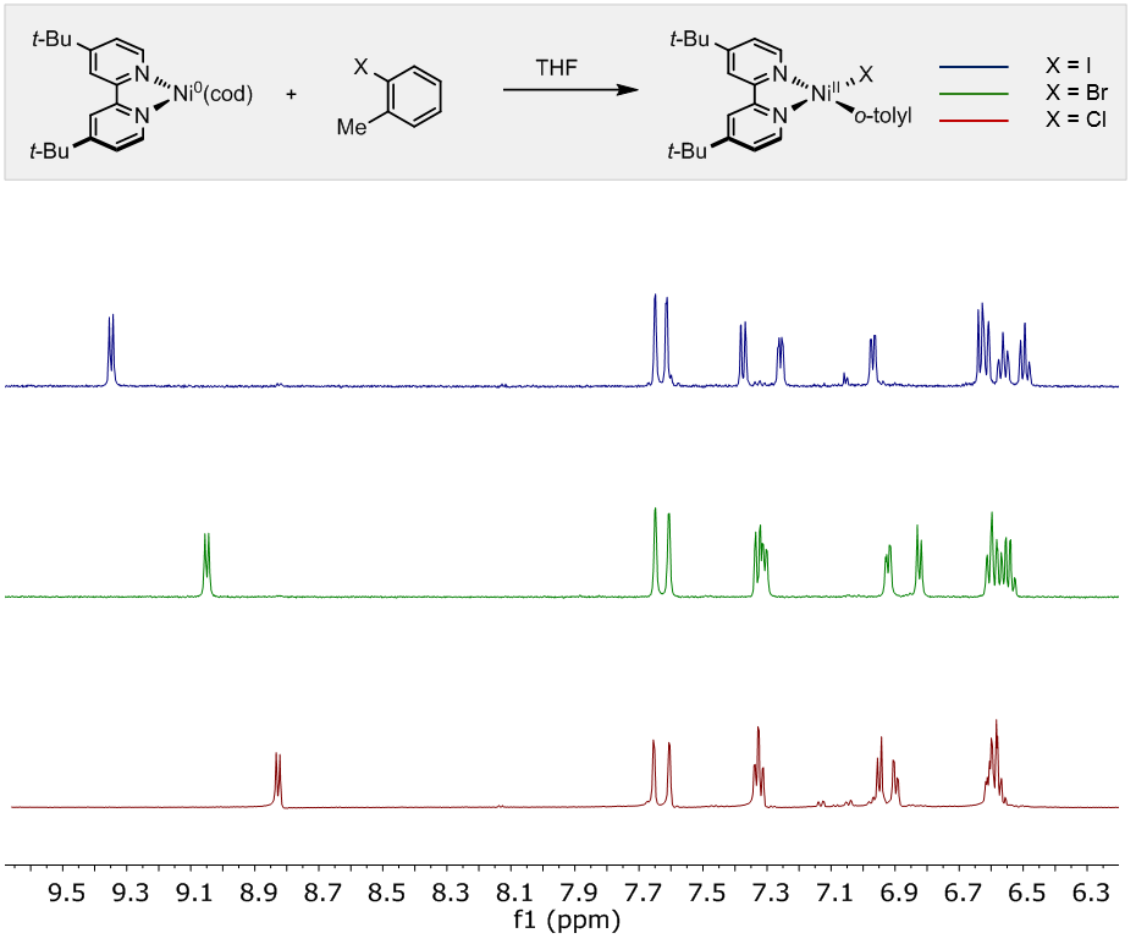

Fig. S1. Preparation of Ni(II)(dtbbpy)(*o*-tolyl) halide complexes. ^{1}H NMR shows diagnostic shifts in the 6-pyridyl proton resonances with halide substitution.

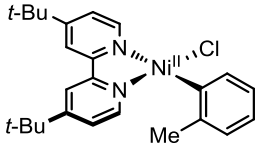

Ni(dtbbpy)(*o*-tolyl)Cl (1–Cl). In a nitrogen filled glove box a reaction tube equipped with a PTFE-coated stir bar was charged with $Ni(cod)_2$ (550 mg, 2.0 mmol), 4,4′-di-*tert*-butyl-2,2′-pyridine (537 mg, 2.0 mmol) and THF (5 mL). The resulting deep purple solution was left to stir for 1 hour at ambient temperature. To the reaction tube was added 2-chlorotoluene (12 mL, 103 mmol) and left to stir for 20 min. The resulting dark red solution was removed from the glove box and triturated with pentane. The precipitate was collected on a frit, rinsed with pentane and residual solvent was removed under high vacuum to give the title compound as a light red powder (700 mg, 1.54 mmol, 77% yield), with trace residual aryl chloride as an impurity. The title compound was used for spectroscopic studies without further purification. Diffraction quality crystals of **1–Cl** were grown by slow evaporation in THF.

^{1}H NMR (501 MHz, CD_2Cl_2): δ 9.03 (d, *J* = 5.9 Hz, 1H), 7.85 (s, 1H), 7.80 (d, *J* = 1.6 Hz, 1H), 7.57 – 7.50 (m, 2H), 7.15 (d, *J* = 6.2 Hz, 1H), 7.10 (dd, *J* = 6.2, 1.9 Hz, 1H), 6.83–6.75 (m, 3H), 3.05 (s, 3H), 1.42 (s, 9H), 1.34 (s, 9H).

^{13}C NMR (126 MHz, CD_2Cl_2): δ 164.08, 163.07, 156.43, 153.04, 151.49, 151.12, 149.46, 142.80, 135.89, 127.64, 124.10, 123.74, 123.39, 122.91, 117.99, 117.19, 35.89, 35.80, 30.58, 30.35, 25.33.

HRMS: (ESI-TOF) calculated for ($[C_{25}H_{31}ClN_2Ni - Cl + MeCN]^+$): 458.2101, found: 458.2102.

FTIR (ATR, cm^{-1}): 3042, 2961, 1614, 1546, 1480, 1409, 1365, 1251, 1202, 1120, 1041, 1071, 899, 847, 736.

X-Ray Crystallography: The crystal structure of **1–Cl** was 37% disordered. Figure S2 shows the refined structure with disorder modeled (left) and the major conformer (right). Note: *checkcif* gives multiple alerts associated with the disorder and constraints used in refinement (three C-type alerts and several G-type alerts). Without disorder modeling the structure does not pass *checkcif*. Both CIF files are included in separate SI documents.

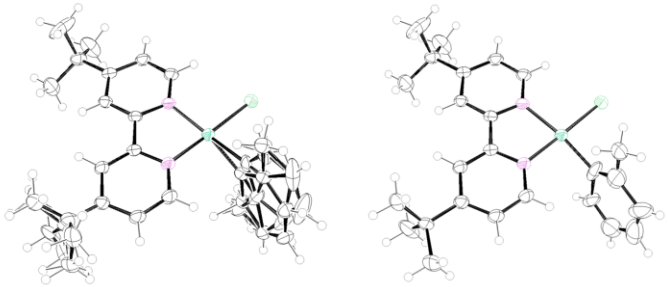

Fig. S2. X-Ray Crystal Structure of complex **1–Cl** with disorder modeled (left) and major conformer (right).

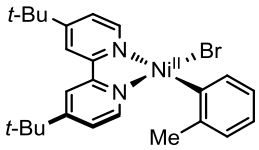

Ni[(dtbbpy)(*o*-tolyl)Br (1–Br). In a nitrogen filled glove box a vial equipped with a PTFE-coated stir bar was charged with $Ni(cod)_2$ (275 mg, 1.0 mmol), 4,4′-di-*tert*-butyl-2,2′-pyridine (268 mg, 1.0 mmol) and THF (3 mL). The resulting deep purple solution was left to stir for 2 hours at ambient temperature. 2-Bromotoluene (0.5 mL, 4.15 mmol) was added and the reaction vial was left to stir for 20 min. The resulting dark red solution was triturated with pentane (10 mL). The precipitate was collected on a frit, rinsed with pentane and residual solvent was removed under vacuum to give the title compound as a light red powder (280 mg, 0.56 mmol, 56% yield). The title compound was used for spectroscopic studies without further purification.

^{1}H NMR (501 MHz, CD_2Cl_2): δ 9.24 (d, *J* = 5.9 Hz, 1H), 7.84 (s, 1H), 7.79 (s, 1H), 7.52 (dd, *J* = 7.3, 1.3 Hz, 1H), 7.49 (dd, *J* = 5.9, 1.7 Hz, 1H), 7.11 (dd, *J* = 6.2, 1.9 Hz, 1H), 7.01 (d, *J* = 6.2 Hz, 1H), 6.82–6.70 (m, 3H), 3.01 (s, 3H), 1.40 (s, 9H), 1.32 (s, 9H).

^{13}C NMR (126 MHz, CD_2Cl_2): δ 163.98, 163.15, 156.39, 153.30, 151.11, 150.96, 149.90, 143.04, 136.59, 127.77, 124.17, 123.93, 123.50, 122.83, 118.03, 117.36, 35.90, 35.86, 30.59, 30.37, 25.88.

HRMS: (ESI-TOF) calculated for ($[C_{25}H_{31}BrN_2Ni - Br + MeCN]^+$): 458.2101, found: 458.2100.

FTIR (ATR, cm^{-1}): 3042, 2961, 1615, 1568, 1543, 1480, 1456, 1409, 1364, 1303, 1252, 1202, 1158, 1121, 1040, 1016, 900, 885, 862, 839, 722.

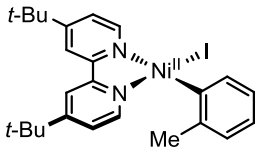

Ni[(dtbbpy)(*o*-tolyl)I (1–I). In a nitrogen filled glove box a Schlenk tube equipped with a PTFE-coated stir bar was charged with $Ni(cod)_2$ (250 mg, 0.909 mmol), 4,4′-di-*tert*-butyl-2,2′-pyridine (244 mg, 0.909 mmol) and THF (7 mL) and left to stir for 1 hour to give a deep purple solution. The tube was fitted with a 10 mm bore stopcock, sealed with a septum, removed from the glovebox, placed in a dry ice acetone bath, and set to stir. The inlet of the Schlenk tube was connected to a manifold, a needle from the manifold was plunged through the septa, and following three vacuum purge cycles the stopcock and Schlenk inlet were opened and left under positive nitrogen pressure. Next 2-iodotoluene (238 mg, 0.139 mL, 1.091 mmol) was added via syringe, the reaction mixture was allowed to warm to ~ 10°C, the stopcocks were closed, and the reaction mixture was brought into the glovebox. The reaction mixture was still purple, indicating the presence of Ni(dtbbpy)(cod). The reaction mixture was diluted into pentanes (50 mL) and the solution was allowed to stir for 1 hour. The resulting red precipitate was collected on a frit, rinsed with pentane, and residual solvent was removed under vacuum to give the title compound as a red/brown powder (109 mg, 0.20 mmol, 22% yield). The title compound was used for spectroscopic studies without further purification.

^{1}H NMR (501 MHz, CD_2Cl_2): δ 9.54 (d, *J* = 5.9 Hz, 1H), 7.84 (d, *J* = 1.4 Hz, 1H), 7.80 (d, *J* = 1.6 Hz, 1H), 7.56 (d, *J* = 7.3 Hz, 1H), 7.45 (dd, *J* = 5.9, 1.8 Hz, 1H), 7.16 (dd, *J* =

6.2, 2.0 Hz, 1H), 6.84 – 6.78 (m, 2H), 6.75 (t, *J* = 7.1 Hz, 1H), 6.68 (t, *J* = 7.1 Hz, 1H), 2.95 (s, 3H), 1.39 (s, 9H), 1.33 (s, 9H).

^{13}C NMR (126 MHz, CD_2Cl_2): δ 163.72, 163.19, 156.23, 154.21, 153.56, 149.86, 148.22, 143.54, 138.15, 127.85, 124.15 (2C), 123.61, 122.64, 118.01, 117.60, 35.87, 34.68, 30.55, 30.38, 27.06.

HRMS: (ESI-TOF) calculated for ($[C_{25}H_{31}IN_2Ni - I + MeCN]^+$): 458.2101, found: 458.2101.

FTIR (ATR, cm^{-1}): 3042, 2960, 1611, 1548, 1480, 1407, 1366, 1291, 1249, 1202, 1157, 1123, 1016, 930, 895, 850, 840, 736.

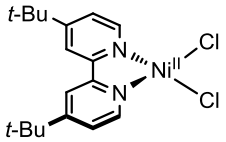

Ni(dtbbpy)Cl_2 (2). A stock solution of the title compound was prepared for spectroscopic studies in the glove box without isolation. To a 10mL volumetric flask $NiCl_2$(DME) (1.1 mg, 0.005 mmol) and 4,4′-di-*tert*-butyl-2,2′-pyridine (1.3 mg, 0.005 mmol) were added, the flask was filled to the line with THF, a stir bar was added, and the resulting light blue/green solution was left to stir for 2 h. A shift in the absorption of dtbbpy from 280 nm to 300 nm indicated formation of the complex (Figure S3). A similar shift was observed in Ni(dtbbpy)(*o*-tolyl) halide complexes.

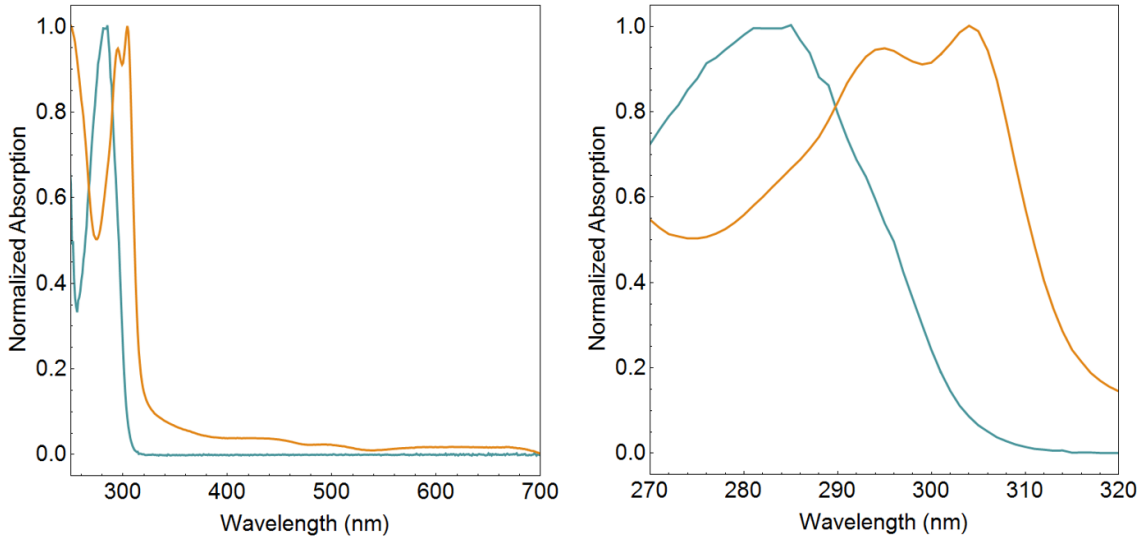

Fig. S3. Preparation of Ni(dtbbpy)Cl_2. Uv-vis spectra of free dtbbpy (teal) and 1:1 mixture of $NiCl_2$(DME) and dtbbpy (yellow).

III. Steady-State Uv-Vis Absorption Spectroscopy

Linear Absorption Data. Linear absorption spectra were collected on an Agilent Cary 60 Spectrophotometer. All reagents were dispensed in stock solutions prepared volumetrically inside a nitrogen filled glove box. In a typical experiment, THF and analyte dispensed in THF were added to screw-top cuvette. The cuvette was then sealed with a septum cap, removed from the glovebox, and a spectrum was collected.

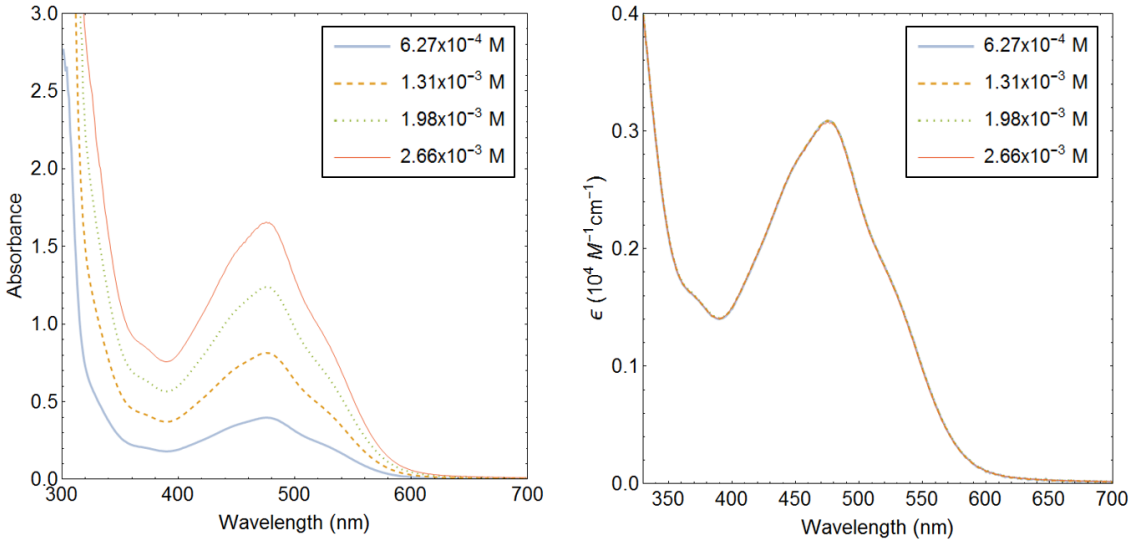

Fig. S4. Comparison of absorption and extinction spectra of Ni(dtbbpy)(*o*-tolyl)Cl (**1–Cl**, 2 mm pathlength optical glass cuvette) in THF at different concentrations. The extinction spectra at different concentrations overlay giving no evidence for ground state aggregation.

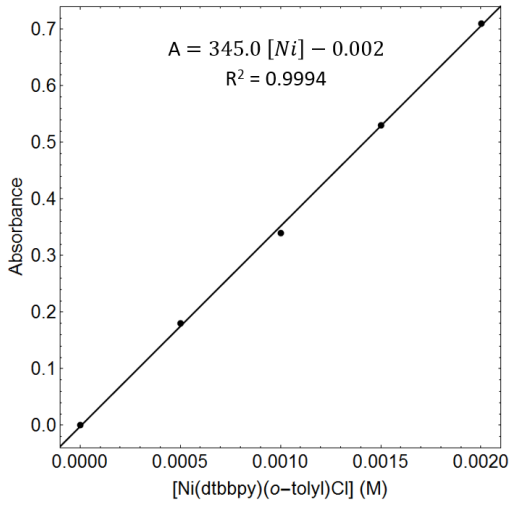

Fig. S5. Single wavelength (412 nm) calibration curve for Ni(dtbbpy)(*o*-tolyl)Cl (**1–Cl**, 2 mm pathlength optical glass cuvette) in THF.

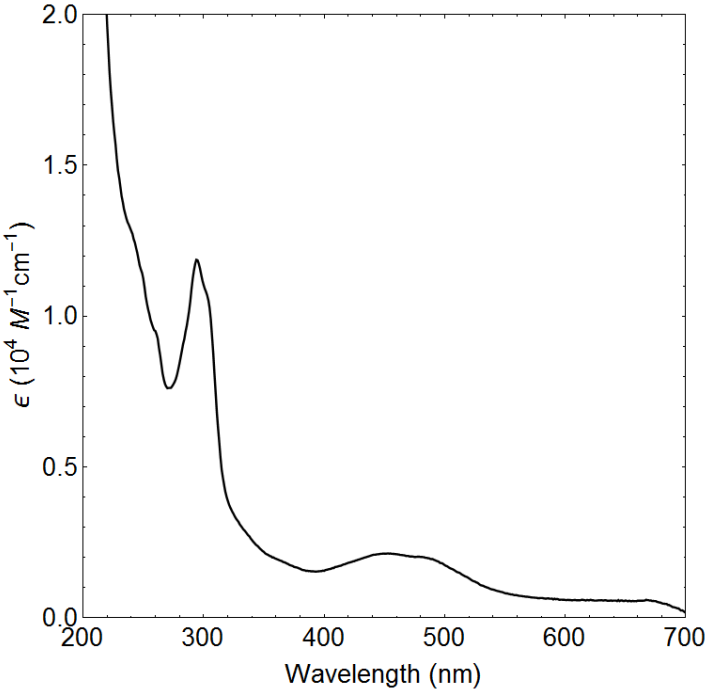

Fig. S6. Extinction spectrum of Ni(dtbbpy)(*o*-tolyl)Cl (**1–Cl**, 3.88 × 10^{-4} M, 1 mm pathlength quartz cuvette) in THF.

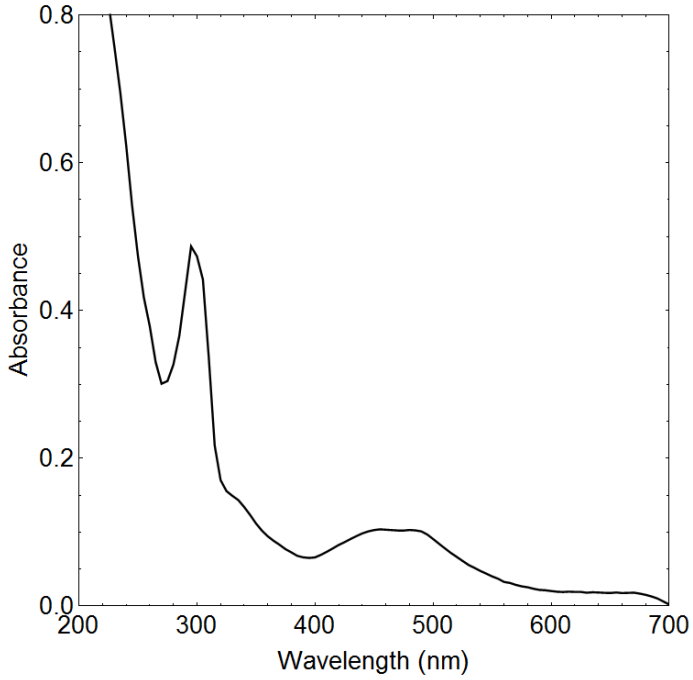

Fig. S7. Absorption spectrum of Ni(dtbbpy)(*o*-tolyl)Br (**1–Br**, 1 mm pathlength quartz cuvette) in THF.

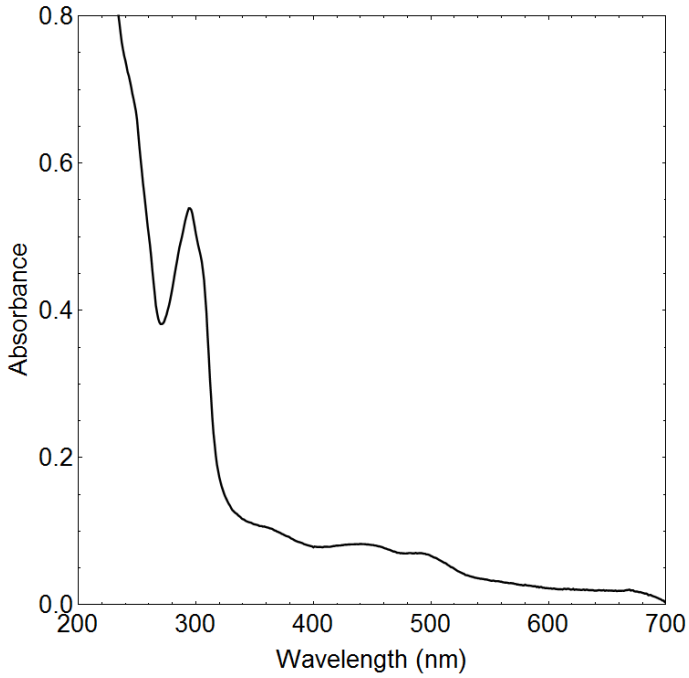

Fig. S8. Absorption spectrum of Ni(dtbbpy)(*o*-tolyl)I (**1–I**, 1 mm pathlength quartz cuvette) in THF.

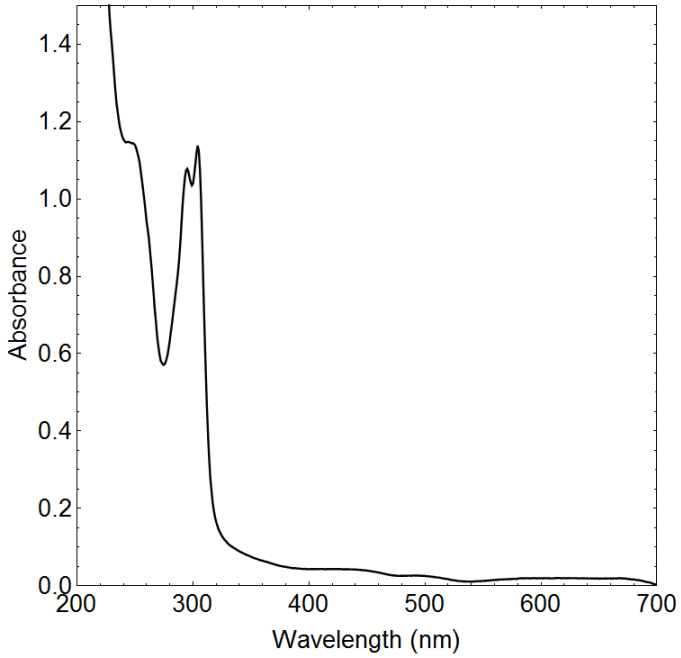

Fig. S9. Absorption spectrum of Ni(dtbbpy)Cl_2 (**2**, 1 mm pathlength quartz cuvette) in THF.

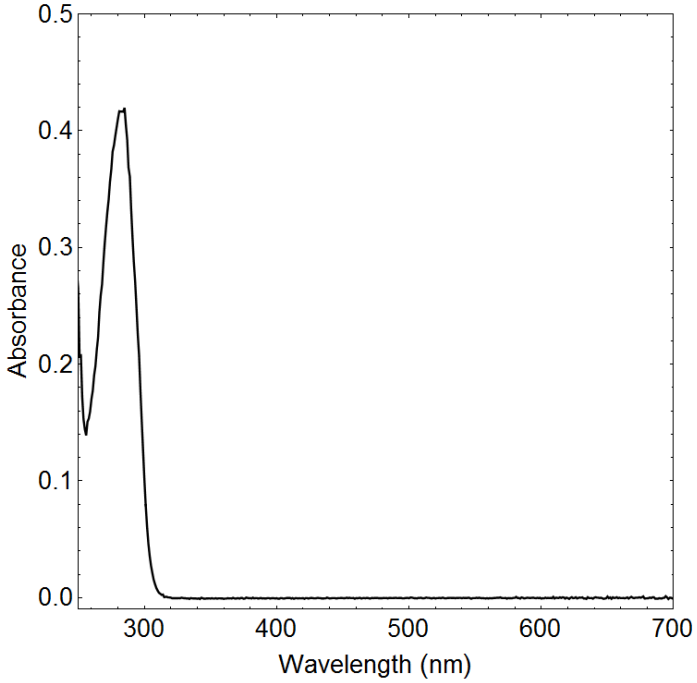

Fig. S10. Absorption spectrum of 4,4'-di-*tert*-butyl-2,2'-bipyridine (1 mm pathlength quartz cuvette) in THF.

IV. Computational Studies

General Methods. Calculations were performed on Gaussian 09 D.01 and Gaussian 16 A.03 software suites.[35,36] For all calculations Becke's three-parameter hybrid exchange-correlation functional (B3LYP) was used based on benchmarking studies (Figure S11 and S12). Several studies suggest that the hybrid B3LYP functional is excellent for the treatment of LC and MLCT states and the computation of S_0–S_N and T_1–T_N excitation energies and oscillator strengths.[37,38] Optimization and frequency calculations were carried out using TZVP (H, C, N, Cl, Br, Ni) and SDD (I) basis sets. All frequency calculations carried out on stationary points gave no imaginary frequencies. Linear response time-dependent DFT (TD-DFT) calculations were carried out on the gas-phase optimized geometry using TZVP (H, C, N, Cl, Br, Ni) and SDD (I) basis sets. The S_0–T_1 gap of complex **1**–Cl was calculated using the sum of electronic and thermal free energies from frequency calculations carried out on the geometry optimized singlet and triplet structures. Triplet–triplet (T_1–T_N) excitation energies and oscillator strengths, for the simulation of the transient absorption spectrum of $^3MLCT_1$ **1**–Cl, were calculated from the geometry optimized T_1 state of **1**–Cl. Transition assignments were made based on orbital contributions and changes in atomic charge calculated by Natural Population Analysis (NPA). Transitions were described by a linear combination of ground state orbitals, resulting from the perturbative response treatment with the B3LYP hybrid exchange-correlation functional. Accordingly, transitions were evaluated using relative Kohn-Sham orbital contributions (tabulated in section XV) and natural population analysis (NPA) to aid the assignment of CT transitions.

Benchmarking Studies. Functional/basis set combinations were evaluated against the absorption spectrum of Ni(dtbbpy)(*o*-tolyl)Cl (**1–Cl**). Becke's three-parameter hybrid exchange-correlation functional (B3LYP) with TZVP basis set best reproduced the experimental absorption spectra.

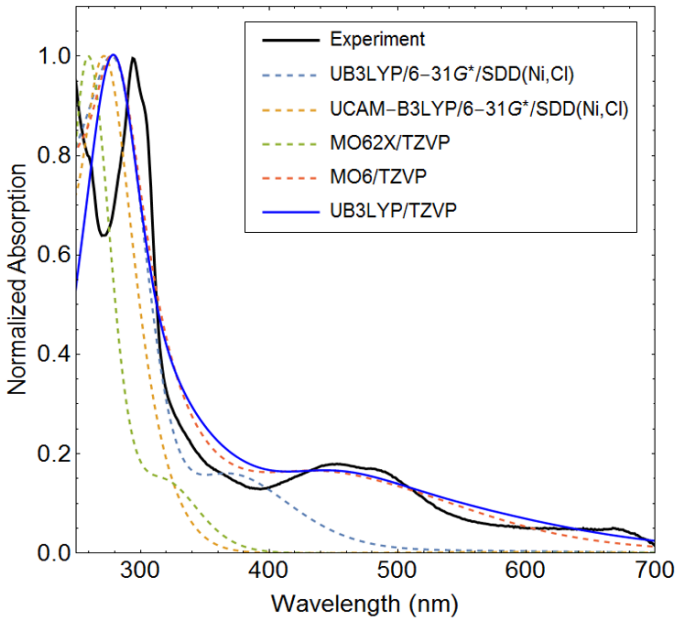

Fig. S11. TD-DFT benchmarking studies for [Ni(dtbbpy)(*o*-tolyl)Cl] (**1–Cl**) various levels of theory.

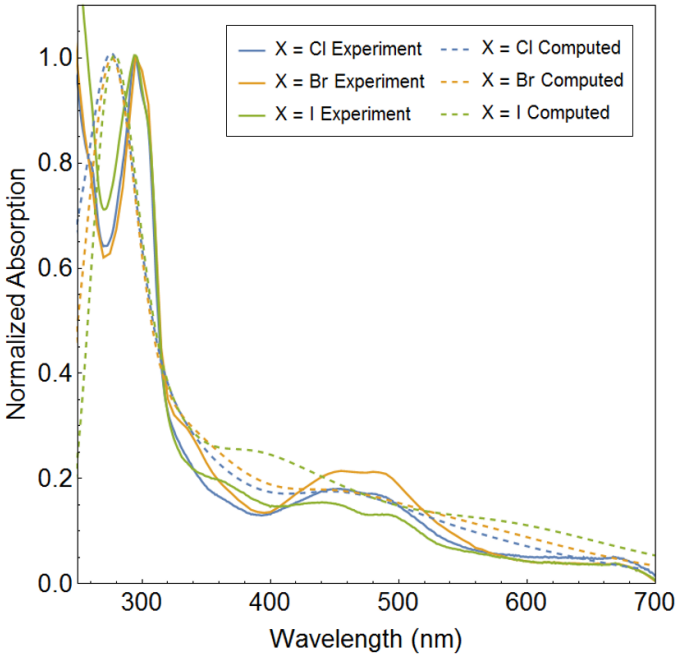

Fig. S12. TD-DFT benchmarking studies for [Ni(dtbbpy)(*o*-tolyl)X] **1** (X = Cl, Br, I).

Kohn-Sham Orbital Diagrams. For complexes with singlet ground states UB3LYP calculations produced identical α and β Kohn-Sham orbitals. Accordingly, for singlets only the computed α orbitals are shown.

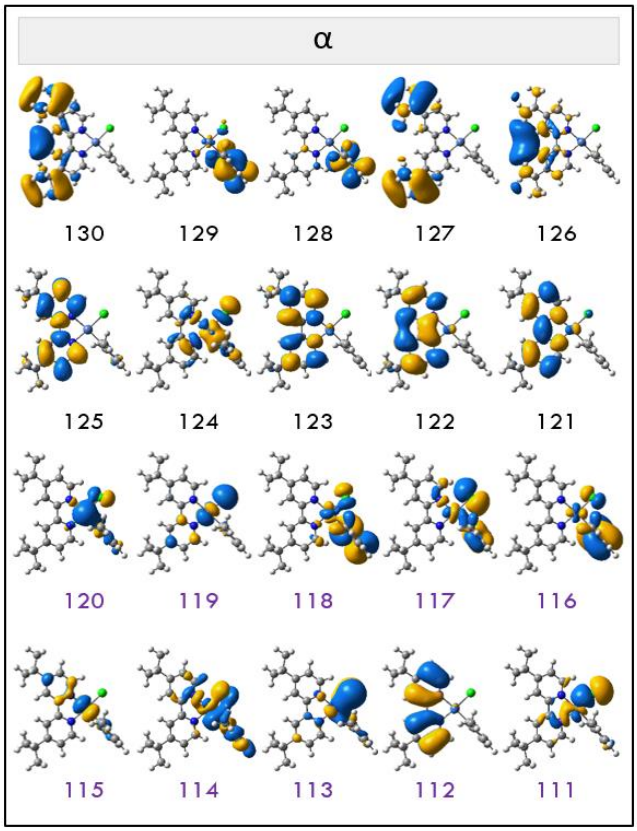

Fig. S13. Frontier molecular orbitals for [Ni(dtbbpy)(*o*-tolyl)Cl] (**1–Cl**) S_0 optimized geometry.

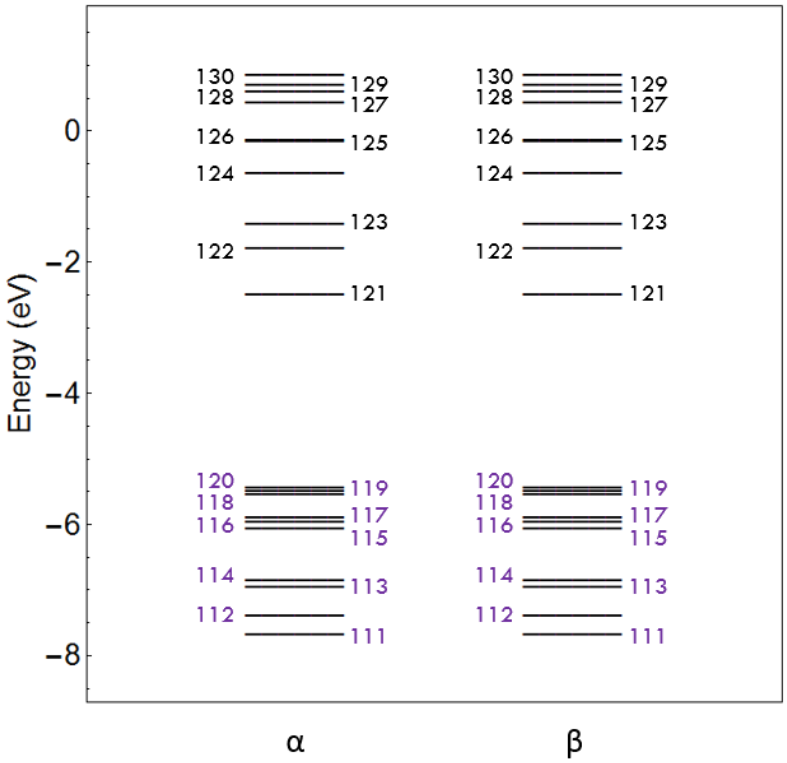

Fig. S14. Energy levels for frontier molecular orbitals of [Ni(dtbbpy)(*o*-tolyl)Cl] (**1–Cl**) S_0 optimized geometry.

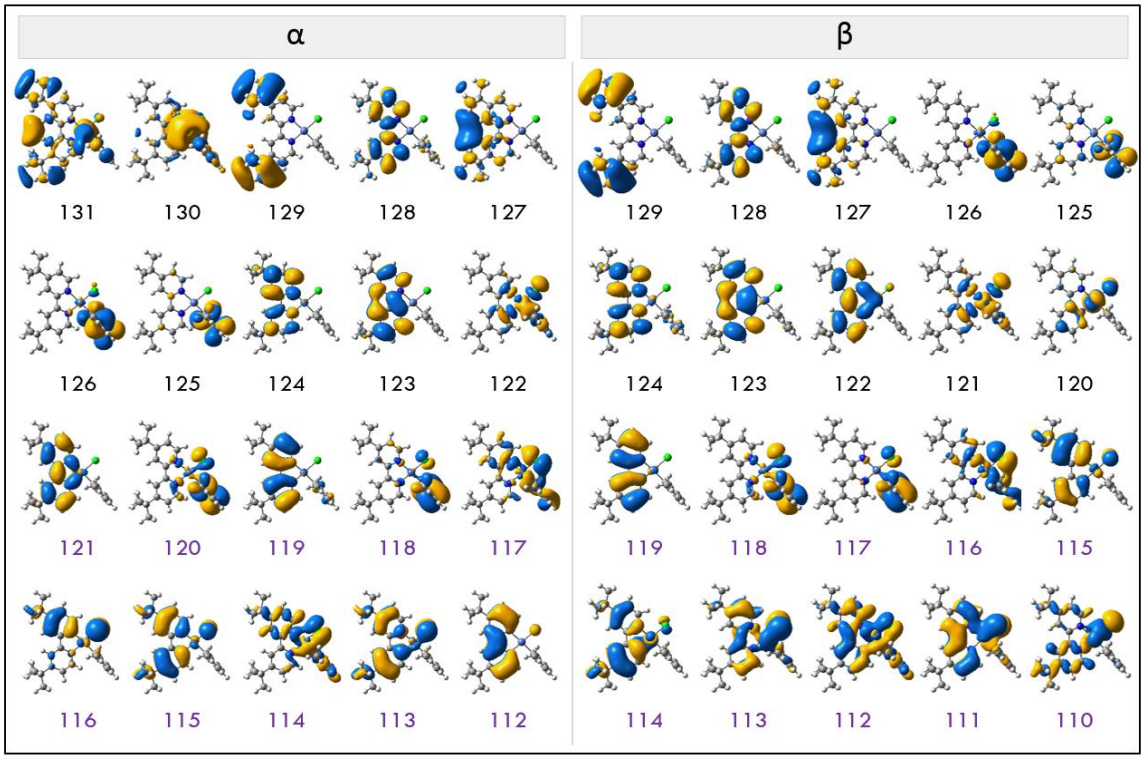

Fig. S15. Frontier molecular orbitals for [Ni(dtbbpy)(*o*-tolyl)Cl] (**1–Cl**) T_1 optimized geometry.

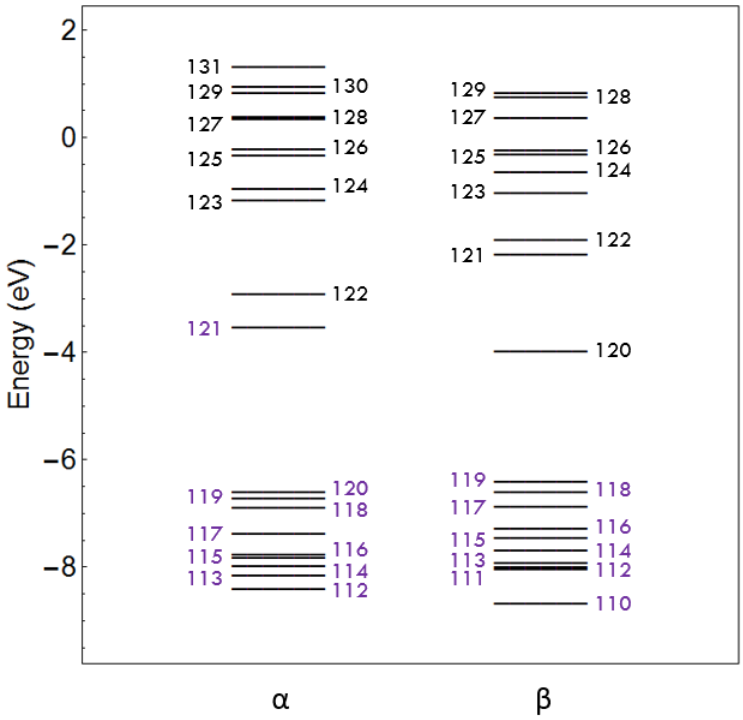

Fig. S16. Energy levels for frontier molecular orbitals of [Ni(dtbbpy)(*o*-tolyl)Cl] (**1–Cl**) T_1 optimized geometry.

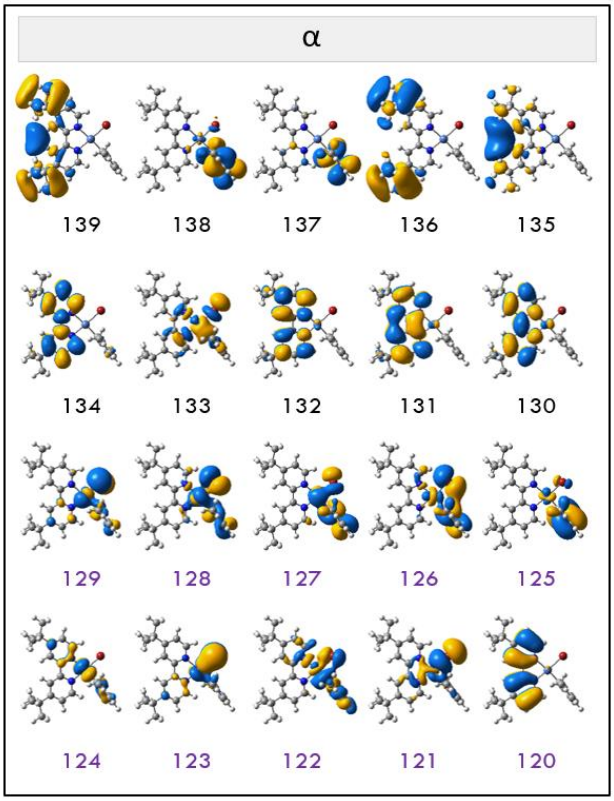

Fig. S17. Frontier molecular orbitals for [Ni(dtbbpy)(*o*-tolyl)Br] (**1–Br**) S_0 optimized geometry.

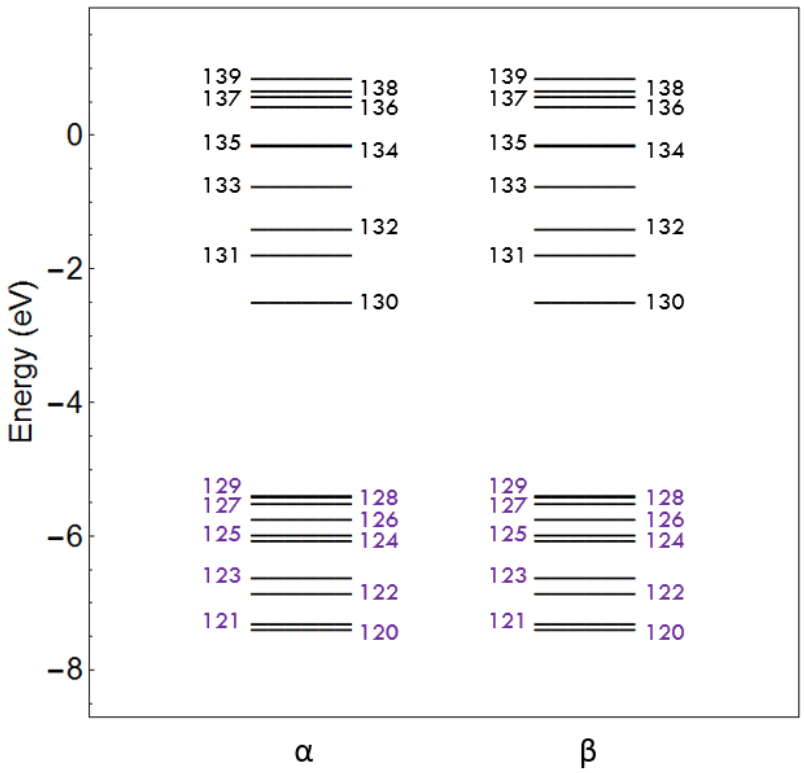

Fig. S18. Energy levels for frontier molecular orbitals of [Ni(dtbbpy)(*o*-tolyl)Br] (**1**–**Br**) S_0 optimized geometry.

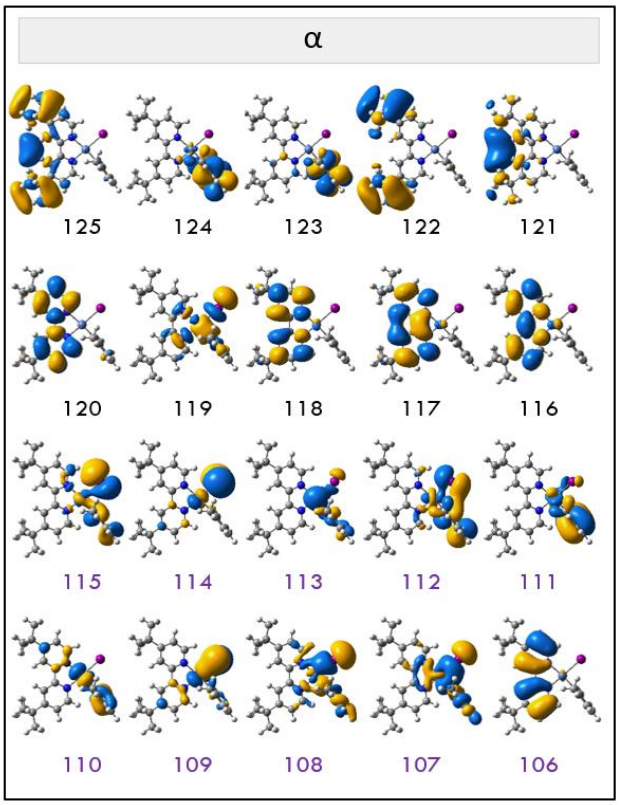

Fig. S19. Frontier molecular orbitals for [Ni(dtbbpy)(*o*-tolyl)I] S_0 (**1–I**) optimized geometry.

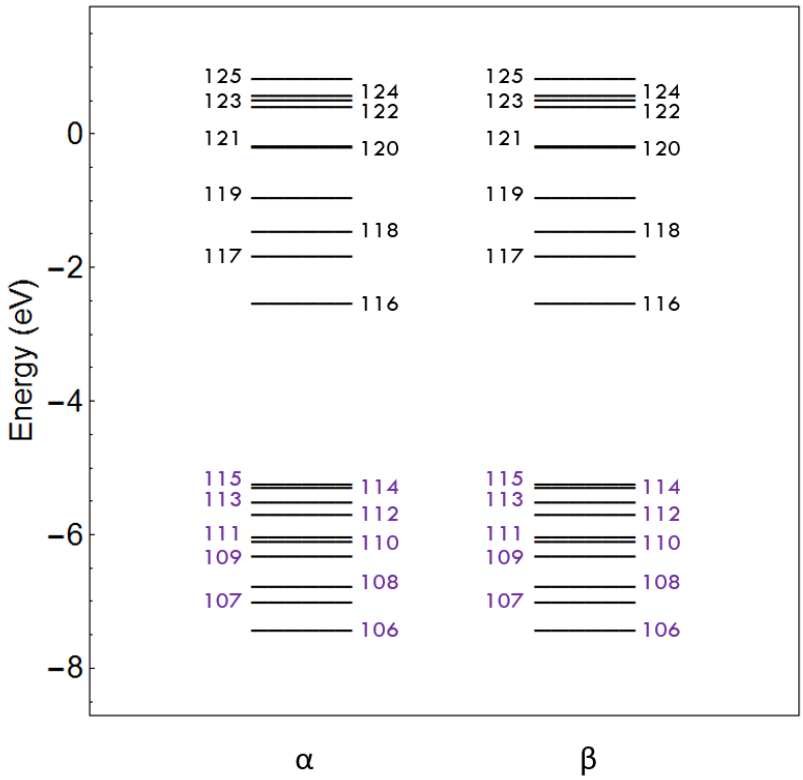

Fig. S20. Energy levels for frontier molecular orbitals of [Ni(dtbbpy)(*o*-tolyl)I] (**1–I**) S_0 optimized geometry.

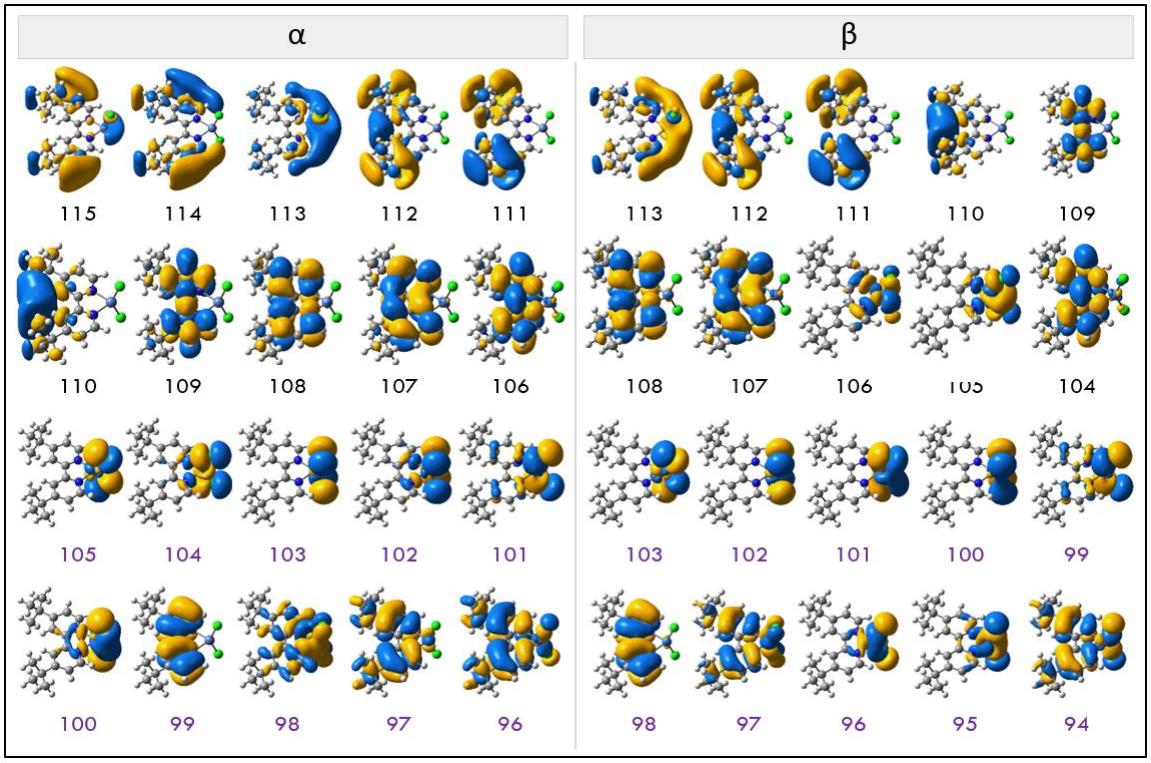

Fig. S21. Frontier molecular orbitals for [Ni(dtbbpy)Cl_2] (**2**) T_0 optimized geometry.

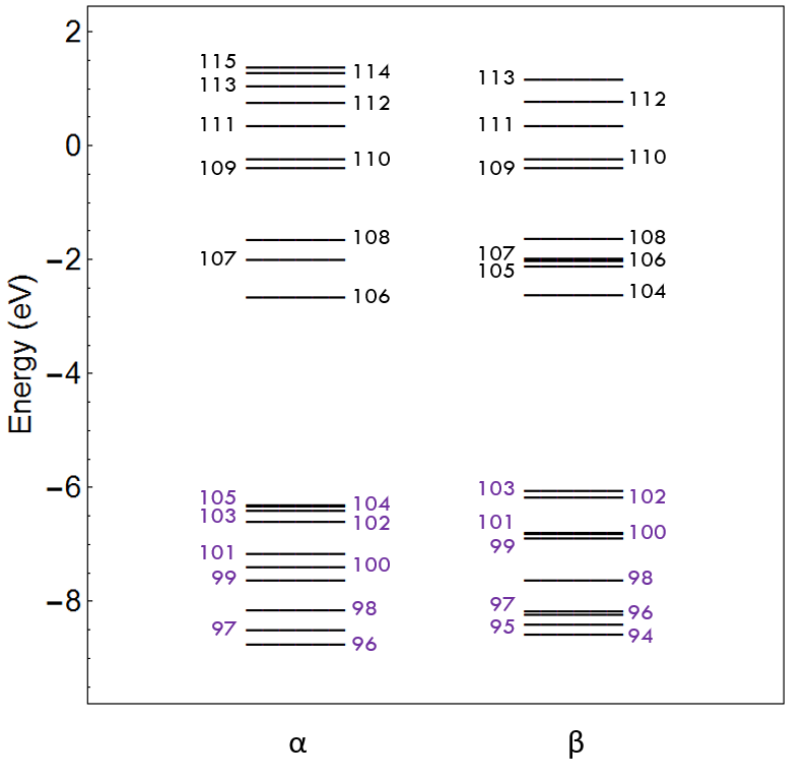

Fig. S22. Energy levels for frontier molecular orbitals of [Ni(dtbbpy)Cl_2] (**2**) T_0 optimized geometry.

Linear Response Time-Dependent Density Functional Theory.

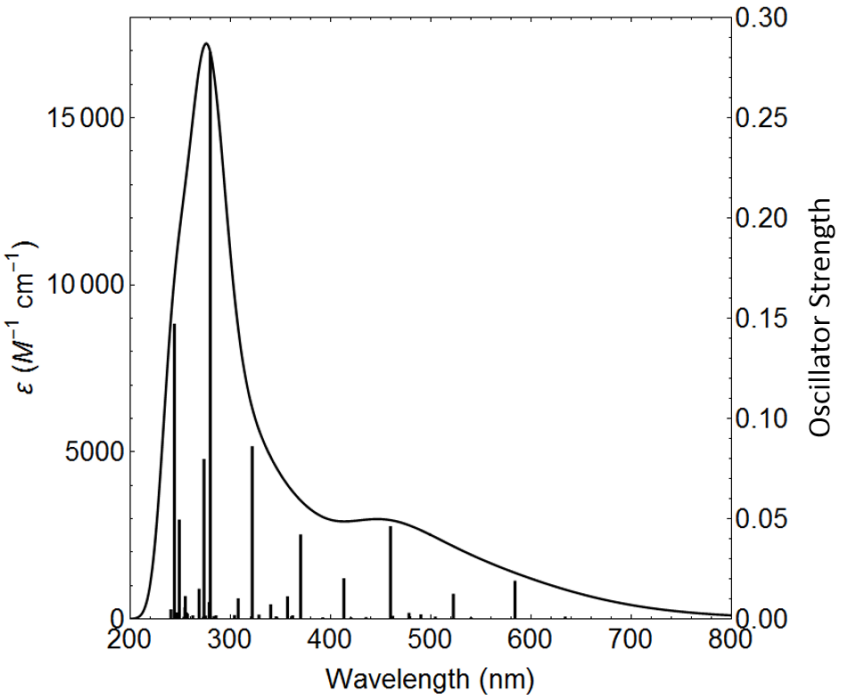

Fig. S23. Calculated absorption spectrum (solid black line) and TD-DFT calculated oscillators (solid bars: first 100 excited states) of [Ni(dtbbpy)(*o*-tolyl)Cl] (**1–Cl**) S_0.

Table S1. TD-DFT calculated transitions 1-50 for [Ni(dtbbpy)(*o*-tolyl)Cl](**1–Cl**) S_0.

Excited State	λ (nm)	f	<S**2>	Excited State	λ (nm)	f	<S**2>
1	1354.17	0	2	26	397.17	0	2
2	1091.22	0	2	27	394.25	0	2
3	900.98	0	2	28	392.22	0.0001	0
4	663.48	0	2	29	391.99	0	2
5	661.18	0	2	30	389.57	0	0
6	655.94	0	2	31	378.44	0	2
7	634.12	0.0004	0	32	370.06	0.0414	0
8	583.99	0.0183	0	33	367.45	0	2
9	540.2	0.0001	0	34	363.64	0	2
10	522.38	0.0118	0	35	362.11	0.001	0
11	520.92	0	2	36	356.94	0.0106	0
12	509.6	0	2	37	353.45	0	2
13	504.5	0.0004	0	38	346.71	0	2
14	490.01	0.0015	0	39	346.33	0.0002	0
15	480.67	0	2	40	345.58	0.0005	0
16	478.24	0.0023	0	41	344.57	0	2
17	461.89	0.0008	0	42	340.13	0.0066	0
18	459.69	0.0456	0	43	339.25	0	2
19	445.94	0	2	44	337.11	0	2
20	438.87	0	2	45	331.43	0	2
21	435.36	0.0002	0	46	329.97	0	2
22	435.02	0	2	47	328.97	0	0
23	421.37	0	2	48	328.48	0.0014	0
24	420.31	0.0001	0	49	321.63	0.0854	0
25	413.2	0.0195	0	50	309.46	0	2

Table S2. TD-DFT calculated transitions 51-100 for [Ni(dtbbpy)(*o*-tolyl)Cl](**1–Cl**) S_0.

Excited State	λ (nm)	f	<S**2>	Excited State	λ (nm)	f	<S**2>
51	307.73	0.0095	0	76	266.9	0	2
52	304.59	0	2	77	265.83	0	2
53	304.02	0.0012	0	78	262.44	0.001	0
54	303.26	0	2	79	257.01	0.0019	0
55	290.69	0	2	80	256.79	0	2
56	287.96	0	2	81	255.94	0.0025	0
57	286.25	0	2	82	255.43	0	2
58	285.52	0.001	0	83	255.19	0	2
59	283.28	0.0007	0	84	254.97	0.0107	0
60	282.49	0	2	85	254.54	0.0051	0
61	279.85	0.2821	0	86	253.87	0	2
62	279.58	0	2	87	253.53	0	2
63	279.02	0	2	88	253.45	0.0003	0
64	278.8	0.0077	0	89	248.96	0.0488	0
65	278.69	0	2	90	246.06	0	2
66	277.25	0	2	91	245.96	0.0025	0
67	276.67	0	2	92	245.72	0	2
68	275.15	0	2	93	245.29	0	2
69	275.14	0.0009	0	94	244.83	0.0012	0
70	273.57	0.0791	0	95	244.79	0	2
71	272.76	0.0003	0	96	244.24	0	2
72	269.89	0	2	97	244.1	0.1465	0
73	269.21	0	2	98	242.4	0	0
74	269	0	2	99	241.25	0	2
75	268.68	0.0143	0	100	240.52	0.004	0

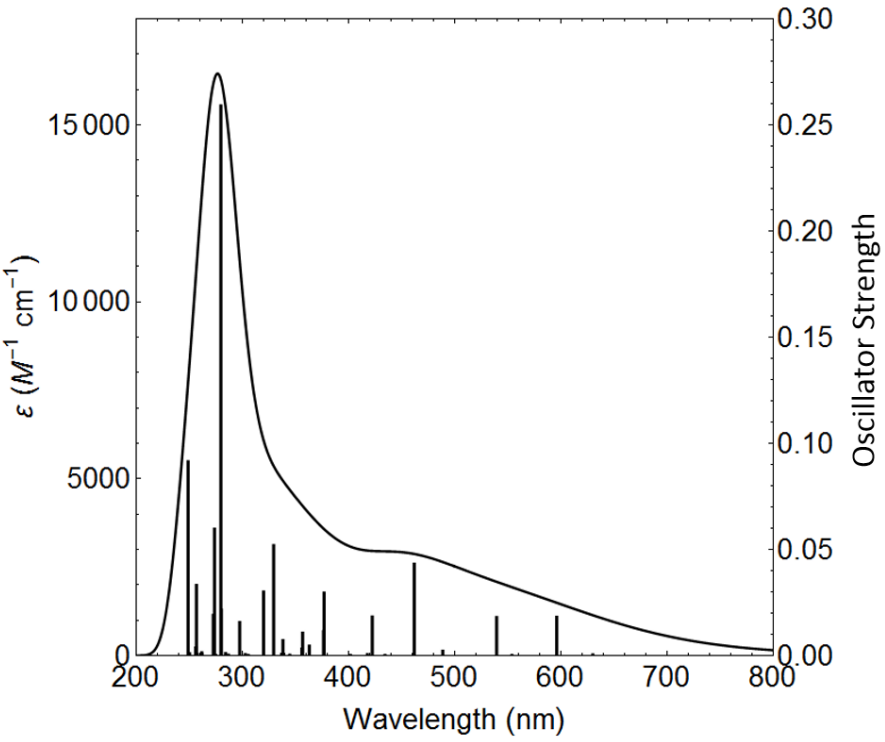

Fig. S24. Calculated absorption spectrum (solid black line) and TD-DFT calculated oscillators (solid bars: first 100 excited states) of [Ni(dtbbpy)(*o*-tolyl)Br](**1**–**Br**) S_0.

Table S3. TD-DFT calculated transitions 1-50 for [Ni(dtbbpy)(*o*-tolyl)Br](**1–Br**) S_0.

Excited State	λ (nm)	f	<S**2>	Excited State	λ (nm)	f	<S**2>
1	1422.16	0	2	26	403.63	0	2
2	1126.66	0	2	27	402.58	0	2
3	930.37	0	2	28	401.75	0.0001	0
4	674.71	0	2	29	391.38	0	2
5	662.87	0	2	30	388.82	0	0
6	656.03	0	2	31	381.87	0	2
7	630.1	0.0003	0	32	378.79	0	2
8	596.05	0.0181	0	33	376.91	0.0294	0
9	553.87	0.0001	0	34	376.4	0.0113	0
10	539.49	0.0179	0	35	371.65	0	2
11	530.83	0	2	36	366.35	0	2
12	525.29	0	0	37	363.05	0.0044	0
13	516.73	0	2	38	357.72	0	2
14	504.2	0	0	39	356.68	0.0106	0
15	500.25	0	2	40	356.05	0.003	0
16	488.63	0.002	0	41	351.31	0	2
17	480.44	0	0	42	344.59	0.0002	0
18	476.38	0	2	43	343.71	0	2
19	461.82	0.0431	0	44	338.94	0	2
20	444.41	0	2	45	338.62	0	2
21	437.63	0	2	46	338.15	0.007	0
22	434.34	0.0001	0	47	336.96	0.0005	0
23	422.27	0.0182	0	48	331.88	0	2
24	419.19	0	2	49	329.39	0.0518	0
25	417.63	0.0004	0	50	320.87	0	2

Table S4. TD-DFT calculated transitions 51-100 for [Ni(dtbbpy)(*o*-tolyl)Br] (**1–Br**) S_0.

Excited State	λ (nm)	f	<S**2>	Excited State	λ (nm)	f	<S**2>
51	319.9	0.0299	0	76	273.67	0.0596	0
52	310.4	0	2	77	272.54	0.0189	0
53	305.52	0	2	78	271.18	0	2
54	305.48	0.0001	0	79	271.02	0	2
55	302.85	0	2	80	266.12	0	2
56	302.66	0.0004	0	81	265.12	0	2
57	300.05	0	2	82	262.1	0.0006	0
58	299.75	0	2	83	261.66	0.0013	0
59	297.4	0.0156	0	84	260.45	0	2
60	292.04	0	2	85	257.74	0	2
61	289.4	0	2	86	257.46	0.0005	0
62	288.18	0	2	87	256.86	0	2
63	286.8	0.0002	0	88	256.73	0.033	0
64	285.75	0.0001	0	89	256.71	0	2
65	285.59	0	2	90	256.07	0.0036	0
66	284.15	0.0009	0	91	255.6	0	0
67	281.77	0	2	92	251.1	0	2
68	281.37	0	2	93	250.28	0.0008	0
69	280.2	0.0214	0	94	250.15	0	2
70	279.68	0.2589	0	95	249.71	0	2
71	278.67	0	2	96	249.6	0.0007	0
72	275.99	0	2	97	248.83	0.0913	0
73	274.97	0	2	98	246.66	0	2
74	274.77	0.0001	0	99	244.86	0	2
75	274.14	0	2	100	244.16	0	2

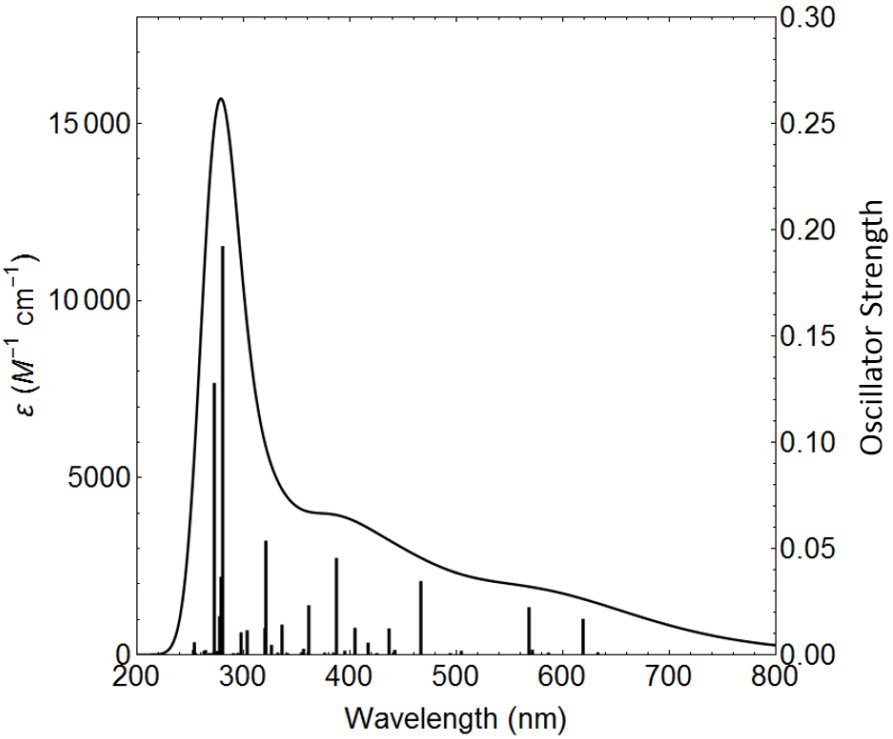

Fig. S25. Calculated absorption spectrum (solid black line) and TD-DFT calculated oscillators (solid bars: first 100 excited states) of [Ni(dtbbpy)(*o*-tolyl)I](**1–I**) S_0.

Table S5. TD-DFT calculated transitions 1-50 for [Ni(dtbbpy)(*o*-tolyl)I](**1–I**) S_0.

Excited State	λ (nm)	f	<S**2>	Excited State	λ (nm)	f	<S**2>
1	1585.52	0	2	26	425.27	0.0001	0
2	1209.41	0	2	27	417.09	0.0049	0
3	988.94	0	2	28	414.74	0	2
4	696.75	0	2	29	404.74	0.0119	0
5	675.94	0	2	30	403.56	0	2
6	657.18	0	2	31	397.61	0	2
7	632.82	0.0004	0	32	395.17	0.0012	0
8	619	0.0162	0	33	387.28	0.0448	0
9	588	0	2	34	386.47	0	2
10	586.45	0.0003	0	35	384.43	0.0003	0
11	571.36	0.0017	0	36	383.36	0	2
12	568.15	0.0217	0	37	377.69	0	2
13	541.25	0	2	38	376.27	0.0003	0
14	520.07	0	0	39	366.62	0	2
15	511.94	0	2	40	361.44	0	2
16	506	0	2	41	361.28	0.0226	0
17	504.55	0.0012	0	42	356.47	0.002	0
18	494.21	0.0001	0	43	354.44	0.0004	0
19	466.56	0.0339	0	44	352.45	0	2
20	459.24	0	2	45	343.85	0	2
21	444.16	0	2	46	342.52	0	2
22	442.18	0.0016	0	47	341.85	0	2
23	436.73	0.0117	0	48	341.35	0.0001	0
24	431.23	0	2	49	338.38	0	2
25	427.93	0	2	50	337.93	0	2

Table S6. TD-DFT calculated transitions 51-100 for [Ni(dtbbpy)(*o*-tolyl)I] (**1–I**) S_0.

Excited State	λ (nm)	f	<S**2>	Excited State	λ (nm)	f	<S**2>
51	336.25	0.0134	0	76	277.53	0.0174	0
52	332.32	0.0003	0	77	277.32	0	2
53	331.86	0	2	78	276.06	0	2
54	328.9	0	2	79	275.2	0.001	0
55	326.32	0.0039	0	80	274.38	0	2
56	321.1	0.0529	0	81	273.26	0	2
57	320.21	0.0118	0	82	272.59	0.1272	0
58	308.93	0	2	83	271.36	0.0003	0
59	304.58	0	2	84	271.29	0	2
60	303.49	0.0108	0	85	270.49	0	2
61	303.28	0	2	86	269.03	0	2
62	300.9	0	2	87	267.84	0.0001	0
63	300.4	0	2	88	266.39	0	2
64	297.72	0.0098	0	89	264.65	0	2
65	296.61	0.0001	0	90	264.47	0.0014	0
66	294.68	0.0002	0	91	263.17	0	2
67	294.36	0	2	92	262.94	0.001	0
68	291.83	0	2	93	258.15	0	2
69	290.4	0.0001	0	94	254.99	0.0001	0
70	288.65	0	2	95	254.82	0	2
71	286.27	0	2	96	253.84	0.0052	0
72	283.11	0	2	97	253.08	0.0016	0
73	280.41	0.1916	0	98	252.57	0	2
74	279.06	0	2	99	249.71	0	2
75	278.88	0.0359	0	100	249.03	0	2

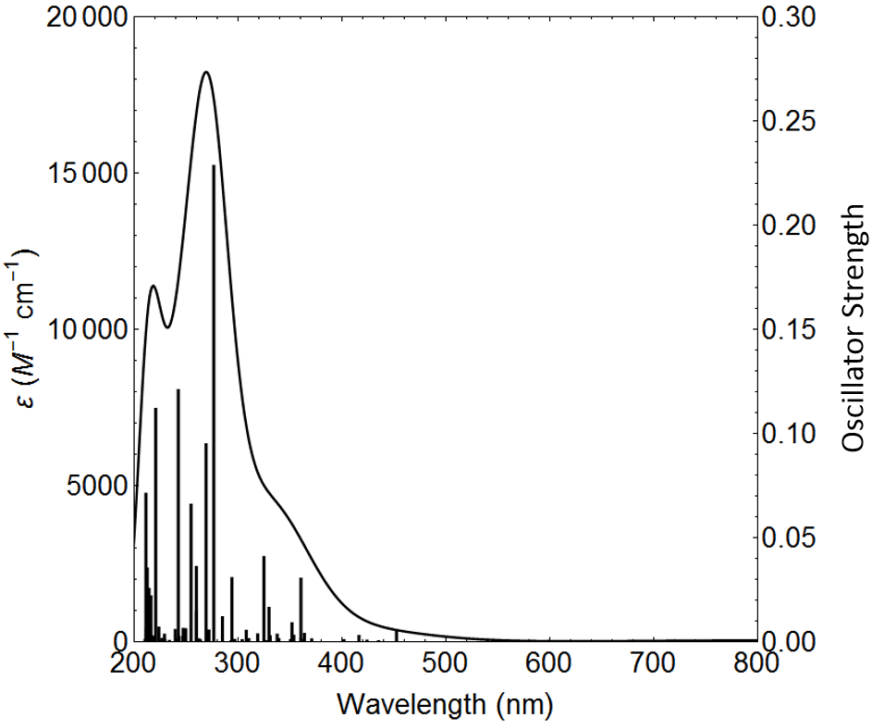

Fig. S26. Calculated absorption spectrum (solid black line) and TD-DFT calculated oscillators (solid bars: first 100 excited states) of [Ni(dtbbpy)Cl_2](**2**) T_0.

Table S7. TD-DFT calculated transitions 1-50 for [Ni(dtbbpy)Cl_2](**2**) T_0.

Excited State	λ (nm)	f	<S**2>	Excited State	λ (nm)	f	<S**2>
1	1514.53	0.0005	2.004	26	337.53	0.0032	2.826
2	1479.07	0	2.005	27	330.76	0.0024	2.126
3	973.03	0.0001	2.005	28	330.21	0.0015	3.107
4	819.81	0	2.007	29	329.66	0.016	2.045
5	814.23	0.0011	2.008	30	326.98	0.0001	2.985
6	540.2	0.0001	2.011	31	324.85	0.0404	2.438
7	452.43	0.0049	3.202	32	318.87	0.0033	3.052
8	435.24	0.0001	3.08	33	318.82	0	2.687
9	424.01	0.0003	2.52	34	310.27	0.001	2.898
10	416.34	0.0025	2.802	35	309.89	0	2.605
11	401.8	0.0005	2.921	36	309.37	0.0007	2.954
12	389.08	0	2.754	37	307.77	0.0051	3.79
13	388.03	0	3.995	38	303.94	0.0005	3.935
14	370.85	0.0009	2.049	39	300.11	0	3.01
15	363.87	0.0035	3.073	40	296.81	0.0007	2.976
16	361.48	0	2.023	41	295.63	0	2.997
17	360.74	0.0008	2.178	42	294.05	0.0303	2.053
18	360.39	0.03	2.084	43	293.23	0.0001	3.957
19	354.86	0	2.049	44	292.17	0	2.756
20	353.58	0.0027	2.965	45	286.24	0	2.096
21	353.07	0	2.763	46	285	0.0115	2.92
22	351.84	0.0087	3.499	47	281.26	0	2.737
23	350.4	0.0006	2.996	48	276.54	0.2282	2.082
24	347.08	0	2.235	49	276.08	0	3.994
25	339.17	0.001	2.492	50	273.95	0	3.004

Table S8. TD-DFT calculated transitions 51-100 for [Ni(dtbbpy)Cl_2](**2**) T_0.

Excited State	λ (nm)	f	<S**2>	Excited State	λ (nm)	f	<S**2>
51	272.96	0	2.984	76	229.05	0.0001	3.03
52	271.93	0.0052	3.196	77	227.15	0.0005	3.018
53	271.43	0.0039	2.194	78	226.83	0	2.91
54	269.25	0.0945	3.271	79	226.56	0.0012	2.958
55	263.58	0.0004	3.95	80	224.29	0	3.027
56	263.14	0.0003	2.989	81	224.09	0.0002	2.765
57	262.49	0.0009	2.908	82	223.7	0.0066	2.596
58	260.96	0	2.031	83	220.64	0.1116	2.719
59	259.83	0.0357	2.084	84	219.18	0.0003	2.976
60	259.71	0.0143	2.457	85	218.85	0.0017	2.544
61	258.19	0	2.024	86	218.71	0.0023	2.971
62	254.69	0.0655	2.557	87	216.34	0	2.034
63	249.52	0.0058	2.991	88	216.17	0.0216	2.553
64	247.16	0.0059	3.048	89	215.49	0	3.001
65	246.74	0	2.903	90	215.09	0	2.984
66	246.61	0.0021	3.7	91	214.64	0.0001	2.039
67	242.78	0.0022	3.583	92	214.54	0	3.006
68	242.49	0.1206	2.53	93	214.36	0.0252	3.435
69	241.05	0.0008	2.986	94	214.34	0	3.011
70	239.56	0.0054	2.503	95	213.96	0.0002	2.981
71	238.59	0	2.692	96	212.94	0.001	3.077
72	234.46	0	2.541	97	212.62	0.0349	2.317
73	233.99	0.0002	2.974	98	211.72	0.0058	3.185
74	229.42	0.0005	2.967	99	211.29	0.0708	2.191
75	229.16	0.0032	2.97	100	210.46	0.0007	2.047

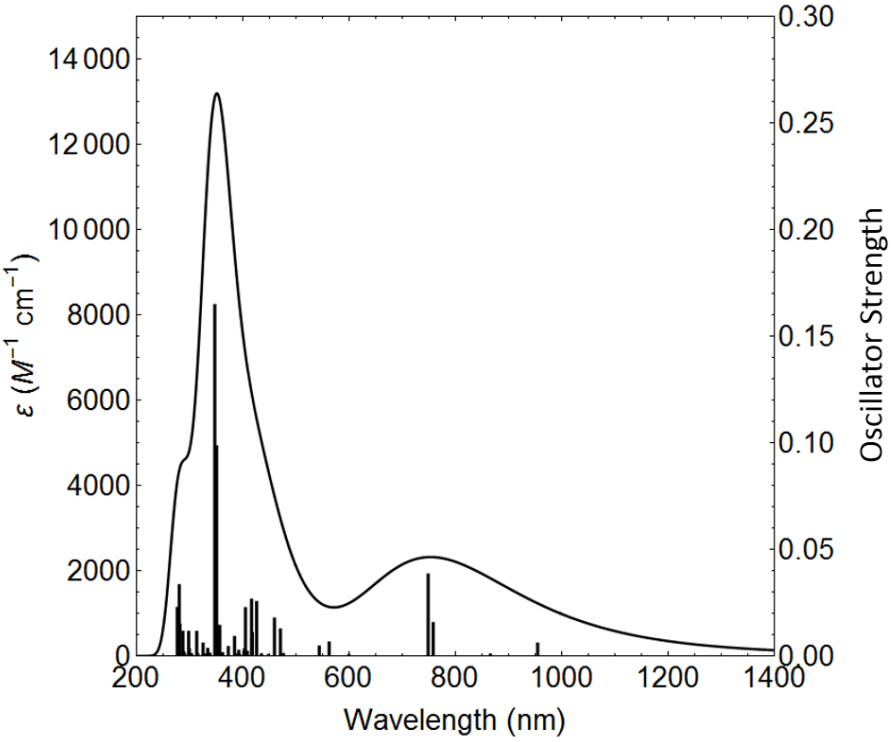

Fig. S27. Calculated absorption spectrum (solid black line) and TD-DFT calculated oscillators (solid bars: first 50 excited states) of geometry optimized [Ni(dtbbpy)(*o*-tolyl)Cl](**1–Cl**) T_1.

Difference Density Isosurfaces. Mapped difference density isosurfaces were generated by subtracting the electron density from total SCF density for the ground state from the electron density from total SCF density of a given excited state. All calculations were carried out at constant isovalue (0.0004).

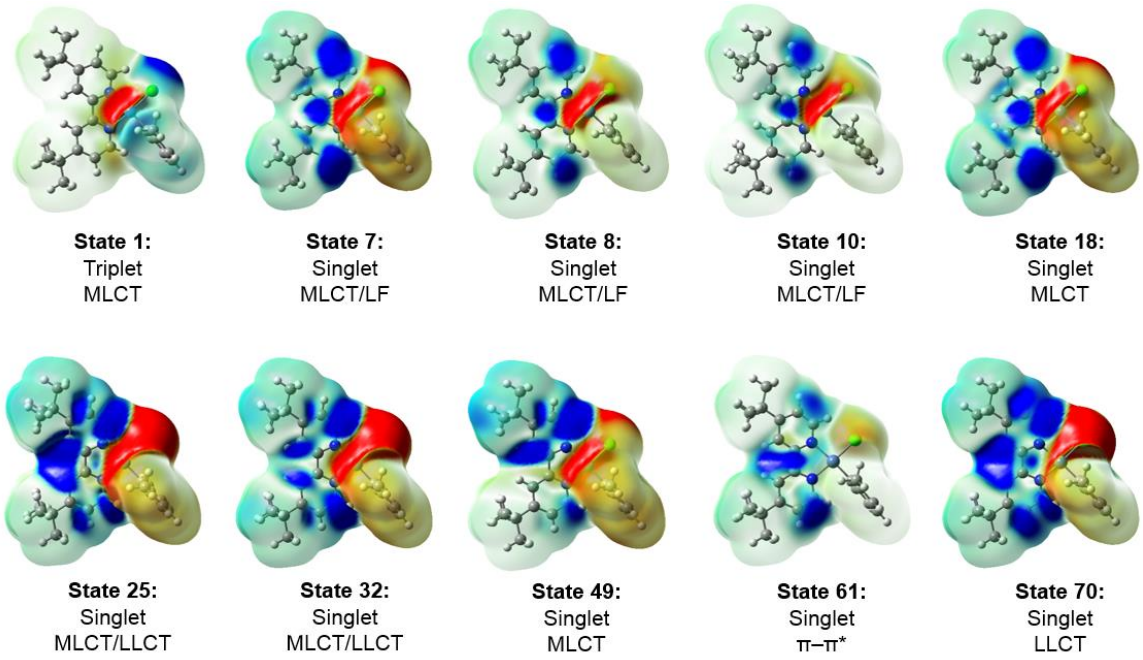

Figure S28. Difference density isosurfaces for select calculated transitions for [Ni(dtbbpy)(*o*-tolyl)Cl](**1–Cl**) S_0 displayed with multiplicity and transition assignments. Difference density isosurfaces demonstrate the loss (red) and build-up (blue) of electron density.

Natural Population Analysis. Atomic charges for **1–Cl** in various electronic states were computed via Natural Population Analysis (NPA) to quantify MLCT character. First the difference in atomic charge

$$\Delta\delta\mathrm{Ni}_{\mathrm{ES}} = \delta\mathrm{Ni}_{\mathrm{ES}} - \delta\mathrm{Ni}_{\mathrm{GS}}$$

between each excited state ($\delta\mathrm{Ni}_{\mathrm{ES}}$) and the ground state ($\delta\mathrm{Ni}_{\mathrm{GS}}$) were calculated. Next the charge differences $\Delta\delta\mathrm{Ni}_{\mathrm{ES}}$ were normalized against the difference in atomic charge between Ni(III) **1**–**Cl**$^{+}$ ($\Delta\delta$Ni(III)) and Ni(II) **1–Cl** ($\delta\mathrm{Ni}_{\mathrm{GS}}$) ground state at constant geometry according to

$$\overline{\Delta\delta\mathrm{Ni}_{\mathrm{ES}}} = \frac{\Delta\delta\mathrm{Ni}_{\mathrm{ES}}}{\delta\mathrm{Ni(III)} - \delta\mathrm{Ni}_{\mathrm{GS}}}$$

where $\overline{\Delta\delta\mathrm{Ni}_{\mathrm{ES}}}$ is the normalized change in charge associated with a given transition such that $\Delta\delta\mathrm{Ni(III)} - \Delta\delta\mathrm{Ni}_{\mathrm{GS}} = 1$. When $\overline{\Delta\delta\mathrm{Ni}_{\mathrm{ES}}} \approx 1$ the change in charge on Ni is similar to the change in charge associated with formal oxidation of the complex, indicating a transition with significant MLCT character.

Table S9. Natural population analysis of select calculated transitions for [Ni(dtbbpy)(*o*-tolyl)Cl](**1–Cl**) S_0. Note that T_1(opt) is the geometry optimized first triplet state while ES1 is the vertical transition computed via TD-DFT.

State	δNi	ΔδNi	$\overline{\Delta\delta\mathrm{Ni}_{\mathrm{ES}}}$
GS	0.40647	-	-
Ni(III)	0.77543	0.36896	1.00
T_1(opt)	0.74438	0.33791	0.92
ES1 (T_1)	0.85778	0.45131	1.22
ES7 (S_1)	0.75710	0.35063	0.95
ES8	0.71071	0.30424	0.82
ES10	0.68026	0.27379	0.74
ES18	0.70966	0.30319	0.82
ES25	0.65403	0.24756	0.67
ES32	0.65570	0.24923	0.68
ES49	0.68935	0.28288	0.77
ES61	0.41286	0.00639	0.02
ES70	0.52779	0.12132	0.33

Simulating $^3MLCT_1$ Ni(dtbbpy)(*o*-tolyl)Cl ΔA Spectrum. The difference absorption spectrum for $^3MLCT_1$ **1–Cl** was simulated by subtraction of the steady state absorption spectrum of Ni(II) from the computed triplet-triplet absorption spectrum.

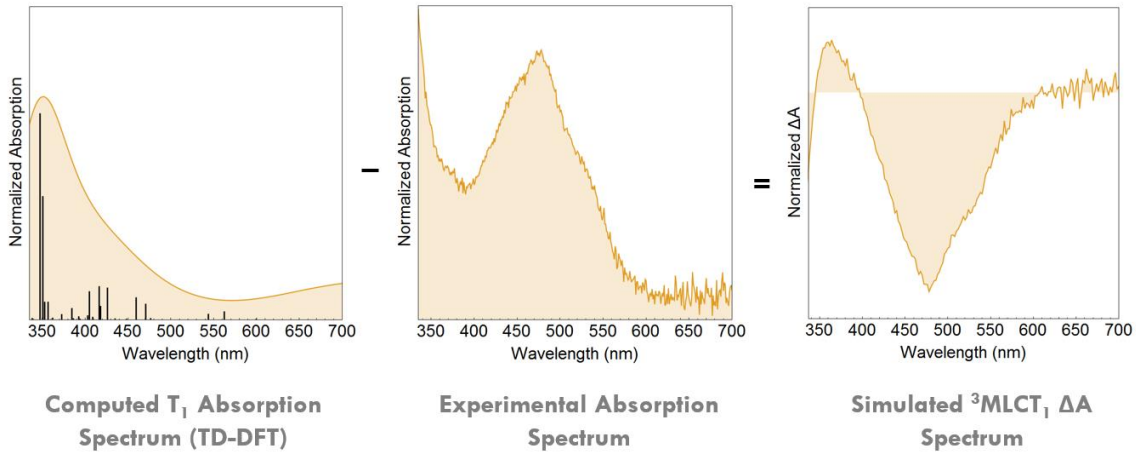

Fig. S29. Method for simulating transient absorption spectrum for $^3MLCT_1$ **1–Cl**.

Excited State Redox Potentials. The excited state reduction potentials for $^3MLCT_1$ Ni(dtbbpy)(*o*-tolyl)Cl were calculated from the ground state peak potentials for the first reduction and first oxidation, measured via cyclic voltammetry, and computed free energy difference between S_0 and $^3MLCT_1$ computed via DFT (B3LYP/TZVP).

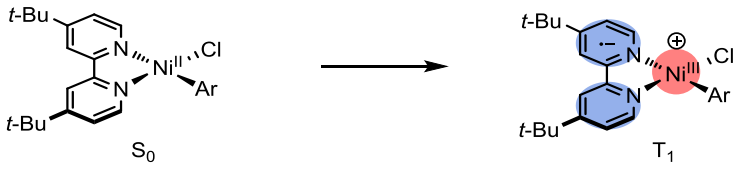

S_0-T_1 (kcal mol^{-1})	
ΔG	37.7
ΔH	38.6

	Ni(dtbbpy)(*o*-tolyl)Cl T_1	Ni(dtbbpy)(*o*-tolyl)Cl S_0
Sum of Electronic and Thermal Free Energies	-3049.401234	-3049.461391
Sum of Electronic and Thermal Enthalpies	-3049.305749	-3049.367197

Fig. S30. DFT calculated ΔSCF S_0–T_1 gap for Ni(dtbbpy)(*o*-tolyl)Cl (**1–Cl**). Tabulated energies are in hartrees.

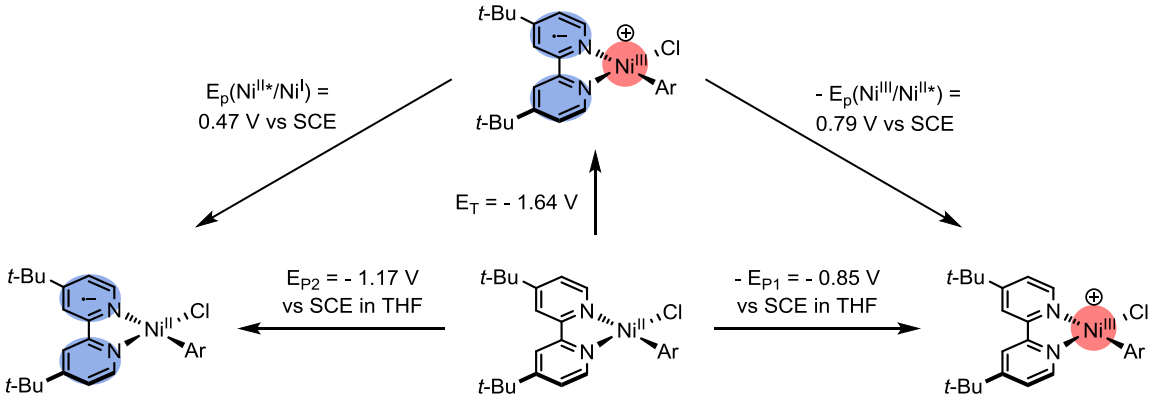

Fig. S31. Thermodynamic cycle summarizing ground state and excited state reduction potentials for Ni(dtbbpy)(*o*-tolyl)Cl (**1–Cl**).

Spin State of Ni(dtbbpy)Cl_2. The spin state of Ni(dtbbpy)Cl_2 was predicted via DFT from the computed free energy difference between geometry optimized singlet and triplet structures.

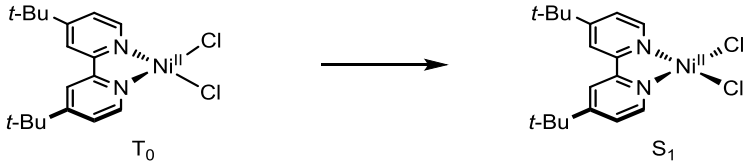

T_0-S_1 (kcal mol^{-1})	
ΔG	11.1
ΔH	8.5

	Ni(dtbbpy)Cl_2 T_0	Ni(dtbbpy)Cl_2 S_1
Sum of Electronic and Thermal Free Energies	-3238.810536	-3238.792782
Sum of Electronic and Thermal Enthalpies	-3238.724621	-3238.711147

Fig. S32. DFT calculated T_0–S_1 gap for Ni(dtbbpy)Cl_2 (**2**). Tabulated energies are in hartrees. The triplet optimized to a tetrahedral geometry while the singlet optimized to a square planar geometry.

C–O Cross Coupling Thermodynamics. A preliminary evaluation of the thermodynamics for C–O reductive elimination from possible Ni(II) and Ni(III) intermediates in C–O coupling experiments was carried out via DFT. The favorability for aryl halide oxidative addition with Ni(I)(dtbbpy)(OR) complexes was evaluated to probe the possibility of a photoinitiated thermal C–O cycle proceeding via a Ni(I)/Ni(III) cycle.

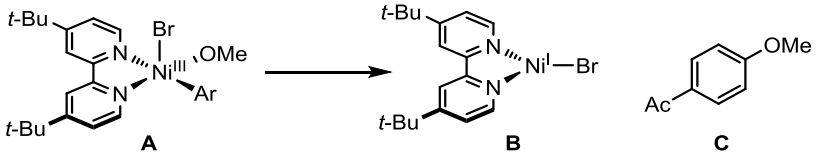

Thermodynamics (kcal mol^{-1})	
ΔG	-39.4
ΔH	-26.2

	A	B	C
Sum of Electronic and Thermal Free Energies	-5391.898905	-4892.500703	-499.461036
Sum of Electronic and Thermal Enthalpies	-5391.790178	-4892.418774	-499.413088

Fig. S33. DFT calculated Ni(III) C–O reductive elimination thermodynamics. Tabulated energies are in hartrees.

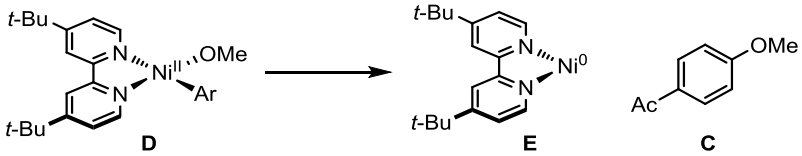

Thermodynamics (kcal mol^{-1})	
ΔG	44.7
ΔH	55.9

	D	E	C
Sum of Electronic and Thermal Free Energies	-2817.696391	-2318.164061	-499.461036
Sum of Electronic and Thermal Enthalpies	-2817.593254	-2318.091121	-499.413088

Fig. S34. DFT calculated Ni(II) C–O reductive elimination thermodynamics. Tabulated energies are in hartrees.

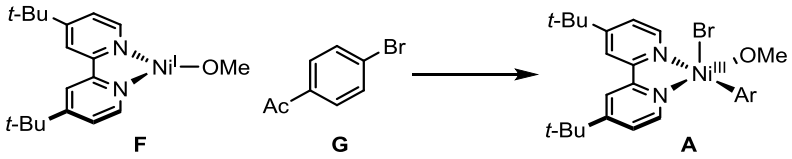

Thermodynamics (kcal mol^{-1})	
ΔG	4.0
ΔH	-11.6

	F	G	A
Sum of Electronic and Thermal Free Energies	-2433.39232	-2958.513033	-5391.898905
Sum of Electronic and Thermal Enthalpies	-2433.305296	-2958.466468	-5391.790178

Fig. S35. DFT calculated Ni(I) oxidative addition thermodynamics. Tabulated energies are in hartrees.

V. Ultrafast Transient Absorption Spectroscopy

Primer. Transient absorption spectroscopy is a time-resolved technique which allows the tracking of how a photoexcited molecule evolves from its original photoexcited state either to other states or back to the ground state. Sometimes called pump-probe spectroscopy, this technique relies on an actinic "pump" pulse of light which is resonant with an electronic transition in the sample to bring it to an excited electronic state. This photoexcited state can have a completely distinct absorption spectrum from the ground state, meaning that it can absorb different wavelengths of light. The absorption spectrum of this transient species (hence, transient absorption spectroscopy) is measured by directing a polychromatic probe pulse to the same sample position and measuring its transmission. In this work, we use a "white light" probe, composed of a broad bandwidth of light ranging from 350 to 775 nm. The difference in the transmission of the probe pulse through the sample with and without a preceding pump pulse constitutes a transient absorption spectrum.

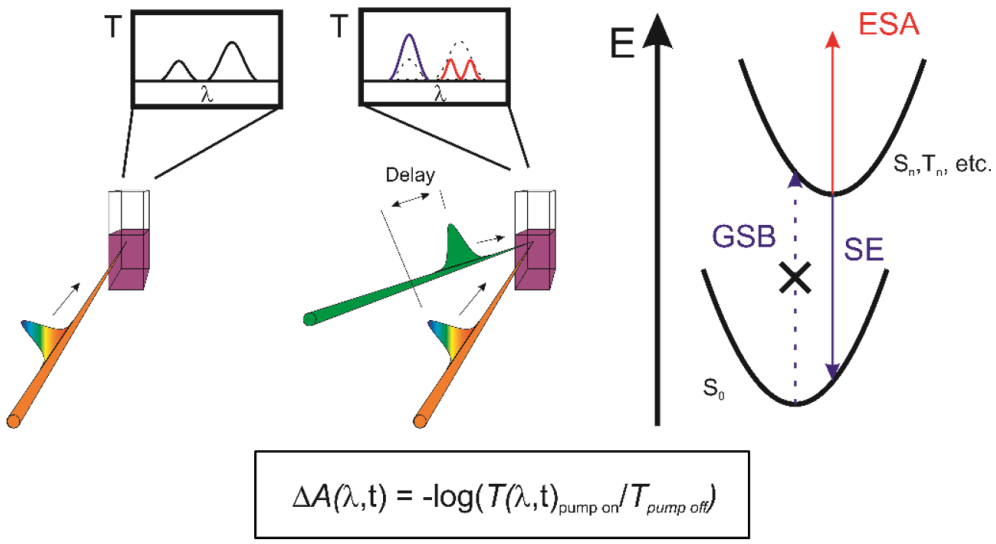

Fig. S36. General principles of transient absorption spectroscopy.

There are three main types of signals in a transient absorption spectrum. One negative signal is the ground state bleach (GSB). GSB signals arise from the depletion of the sample's ability to absorb light at a particular wavelength because some of the absorbers in that sample are in the excited state. While common conceptions of photobleaching in organic chemistry usually occur due to decomposition of the absorbing unit, the GSB signal we refer to is a transient bleaching signal due to generally distinct absorbing properties of the system measured. In practice, the GSB signal is visible if the probe spectral bandwidth encompasses absorption features of the sample, and it decays with the lifetime of the overall excited-state lifetime of the sample itself. For example, if the sample was first photoexcited into a singlet state and then underwent intersystem crossing to form a triplet state, the GSB would only decay with the lifetime of the triplet state.

Another negative signal is the stimulated emission (SE). SE signals arise when the probe photon interacts with an emissive electronically excited state, stimulating that entity to relax to a lower electronic state with the emission of a photon with energy equal to the

difference in the energies of the two states. This SE signal normally presents itself at the wavelengths associated with a sample's emission spectrum while that sample is in a photoexcited emissive states. For systems with small Stokes' shift[39], this signal is usually overlapping with the GSB, although with independent dynamics. Hence, the conversion from some initial photoexcited state to some non-emissive state, i.e. a triplet, would result in the decay of the SE feature in the TA spectrum. Further, if a sample is excited to some excited state higher than that (S_n) of the lowest excited state singlet (S_1), there would first be an SE signal associated with the S_n state with the formation of the S_1 SE arising with the rate of the internal conversion of S_n to S_1.

Positive signals in the TA spectra are the excited-state absorptions (ESA), sometimes also denoted photo-induced absorptions (PIA). ESA signals arise from new electronic transitions that are available from the new photoexcited states. The spectral positioning of these signals is not only dependent on the existence of energy levels accessible by the various wavelengths of light in the probe pulse, but also the extinction coefficient of those transitions according to optical selection rules. One example is that of intersystem crossing (ISC), where an excitation that originates on the singlet spin manifold relaxes to a state on the triplet manifold. In the singlet manifold, transitions to other higher lying singlet excited states accessible within the probe photon energies are likely observed as ESA signals—after the ISC, a new set of ESA signals corresponding to transitions to higher lying triplet excited states are now observed where they weren't before due to the spin optical selection rule. The evolution from one set of ESA features to another is usually assigned to some excited state dynamics which can take many forms, although the existence of an excited state absorption evolution without supplementary experimental or computational confirmations does not necessarily designate a specific excited-state process.

While the features themselves are a major component of TA spectroscopy, the ability to track their evolutions in time is the key aspect of this technique. By delaying the probe pulse with respect to the pump pulse, our experiments allow the excited state to evolve independently for a controllable amount of time before interrogating the excited state of the system with the probe pulse. As suggested previously, different excited states will likely have different transient features, such that the interconversion from one state to another can be tracked by the evolution of one state's features to another's. Hence, if a particular feature is associated with a particular excited state, like SE and ESA features usually are, correlating the disappearance or appearance of these features with the pump-probe delays over which the evolution occurs allows a designation of a kinetics for that conversion.

Figure S37A shows a TA map, which reports the excited state dynamics of **1-Cl** upon photoexcitation at 295 nm, which is particularly instructive because it is composed of both positive and negative signals dictated by the existence of GSB, SE, and ESA as described above. In this map, horizontal slices at particular pump probe delays report the transient spectrum at that delay (Figure S37B), while vertical slices at particular wavelengths reports the intensity of the transient absorption (positive for ESA, negative for GSB and SE) at that wavelength over the pump-probe delays investigated (Figure S37C). As noted in Figure 2b, an excitation of the **1-Cl** with 295 nm light will excite a predominantly dtbbpy centered transition, formally a high-lying singlet transition of the entire complex. Hence, the signals we might expect at early-pump probe delays would consist of the ESA signatures of the dtbbpy transition, which are peaks at 390, 520, and 740 nm, with the inclusion of the bleach features of the entire complex's absorption, which with the use of the visible probe, should

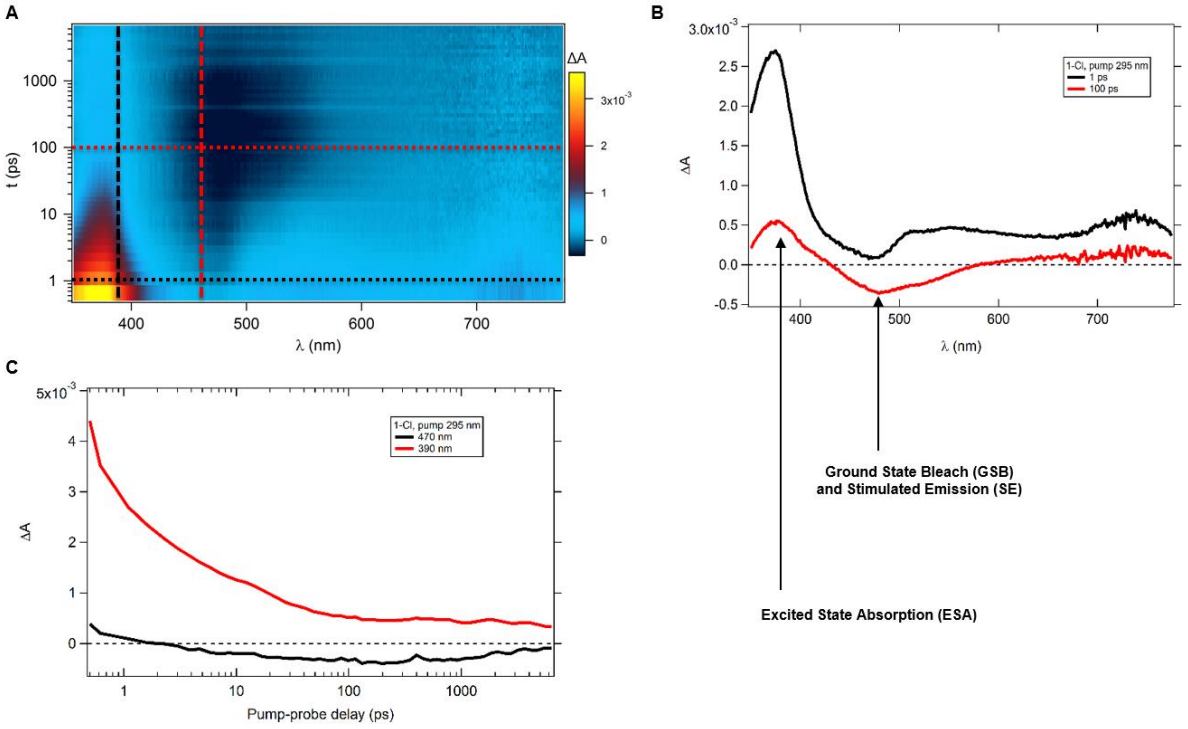

Fig. S37. Data summary and analysis of transient absorption spectra. (A) TA contour map with horizontal dotted lines corresponding to the transient spectrum at the reported time delay (B) and vertical lines corresponding to single wavelength kinetic traces (C).

appear as a negative feature at 470 nm. Indeed, at early times, meaning small pump-probe delays, this is exactly what is observed. Furthermore, we can motivate the internal conversion from this predominantly dtbbpy-centered transition to a ^{1}MLCT-type excited state by the reduction of ESA intensities assigned to the dtbbpy-centered excited state with an increase in the intensity of the negative signal near the GSB maximum, which is likely a formation of a SE signal. It is exactly this type of signal analysis which informs our assignments of the excited-state dynamics in this work.

Methods. A 1 kHz regeneratively amplified Ti:Sapphire laser (Coherent Libra, Santa Clara, California) with an output pulse duration of approximately 45 fs centered at 800 nm with output power 3.6 W is split with a 90-10 beamsplitter to generate the pump and probe. To generate the pump, the reflected portion of the Ti:Sapphire output is directed into a commercial optical parametric amplifier (OPerA Solo, Vilnius, Lithuania), which in our work we use to generate light at 295, 400, and 412 nm. Both the output of the OPerA Solo as well as the remainder of the originally transmitted 800 nm light were directed into a commercial transient absorption spectrometer (Ultrafast Systems Helios, Sarasota, Florida). The pump pulse is chopped at 500 Hz and is focused with a 500 mm focal length lens to the sample position. In the case of the experiments using 412 nm pump pulses, a broadband λ/2 waveplate was used to control its polarization, resulting in a pulse duration of approximately 100 fs. For the experiments using 400 nm light, neutral density filters were removed from the pump beam path and instead of a 500 mm focal length lens to focus the beam, we instead use a 400 nm high reflective spherical mirror with a 300 mm focal length to achieve a <100 fs pulse duration.

The remaining 800 nm light is first passes onto a delay stage before passing through a λ/2 waveplate and polarizer combination to control its intensity and polarization before being focused into a either a 2 mm thick translating CaF_2 crystal to generate a white light continuum from 325 nm to 800 nm or a 2 mm thick sapphire crystal to generate a white light continuum from 425 to 800 nm. The white light was then sent through a filter to remove the remaining fundamental light. A variable neutral density filter takes a portion of the probe light after the filter and directs the reflected portion to a separate camera for balance detection, whereas the transmitted portion is focused into the sample. The samples were prepared in a N_2-filled glovebox using 1 mm quartz cuvette (Starna Cells, Inc., Atascadero, California) equipped with a septum cap or a 2 mm optical glass cuvette (Starna Cells, Inc., Atascadero, California) which was adapted in house with a J. Young fitting and were stirred during experiments using a magnetic stirrer. All experiments were done at magic angle to avoid reorientation effects of the samples—in the case of the experiments photoexciting at 295 nm or 400 nm, the relative polarization angles between the pump and probe were controlled using the polarizer before the white light generation, as the polarization of the supercontinuum does not deviate from the incoming polarization of light.

The resultant data were background subtracted by subtracting the averaged transient spectra before the coherent artifact. Scattering peaks appear as positive signals at long pump-probe delays possibly due to minor changes in probe transmission at different delay stage positions, as well as alternating positive and negative peaks reflecting small fluctuations in pump power. The coherent artifact was also fit to a polynomial to correct for the temporal chirp in the TA maps. For samples which displayed degradation over the course of the experiment, only the first 50 scans were averaged for post-processing and analysis, which with 1s averaging per point and ~200 points per scan, corresponds to ~3 hours of experiment time analyzed.

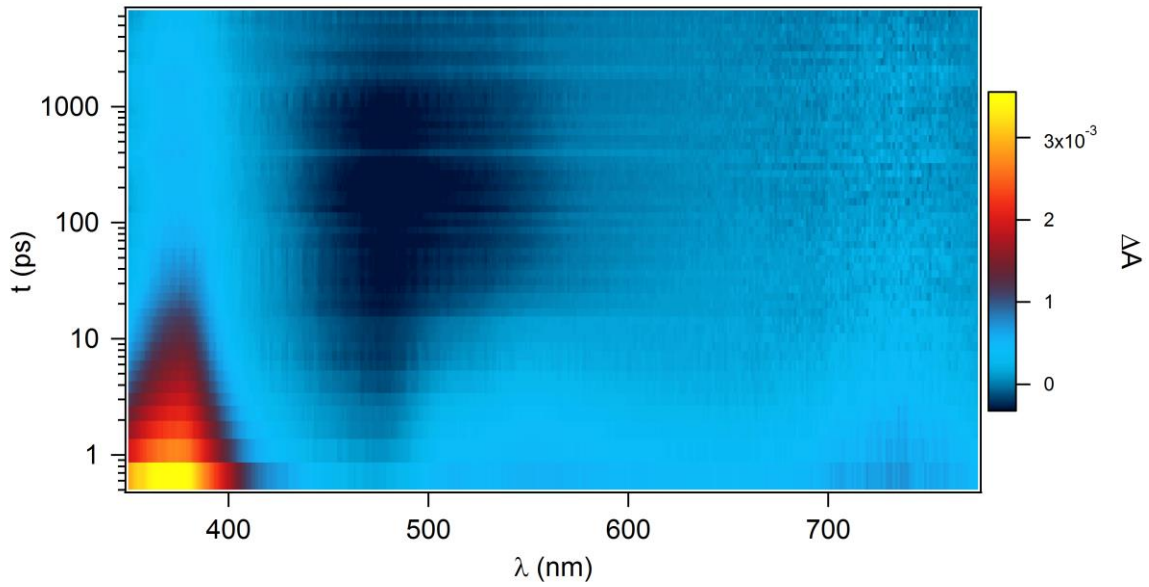

Fig. S38. Contour plot for transient absorption spectra of Ni(dtbbpy)(*o*-tolyl)Cl (**1–Cl**) after photoexcitation at 295 nm (pump power = 20 µW, first 50 scans, CaF_2 probe, 1mm quartz cuvette).

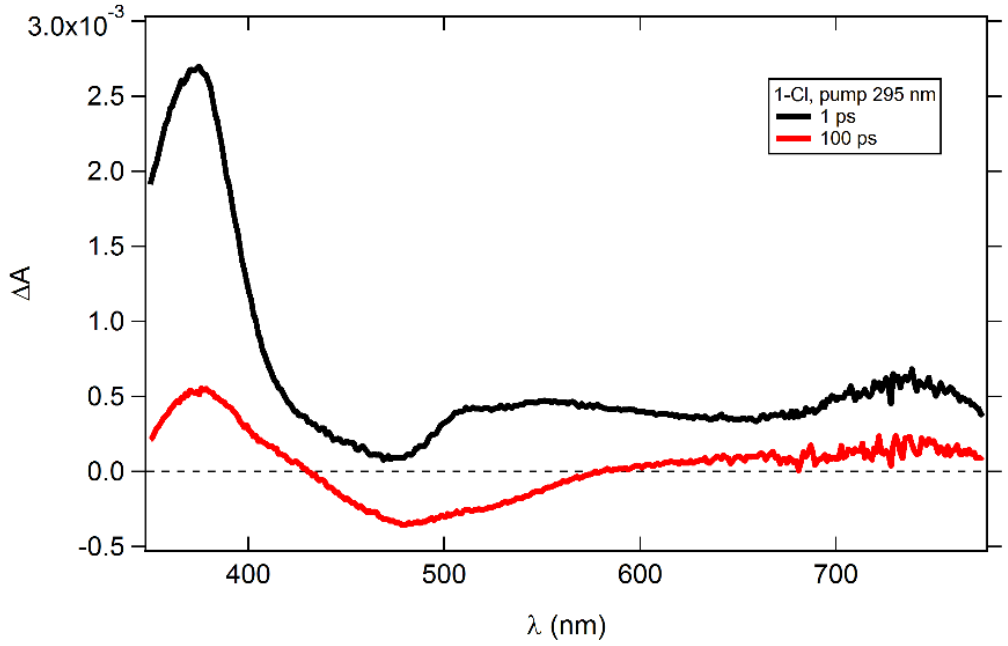

Fig. S39. Transient absorption spectra of Ni(dtbbpy)(*o*-tolyl)Cl (**1–Cl**) after photoexcitation at 295 nm at select probe delays (pump power = 20 µW, first 50 scans, CaF_2 probe, 1mm quartz cuvette).

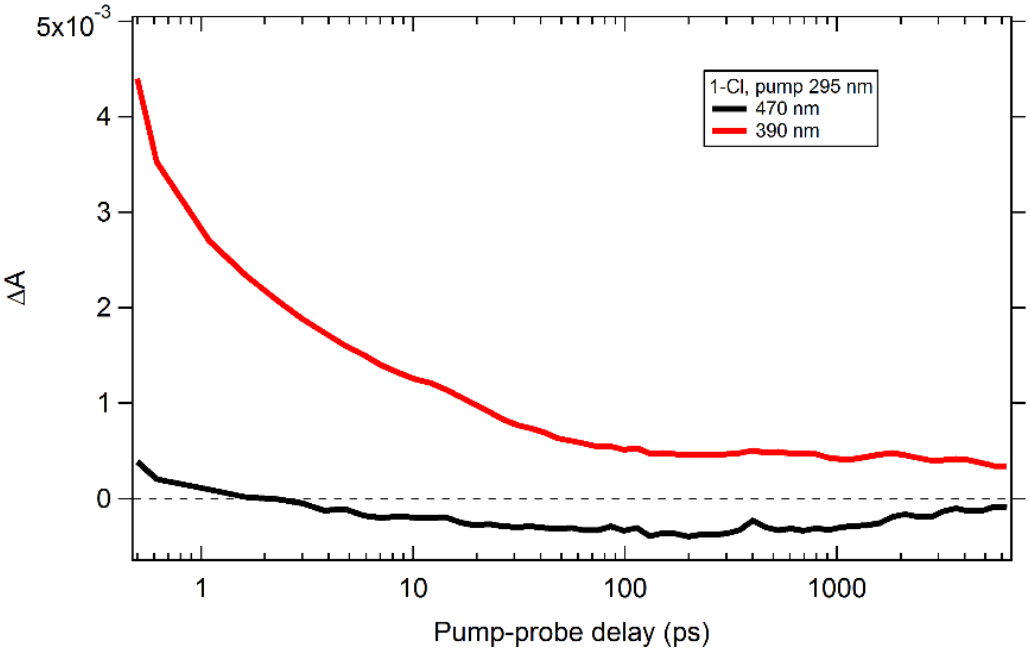

Fig. S40. Single wavelength kinetics for transient absorption spectra of Ni(dtbbpy)(*o*-tolyl)Cl (**1–Cl**) after photoexcitation at 295 nm at select wavelengths (pump power = 20 μW, first 50 scans, CaF_2 probe, 1mm quartz cuvette).

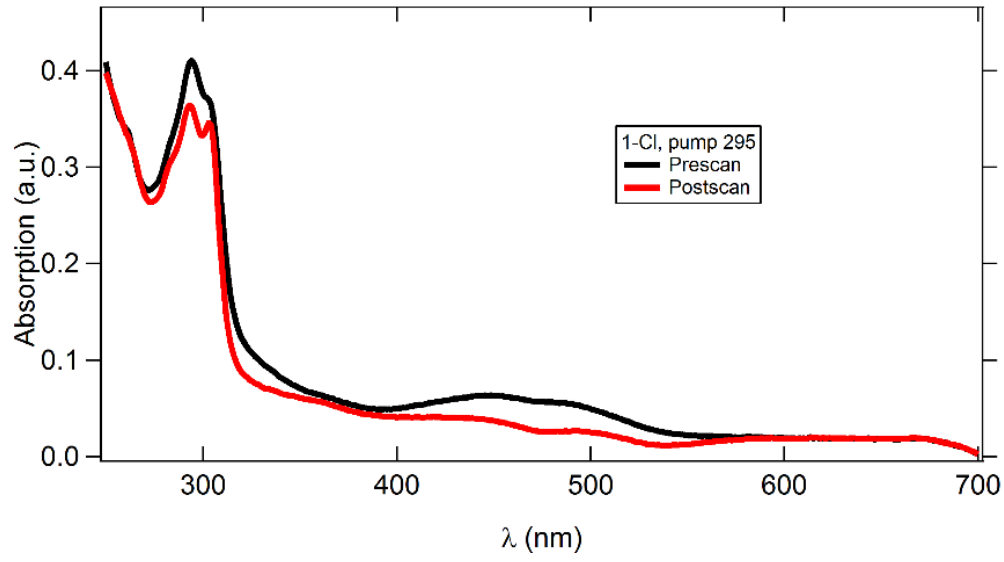

Fig. S41. Absorption spectra of Ni(dtbbpy)(*o*-tolyl)Cl (**1–Cl**) before and after transient absorption experiment (295 nm photoexcitation, pump power = 20 μW, 115 total scans, CaF_2 probe, 1mm quartz cuvette).

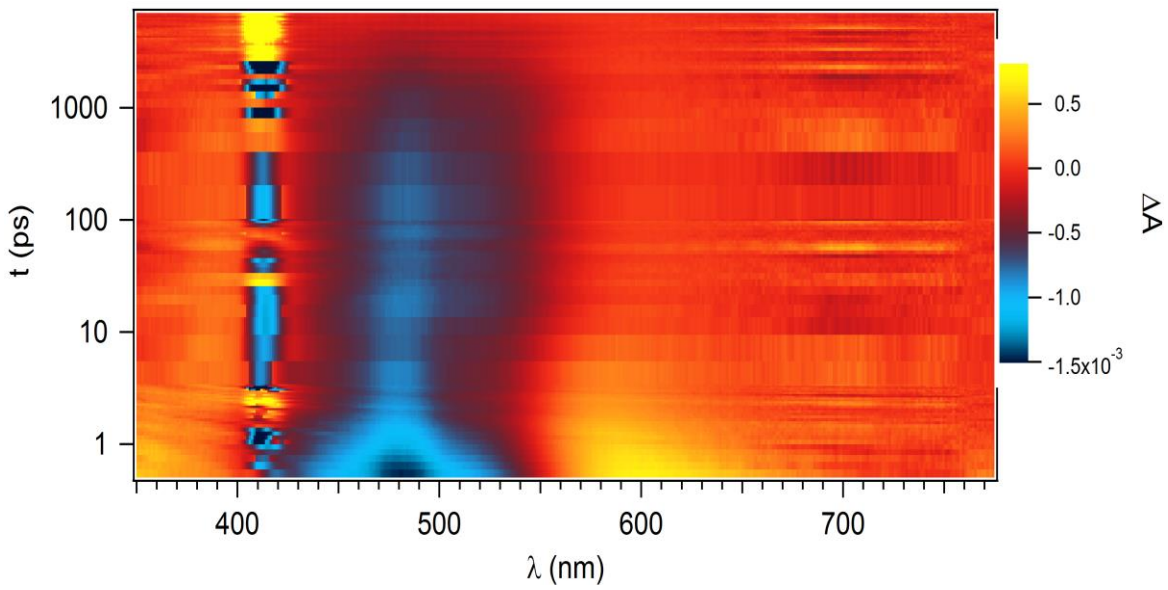

Fig. S42. Contour plot for transient absorption spectra of Ni(dtbbpy)(*o*-tolyl)Cl (**1–Cl**) after photoexcitation at 412 nm (pump power = 800 µW, 46 scans, CaF_2 probe, 2mm optical glass cuvette).

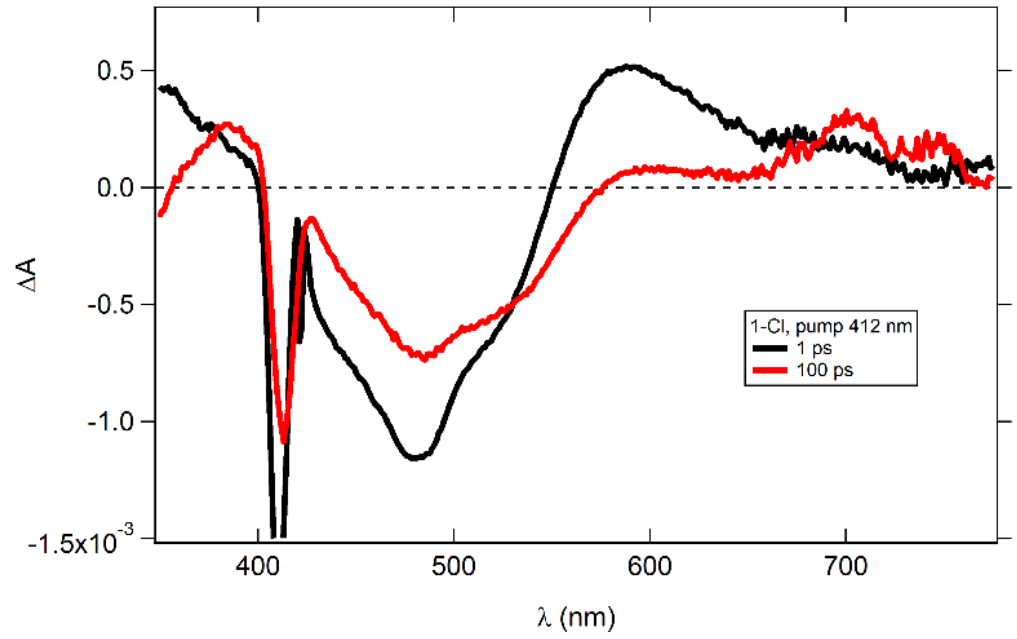

Fig. S43. Transient absorption spectra of Ni(dtbbpy)(*o*-tolyl)Cl (**1–Cl**) after photoexcitation at 412 nm at select probe delays (pump power = 800 µW, 46 scans, CaF_2 probe, 2mm optical glass cuvette).

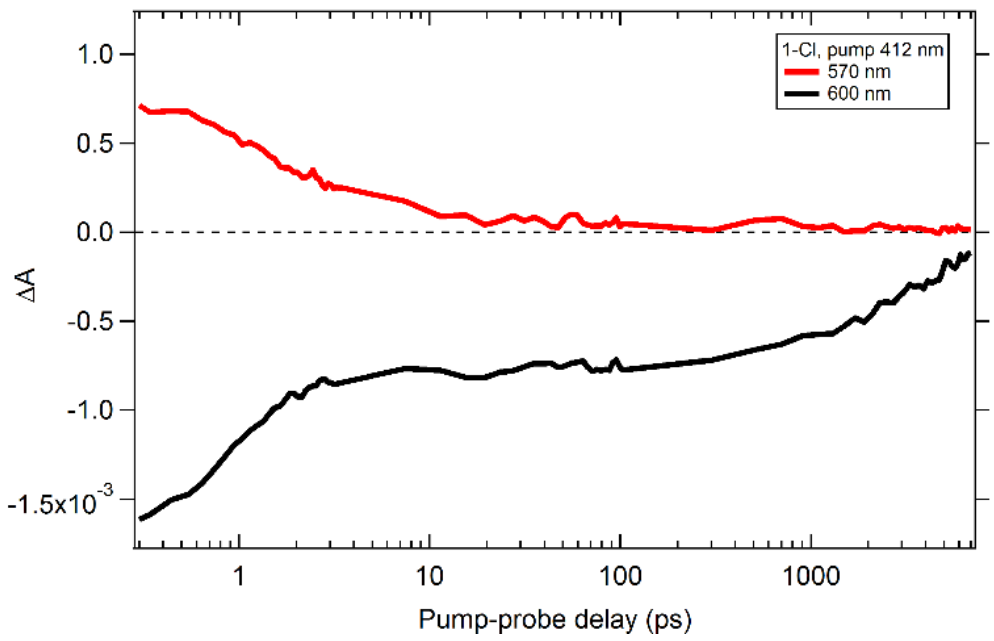

Fig. S44. Single wavelength kinetics for transient absorption spectra of Ni(dtbbpy)(*o*-tolyl)Cl (**1–Cl**) after photoexcitation at 412 nm at select wavelengths (pump power = 800 µW, 46 scans, CaF_2 probe, 2mm optical glass cuvette).

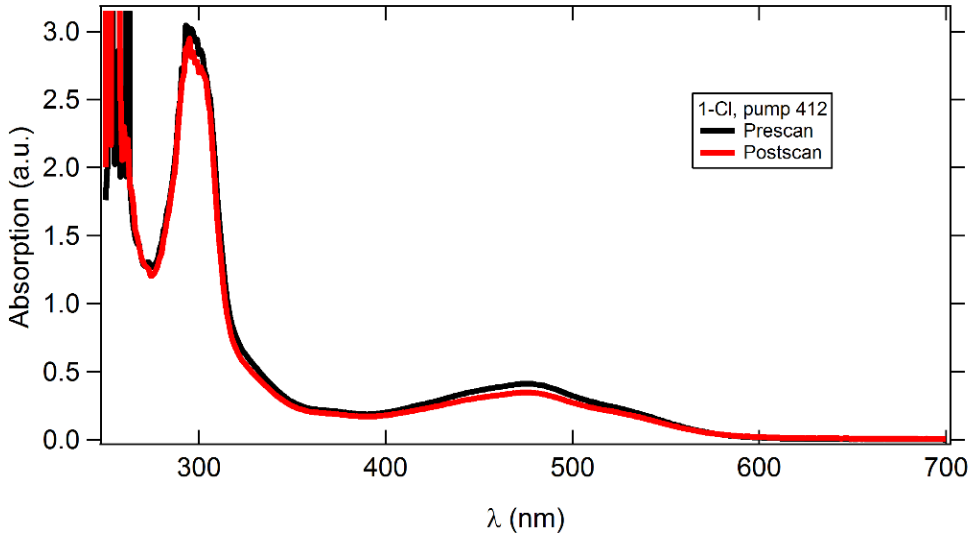

Fig. S45. Absorption spectra of Ni(dtbbpy)(*o*-tolyl)Cl (**1–Cl**) before and after transient absorption experiment (412 nm photoexcitation, pump power = 800 µW, 46 total scans, CaF_2 probe, 2mm optical glass cuvette).

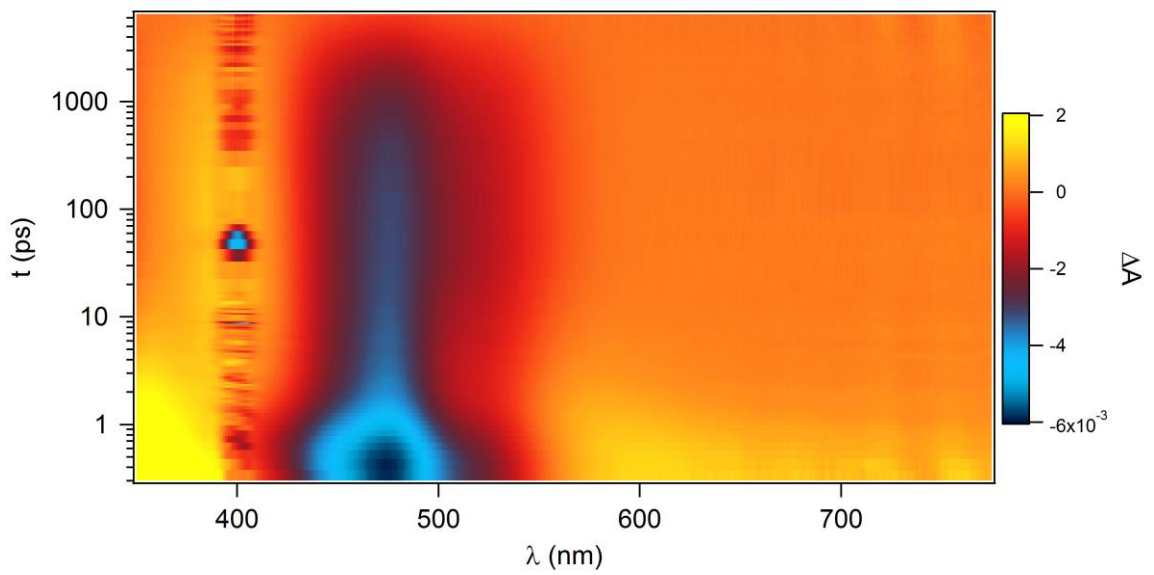

Fig. S46. Contour plot for transient absorption spectra of Ni(dtbbpy)(*o*-tolyl)Cl (**1–Cl**) after photoexcitation at 400 nm (pump power = 500 µW, first 50 scans, CaF_2 probe, 2mm optical glass cuvette).

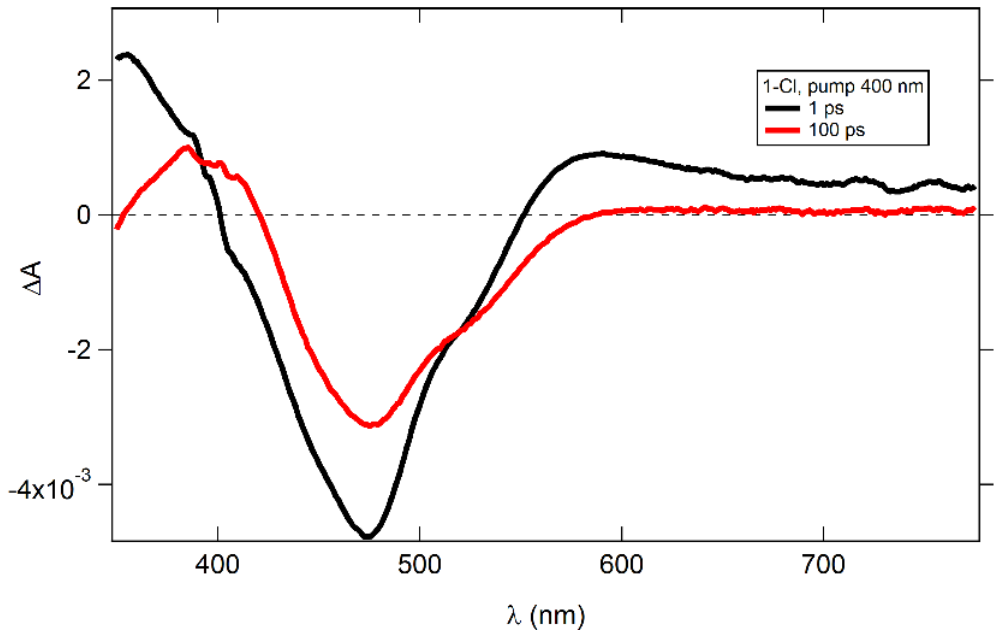

Fig. S47. Transient absorption spectra of Ni(dtbbpy)(*o*-tolyl)Cl (**1–Cl**) after photoexcitation at 400 nm at select probe delays (pump power = 500 µW, first 50 scans, CaF_2 probe, 2mm optical glass cuvette).

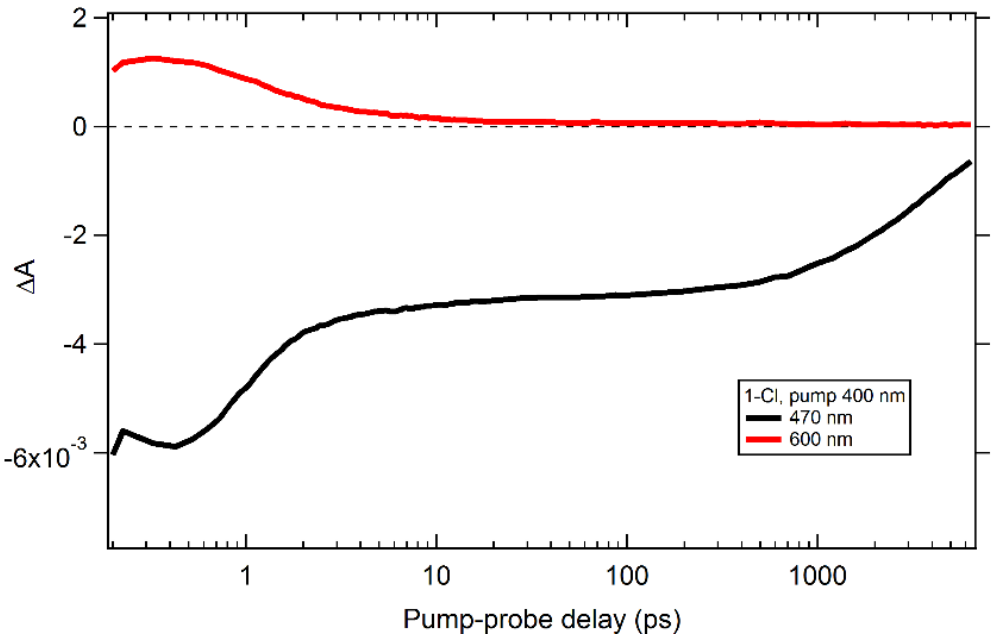

Fig. S48. Single wavelength kinetics for transient absorption spectra of Ni(dtbbpy)(*o*-tolyl)Cl (**1–Cl**) after photoexcitation at 400 nm at select wavelengths (pump power = 500 µW, first 50 scans, CaF_2 probe, 2mm optical glass cuvette).

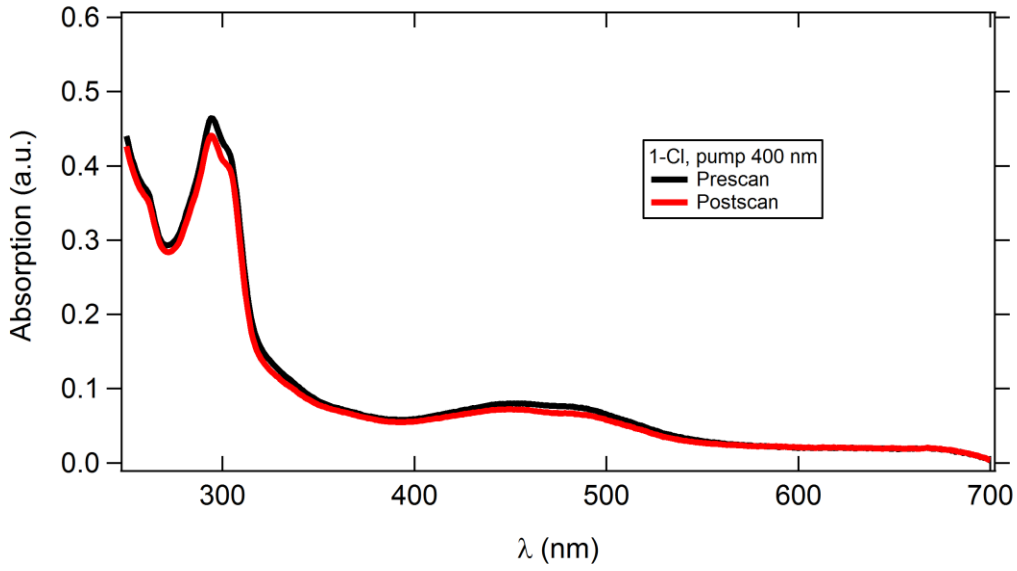

Fig. S49. Absorption spectra of Ni(dtbbpy)(*o*-tolyl)Cl (**1–Cl**) before and after transient absorption experiment (400 nm photoexcitation, pump power = 500 µW, 229 total scans, CaF_2 probe, 2mm optical glass cuvette).

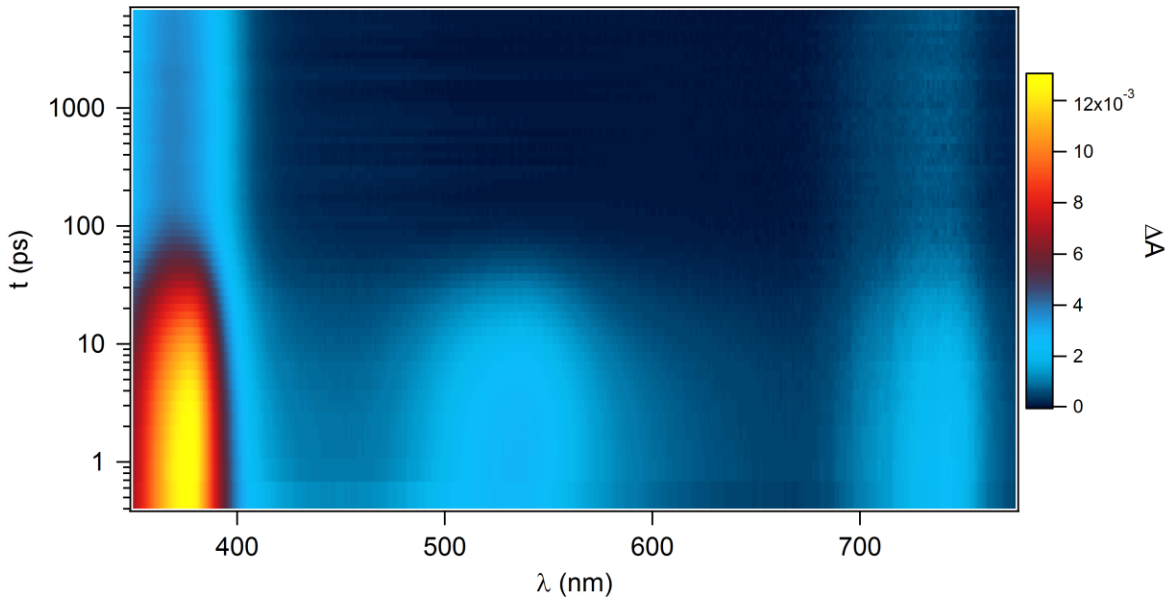

Fig. S50. Contour plot for transient absorption spectra of 4,4'-di-*tert*-butyl-2,2'-bipyridine after photoexcitation at 305 nm (pump power = 10 µW, 100 scans, CaF_2 probe, 1mm quartz cuvette).

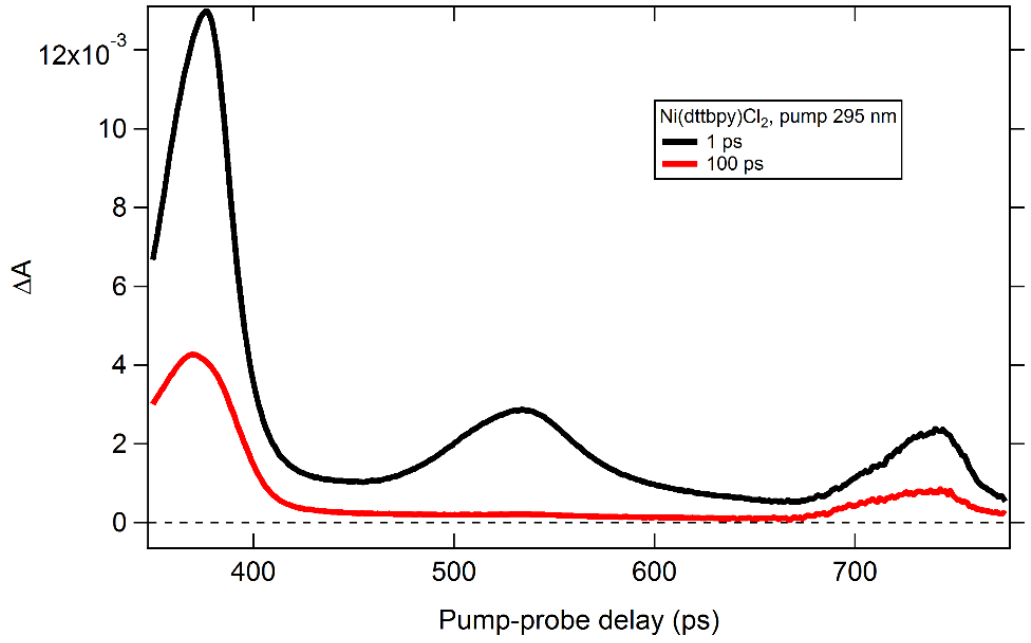

Fig. S51. Transient absorption spectra of 4,4'-di-*tert*-butyl-2,2'-bipyridine after photoexcitation at 305 nm at select probe delays (pump power = 10 µW, 100 scans, CaF_2 probe, 1mm quartz cuvette).

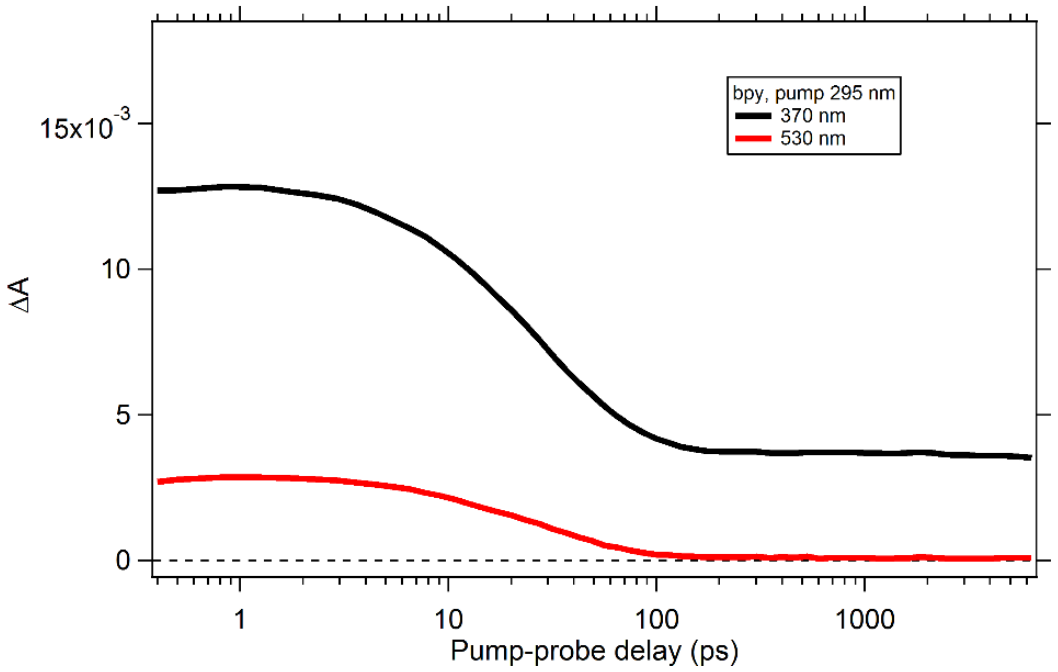

Fig. S52. Single wavelength kinetics for transient absorption spectra of 4,4'-di-*tert*-butyl-2,2'-bipyridine after photoexcitation at 305nm at select wavelengths (pump power = 10 µW, 100 scans, CaF_2 probe, 1mm quartz cuvette).

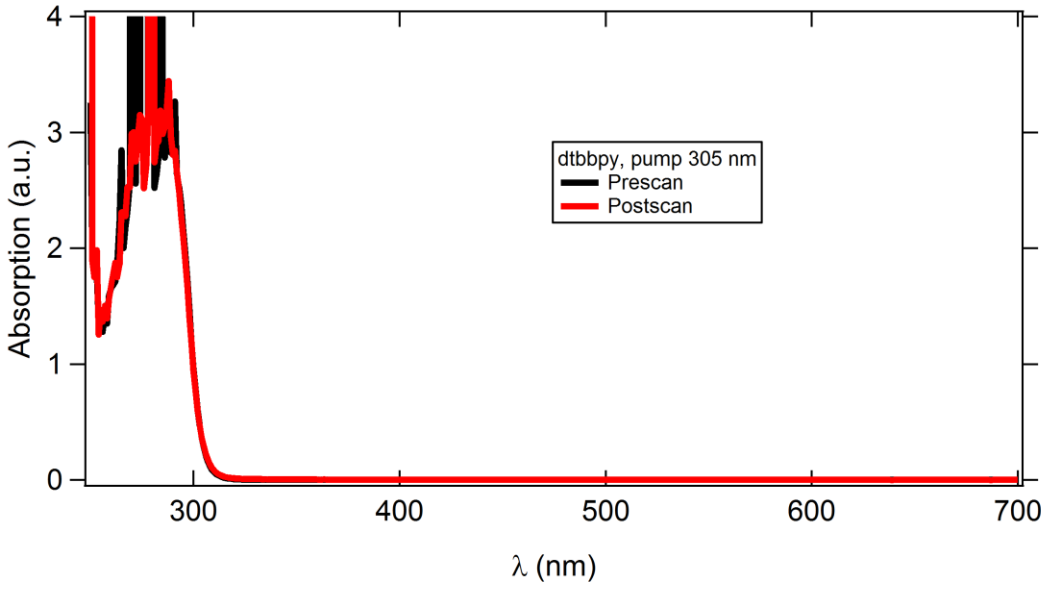

Fig. S53. Absorption spectra of 4,4'-di-*tert*-butyl-2,2'-bipyridine before and after transient absorption experiment (305 nm photoexcitation, pump power = 10 µW, 100 scans, CaF_2 probe, 1mm quartz cuvette).

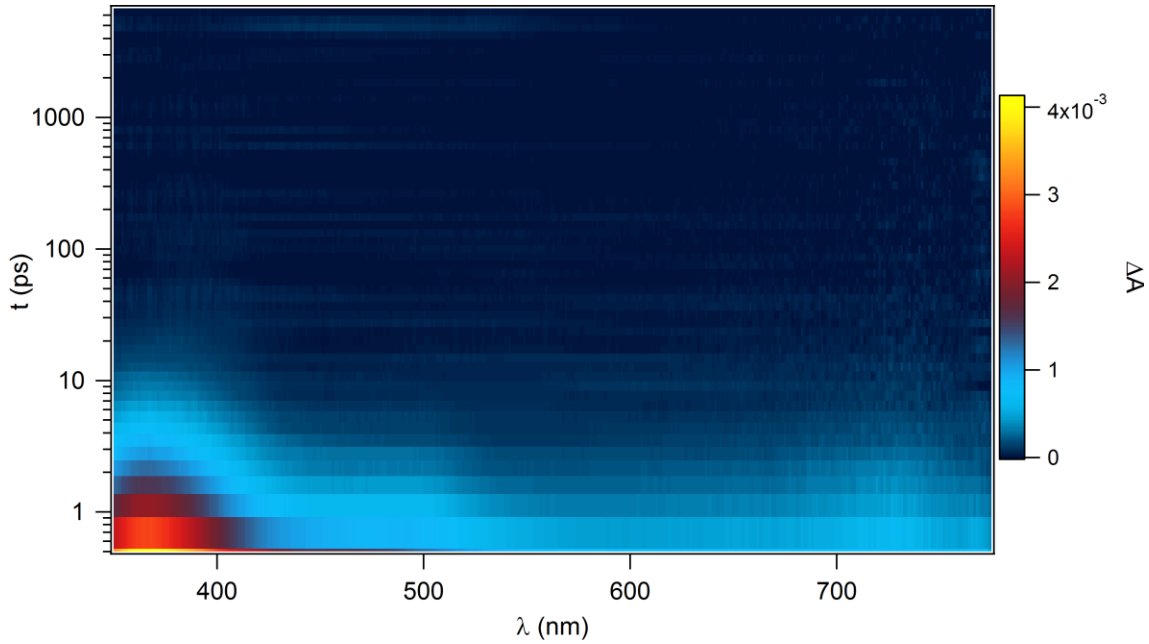

Fig. S54. Contour plot for transient absorption spectra of Ni(dtbbpy)Cl_2 (**2**) after photoexcitation at 295 nm (pump power = 20 µW, 50 scans, CaF_2 probe, 1mm quartz cuvette).

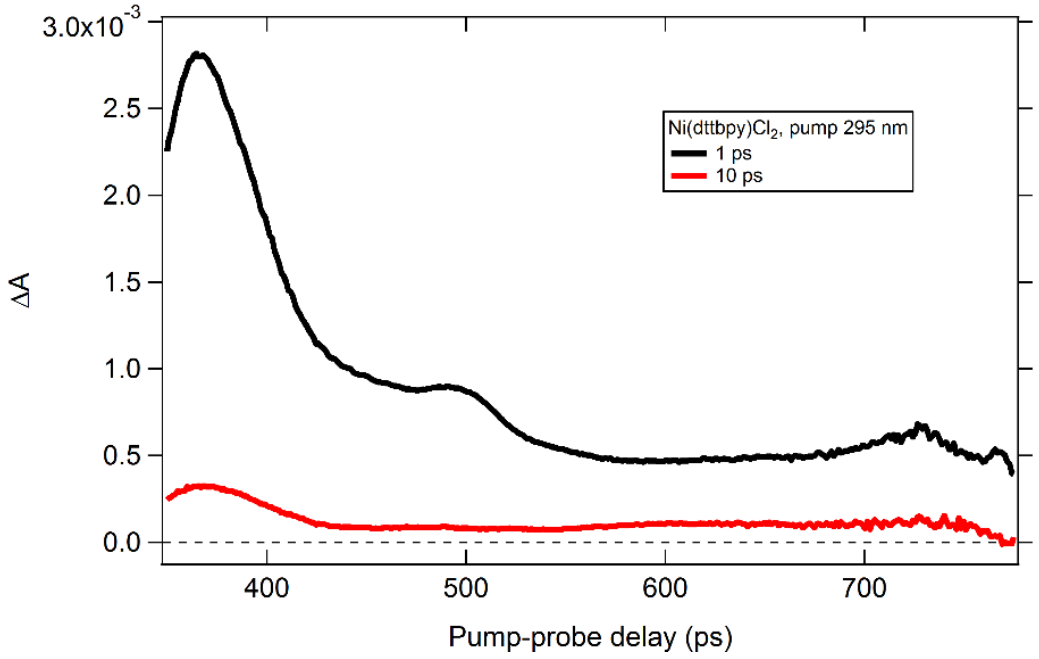

Fig. S55. Transient absorption spectra of Ni(dtbbpy)Cl_2 (**2**) after photoexcitation at 295 nm at select probe delays (pump power = 20 µW, 50 scans, CaF_2 probe, 1mm quartz cuvette).

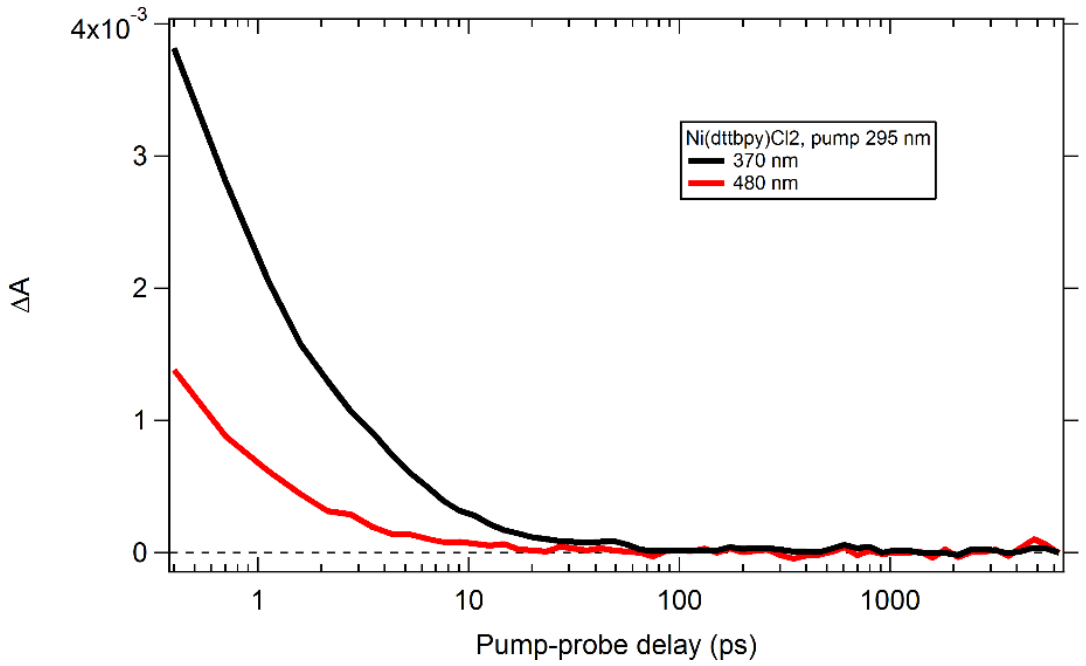

Fig. S56. Single wavelength kinetics for transient absorption spectra of Ni(dtbbpy)Cl_2 (**2**) after photoexcitation at 295 nm at select wavelengths (pump power = 20 μW, 50 scans, CaF_2 probe, 1mm quartz cuvette).

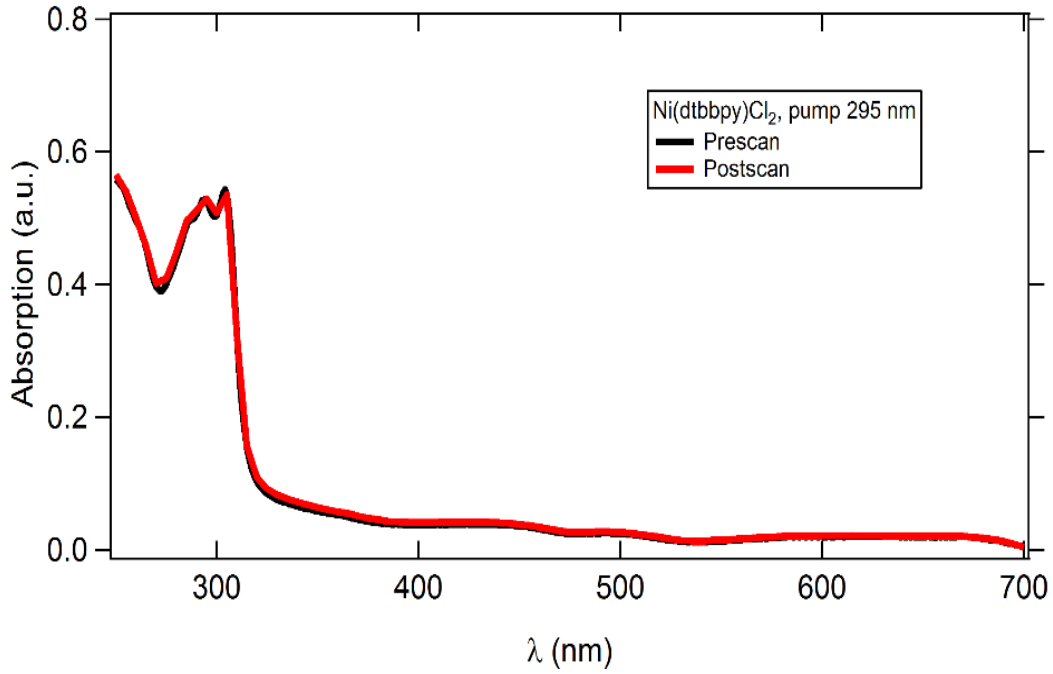

Fig. S57. Absorption spectra of Ni(dtbbpy)Cl_2 (**2**) before and after transient absorption experiment (295 nm photoexcitation, pump power = 20 μW, 50 scans, CaF_2 probe, 1mm quartz cuvette).

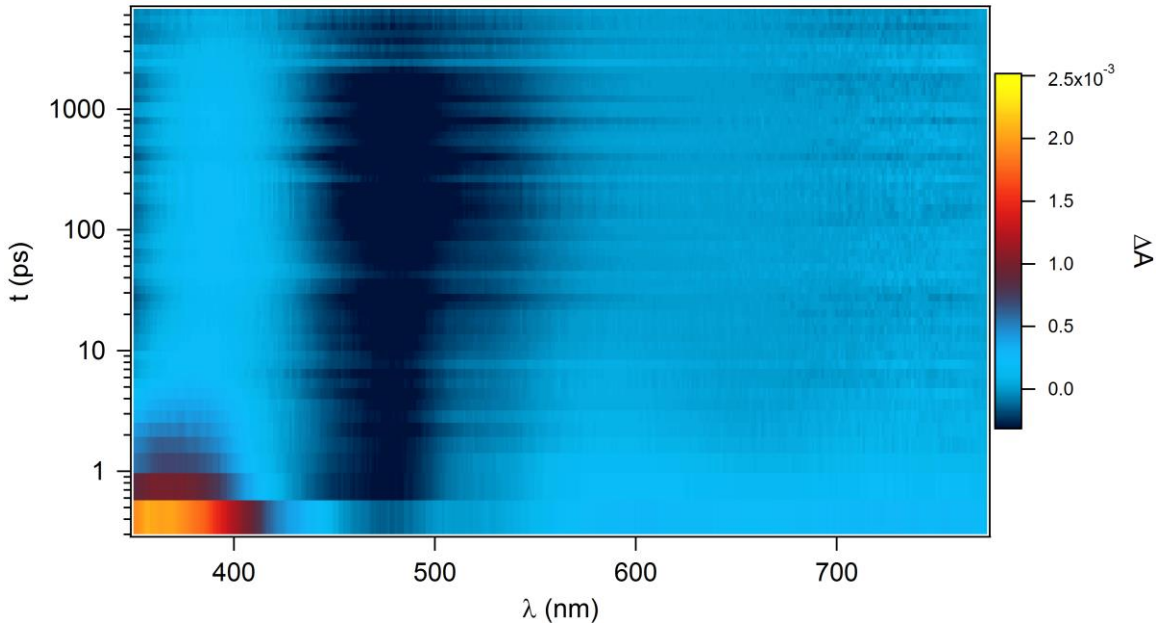

Fig. S58. Contour plot for transient absorption spectra of Ni(dtbbpy)(*o*-tolyl)Br (**1–Br**) after photoexcitation at 295 nm (pump power = 20 µW, first 50 scans, CaF_2 probe, 1mm quartz cuvette).

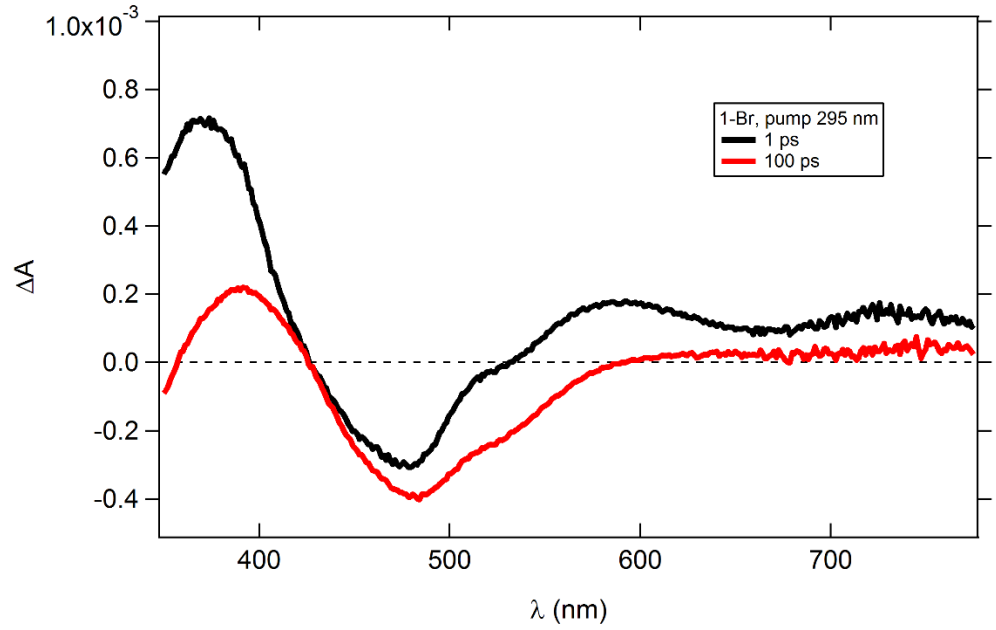

Fig. S59. Transient absorption spectra of Ni(dtbbpy)(*o*-tolyl)Br (**1–Br**) after photoexcitation at 295 nm at select probe delays (pump power = 20 µW, first 50 scans, CaF_2 probe, 1mm quartz cuvette).

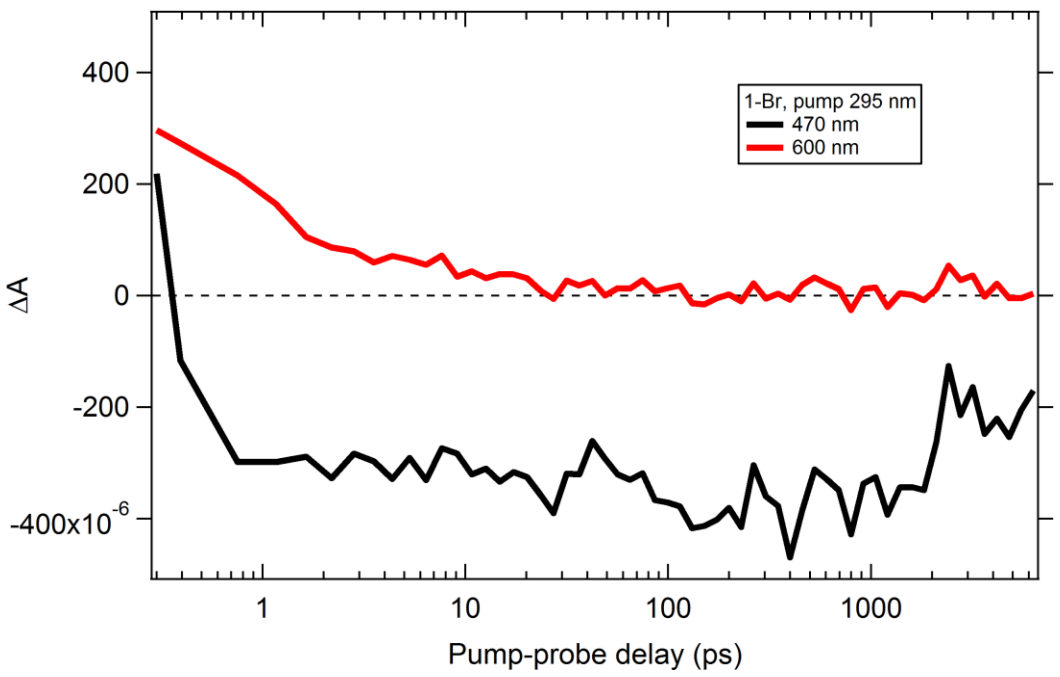

Fig. S60. Single wavelength kinetics for transient absorption spectra of Ni(dtbbpy)(*o*-tolyl)Br (**1–Br**) after photoexcitation at 295 nm at select wavelengths (pump power = 20 μW, first 50 scans, CaF_2 probe, 1mm quartz cuvette).

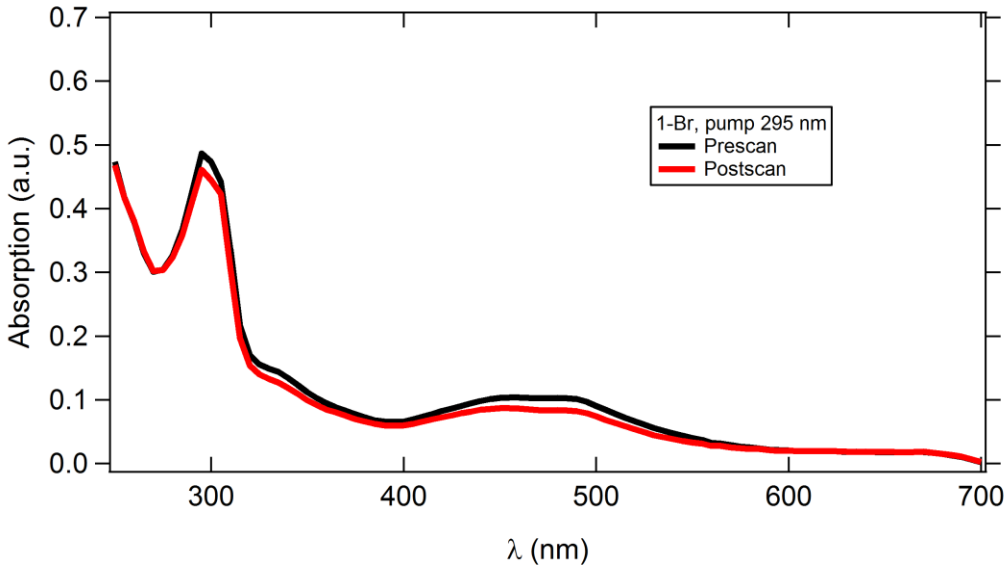

Fig. S61. Absorption spectra of Ni(dtbbpy)(*o*-tolyl)Br (**1–Br**) before and after transient absorption experiment (295 nm photoexcitation, pump power = 20 μW, 233 total scans, CaF_2 probe, 1mm quartz cuvette).

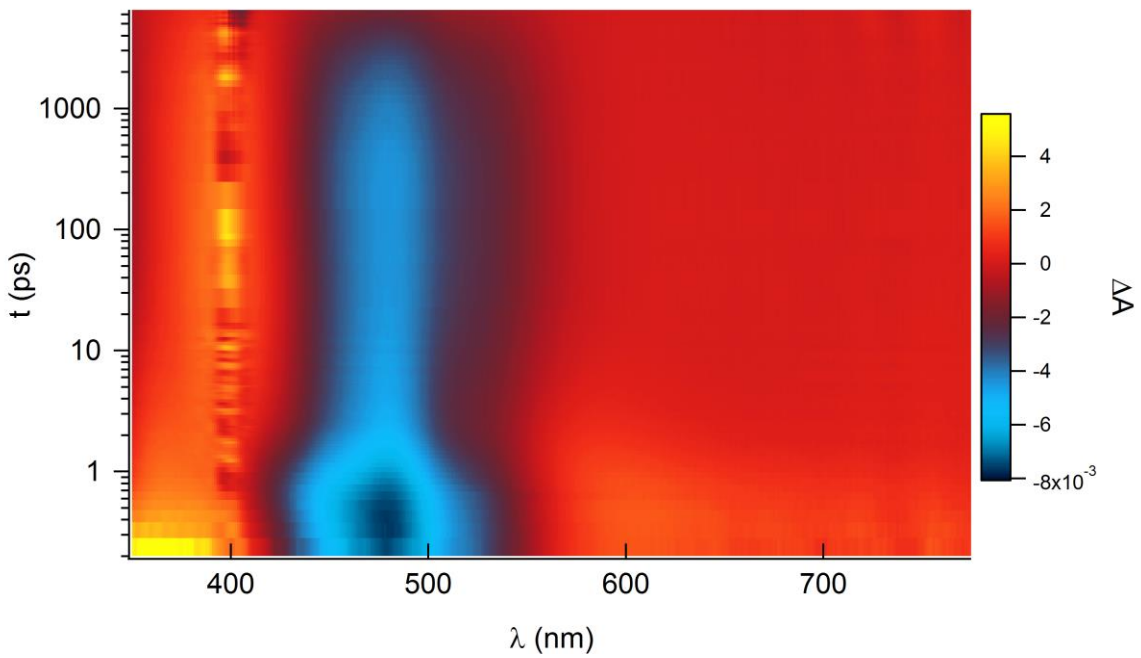

Fig. S62. Contour plot for transient absorption spectra of Ni(dtbbpy)(*o*-tolyl)Br (**1–Br**) after photoexcitation at 400 nm (pump power = 500 µW, first 50 scans, CaF_2 probe, 2mm optical glass cuvette).

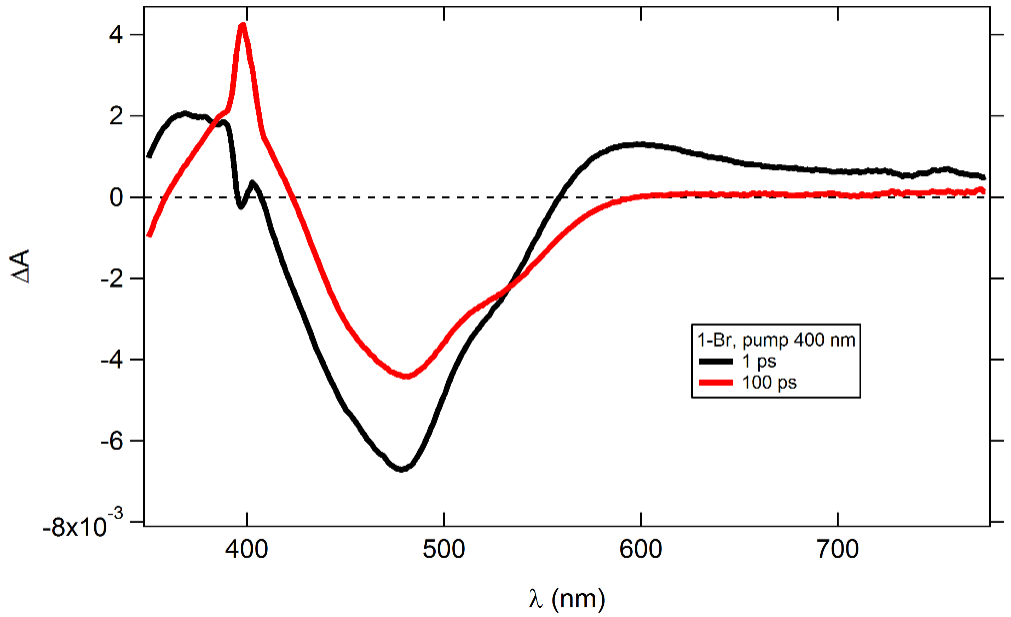

Fig. S63. Transient absorption spectra of Ni(dtbbpy)(*o*-tolyl)Br (**1–Br**) after photoexcitation at 400 nm at select probe delays (pump power = 500 µW, first 50 scans, CaF_2 probe, 2 mm optical glass cuvette).

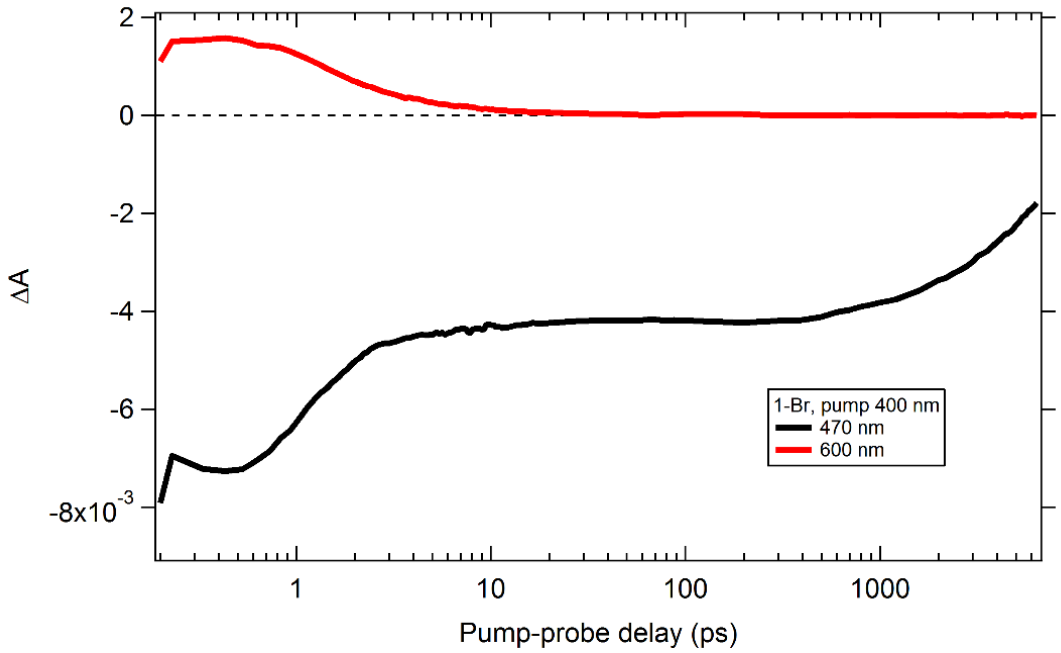

Fig. S64. Single wavelength kinetics for transient absorption spectra of Ni(dtbbpy)(*o*-tolyl)Br (**1–Br**) after photoexcitation at 400 nm at select wavelengths (pump power = 500 μW, first 50 scans, CaF_2 probe, 2mm optical glass cuvette).

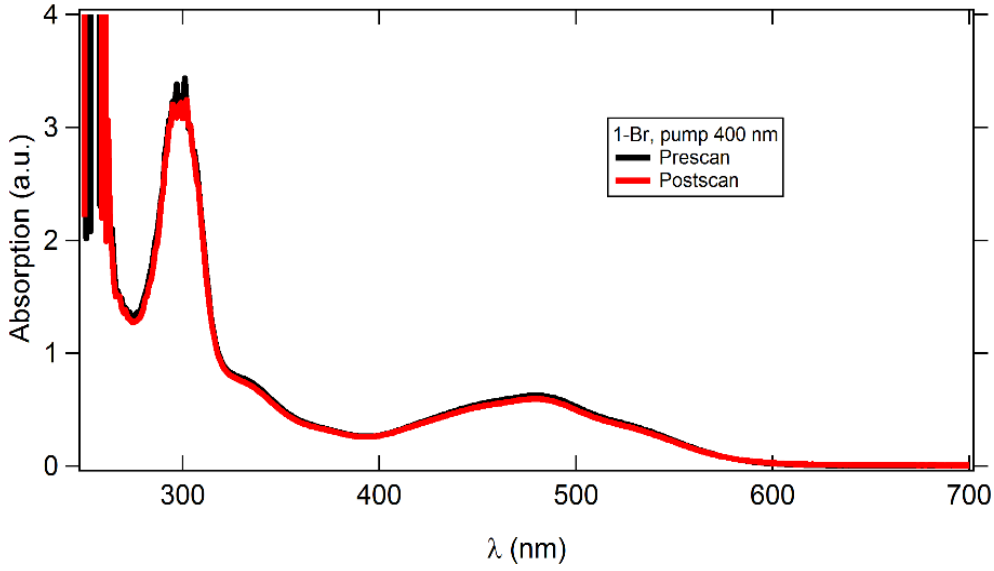

Fig. S65. Absorption spectra of Ni(dtbbpy)(*o*-tolyl)Br (**1–Br**) before and after transient absorption experiment (400 nm photoexcitation, pump power = 500 μW, 78 total scans, CaF_2 probe, 2mm optical glass cuvette).

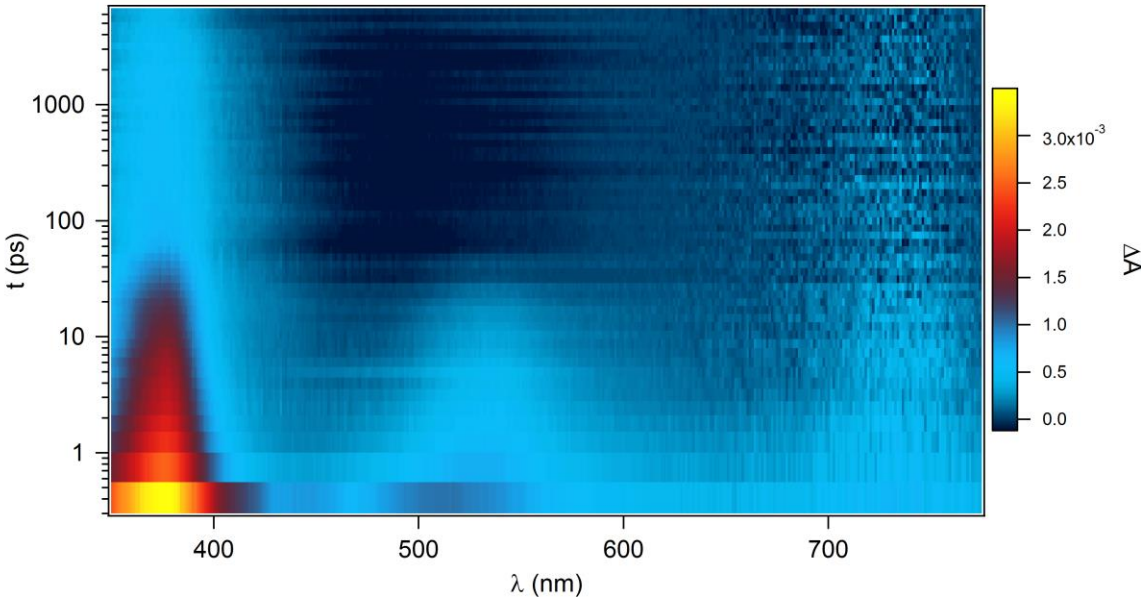

Fig. S66. Contour plot for transient absorption spectra of Ni(dtbbpy)(*o*-tolyl)I (**1–I**) after photoexcitation at 295 nm (pump power = 20 μW, first 50 scans, CaF_2 probe, 1mm quartz cuvette).

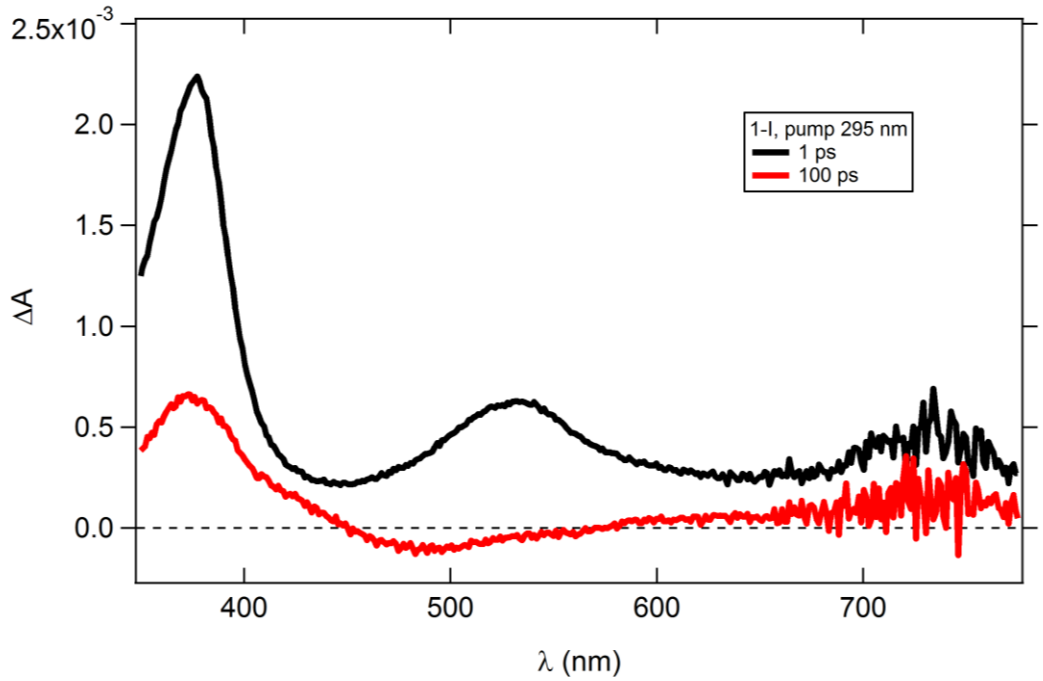

Fig. S67. Transient absorption spectra of Ni(dtbbpy)(*o*-tolyl)I (**1–I**) after photoexcitation at 295 nm at select probe delays (pump power = 20 μW, first 50 scans, CaF_2 probe, 1mm quartz cuvette).

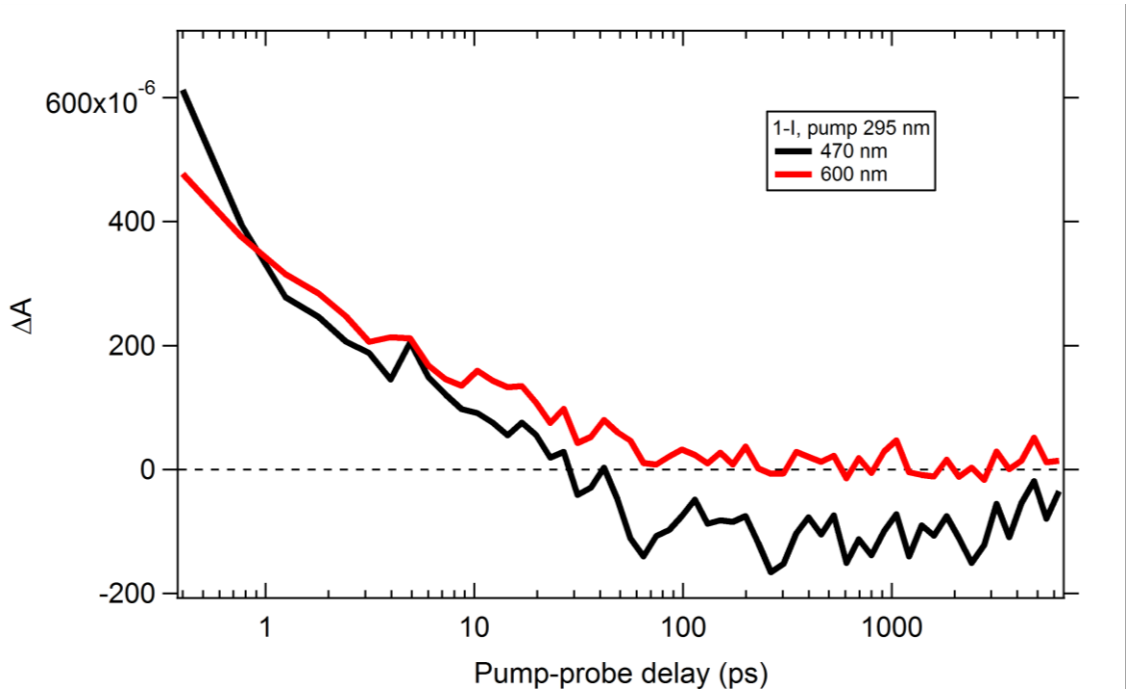

Fig. S68. Single wavelength kinetics for transient absorption spectra of Ni(dtbbpy)(*o*-tolyl)I (**1–I**) after photoexcitation at 295 nm at select wavelengths (pump power = 20 μW, first 50 scans, CaF_2 probe, 1mm quartz cuvette).

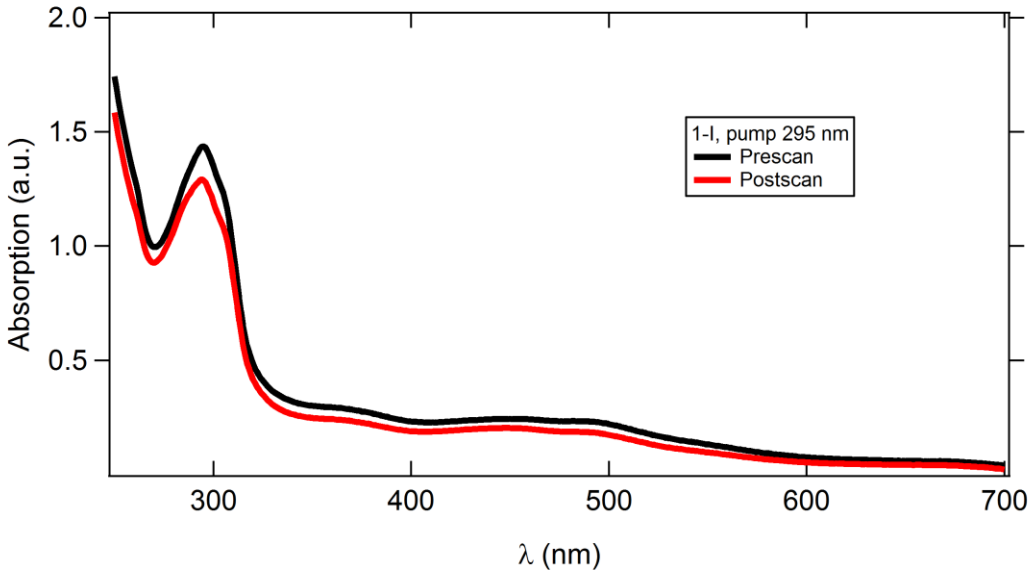

Fig. S69. Absorption spectra of Ni(dtbbpy)(*o*-tolyl)I (**1–I**) before and after transient absorption experiment (295 nm photoexcitation, pump power = 20 μW, 298 total scans, CaF_2 probe, 1mm quartz cuvette).

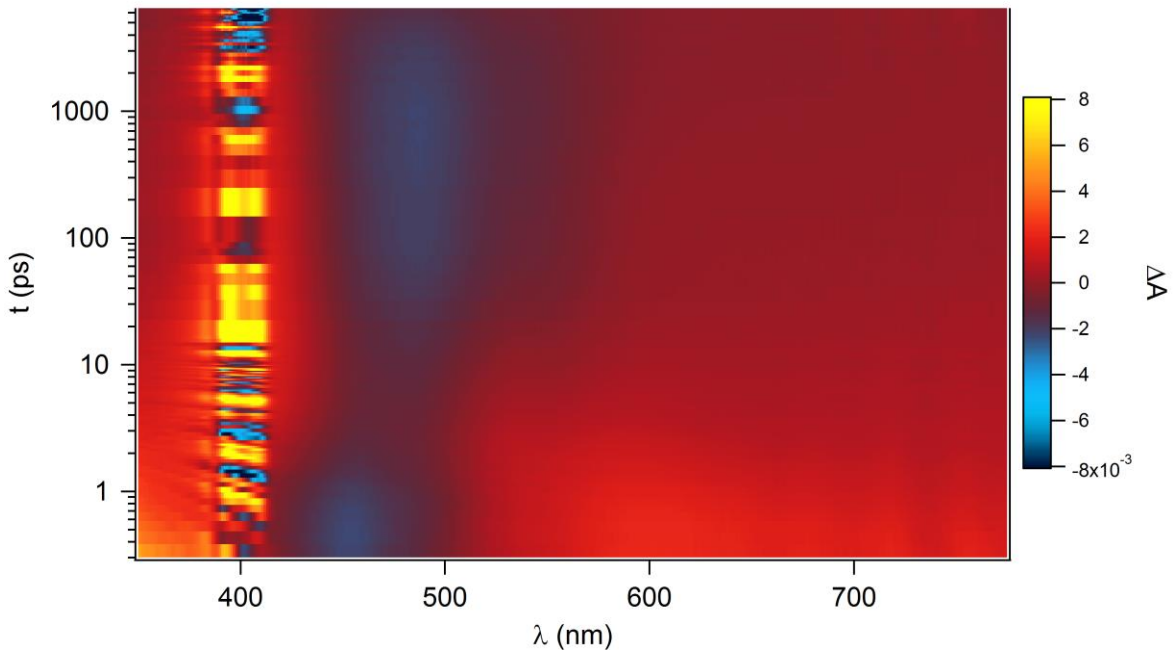

Fig. S70. Contour plot for transient absorption spectra of Ni(dtbbpy)(*o*-tolyl)I (**1–I**) after photoexcitation at 400 nm (pump power = 500 µW, first 50 scans, CaF_2 probe, 2mm optical glass cuvette).

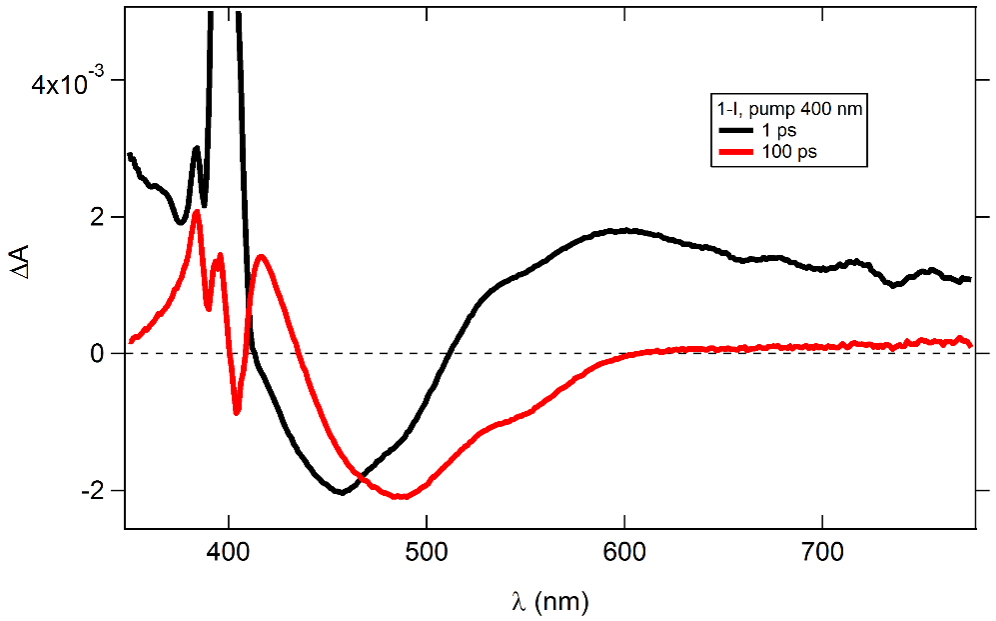

Fig. S71. Transient absorption spectra of Ni(dtbbpy)(*o*-tolyl)I (**1–I**) after photoexcitation at 400 nm at select probe delays (pump power = 500 µW, first 50 scans, CaF_2 probe, 2mm optical glass cuvette).

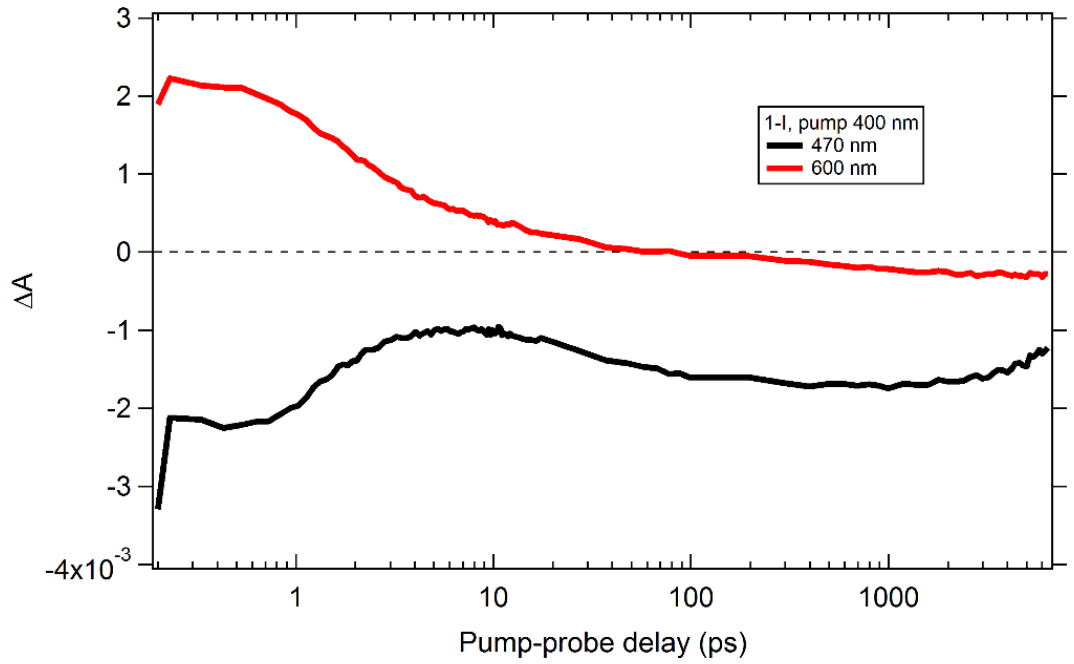

Fig. S72. Single wavelength kinetics for transient absorption spectra of Ni(dtbbpy)(*o*-tolyl)I (**1–I**) after photoexcitation at 400 nm at select wavelengths (pump power = 500 µW, first 50 scans, CaF_2 probe, 2mm optical glass cuvette).

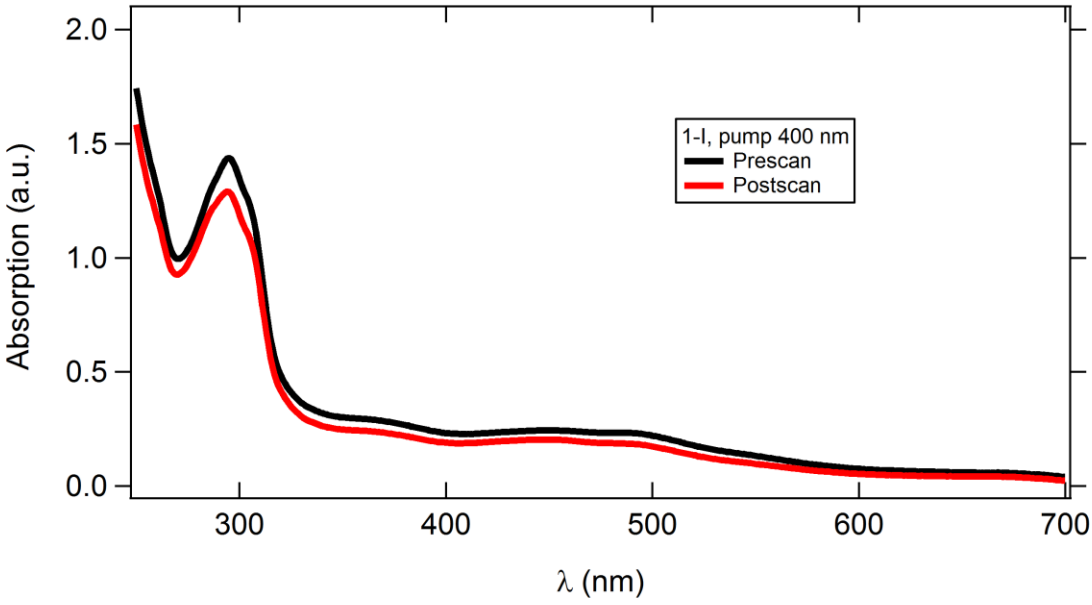

Fig. S73. Absorption spectra of Ni(dtbbpy)(*o*-tolyl)I (**1–I**) before and after transient absorption experiment (400 nm photoexcitation, pump power = 500 µW, 280 total scans, CaF_2 probe, 2mm optical glass cuvette).

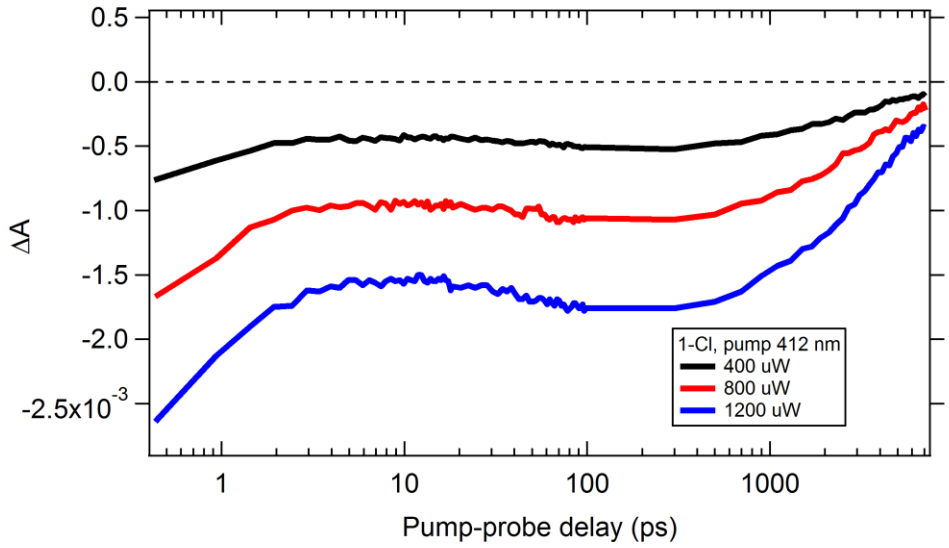

Fig. S74. Power dependence for Ni(dtbbpy)(*o*-tolyl)Cl (**1–Cl**). Single wavelength kinetics (460 nm) for transient absorption spectra of **1–Cl** after photoexcitation at 412 nm at select pump powers.

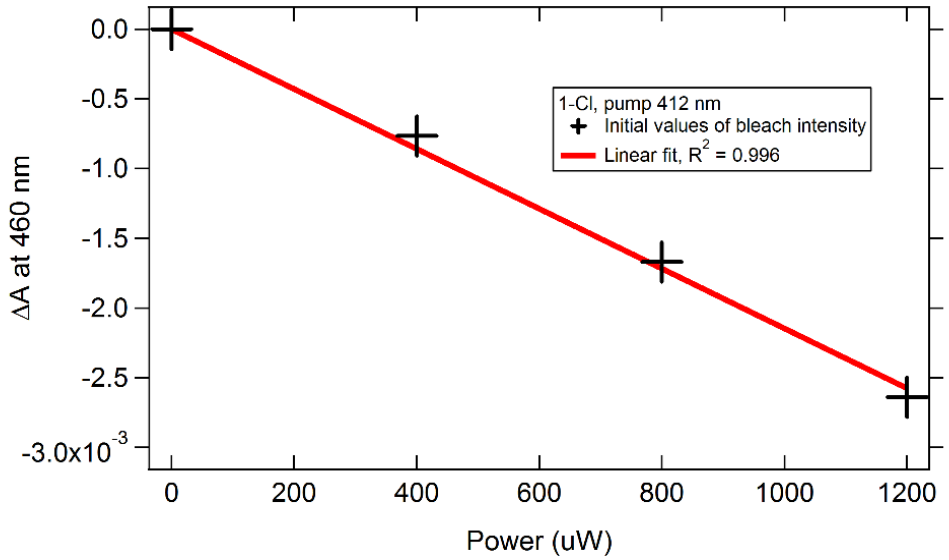

Fig. S75. Power dependence for Ni(dtbbpy)(*o*-tolyl)Cl (**1–Cl**). Initial values of bleach intensity (400 fs time delay) versus pump power plotted together with linear fit.

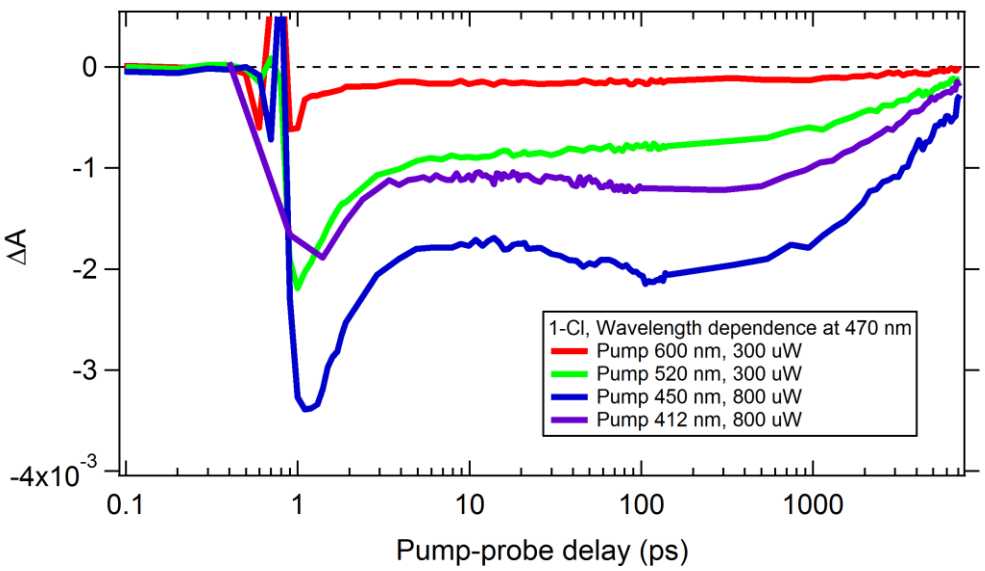

Fig. S76. Wavelength dependence for Ni(dtbbpy)(*o*-tolyl)Cl (**1–Cl**). Single wavelength kinetics (470 nm) for transient absorption spectra of **1–Cl** after photoexcitation at various wavelengths.

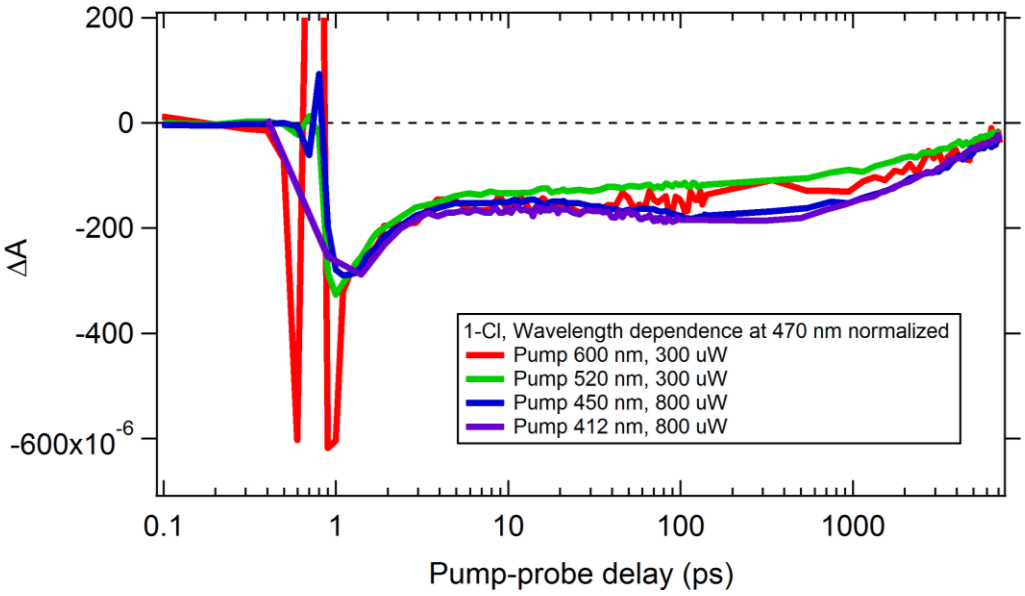

Fig. S77. Wavelength dependence for Ni(dtbbpy)(*o*-tolyl)Cl (**1–Cl**). Normalized single wavelength kinetics (470 nm) for transient absorption spectra of **1–Cl** after photoexcitation at various wavelengths.

VI. Global Analysis

Methods. Global analysis was employed for kinetic modeling of transient absorption data to evaluate the proposed models and extract kinetic parameters. Global analysis was carried out using two software packages in this study: (1) the R-package *TIMP*[40] and graphical user interface *Glotaran*[41] and (2) a *Mathematica* package developed in house. The *Mathematica* package will be published open source upon completion; please don't hesitate to contact us regarding the preliminary code should you be interested in carrying out a similar analysis before that time. Note that this package is based on the same principles as other popular software such as *TIMP*, but carries out kinetic modeling using numerical solutions to systems ordinary differential equations (ODEs) and numerical minimization of fit residuals rather than using separable systems of linear ODEs with time dependent concentration solutions assumed to be the weighted sum of exponential decay functions (first order kinetics). The numerical minimization approach allows one to avoid the unimolecular assumptions of other methods. In this study the software was employed only to evaluate fitting error via bootstrap error analysis simulations and was critical to assessing the statistical significance of concentration dependent dynamics experiments. For the analysis of the full time course of transient absorption spectra global analysis was carried out using sequential models with unimolecular steps employing two, three, and four components.

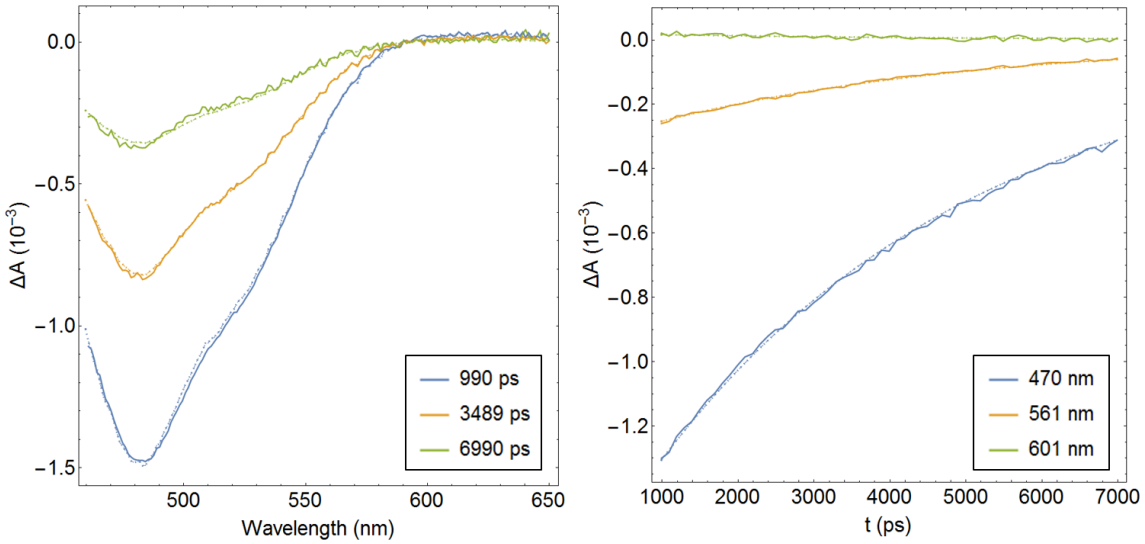

Fig. S78. Comparison of global analysis of late time dynamics using *Glotaran* and *Mathematica* packages (solid line = data, dashed line = *Glotaran*, dotted line = *Mathematica*). Select time slices (left) and single wavelength kinetics (right) for example data. Fit rate constants: $k_{\text{Glotaran}} = 2.3892\times10^{-4}$ ps^{-1}, $k_{\text{Mathematica}} = 2.3885\times10^{-4}$ ps^{-1}.

The following section outlines the general algorithm for bootstrap error analysis used in concentration dependent kinetic experiments.

1. Global analysis of the experimental data is carried out and the residuals between fit and experimental data are calculated according to

$$Y = CA + R$$

where Y is the experimental data matrix, $X = CA$ is the fit data matrix (C is the time dependent concentration profile matrix and A is the pure component spectra matrix) and $R = \{R_1, R_2, \dots, R_t\}$ is the residuals matrix (R_t is a time vector residual, i.e. the residual spectrum at each time delay). Note that the software works by simply minimizing R with respect to the rate constants for specified steps in a mechanism, where the system of equations describing the mechanism is solved numerically on each iteration of the minimization.

2. A bootstrapped residual matrix $\widehat{R^*} = \{\widehat{R_1^*}, \widehat{R_2^*}, \dots, \widehat{R_t^*}\}$, for fixed regressor bootstrap analysis, is generated by randomly sampling the time vector residuals (R_t) with replacement.

3. Next, the bootstrapped residual matrix ($\widehat{R^*}$) is added to the fit data matrix (X)

$$\hat{Y} = X + \widehat{R^*}$$

and the resulting bootstrapped data set ($\hat{Y}$) is fit using global analysis to give a set of bootstrapped rate constants. This process is repeated N times, each time generating a new bootstrapped residual matrix and tabulating the resulting rate constants. In the limit, the rate constant distribution calculated in this way gives the probability of a given rate constant. Accordingly, one can empirically check for convergence of the bootstrap algorithm by plotting bootstrap standard error as a function of the number of iterations. For this work, N = 500 was found to be sufficient (figure S79).

4. Finally, the resulting set of bootstrapped rate constants can be treated as analogous to the true probability distribution for statistical inference. The bootstrap standard error can be calculated via the standard deviation of the set of bootstrapped rate constants. The standard error can then be Studentized to give confidence intervals for kinetic parameters.

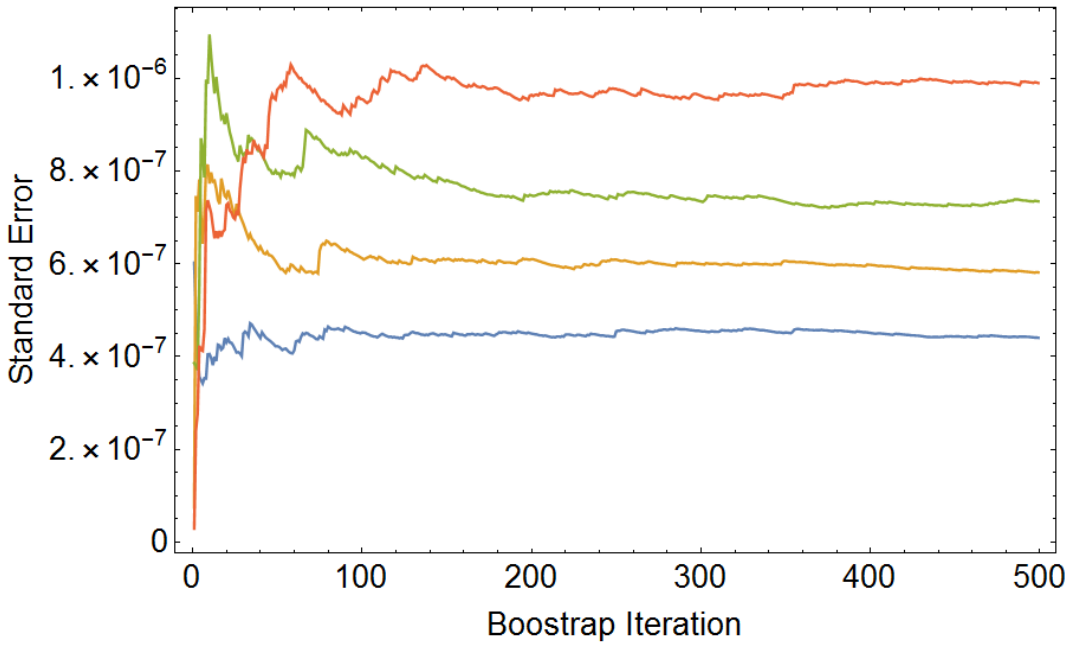

Fig. S79. Convergence of bootstrap standard error. The above data was generated via global analysis of the long time constant (fit after 1 ns delay) from concentration dependence experiments. Standard error: blue ([Ni] = 0.63 mM, 237 scans), yellow ([Ni] = 1.31 mM, 113 scans), green ([Ni] = 1.98 mM, 189 scans), red ([Ni] = 2.66 mM, 587 scans).

Global Analysis Summary. Computational studies suggest that photoexcitation of complexes **1–Cl**, **–Br**, **–I** with 295 nm and 400 nm laser pulses initially generate $^1\pi$–π^* and ^{1}MLCT upper excited states respectively. Therefore, it was assumed that the transient absorption spectra from these experiments evolved from $^1\pi$–π^*_N and $^1MLCT_N$ states. For data collected with 295 nm photoexcitation the initial transient signal, which we ascribe to $^1\pi$–π^*_N upper excited states, is coevolved with the instrument response but clearly present in the first picosecond. For data collected with 400 nm photoexcitation, cooling of the initial transient signal, which we assign to $^1MLCT_N$ upper excited states, is resolved as shown in figure 4B of the manuscript. However, for these data the presence of scattering at 400 nm complicates global analysis. Accordingly, during our modeling studies the spectra were truncated to 420 nm and as a result the initial decay is not captured in global analysis.

In transient spectra for **1–Cl**, **–Br**, **–I** there is an observable bleach broadening which accompanies cooling of the blue ESA feature (figure 4D). We ascribe this feature to formation of an excimer on the basis of concentration dependence and modeling studies. Given that this step is not unimolecular, global analysis can be viewed as a fitting tool for deconvoluting excimer formation. The "rate constants" reported for this step, should not be taken as the true rate of bimolecular excimer formation. In this section simple models without concentration dependent excimer formation or electron transfer reactions (Section IX) were chosen to capture the overall unimolecular excited state dynamics of the complexes.

With these considerations in mind we have selected sequential models that best fit each set of experimental data, though the fitting results for two, three, and four component models are tabulated for completeness. For 295 nm photoexcitation the complexes a four-component model (scheme 1) in which the first, second, and fourth components represent unimolecular decays while the third component captures the bleach broadening associated with excimer formation were expected to best fit the data.

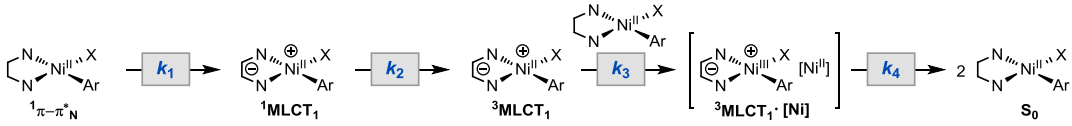

(1)

However, a simpler three-component model, without excimer formation, was ultimately employed (scheme 2).

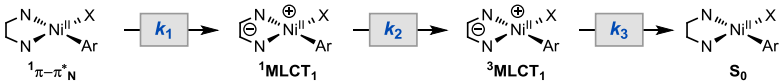

(2)

In this case, the temporal resolution and data quality of the experiment was not sufficient to capture bleach broadening with global analysis. For 400 nm photoexcitation of **1–Cl**, **–Br**, and **–I** a three-component model (scheme 3)

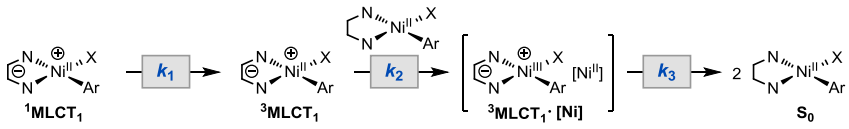

(3)

represented that data well. For this model, the second component captures excimer formation. Some additional evidence for this assignment can be seen in the contour plot (figure S115) and single wavelength kinetics (figure S117) of the transient absorption

spectra of **1–I** after 400 nm photoexcitation. The amplitude of the negative signal doubles on the tens to hundreds of picoseconds timescale.

Table S10 and S11 summarize the final global analysis results. For each complex the late time dynamics are similar, with lifetimes on the order of 10 ns. Table S12, S13, and S14 summarize the two-, three-, and four-component fitting results. The errors reported here are those calculated by *Glotaran*. The bootstrap approach presented above was developed for concentration dependence experiments because it is not clear how these errors were calculated. For each fit the following section contains contour plot for the data used in global analysis, evolution associated spectra, concentration profiles for each component and a comparison of experimental and fit difference absorption and single wavelength kinetics.

Proposed deexcitation kinetics. Comments on figure 4A. We did not include ligand-field states in the Jablonski diagram based on the following considerations: (i) the allowed transitions of largest oscillator strength in the visible (Table S1, ES18) and UV (Table S2, ES61) were assigned as MLCT and π–π* respectively based on changes in atomic charge (Table S9), difference density isosurfaces (Figure S28), and orbital contributions (Table S29). (ii) The lowest energy excited state, identified by comparing the spectrum for the long-lived component in pump-probe with the computed difference absorption spectrum for T_1, was assigned to $^3MLCT_1$ by DFT, TD-DFT, and NPA analysis. In addition, the optimized T_1 electronic structure has unpaired spin density localized in a dtbbpy π* Kohn-Sham orbital (Fig. S15, orbital α121) and a Ni/aryl/Cl centered Kohn-Sham orbital (Fig. S15, orbital α120) consistent with this assignment. (iii) Excluding exciplex formation, analysis of pump-probe data for visible excitation suggested a three-component sequential model, giving one unassigned observable state. The required initial excitation to a singlet state (singlet ground state) and $^3MLCT_1$ terminal assignment suggest this intermediate state could be a singlet which *we assigned to be S_1 under the assumption that ISC occurs from the lowest excited singlet state*. Computations predict that S_1 (Table S1, ES7) has significant positive charge buildup on Ni (Table S9) and is well described as a HOMO-LUMO transition and thus $^1MLCT_1$. Many states do have some computed 3d contributions and states with larger 3d character are likely along the path to deexcitation *before $^3MLCT_1$*, given the computed density of states. For example, S_2 (Table S1, ES8) has significant ligand field character based on transition orbital contributions (Table S29). Additionally, in the case of hot ISC mentioned in the text, the intermediate species could be an upper triplet state with some LF character. However, based on the above considerations the excited states observed spectroscopically are best described according to Figure 4A. Accordingly, we believe that *ligand-field states are not involved in the deactivation of $^3MLCT_1$ Ni*, rather deexcitation to the ground state likely involves other nonradiative processes such as spin interconversion.

Table S10. Summary of global analysis results for complexes **1–Cl**, **–Br**, **–I** (295 nm photoexcitation) with selected three-component model. The rate and time constants correspond to the models presented on the previous page.

Complex	Pump	Model	k_1 (ps^{-1})	τ_1 (ps)	k_2 (ps^{-1})	τ_2 (ps)	k_3 (ps^{-1})	τ_3 (ns)
1-Cl	295 nm	2	2.7	0.37	9.6×10^{-2}	10.4	1.4×10^{-4}	7.1
1-Br	295 nm	2	2.8	0.36	0.43	2.3	1.1×10^{-4}	9.0
1-I	295 nm	2	4.3	0.23	5.2×10^{-2}	19.2	7.7×10^{-5}	13.1

Table S11. Summary of global analysis results for complexes **1–Cl**, **–Br**, **–I** (400 nm photoexcitation) with selected three-component model. The rate and time constants correspond to the models presented on the previous page.

Complex	Pump	Model	k_1 (ps^{-1})	τ_1 (ps)	k_2 (ps^{-1})	τ_2 (ps)	k_3 (ps^{-1})	τ_3 (ns)
1-Cl	400 nm	3	0.95	1.05	0.15	6.6	2.4×10^{-4}	4.1
1-Br	400 nm	3	0.75	1.34	0.17	6.0	1.3×10^{-4}	7.8
1-I	400 nm	3	0.49	2.04	3.1×10^{-2}	32.2	4.8×10^{-5}	20.8

Table S12. Summary of global analysis results for fitting with a two-component sequential model.

Complex	Pump	Two Component Model			
		k_1 (ps^{-1})	Error	k_2 (ps^{-1})	Error
1-Cl	295 nm	2.3	7.2×10^{-3}	5.5×10^{-4}	1.2×10^{-5}
1-Cl	400 nm	0.86	4.1×10^{-3}	2.3×10^{-4}	7.2×10^{-7}
1-Br	295 nm	2.6	9.3×10^{-3}	1.3×10^{-4}	4.5×10^{-6}
1-Br	400 nm	0.72	3.4×10^{-3}	1.1×10^{-4}	4.1×10^{-7}
1-I	295 nm	3.2	2.0×10^{-2}	1.6×10^{-3}	2.9×10^{-5}
1-I	400 nm	0.11	7.1×10^{-4}	5.5×10^{-6}	1.2×10^{-6}

Table S13. Summary of global analysis results for fitting with a three-component sequential model.

Complex	Pump	Three Component Model					
		k_1 (ps^{-1})	Error	k_2 (ps^{-1})	Error	k_3 (ps^{-1})	Error
1-Cl	295 nm	2.7	5.9×10^{-4}	9.6×10^{-2}	9.1×10^{-4}	1.4×10^{-4}	3.3×10^{-6}
1-Cl	400 nm	0.95	3.0×10^{-3}	0.15	9.3×10^{-4}	2.4×10^{-4}	3.6×10^{-7}
1-Br	295 nm	2.8	1.5×10^{-2}	0.43	8.5×10^{-3}	1.1×10^{-4}	4.4×10^{-6}
1-Br	400 nm	0.75	3.3×10^{-3}	0.17	1.3×10^{-3}	1.3×10^{-4}	2.4×10^{-7}
1-I	295 nm	4.3	1.4×10^{-2}	5.2×10^{-2}	3.4×10^{-4}	7.7×10^{-5}	1.9×10^{-6}
1-I	400 nm	0.49	2.0×10^{-3}	3.1×10^{-2}	2.0×10^{-4}	4.8×10^{-5}	4.3×10^{-7}

Table S14. Summary of global analysis results for fitting with a four-component sequential model.

Complex	Pump	Four Component Model							
		k_1 (ps^{-1})	Error	k_2 (ps^{-1})	Error	k_3 (ps^{-1})	Error	k_4 (ps^{-1})	Error
1-Cl	295 nm	2.7	5.9×10^{-3}	8.4×10^{-4}	2.6×10^{-5}	9.4×10^{-2}	1.2×10^{-3}	8.0×10^{-5}	7.1×10^{-6}
1-Cl	400 nm	0.82	3.2×10^{-2}	0.8	3.7×10^{-3}	7.2×10^{-2}	1.2×10^{-3}	2.4×10^{-4}	3.3×10^{-7}
1-Br	295 nm	2.1	0.65	2.1	0.64	1.3×10^{-2}	4.5×10^{-4}	1.6×10^{-4}	5.1×10^{-6}
1-Br	400 nm	0.64	2.5×10^{-2}	0.65	2.8×10^{-2}	2.6×10^{-2}	5.5×10^{-4}	1.3×10^{-4}	2.4×10^{-7}
1-I	295 nm	5.8	4.6×10^{-2}	1.3	2.0×10^{-2}	3.9×10^{-2}	2.9×10^{-4}	6.8×10^{-5}	1.5×10^{-6}
1-I	400 nm	0.53	1.6×10^{-3}	6.8×10^{-2}	3.0×10^{-4}	1.4×10^{-3}	1.6×10^{-5}	7.7×10^{-5}	5.1×10^{-7}

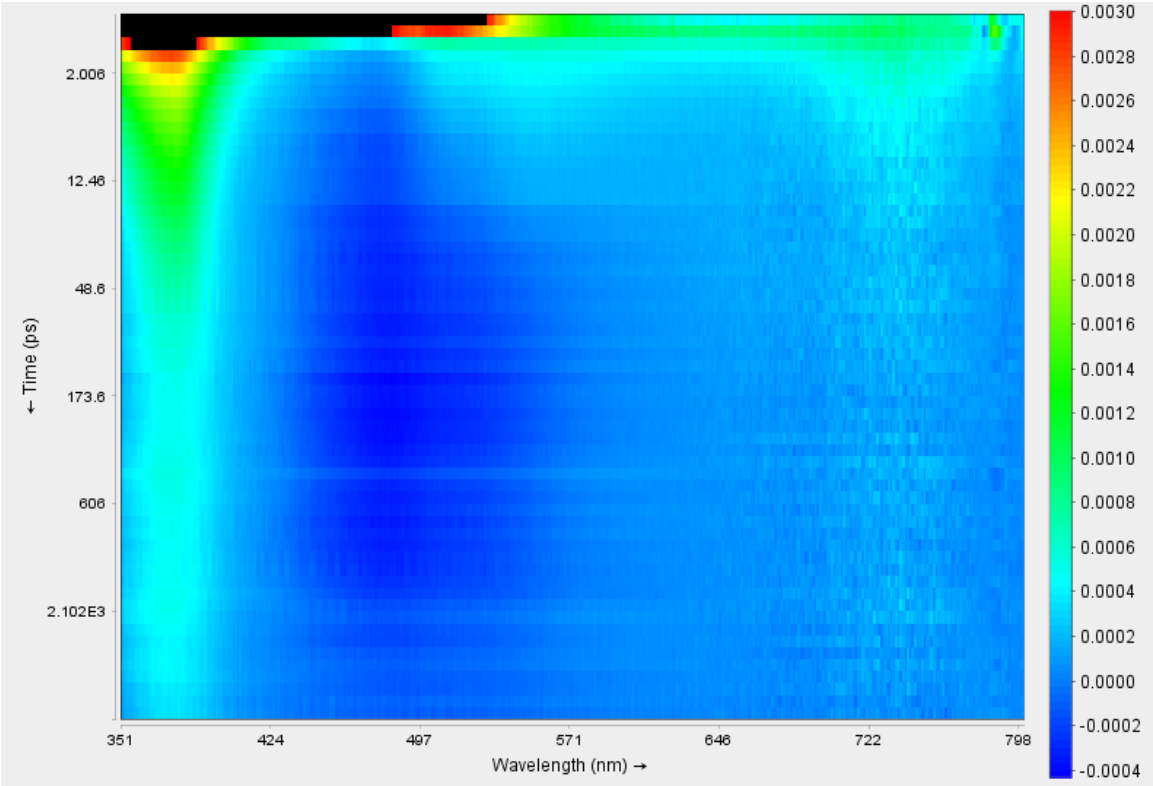

Fig. S80. Contour plot for portion of Ni(dtbbpy)(*o*-tolyl)Cl (**1–Cl**) transient absorption data used for global analysis (295 nm photoexcitation).

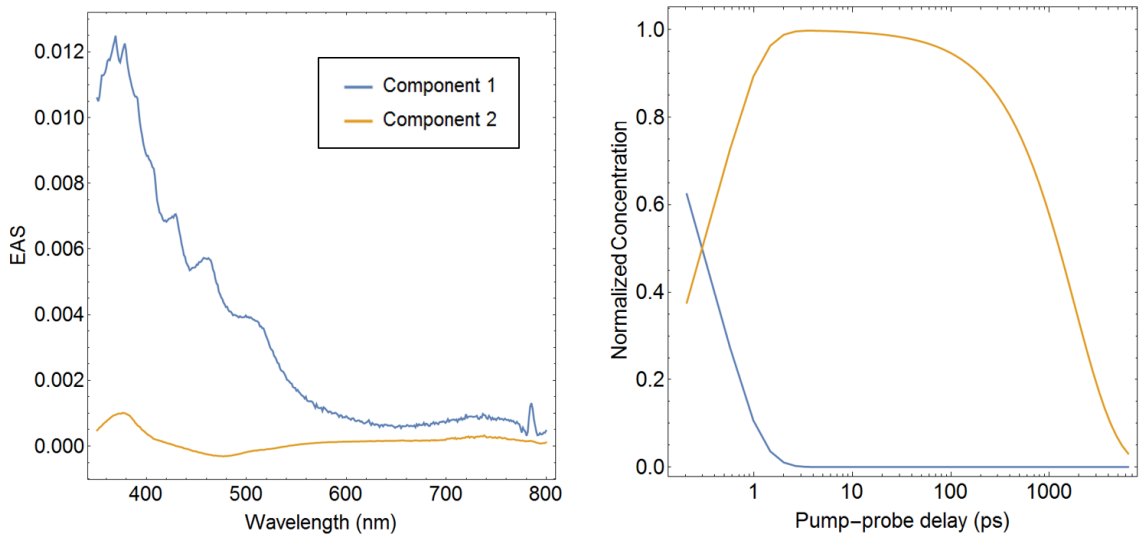

Fig. S81. Summary of **2** component global analysis of Ni(dtbbpy)(*o*-tolyl)Cl (**1–Cl**) transient absorption data (295 nm photoexcitation). Evolution associated spectra (left) and concentration profiles (right).

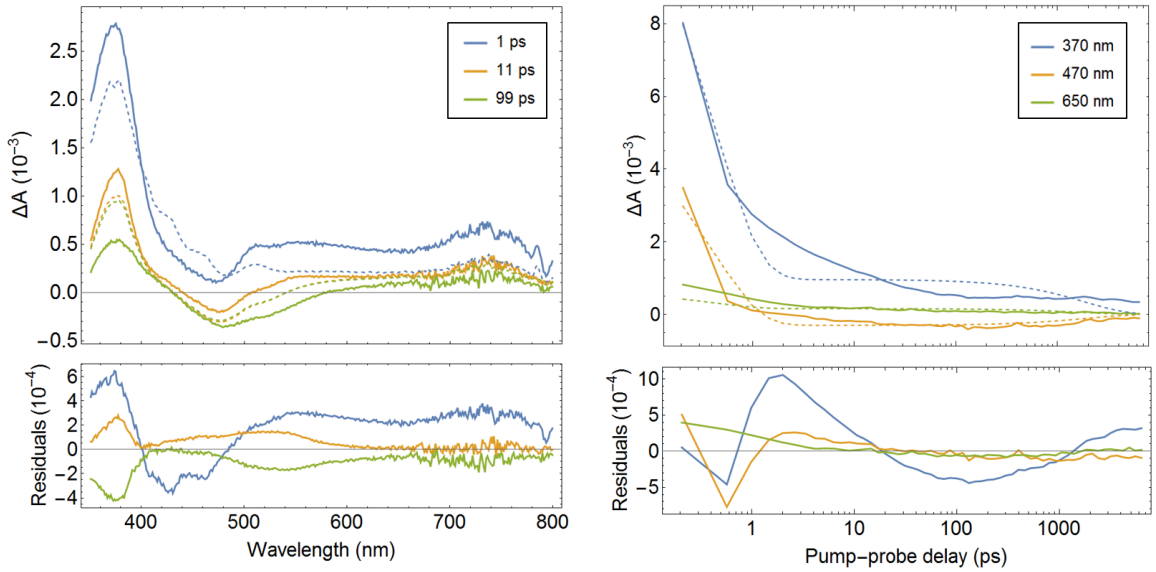

Fig. S82. Summary of **2** component global analysis of Ni(dtbbpy)(*o*-tolyl)Cl (**1–Cl**) transient absorption data (295 nm photoexcitation). Comparison of experimental (solid) and fit (dashed) difference absorption spectra at select pump-probe delays (left) and single wavelength kinetics (right).

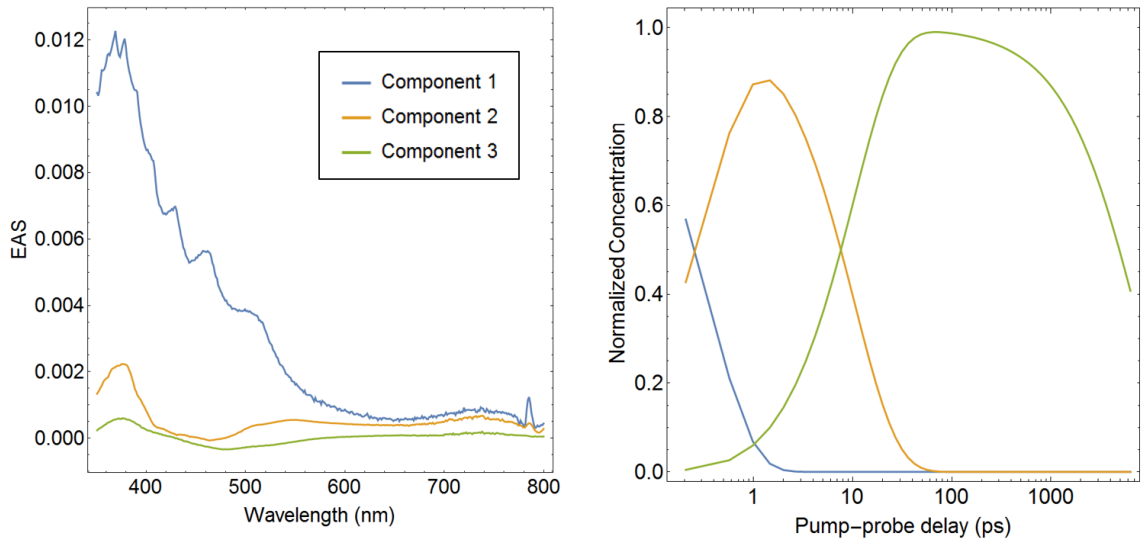

Fig. S83. Summary of **3** component global analysis of Ni(dtbbpy)(*o*-tolyl)Cl (**1–Cl**) transient absorption data (295 nm photoexcitation). Evolution associated spectra (left) and concentration profiles (right).

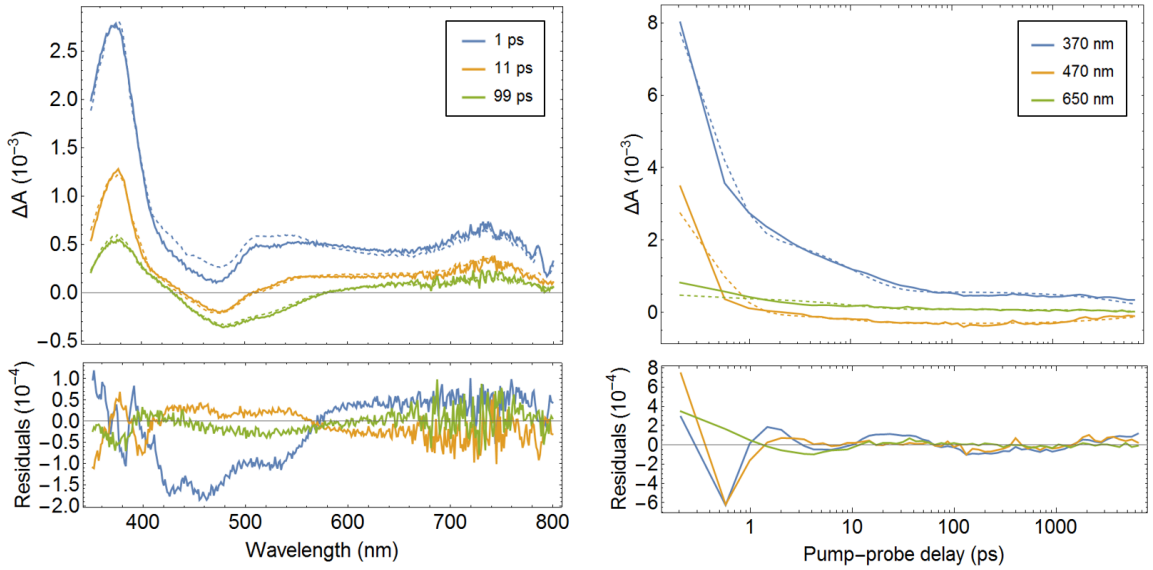

Fig. S84. Summary of **3** component global analysis of Ni(dtbbpy)(*o*-tolyl)Cl (**1–Cl**) transient absorption data (295 nm photoexcitation). Comparison of experimental (solid) and fit (dashed) difference absorption spectra at select pump-probe delays (left) and single wavelength kinetics (right).

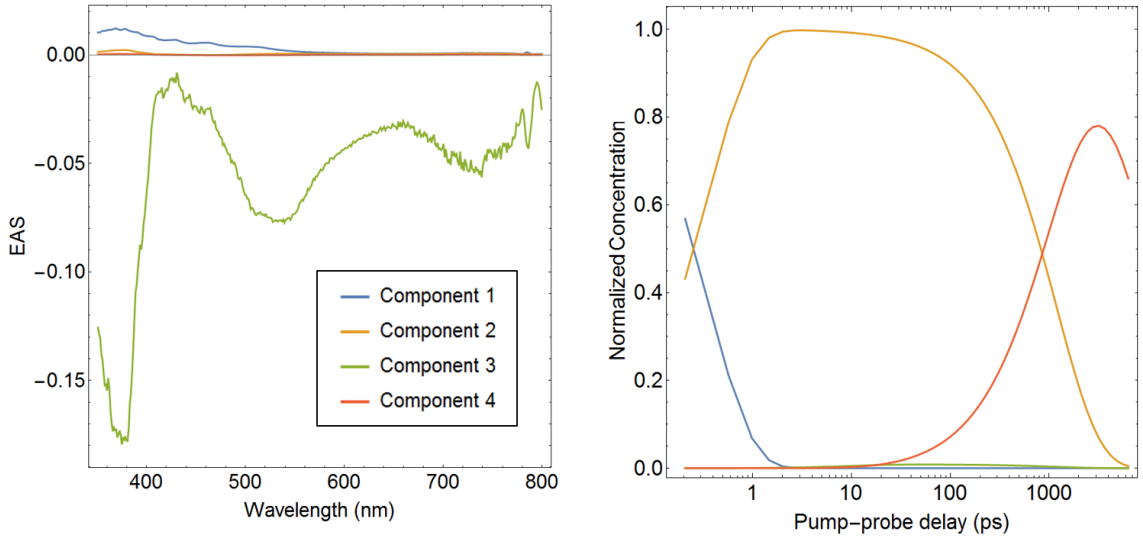

Fig. S85. Summary of **4** component global analysis of Ni(dtbbpy)(*o*-tolyl)Cl (**1–Cl**) transient absorption data (295 nm photoexcitation). Evolution associated spectra (left) and concentration profiles (right).

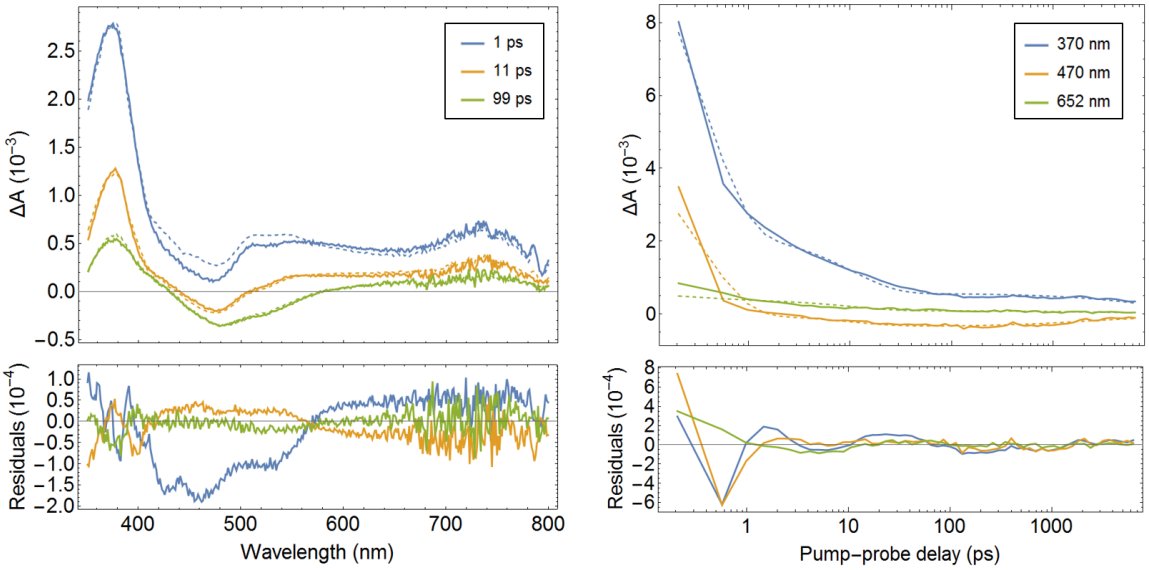

Fig. S86. Summary of **4** component global analysis of Ni(dtbbpy)(*o*-tolyl)Cl (**1–Cl**) transient absorption data (295 nm photoexcitation). Comparison of experimental (solid) and fit (dashed) difference absorption spectra at select pump-probe delays (left) and single wavelength kinetics (right).

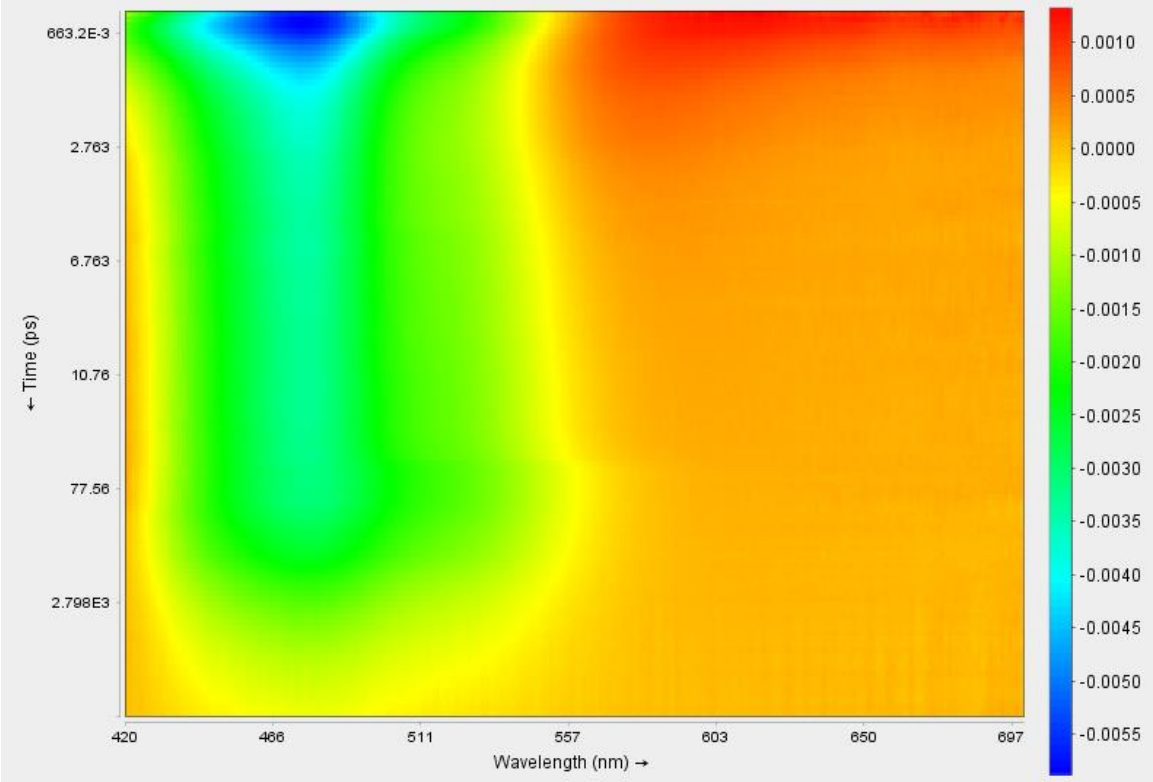

Fig. S87. Contour plot for portion of Ni(dtbbpy)(*o*-tolyl)Cl (**1–Cl**) transient absorption data used for global analysis (400 nm photoexcitation).

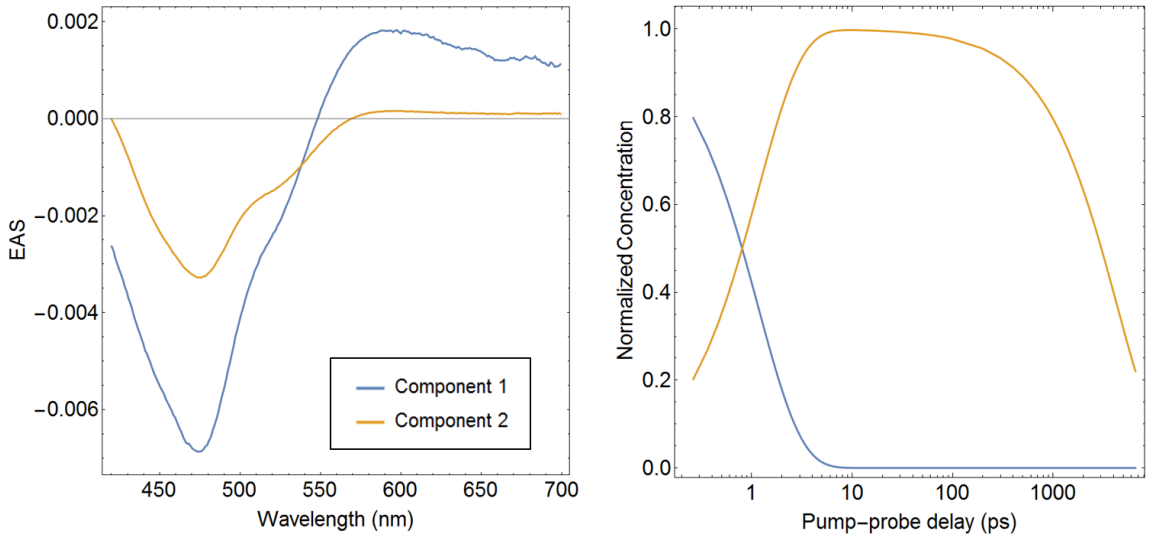

Fig. S88. Summary of **2** component global analysis of Ni(dtbbpy)(*o*-tolyl)Cl (**1–Cl**) transient absorption data (400 nm photoexcitation). Evolution associated spectra (left) and concentration profiles (right).

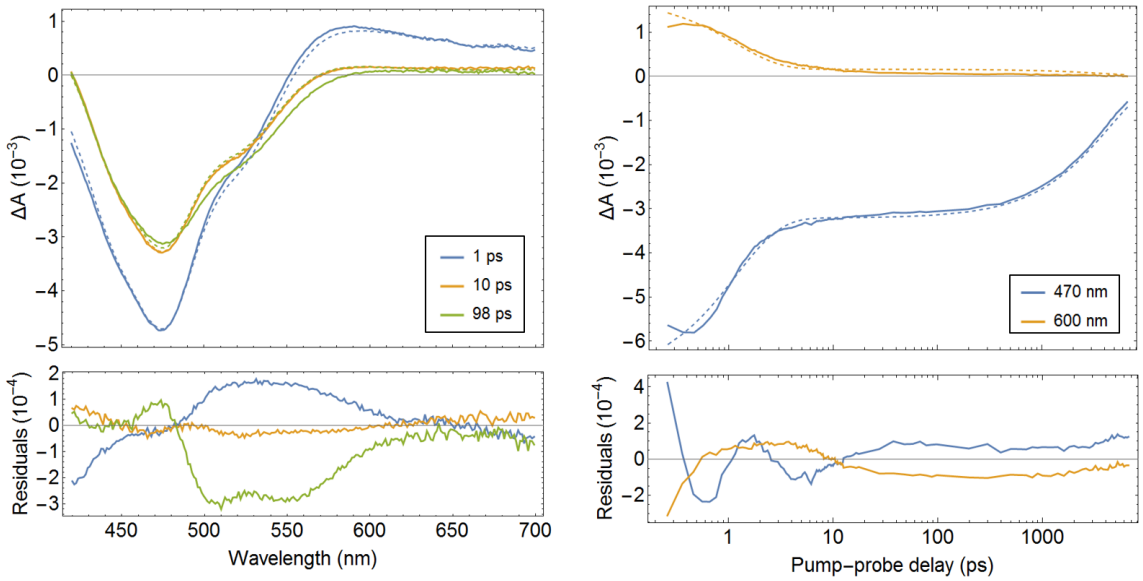

Fig. S89. Summary of **2** component global analysis of Ni(dtbbpy)(*o*-tolyl)Cl (**1–Cl**) transient absorption data (400 nm photoexcitation). Comparison of experimental (solid) and fit (dashed) difference absorption spectra at select pump-probe delays (left) and single wavelength kinetics (right).

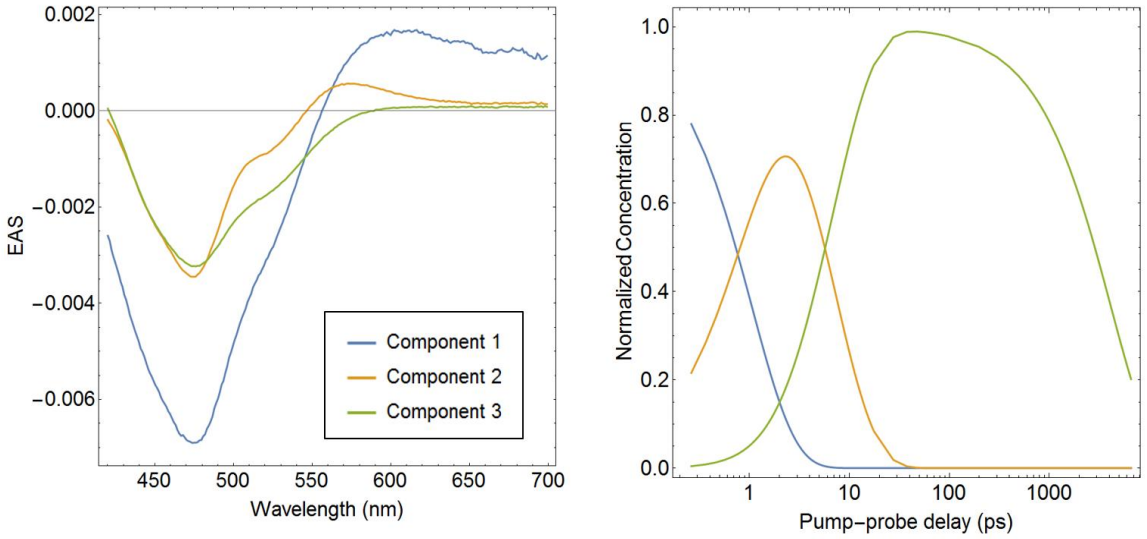

Fig. S90. Summary of **3** component global analysis of Ni(dtbbpy)(*o*-tolyl)Cl (**1–Cl**) transient absorption data (400 nm photoexcitation). Evolution associated spectra (left) and concentration profiles (right).

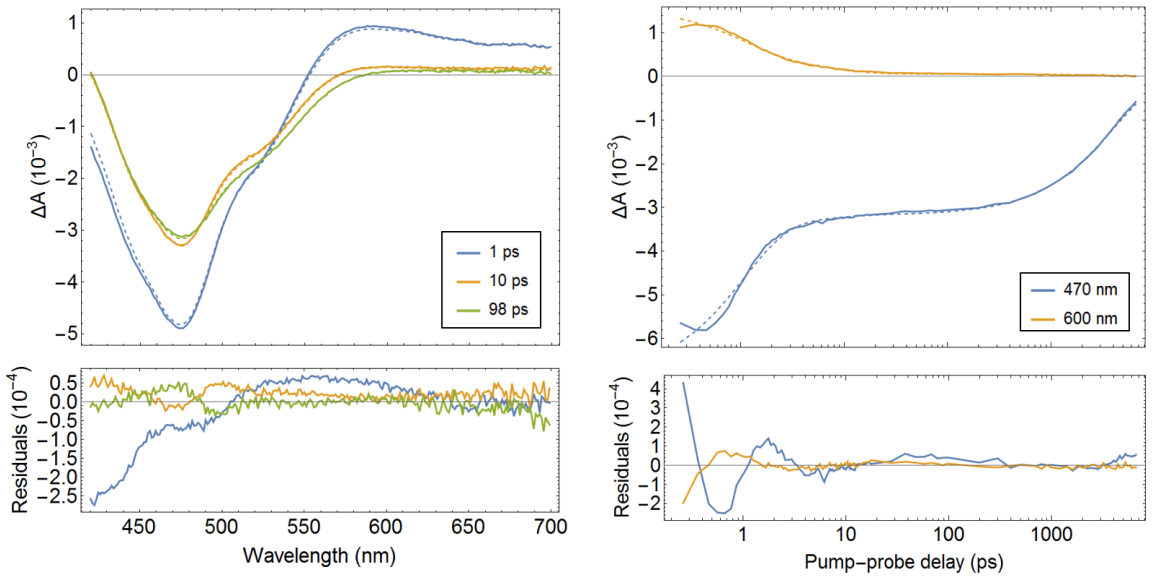

Fig. S91. Summary of **3** component global analysis of Ni(dtbbpy)(*o*-tolyl)Cl (**1–Cl**) transient absorption data (400 nm photoexcitation). Comparison of experimental (solid) and fit (dashed) difference absorption spectra at select pump-probe delays (left) and single wavelength kinetics (right).

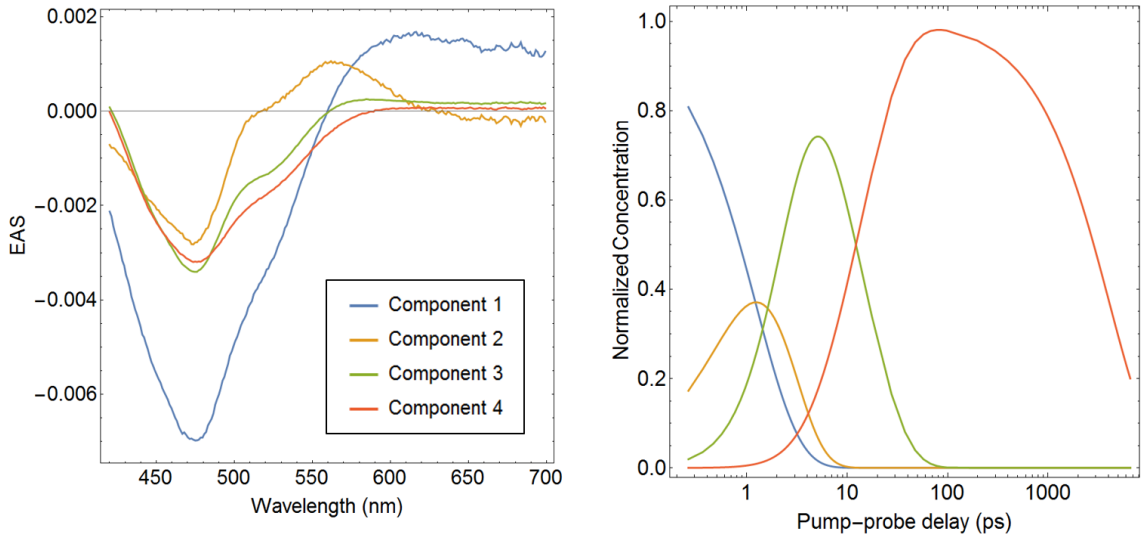

Fig. S92. Summary of **4** component global analysis of Ni(dtbbpy)(*o*-tolyl)Cl (**1–Cl**) transient absorption data (400 nm photoexcitation). Evolution associated spectra (left) and concentration profiles (right).

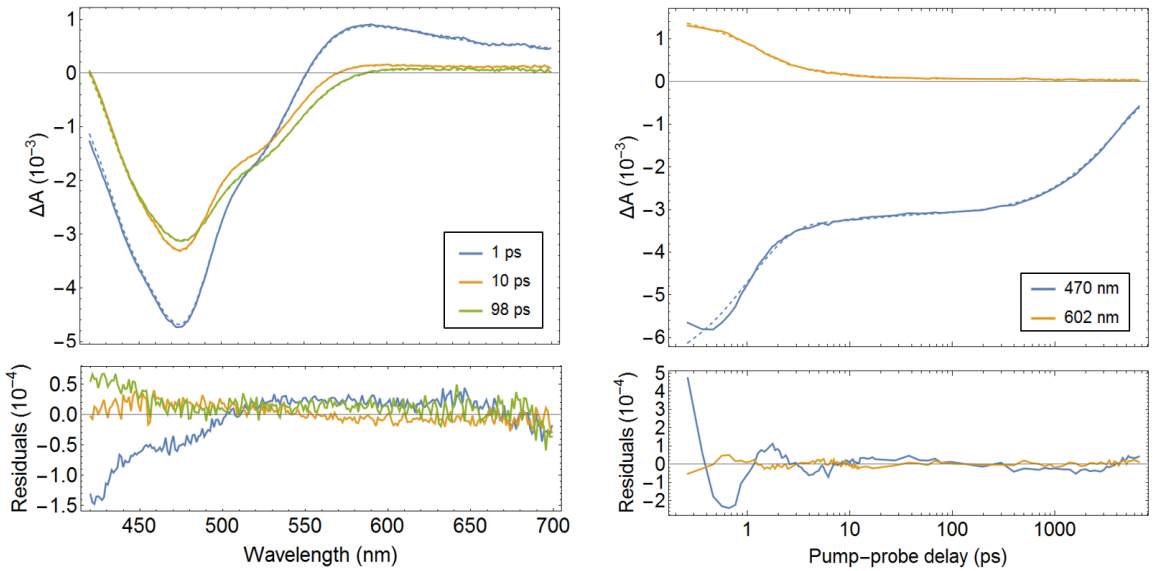

Fig. S93. Summary of **4** component global analysis of Ni(dtbbpy)(*o*-tolyl)Cl (**1–Cl**) transient absorption data (400 nm photoexcitation). Comparison of experimental (solid) and fit (dashed) difference absorption spectra at select pump-probe delays (left) and single wavelength kinetics (right).

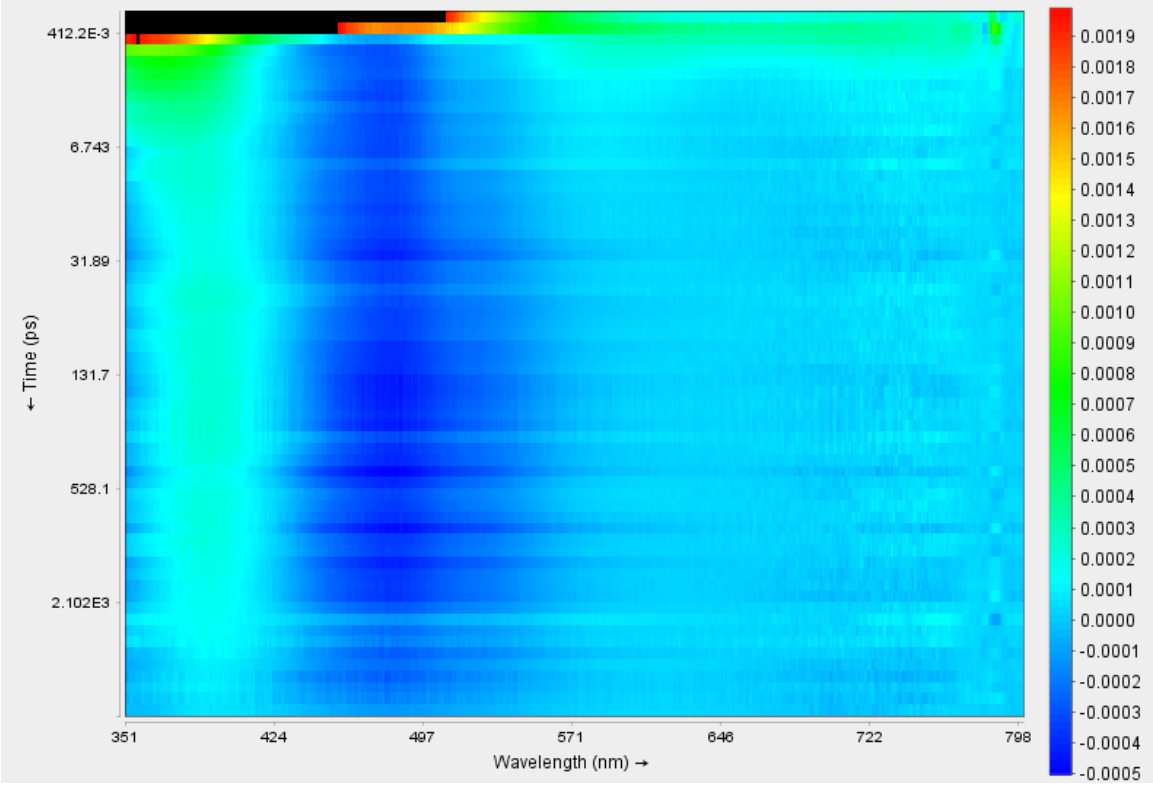

Fig. S94. Contour plot for portion of Ni(dtbbpy)(*o*-tolyl)Br (**1–Br**) transient absorption data used for global analysis (295 nm photoexcitation).

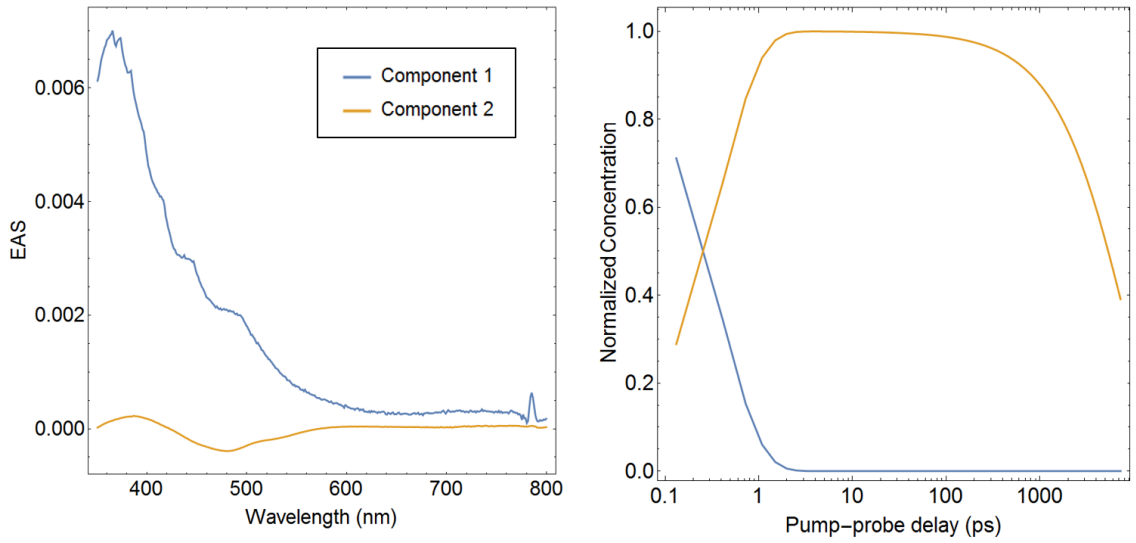

Fig. S95. Summary of **2** component global analysis of Ni(dtbbpy)(*o*-tolyl)Br (**1–Br**) transient absorption data (295 nm photoexcitation). Evolution associated spectra (left) and concentration profiles (right).

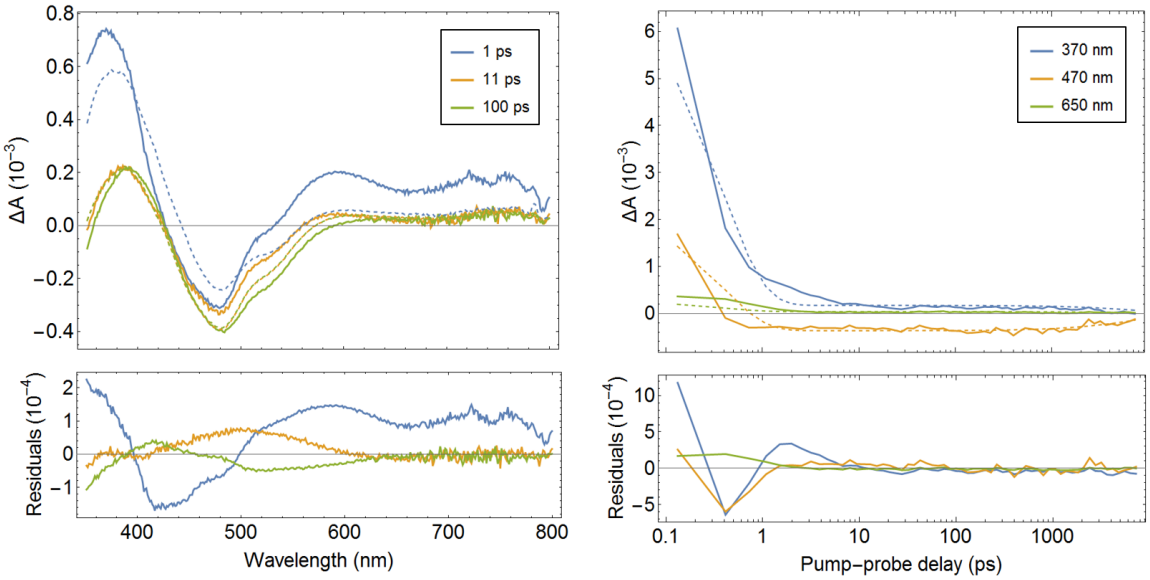

Fig. S96. Summary of **2** component global analysis of Ni(dtbbpy)(*o*-tolyl)Br (**1–Br**) transient absorption data (295 nm photoexcitation). Comparison of experimental (solid) and fit (dashed) difference absorption spectra at select pump-probe delays (left) and single wavelength kinetics (right).

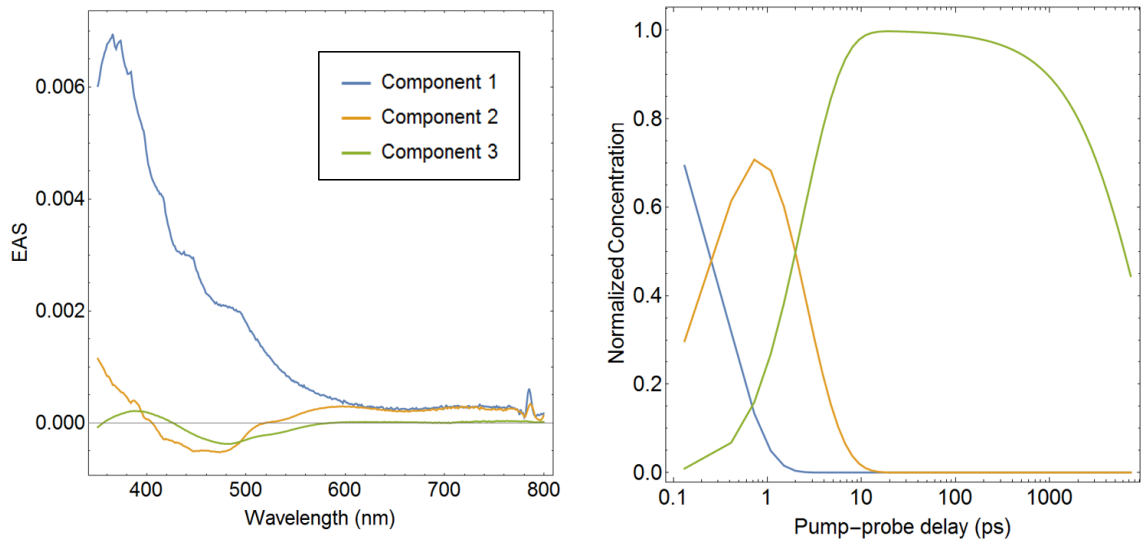

Fig. S97. Summary of **3** component global analysis of Ni(dtbbpy)(*o*-tolyl)Br (**1–Br**) transient absorption data (295 nm photoexcitation). Evolution associated spectra (left) and concentration profiles (right).

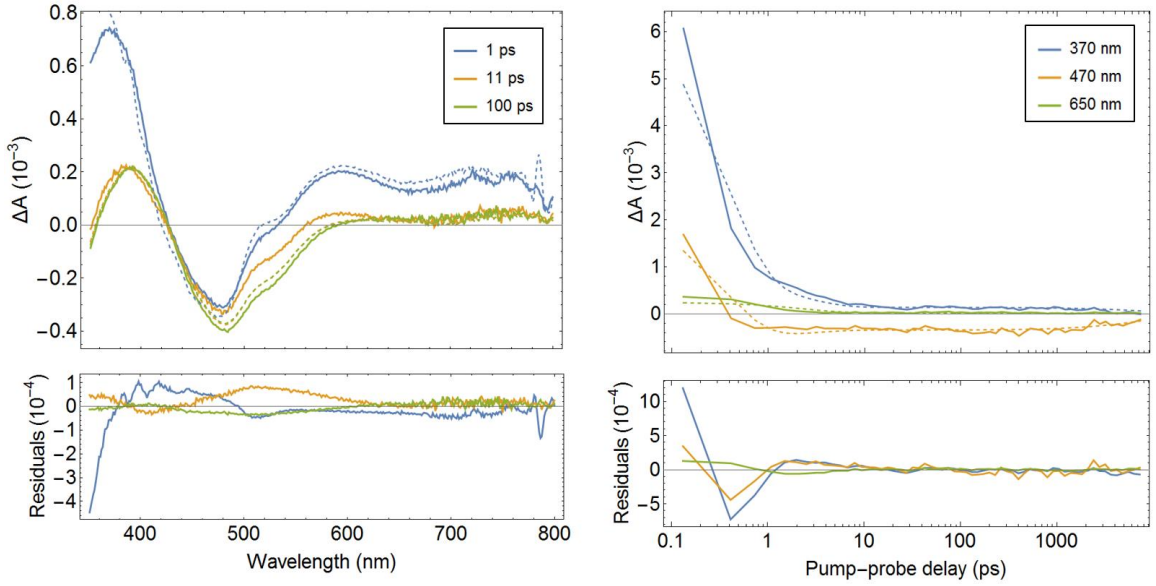

Fig. S98. Summary of **3** component global analysis of Ni(dtbbpy)(*o*-tolyl)Br (**1–Br**) transient absorption data (295 nm photoexcitation). Comparison of experimental (solid) and fit (dashed) difference absorption spectra at select pump-probe delays (left) and single wavelength kinetics (right).

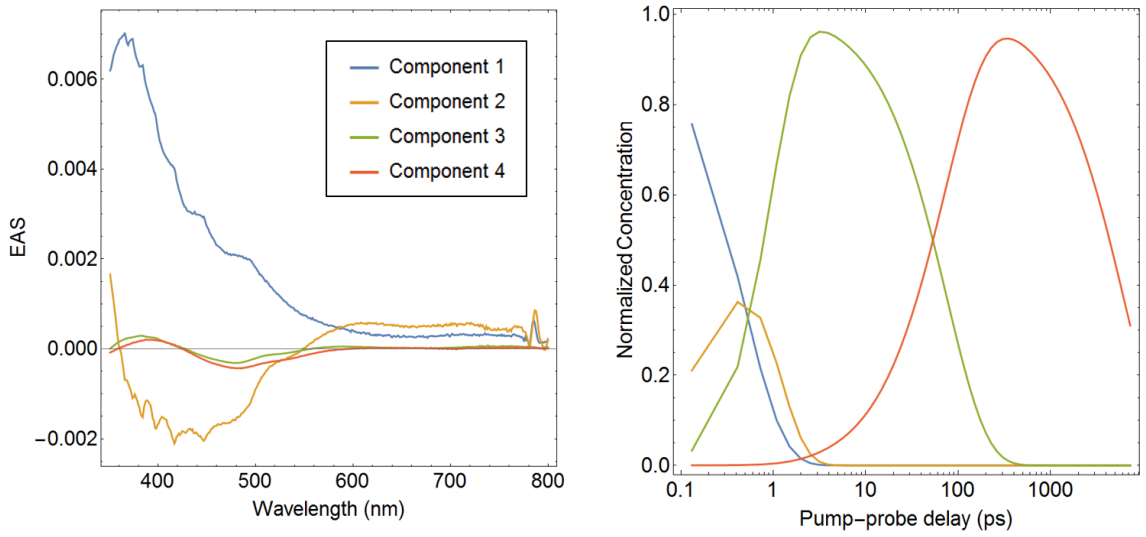

Fig. S99. Summary of **4** component global analysis of Ni(dtbbpy)(*o*-tolyl)Br (**1–Br**) transient absorption data (295 nm photoexcitation). Evolution associated spectra (left) and concentration profiles (right).

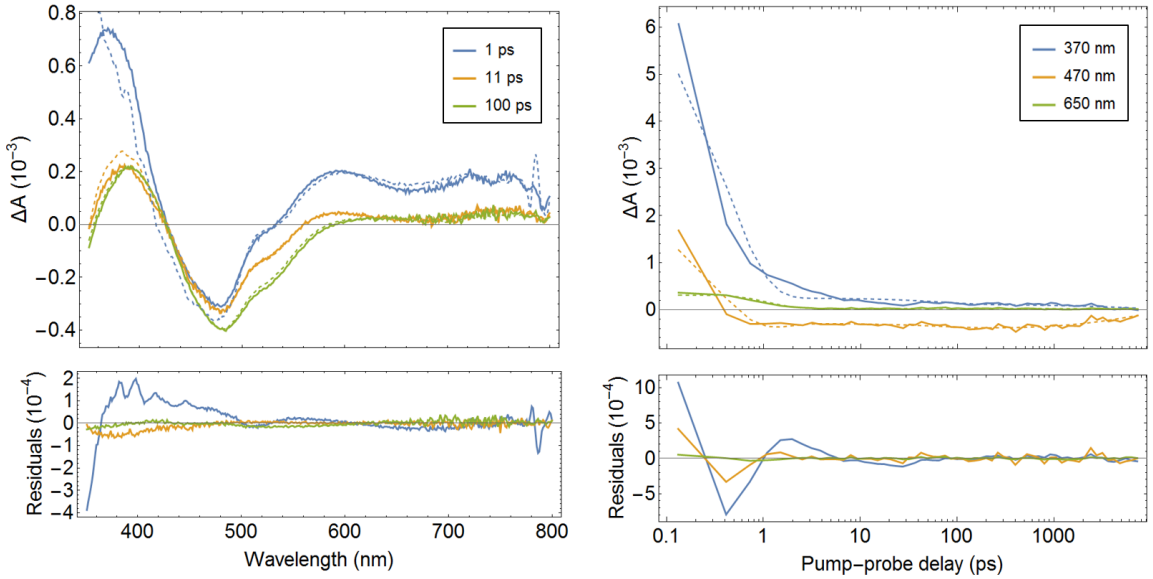

Fig. S100. Summary of **4** component global analysis of Ni(dtbbpy)(*o*-tolyl)Br (**1–Br**) transient absorption data (295 nm photoexcitation). Comparison of experimental (solid) and fit (dashed) difference absorption spectra at select pump-probe delays (left) and single wavelength kinetics (right).

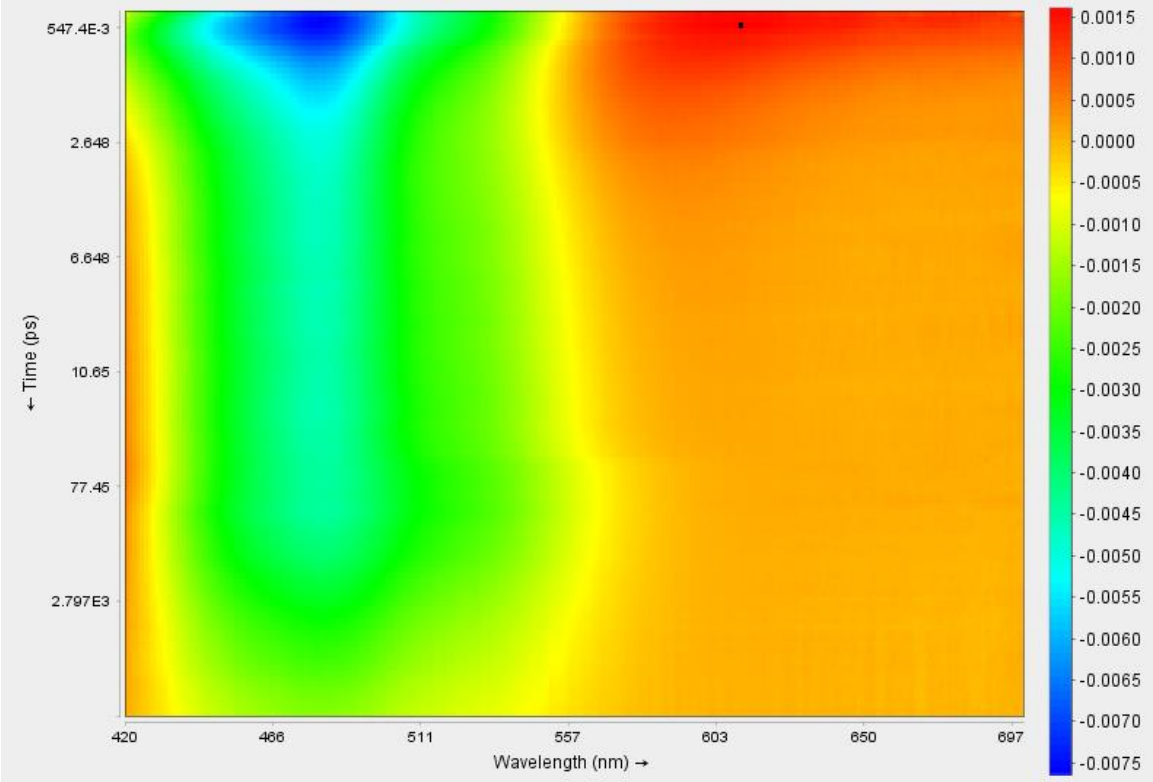

Fig. S101. Contour plot for portion of Ni(dtbbpy)(*o*-tolyl)Br (**1–Br**) transient absorption data used for global analysis (400 nm photoexcitation).

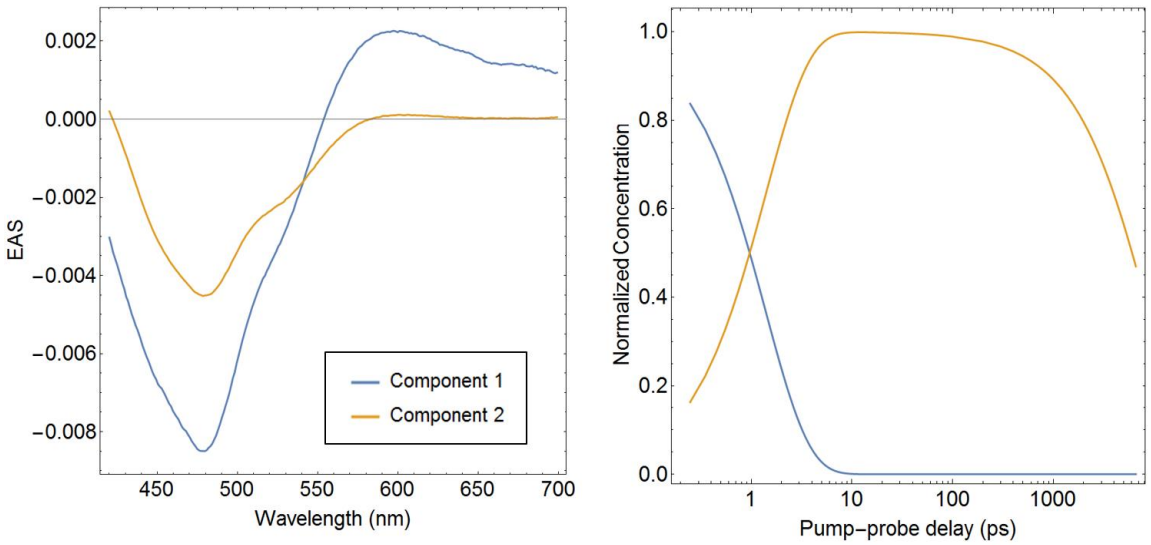

Fig. S102. Summary of **2** component global analysis of Ni(dtbbpy)(*o*-tolyl)Br (**1–Br**) transient absorption data (400 nm photoexcitation). Evolution associated spectra (left) and concentration profiles (right).

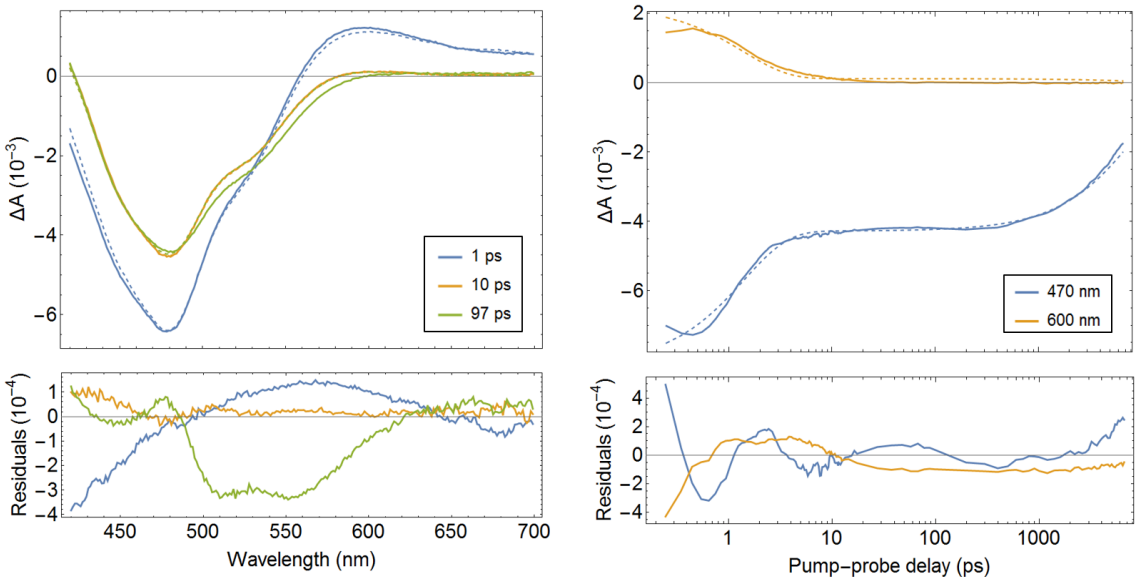

Fig. S103. Summary of **2** component global analysis of Ni(dtbbpy)(*o*-tolyl)Br (**1–Br**) transient absorption data (400 nm photoexcitation). Comparison of experimental (solid) and fit (dashed) difference absorption spectra at select pump-probe delays (left) and single wavelength kinetics (right).

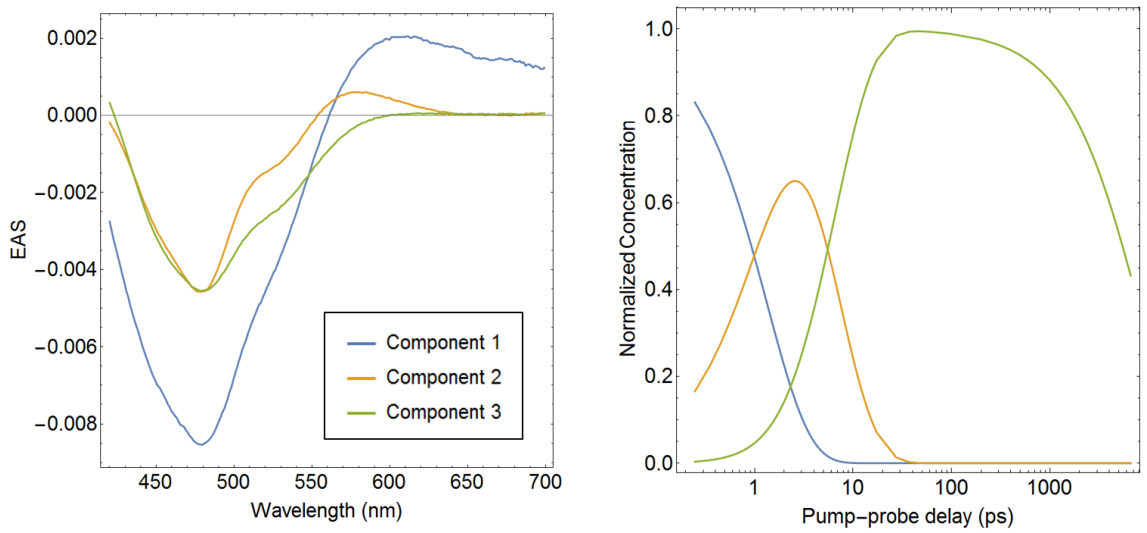

Fig. S104. Summary of **3** component global analysis of Ni(dtbbpy)(*o*-tolyl)Br (**1–Br**) transient absorption data (400 nm photoexcitation). Evolution associated spectra (left) and concentration profiles (right).

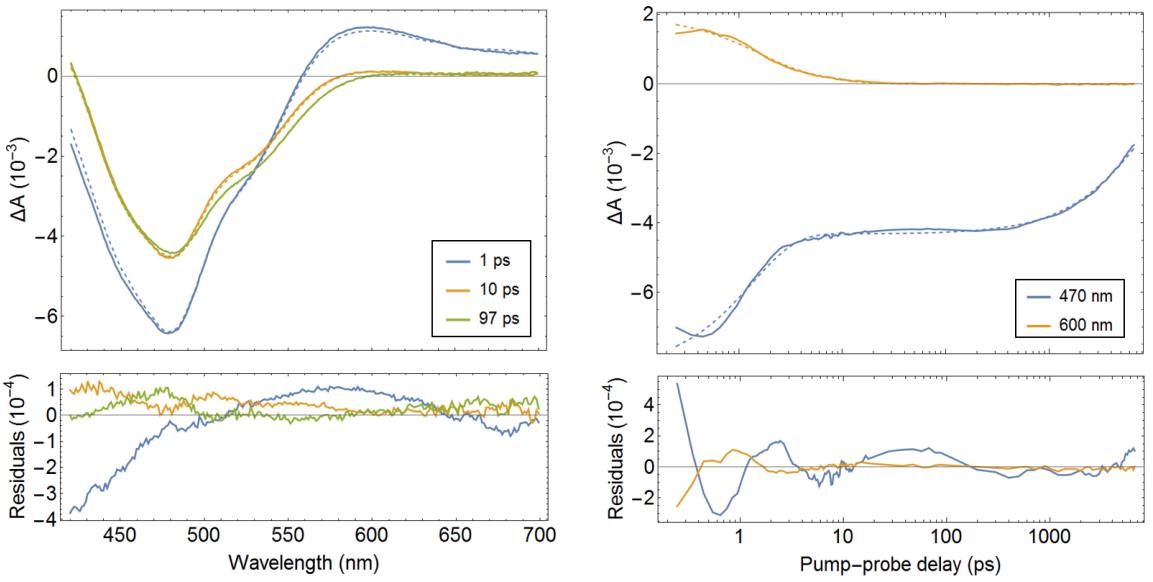

Fig. S105. Summary of **3** component global analysis of Ni(dtbbpy)(*o*-tolyl)Br (**1–Br**) transient absorption data (400 nm photoexcitation). Comparison of experimental (solid) and fit (dashed) difference absorption spectra at select pump-probe delays (left) and single wavelength kinetics (right).

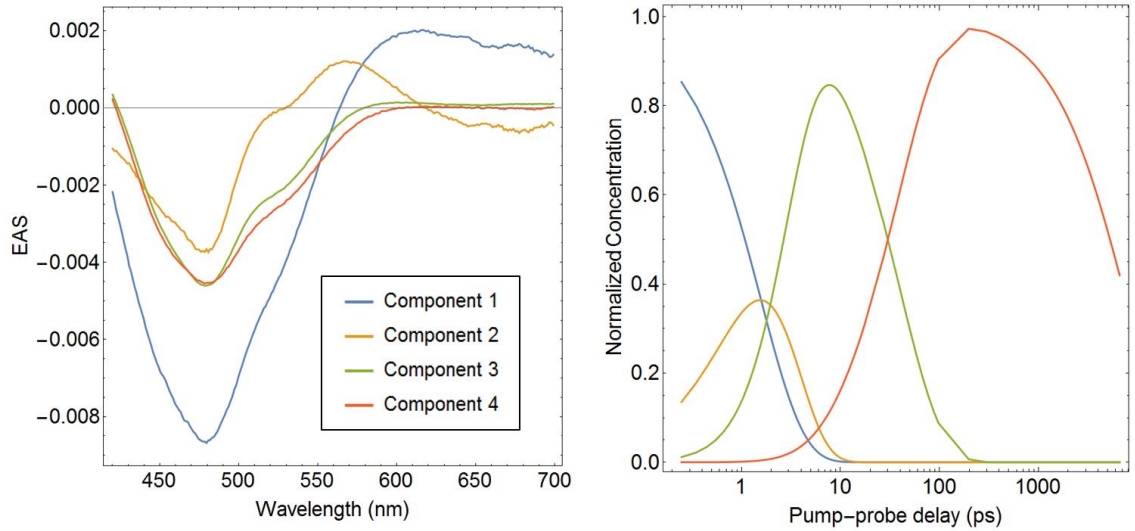

Fig. S106. Summary of **4** component global analysis of Ni(dtbbpy)(*o*-tolyl)Br (**1–Br**) transient absorption data (400 nm photoexcitation). Evolution associated spectra (left) and concentration profiles (right).

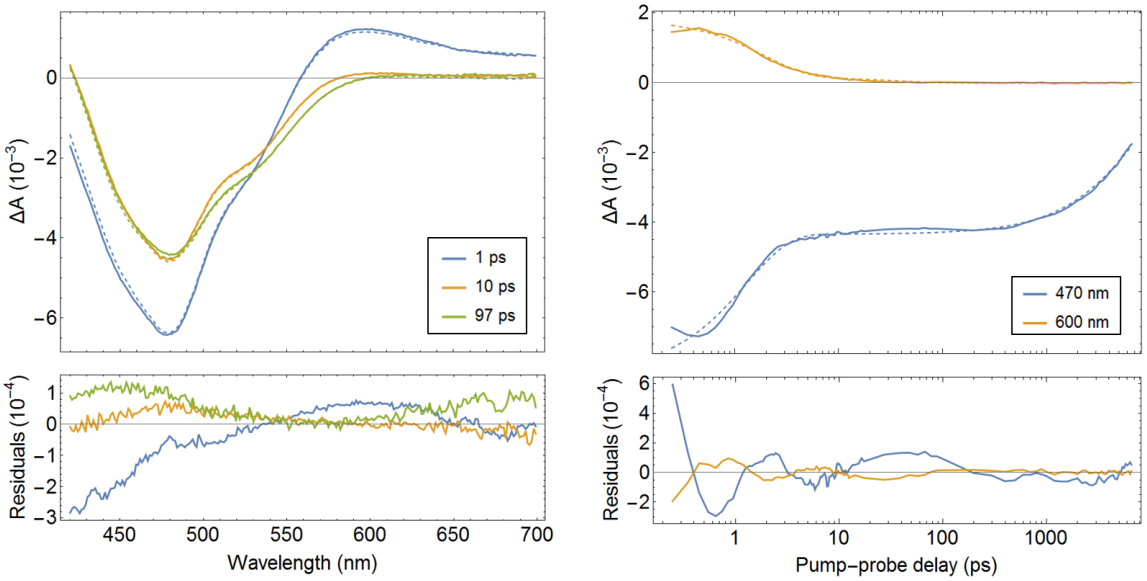

Fig. S107. Summary of **4** component global analysis of Ni(dtbbpy)(*o*-tolyl)Br (**1–Br**) transient absorption data (400 nm photoexcitation). Comparison of experimental (solid) and fit (dashed) difference absorption spectra at select pump-probe delays (left) and single wavelength kinetics (right).

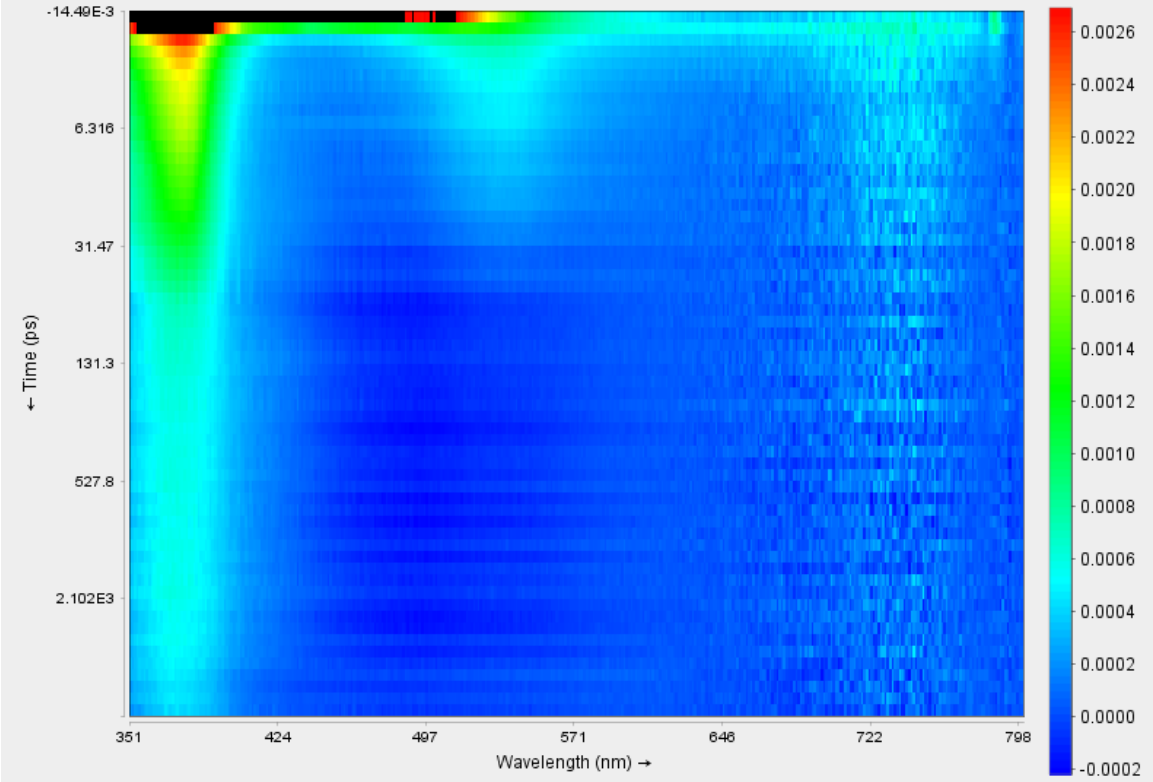

Fig. S108. Contour plot for portion of Ni(dtbbpy)(*o*-tolyl)I (**1–I**) transient absorption data used for global analysis (295 nm photoexcitation).

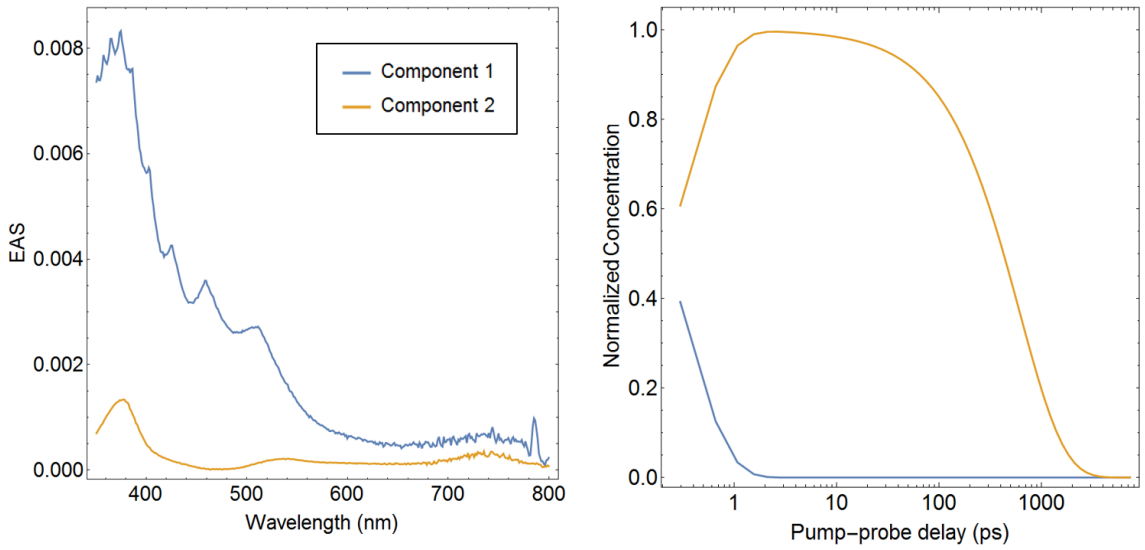

Fig. S109. Summary of **2** component global analysis of Ni(dtbbpy)(*o*-tolyl)I (**1–I**) transient absorption data (295 nm photoexcitation). Evolution associated spectra (left) and concentration profiles (right).

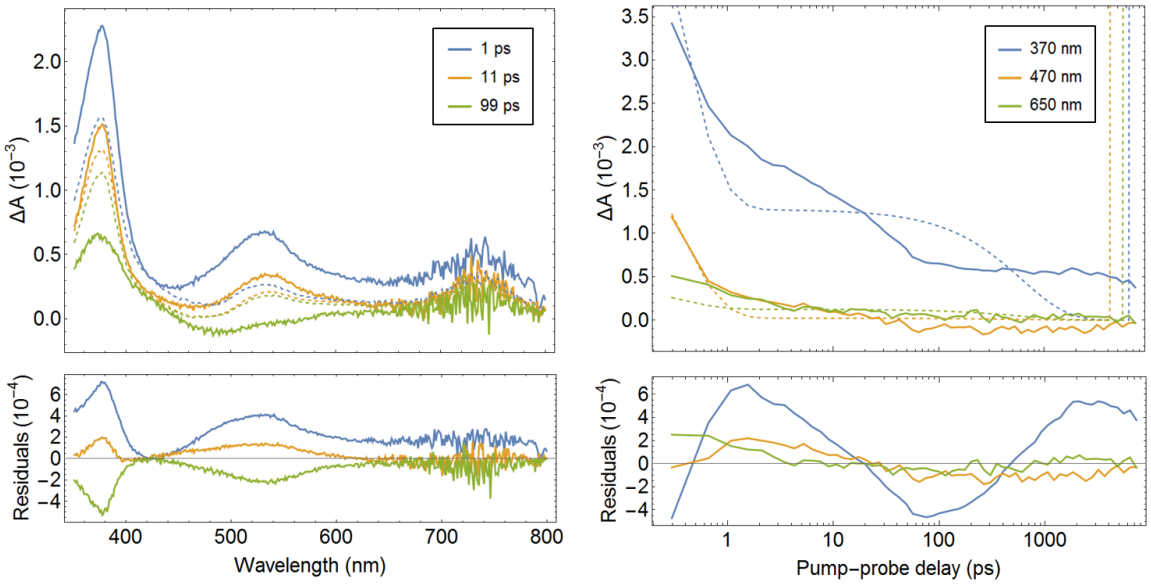

Fig. S110. Summary of **2** component global analysis of Ni(dtbbpy)(*o*-tolyl)I (**1–I**) transient absorption data (295 nm photoexcitation). Comparison of experimental (solid) and fit (dashed) difference absorption spectra at select pump-probe delays (left) and single wavelength kinetics (right).

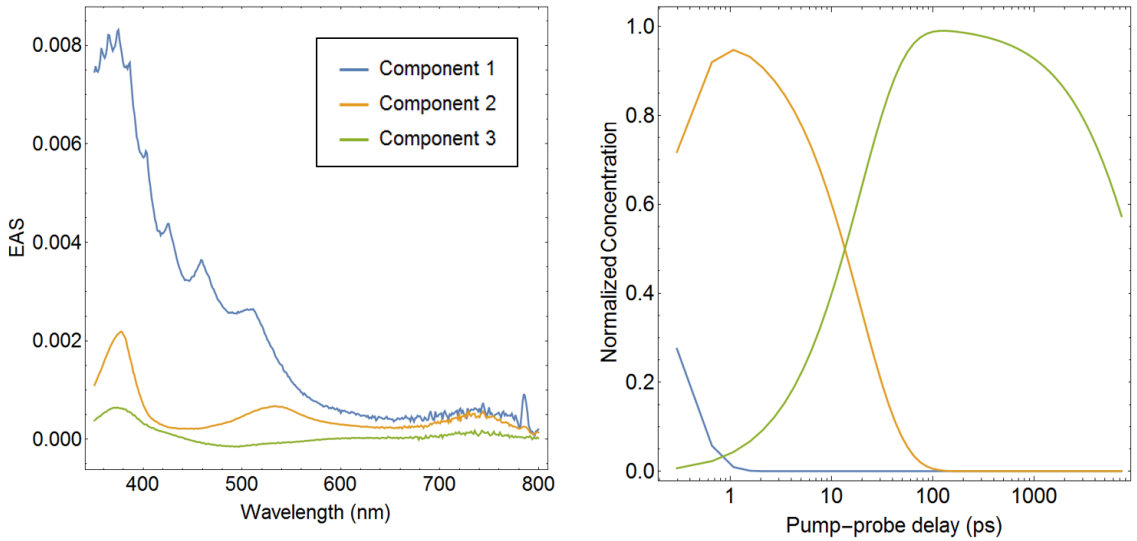

Fig. S111. Summary of **3** component global analysis of Ni(dtbbpy)(*o*-tolyl)I (**1–I**) transient absorption data (295 nm photoexcitation). Evolution associated spectra (left) and concentration profiles (right).

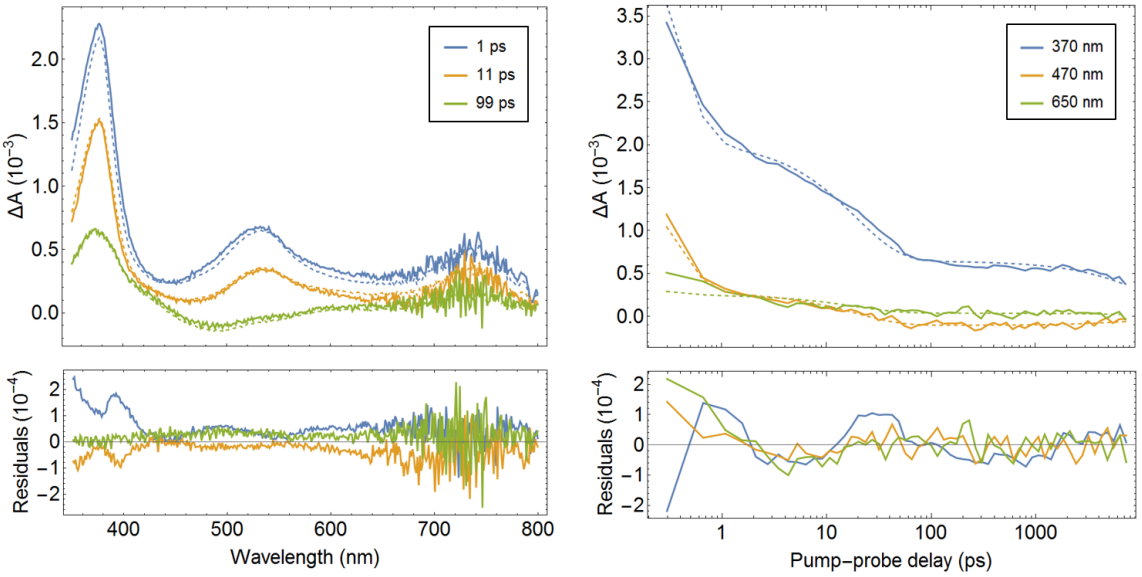

Fig. S112. Summary of **3** component global analysis of Ni(dtbbpy)(*o*-tolyl)I (**1–I**) transient absorption data (295 nm photoexcitation). Comparison of experimental (solid) and fit (dashed) difference absorption spectra at select pump-probe delays (left) and single wavelength kinetics (right).

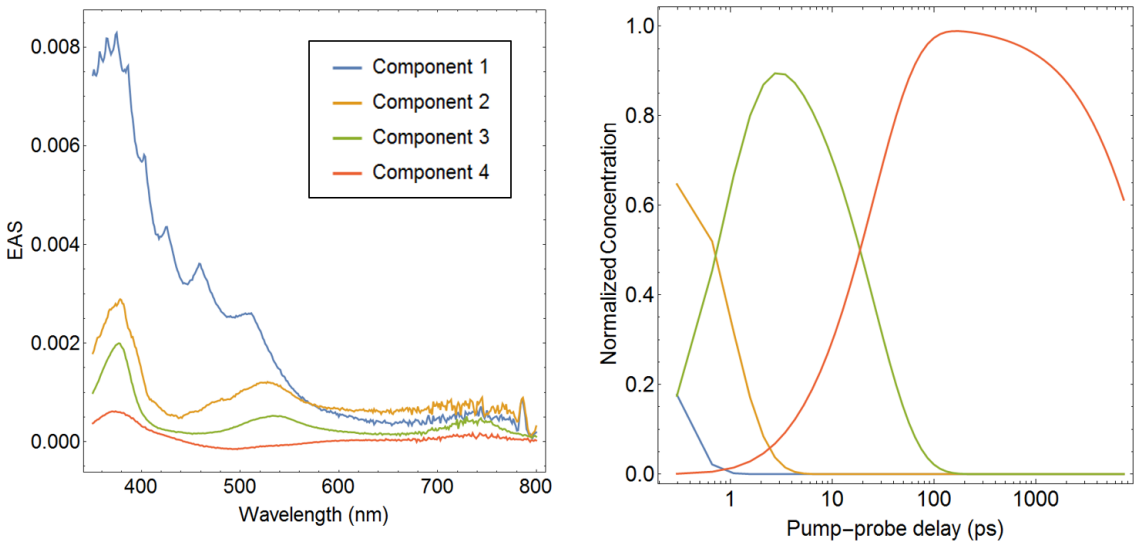

Fig. S113. Summary of **4** component global analysis of Ni(dtbbpy)(*o*-tolyl)I (**1–I**) transient absorption data (295 nm photoexcitation). Evolution associated spectra (left) and concentration profiles (right).

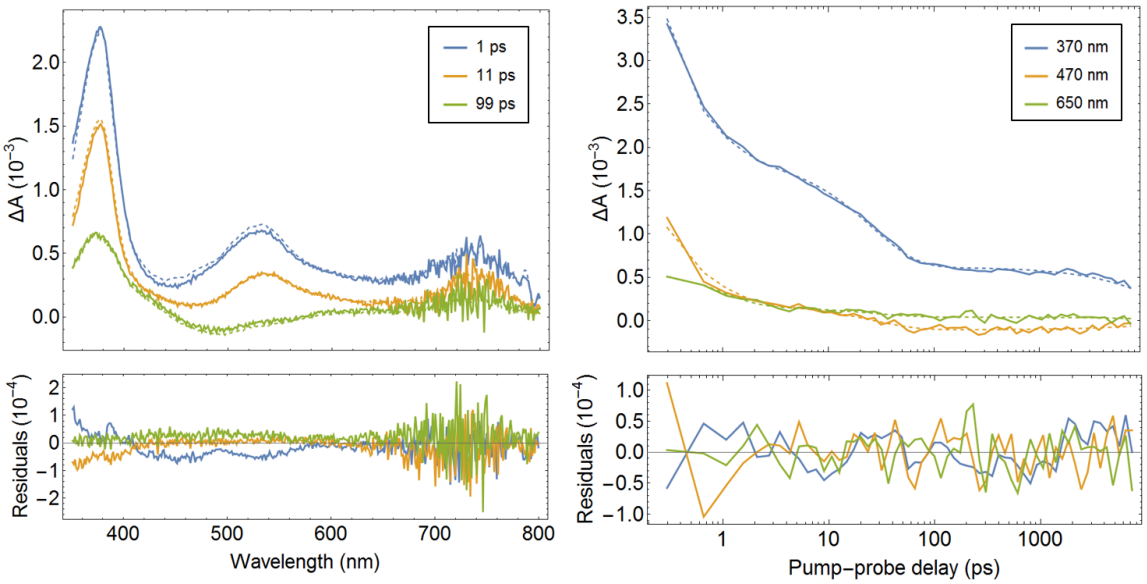

Fig. S114. Summary of **4** component global analysis of Ni(dtbbpy)(*o*-tolyl)I (**1–I**)transient absorption data (295 nm photoexcitation). Comparison of experimental (solid) and fit (dashed) difference absorption spectra at select pump-probe delays (left) and single wavelength kinetics (right).

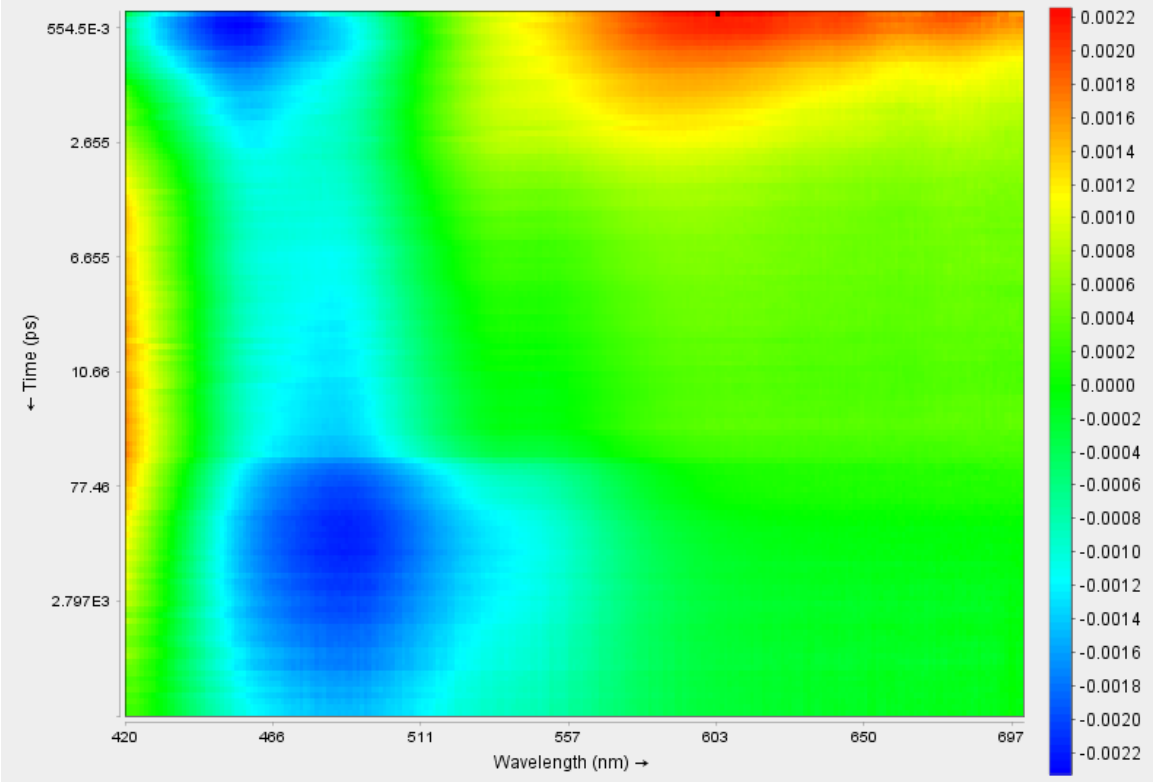

Fig. S115. Contour plot for portion of Ni(dtbbpy)(*o*-tolyl)I (**1–I**) transient absorption data used for global analysis (400 nm photoexcitation).

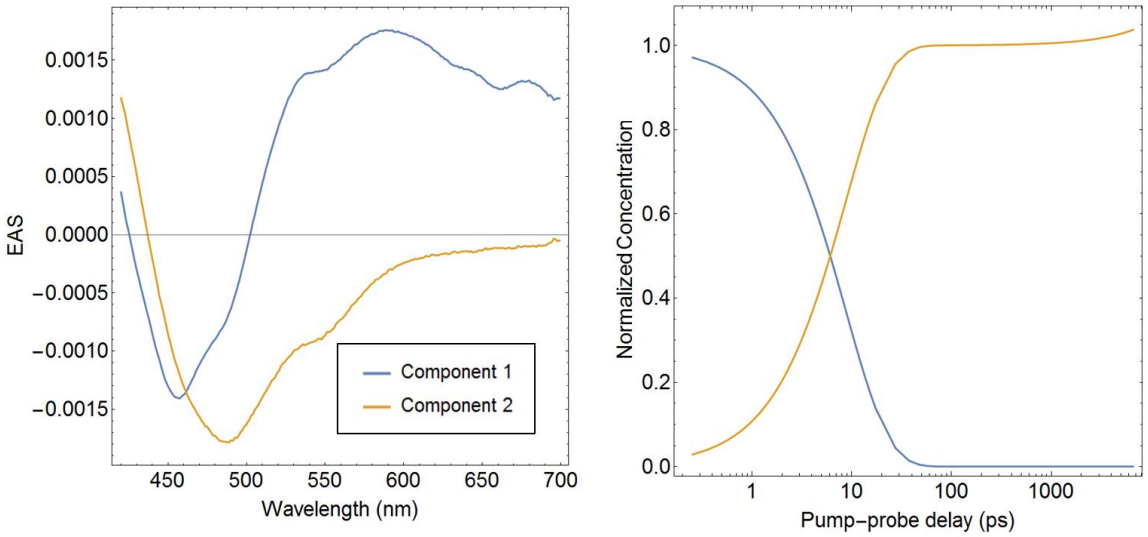

Fig. S116. Summary of **2** component global analysis of Ni(dtbbpy)(*o*-tolyl)I (**1–I**) transient absorption data (400 nm photoexcitation). Evolution associated spectra (left) and concentration profiles (right).

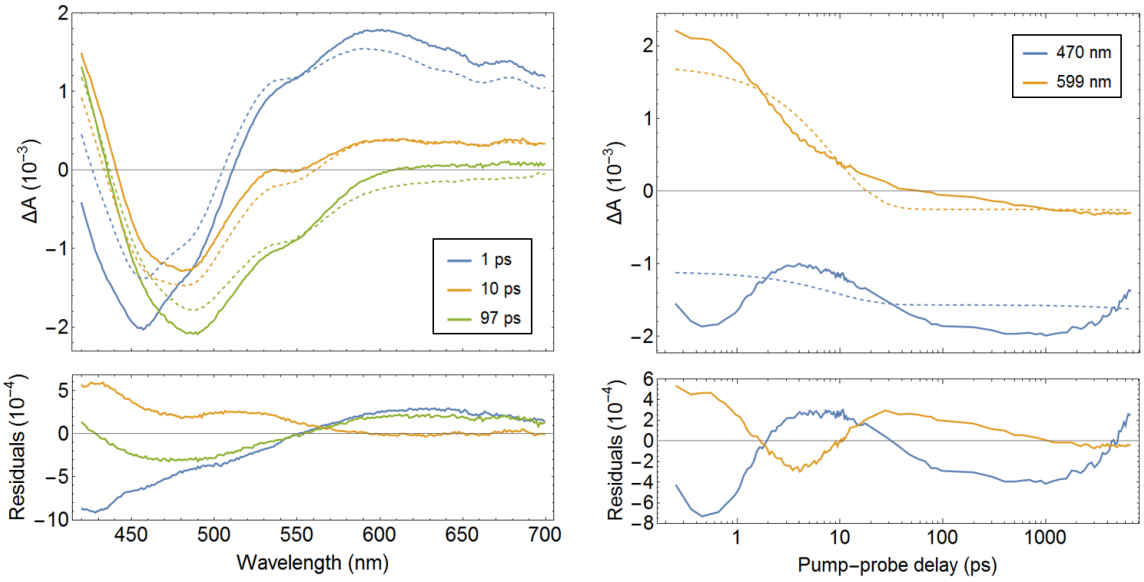

Fig. S117. Summary of **2** component global analysis of Ni(dtbbpy)(*o*-tolyl)I (**1–I**) transient absorption data (400 nm photoexcitation). Comparison of experimental (solid) and fit (dashed) difference absorption spectra at select pump-probe delays (left) and single wavelength kinetics (right).

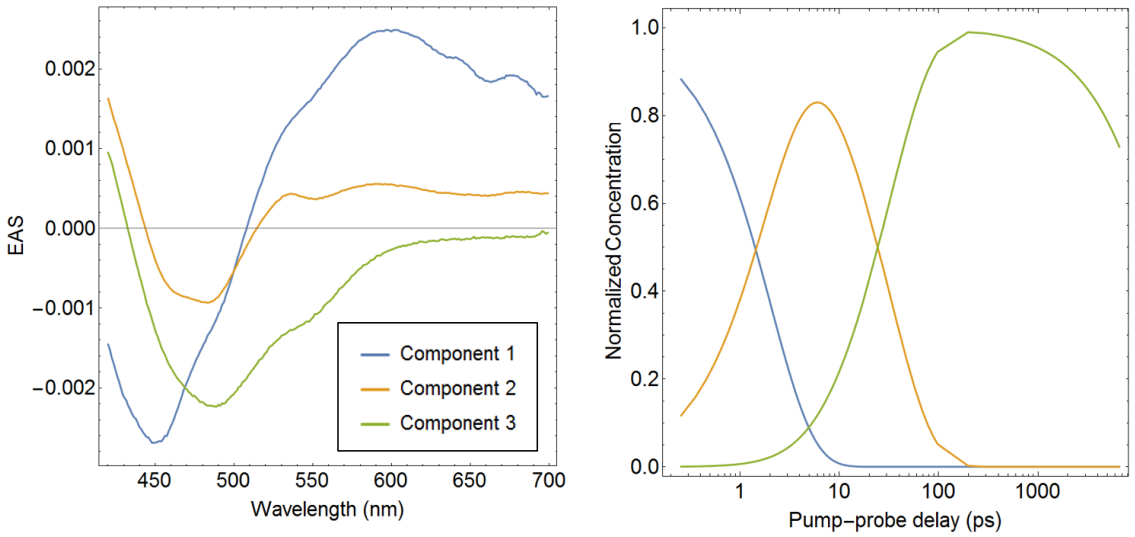

Fig. S118. Summary of **3** component global analysis of Ni(dtbbpy)(*o*-tolyl)I (**1–I**) transient absorption data (400 nm photoexcitation). Evolution associated spectra (left) and concentration profiles (right).

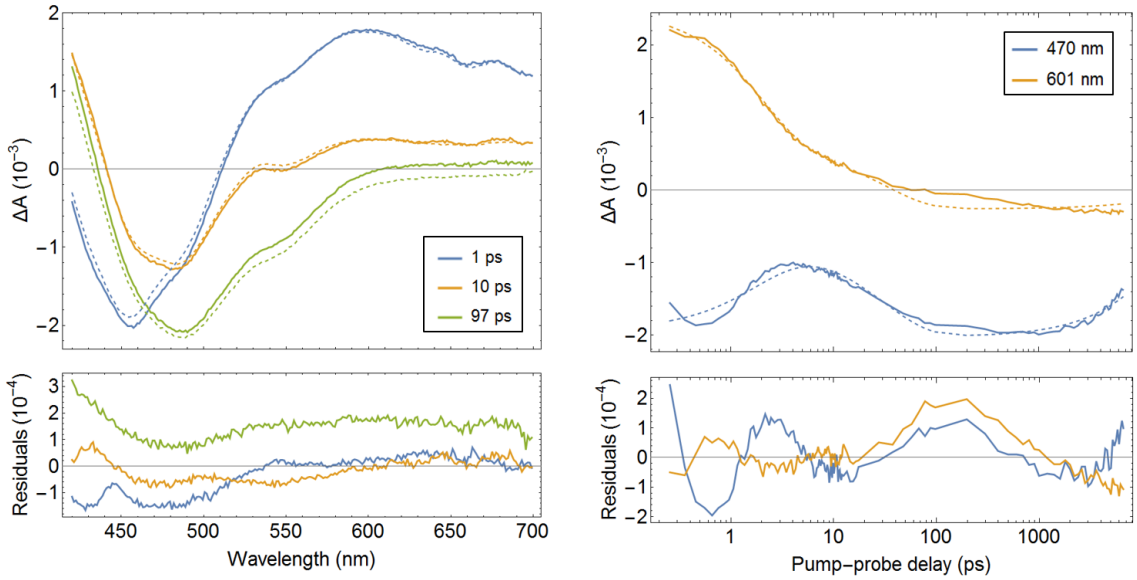

Fig. S119. Summary of **3** component global analysis of Ni(dtbbpy)(*o*-tolyl)I (**1–I**) transient absorption data (400 nm photoexcitation). Comparison of experimental (solid) and fit (dashed) difference absorption spectra at select pump-probe delays (left) and single wavelength kinetics (right).

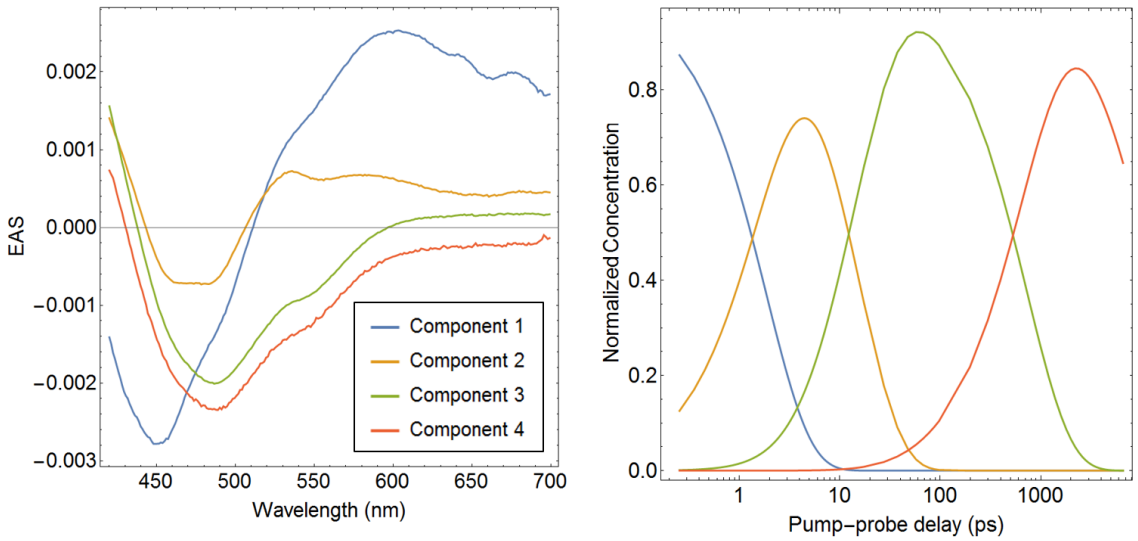

Fig. S120. Summary of **4** component global analysis of Ni(dtbbpy)(*o*-tolyl)I (**1–I**) transient absorption data (400 nm photoexcitation). Evolution associated spectra (left) and concentration profiles (right).

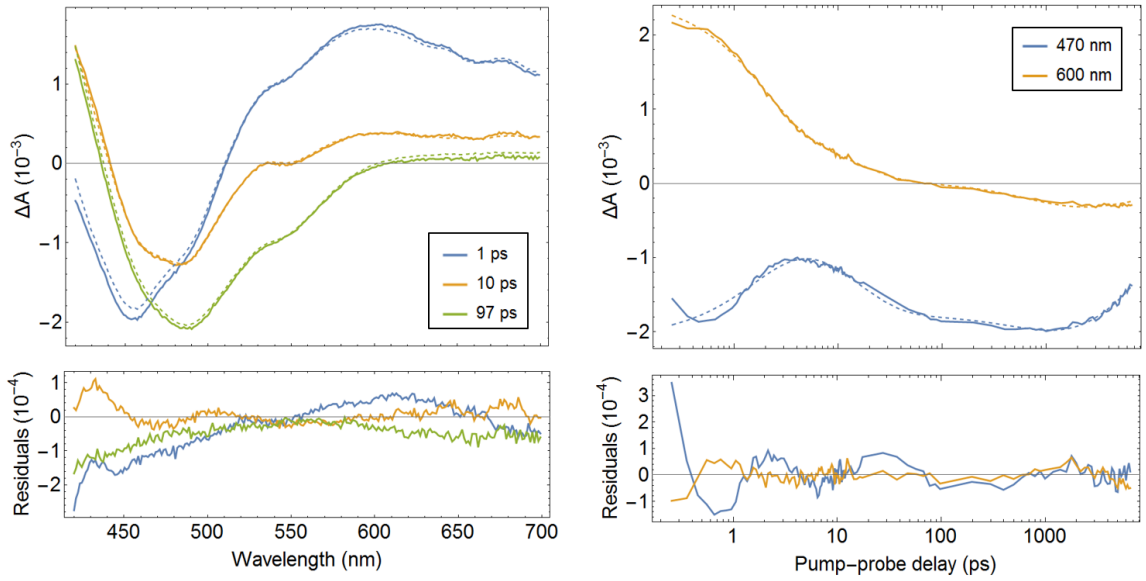

Fig. S121. Summary of **4** component global analysis of Ni(dtbbpy)(*o*-tolyl)I (**1–I**)transient absorption data (400 nm photoexcitation). Comparison of experimental (solid) and fit (dashed) difference absorption spectra at select pump-probe delays (left) and single wavelength kinetics (right).

VII. Photolytic and Thermal Degradation Studies

Degradation Studies. All samples were prepared inside a nitrogen filled glove box. Note that the solution temperature was measured to be 34˚C in a typical photolytic degradation experiment. For ^{1}H NMR degradation studies, a solution of **1–Cl** (8.0 mg, 17.6 µmol) in THF-d8 (1.3 mL, 13.5 mM) was split between two NMR tubes (0.6 mL each). The tubes were then sealed with plastic caps and electrical tape and removed from the glovebox. One sample was then irradiated with a 34 W blue LED (1.5 in away, measured intensity = 4061 µEinsteins $s^{-1}m^{-2}$) while the other was placed in a dark heating bath at 34˚C. After irradiation for the indicated time a spectrum of each sample was collected. For Uv-vis degradation studies, a 5.0×10^{-4} M THF solution of **1–Cl** was added to screw-top 2mm optical glass cuvette. The cuvette was then sealed with a J. Young valve, removed from the glovebox, and irradiated with a 34 W blue LED. After irradiation for the indicated time a spectrum was collected. Note that at room temperature no degradation was observed by Uv-vis after 24 h in the absence of light.

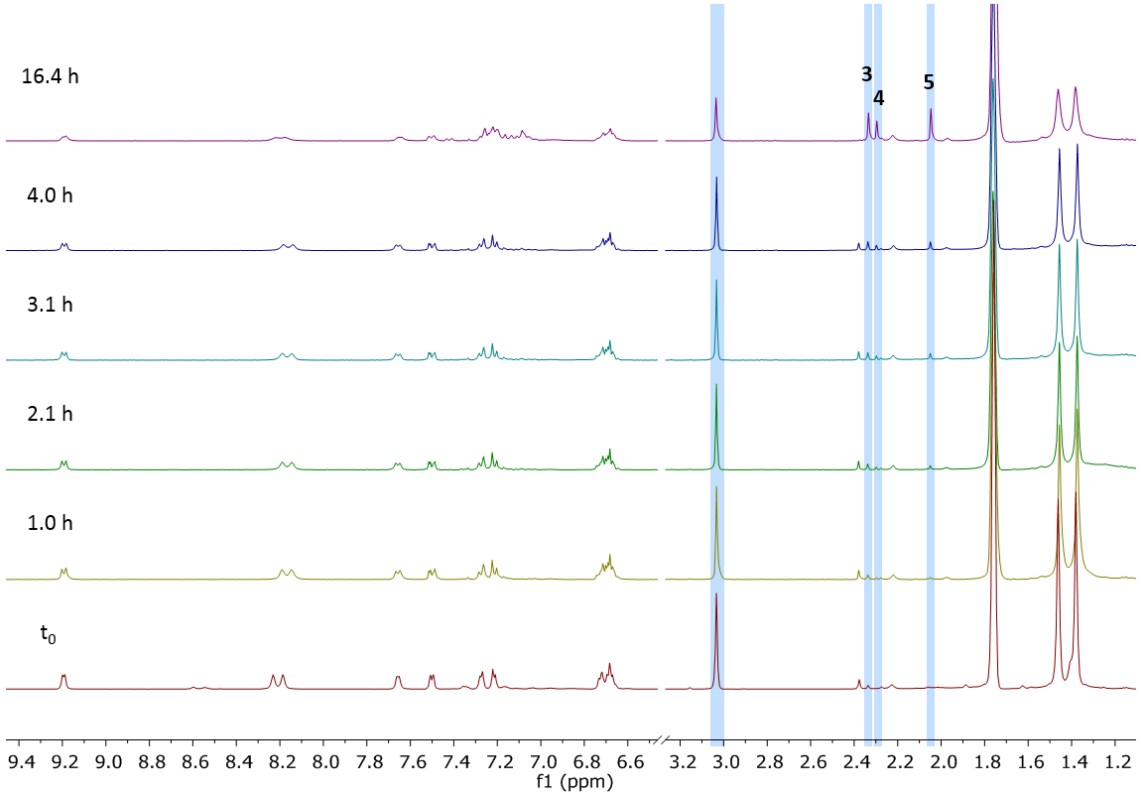

Fig. S122. Photolytic degradation of Ni(dtbbpy)(*o*-tolyl)Cl (**1–Cl**) at 34˚C monitored via ^{1}H NMR over 16.4 h of irradiation. Degradation of **1–Cl** was monitored by the disappearance of the methyl resonance associated with the *o*-tolyl ligand. The production of toluene (**3**), 2-(*o*-tolyl)tetrahydrofuran (**4**), and 2,2'-dimethyl-1,1'biphenyl (**5**) products were detected via methyl resonances associated with the species.

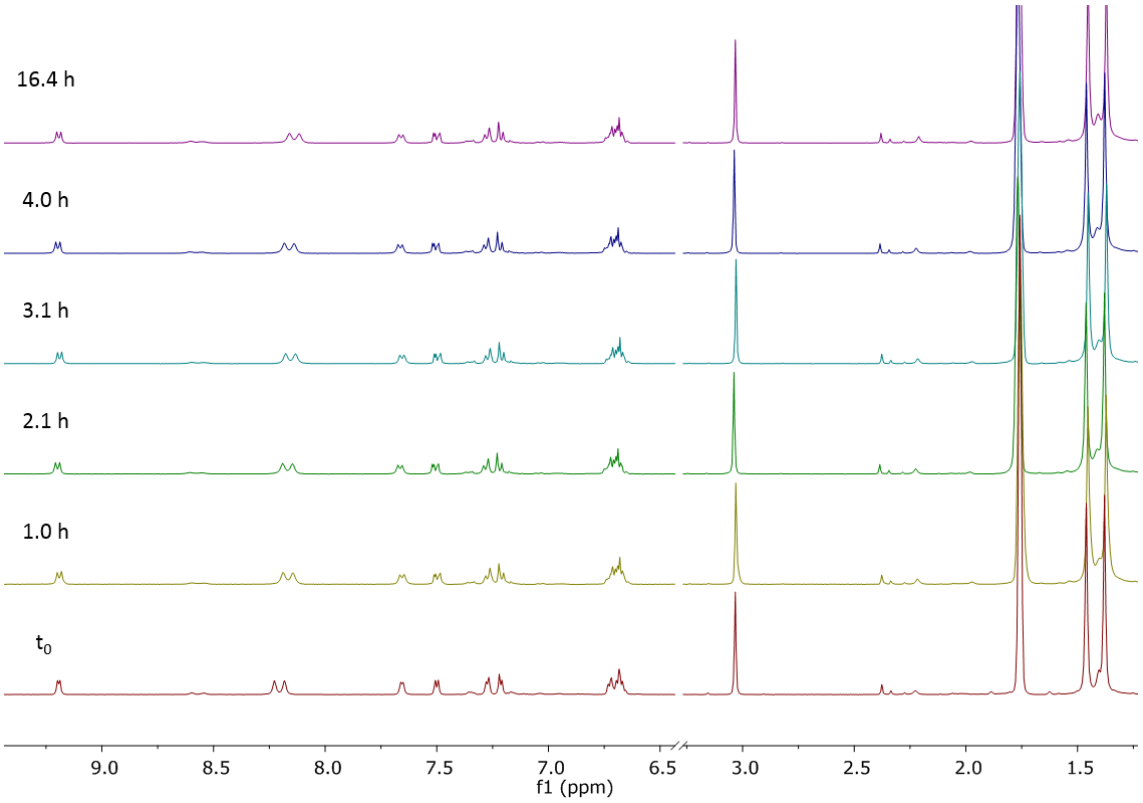

Fig. S123. Thermal degradation control for Ni(dtbbpy)(*o*-tolyl)Cl (**1–Cl**) monitored via ^{1}H NMR over 16.4 h of heating at 34°C. Minimal degradation was detected.

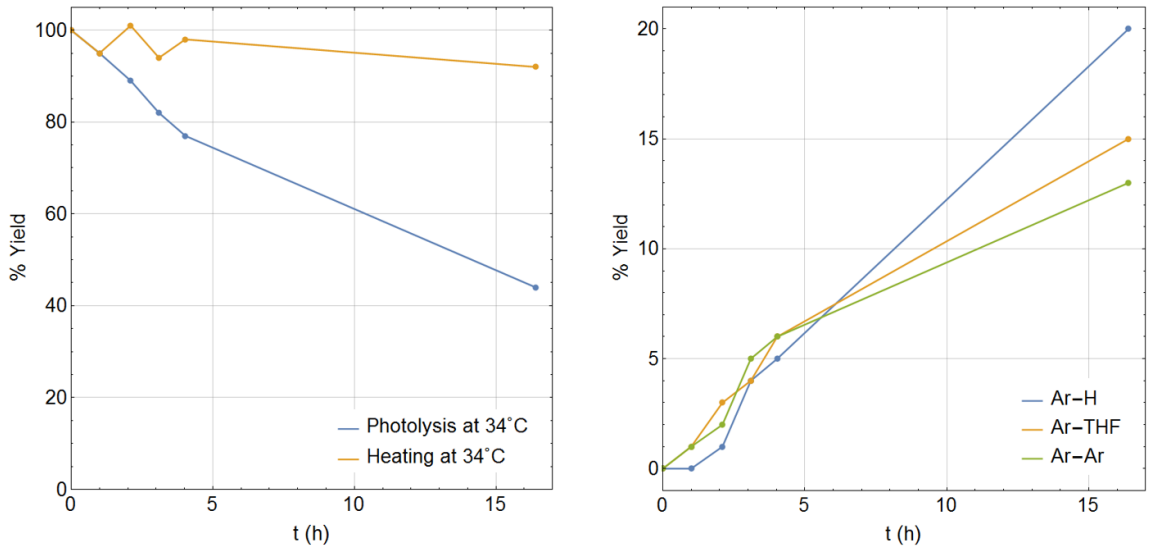

Fig. S124. Quantification of photolytic and thermal degradation (left). Quantification of organic photolytic degradation products (right).

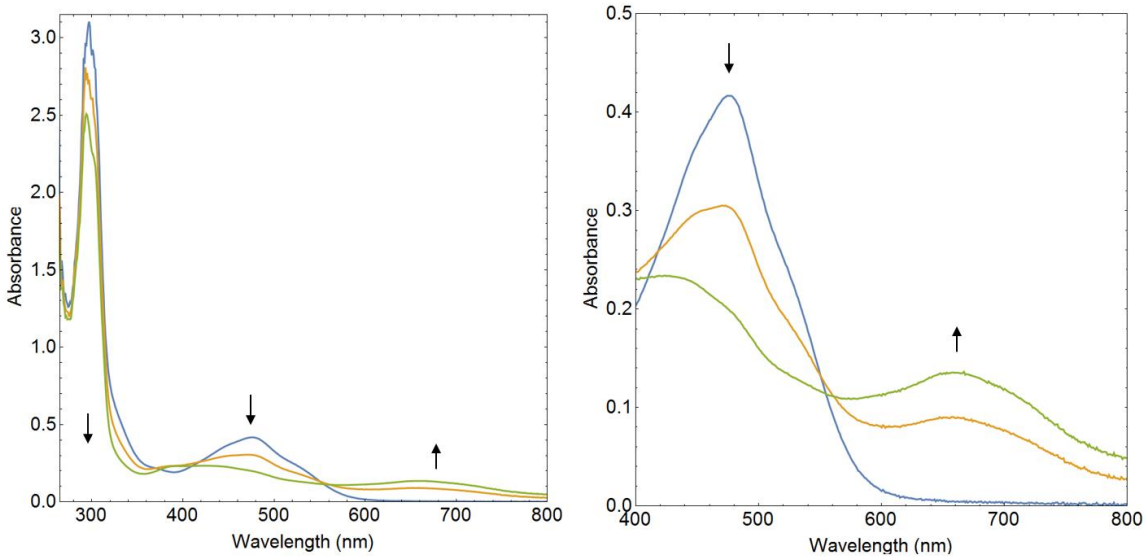

Fig. S125. Photolytic degradation of Ni(dtbbpy)(*o*-tolyl)Cl (**1–Cl**) at 34°C monitored via Uv-vis over 3.25 h of irradiation. The spectra show the generation of unidentified species (λ_{max} = 660 nm) upon irradiation.

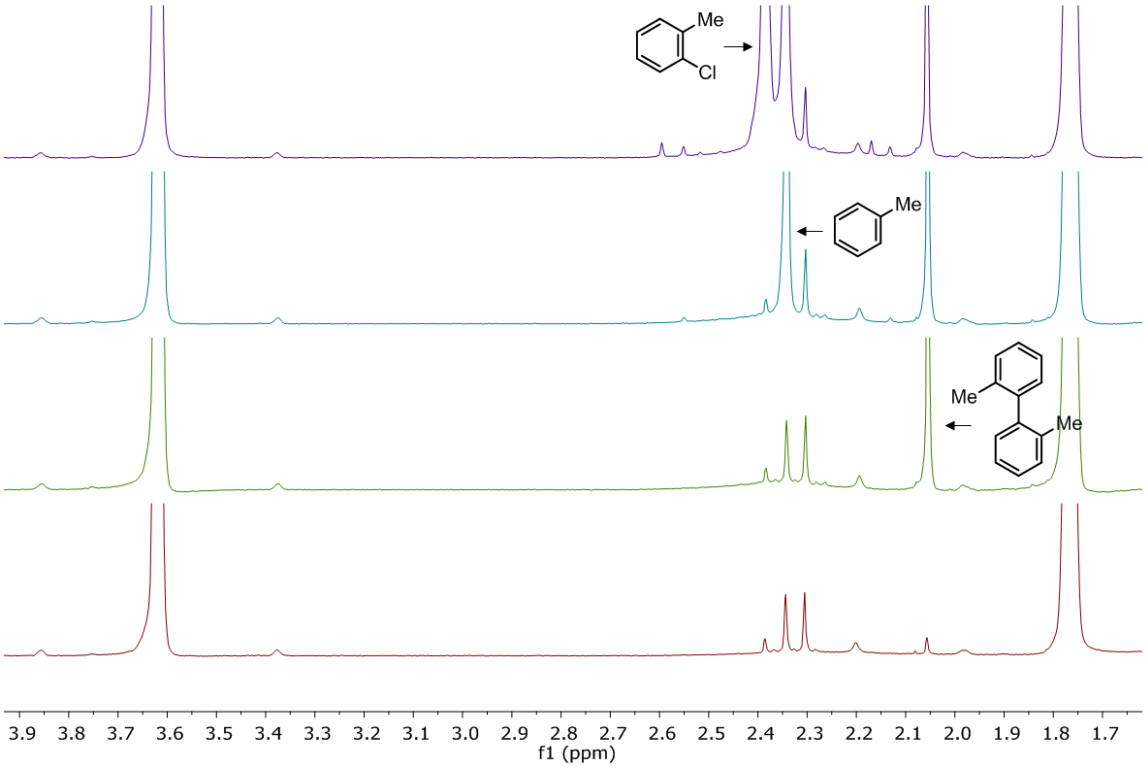

Fig. S126. In a separate photolytic degradation experiment the organic products toluene-d1 (**3**) and 2,2'-dimethyl-1,1'biphenyl (**5**) were positively identified by spiking the crude reaction mixture (bottom) with a pure sample of the corresponding undeuterated compound. The organic product 2-(*o*-tolyl)tetrahydrofuran-d7 (**4**) was identified by comparison to the ^{1}H NMR shift of 2-(*o*-tolyl)tetrahydrofuran-h7.

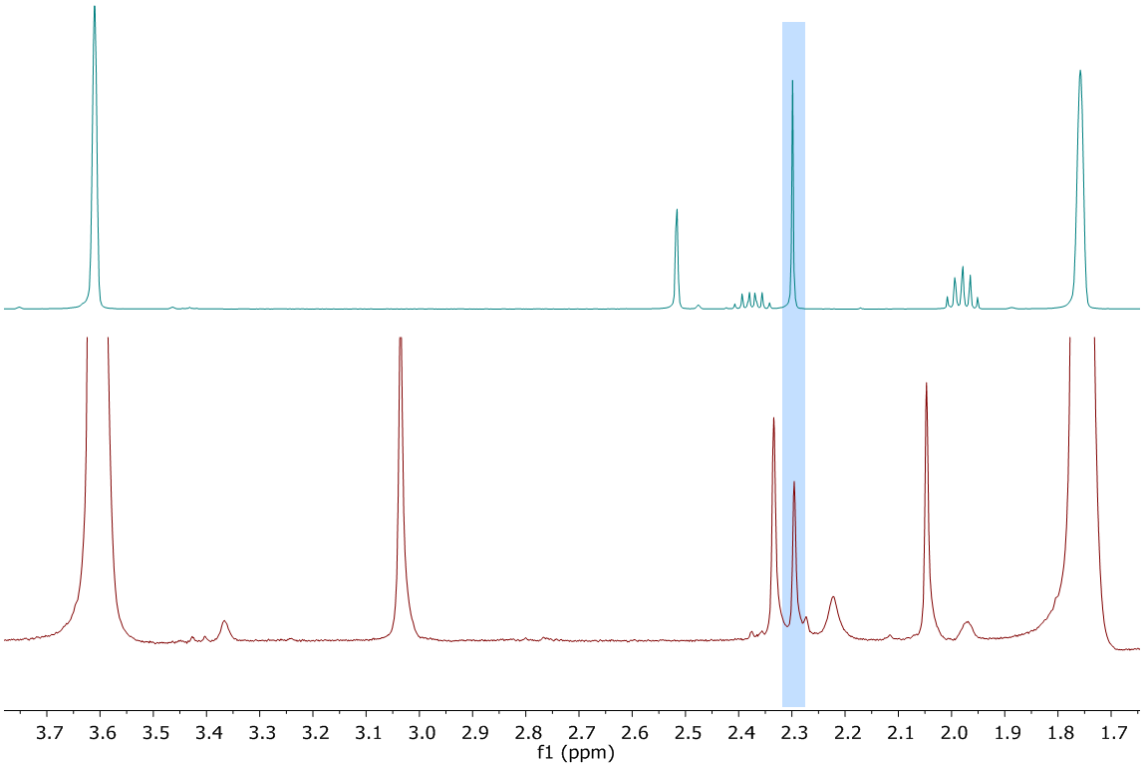

Fig. S127. The organic product 2-(*o*-tolyl)tetrahydrofuran-d7 was identified by comparison to the ^{1}H NMR spectrum of the 2-(*o*-tolyl)tetrahydrofuran-h7 (top) in THF-d8.

VIII. Redox Bracketing Studies

Stoichiometric Oxidation Experiment. A threaded 20 × 125 mm borosilicate reaction tube (Fisher part number: 14-959-37A) equipped with PTFE-coated stir bar was brought into a N_2-filled glove box and charged with Ni(dtbbpy)(*o*-tolyl)Cl (11 mg, 0.025 mmol) followed by THF (9 mL) to give a ruby red solution. To a two dram vial was added ferrocenium tetrakis[3,5-bis(trifluoromethyl)phenyl]borate ($FcBArF^4$, 26 mg, 0.025 mmol) followed by THF (3.5 mL) to give a turquoise solution. The reaction tube and vial were capped with Teflon septum caps, sealed with electrical tape and removed from the glove box. The Ni(dtbbpy)(*o*-tolyl)Cl solution was placed in a acetone/dry ice bath and set to stir (800 rpm) for 15 min. The $FcBArF^4$ solution was cooled in a acetone/dry ice bath. The cooled Ni(dtbbpy)(*o*-tolyl)Cl solution was irradiated with two 34 W blue LED lamps (5 cm away, placed 180° apart). The cooled $FcBArF^4$ solution was titrated drop wise via syringe into the Ni(dtbbpy)(*o*-tolyl)Cl solution. During the titration condensation was washed from the reaction tube with acetone. The reaction mixture changed from ruby red to light yellow after complete addition of the $FcBArF^4$. After addition of $FcBArF^4$ was complete the reaction was warmed to room temperature and the crude product was analyzed by GC-FID relative to 1-fluoronaphthalene as an external standard.

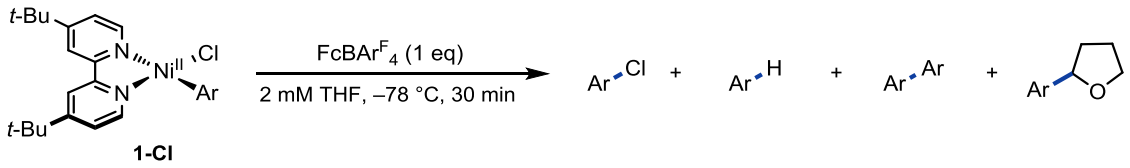

Entry	Conditions	Yield Ar-Cl	Yield Ar-H	Yield Ar-Ar	Yield Ar-THF
1	**dark**	50%	3%	0%	**0%**
2	34 W Blue LED	12%	40%	2%	**7%**
3	no oxidant	5%	2%	0%	**0%**

Fig. S128. Stoichiometric reactions of Ni(dtbbpy)(*o*-tolyl)Cl (**1–Cl**). Yields determined by GC-FID using 1-fluoronaphthalene as an external standard. Reactions were carried out at 0.025 mmol scale. Nickel complex contained trace aryl chloride remaining from synthesis which accounts for the small amount observed in the absence of oxidant.

IX. Concentration Dependent Dynamics

Methods. All samples were dispensed in stock solutions prepared volumetrically inside a nitrogen filled glove box. In a typical experiment, THF and Ni(dtbbpy)(*o*-tolyl)Cl (**1–Cl**) dispensed in THF were added to 2 mm optical glass cuvette equipped with a J. Young valve and a magnetic stir bar. The cuvette was then sealed with a J. Young cap, removed from the glovebox, and an absorption spectrum was collected. Next the sample was set to stir and transient absorption spectra (400 nm photoexcitation, 1000 μW) were collected. Extra care was taken to collect enough spectra such that after averaging the signal to noise gave narrow rate constant distributions (Figure S137). Rate constants were extracted by fitting experimental data between 470 nm and 600 nm (to avoid noise from pump scattering) after 1 ns pump-probe delay (to exclude early time dynamics) via global analysis using a single exponential decay. Rate constant distributions were generated according to the bootstrapping procedure outlined in the global analysis methods section (VI). The increase in optical density of the samples with concentration lead to requirement for additional scans to achieve sufficient averaging. After data collection was complete, the bootstrapped distributions were used to calculate standard error and confidence intervals for the rate constants (Table S15) used for kinetic modeling.

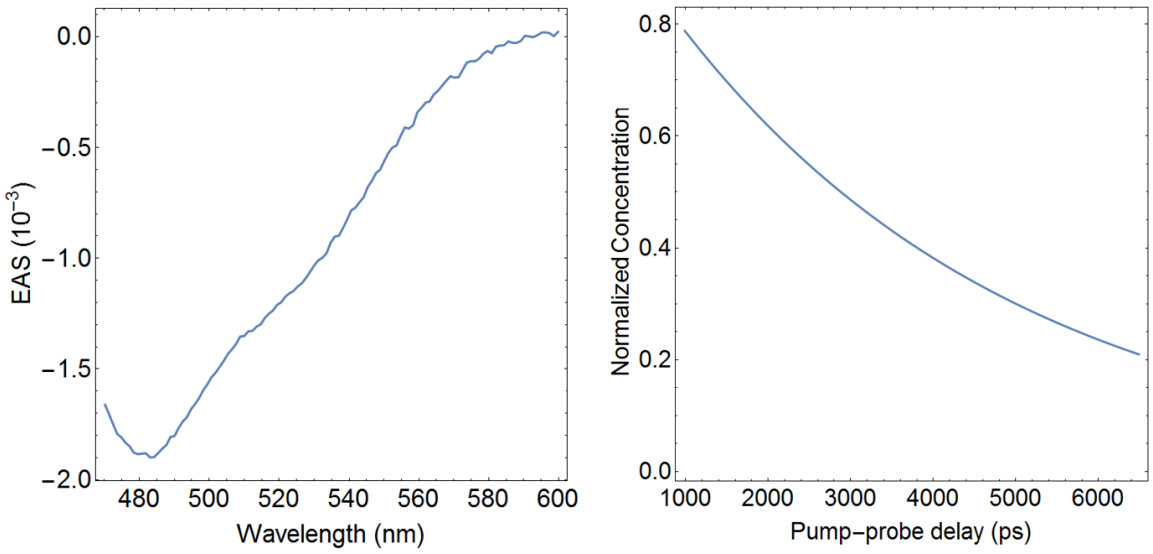

Fig. S129. Global analysis of Ni(dtbbpy)(*o*-tolyl)Cl concentration dependent transient absorption data (412 nm photoexcitation, 1000 µW, 0.63 mM Ni, 237 scans). Evolution associated spectrum (left) and concentration profile (right).

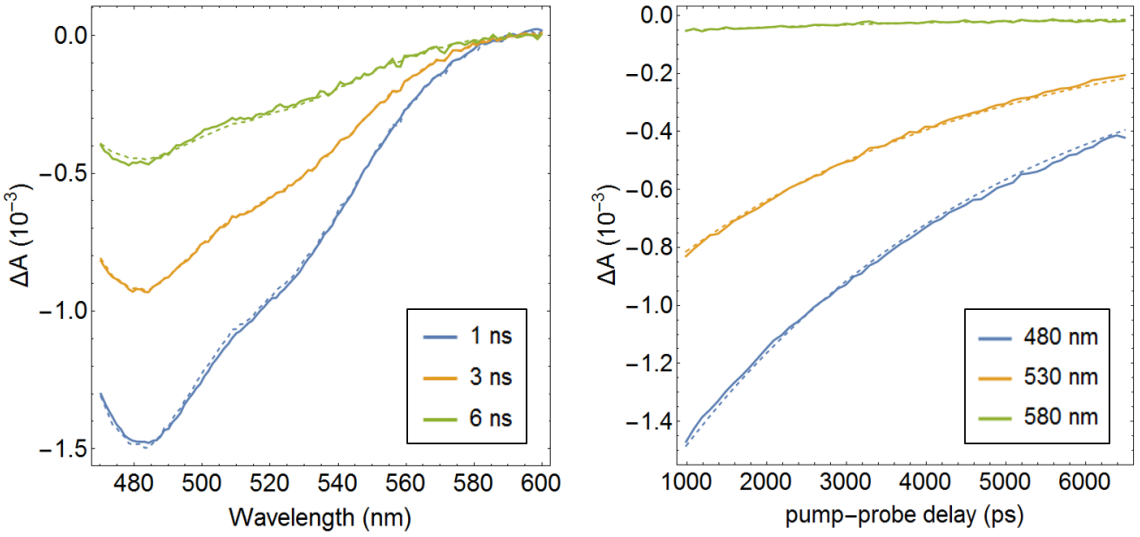

Fig. S130. Global analysis of Ni(dtbbpy)(*o*-tolyl)Cl concentration dependent transient absorption data (412 nm photoexcitation, 1000 µW, 0.63 mM Ni, 237 scans). Comparison of experimental (solid) and fit (dashed) difference absorption spectra at select pump-probe delays (left) and single wavelength kinetics (right).

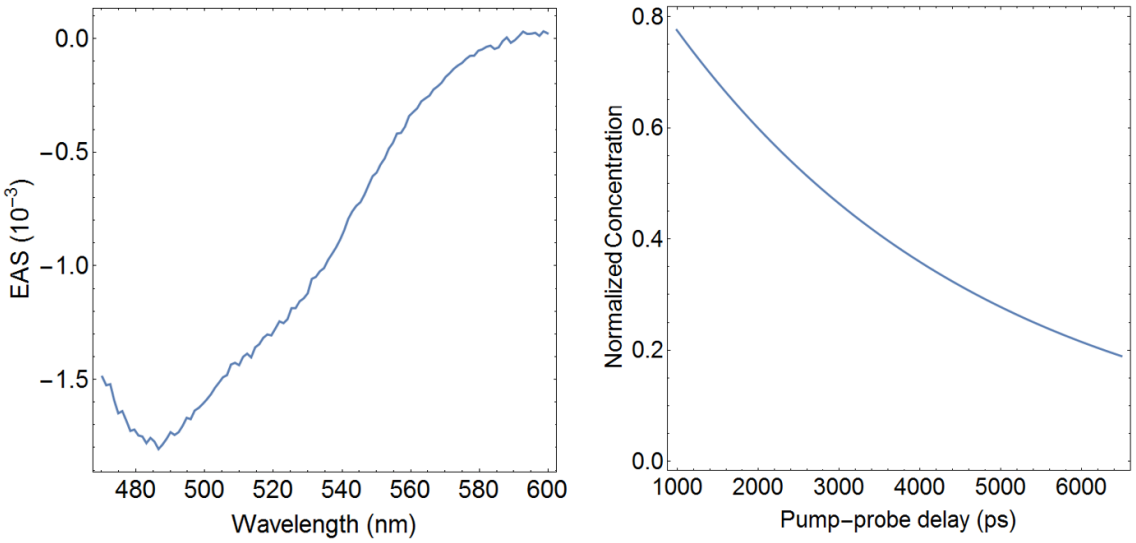

Fig. S131. Global analysis of Ni(dtbbpy)(*o*-tolyl)Cl concentration dependent transient absorption data (412 nm photoexcitation, 1000 µW, 1.31 mM Ni, 113 scans). Evolution associated spectrum (left) and concentration profile (right).

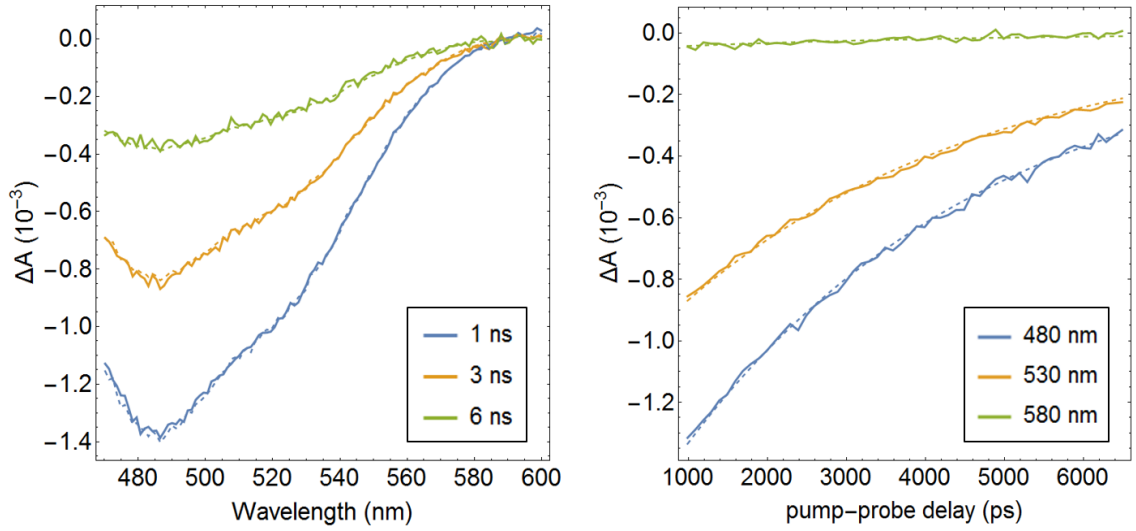

Fig. S132. Global analysis of Ni(dtbbpy)(*o*-tolyl)Cl concentration dependent transient absorption data (412 nm photoexcitation, 1000 µW, 1.31 mM Ni, 113 scans). Comparison of experimental (solid) and fit (dashed) difference absorption spectra at select pump-probe delays (left) and single wavelength kinetics (right).

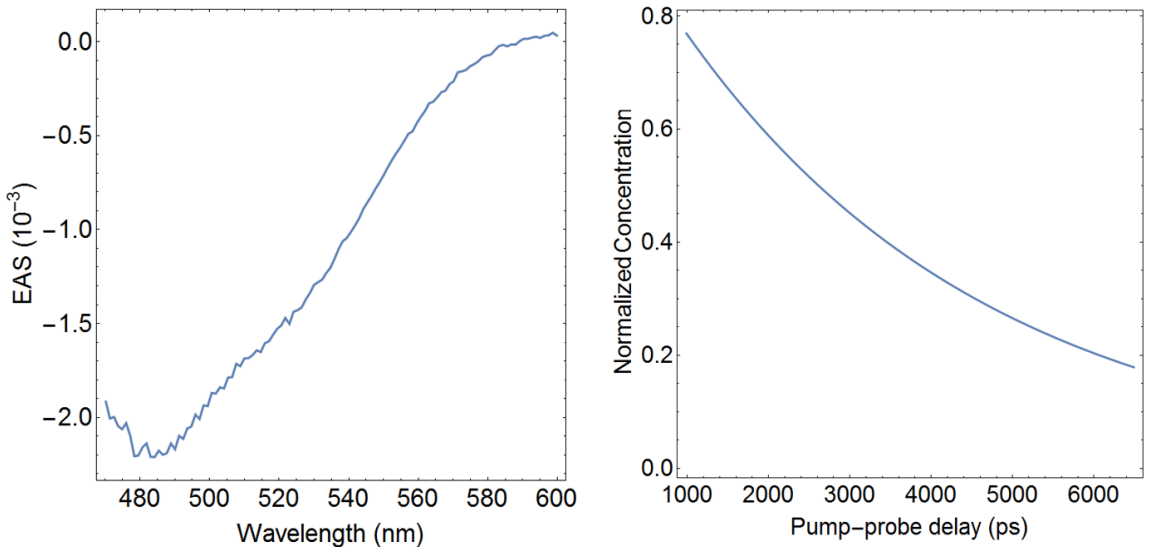

Fig. S133. Global analysis of Ni(dtbbpy)(*o*-tolyl)Cl concentration dependent transient absorption data (412 nm photoexcitation, 1000 µW, 1.98 mM Ni, 181 scans). Evolution associated spectrum (left) and concentration profile (right).

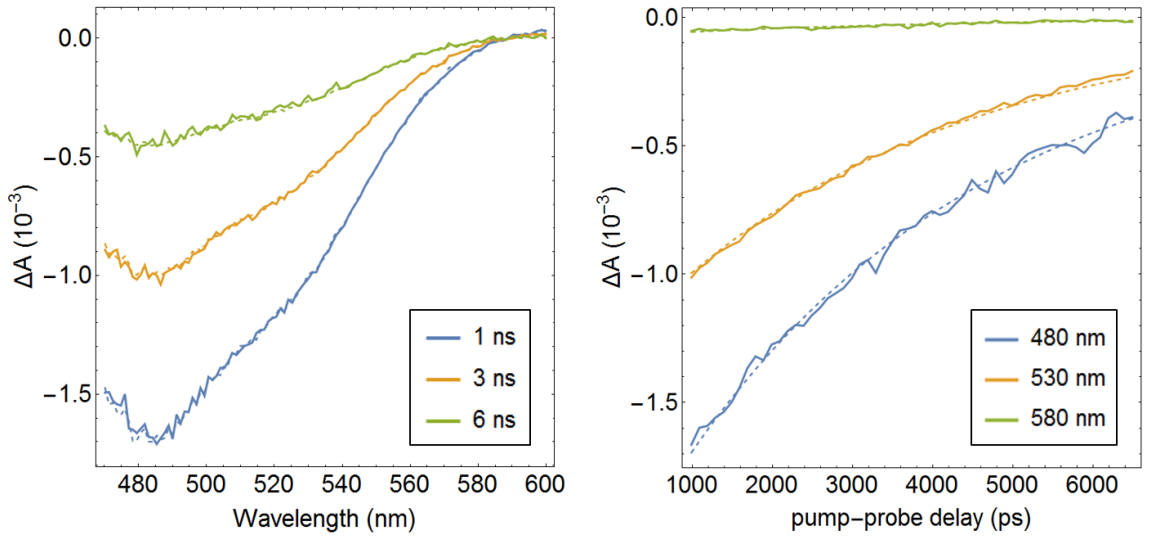

Fig. S134. Global analysis of Ni(dtbbpy)(*o*-tolyl)Cl concentration dependent transient absorption data (412 nm photoexcitation, 1000 µW, 1.98 mM Ni, 181 scans). Comparison of experimental (solid) and fit (dashed) difference absorption spectra at select pump-probe delays (left) and single wavelength kinetics (right).

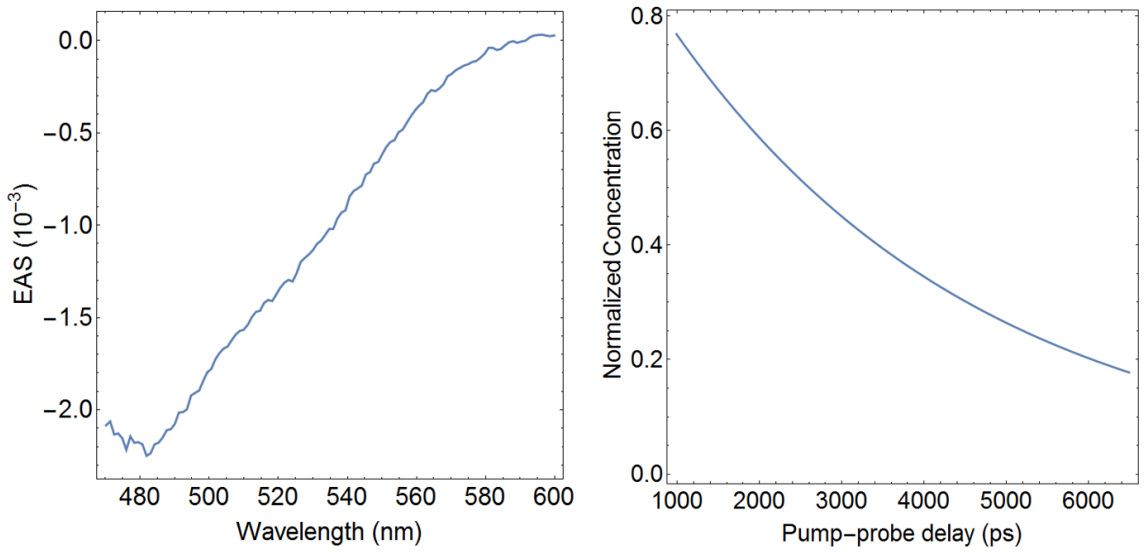

Fig. S135. Global analysis of Ni(dtbbpy)(*o*-tolyl)Cl concentration dependent transient absorption data (412 nm photoexcitation, 1000 µW, 2.66 mM Ni, 587 scans). Evolution associated spectrum (left) and concentration profile (right).

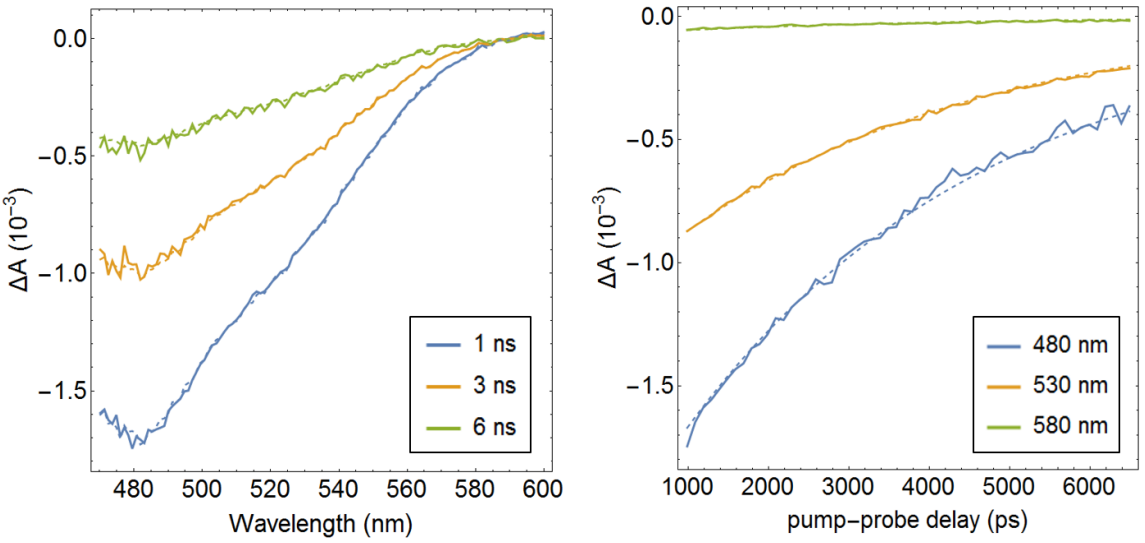

Fig. S136. Global analysis of Ni(dtbbpy)(*o*-tolyl)Cl concentration dependent transient absorption data (412 nm photoexcitation, 1000 µW, 2.66 mM Ni, 587 scans). Comparison of experimental (solid) and fit (dashed) difference absorption spectra at select pump-probe delays (left) and single wavelength kinetics (right).

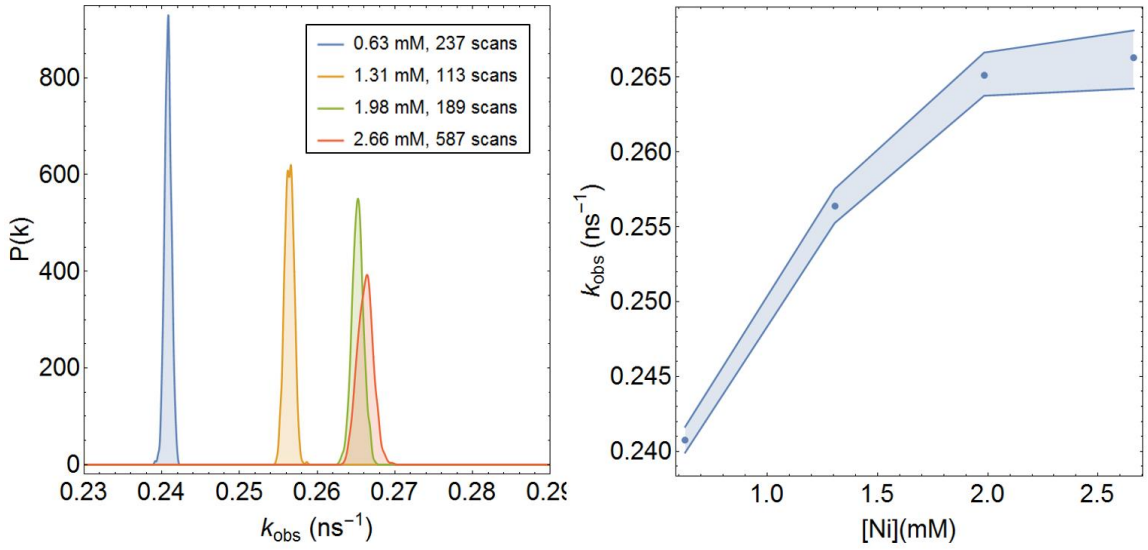

Fig. S137. Rate constant distributions (left) and [Ni] versus k_{obs} plot (right) for concentration dependent transient absorption experiments. The distribution shows smooth histograms representing the empirical rate constant distributions generated by bootstrap global analysis where the rate constants are plotted against the relative probability P(k) in arbitrary units.

[Ni] (M)	k_{obs} (ps^{-1})	SE (ps^{-1})	k_{obs}^{m} (ps^{-1})	$k_{obs}^{m} - t \times$ SE (ps^{-1})	$k_{obs}^{m} + t \times$ SE (ps^{-1})
6.27×10^{-4}	2.41×10^{-4}	4.41×10^{-7}	2.41×10^{-4}	2.40×10^{-4}	2.42×10^{-4}
1.31×10^{-3}	2.56×10^{-4}	5.81×10^{-7}	2.56×10^{-4}	2.55×10^{-4}	2.58×10^{-4}
1.98×10^{-3}	2.65×10^{-4}	7.35×10^{-7}	2.65×10^{-4}	2.64×10^{-4}	2.67×10^{-4}
2.66×10^{-3}	2.66×10^{-4}	9.90×10^{-7}	2.66×10^{-4}	2.64×10^{-4}	2.68×10^{-4}

Table S15. Fitted rate constants for concentration dependent transient absorption experiments. Concentration ([Ni]) and rate constant from initial global analysis (k_{obs}) are displayed with standard error (SE), bootstrap mean rate constant (k_{obs}^{m}) and Studentized 95% (t = 1.96) lower ($k_{obs}^{m} - t \times SE$) and upper ($k_{obs}^{m} + t \times SE$) confidence intervals. Note that k_{obs} was fit with a single exponential and thus given the units of a unimolecular rate constant.

Kinetic Modeling. For a bimolecular reaction, the observed rate of decay of the long-lived component, attributed to ^{3}MLCT$_1$ Ni, should display a Ni concentration dependence which in the limiting case of collisional quenching should take the form of a line with slope and intercept equal to the quenching rate constant and fundamental nonradiative decay rate respectively (Figure S138). Importantly, for a unimolecular decomposition reaction or reaction with solvent no concentration dependence is expected.

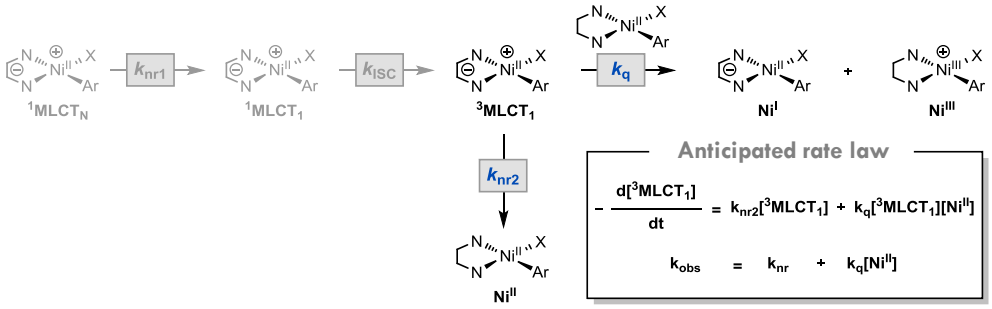

Fig. S138. Kinetics for photoinduced disproportionation via dynamic quenching pathway. A linear relationship between the concentration of Ni(dtbbpy)(*o*-tolyl)Cl (**1–Cl**) and k_{obs} is expected.

When the observed rate constant, fit using Global Analysis after 1 ns delay, is plotted against the concentration of Ni a clear concentration dependence is observed (Figure S137). However, the concentration dependence takes the form of a saturation curve rather than the line necessitated by collisional quenching. The observed negative deviation from linearity could be explained by a Michaelis-Menten-like saturation scheme (Figure S139) in which ^{3}MLCT$_1$ Ni (**c**) either associates with a ground state Ni(II) (**d**) to give excimer **e** or decays to the ground state. Next **e** could undergo charge separation to give ion pair **f** or decay to the ground state. Finally, **f** can either undergo back electron transfer to give two equivalents of **d** or dissociate to form a solvent separated ion pair towards the observed decomposition

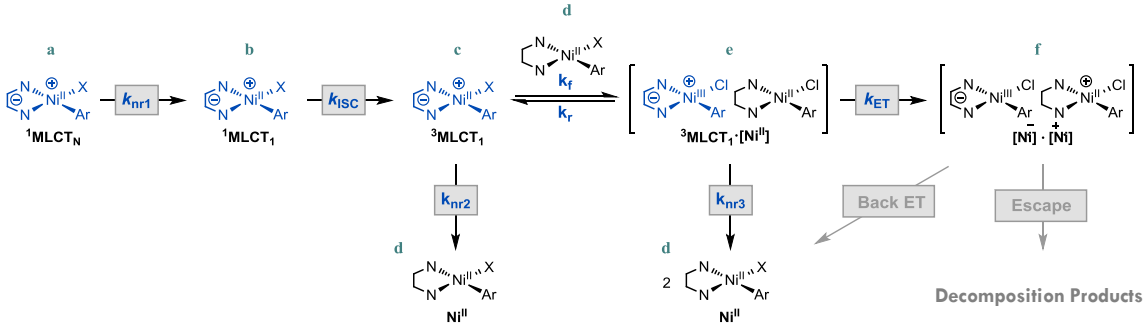

Fig. S139. Kinetics for photoinduced disproportionation via reversible association: Michaelis-Menten-like excited state kinetics.

products. To gauge the feasibility of this mechanism, a modeling approach was taken in which the rate law for the proposed pathway:

$$\frac{d[\mathrm{a}]}{d\mathrm{t}} = -k_{\mathrm{nr1}}[\mathrm{a}]$$

$$\frac{d[\mathrm{b}]}{d\mathrm{t}} = k_{\mathrm{nr1}}[\mathrm{a}] - k_{\mathrm{ISC}}[\mathrm{b}]$$

$$\frac{d[\mathrm{c}]}{d\mathrm{t}} = k_{\mathrm{ISC}}[\mathrm{b}] + k_{\mathrm{r}}[\mathrm{e}] - k_{\mathrm{nr2}}[\mathrm{c}] - k_{\mathrm{f}}[\mathrm{c}][\mathrm{d}]$$

$$\frac{d[\mathrm{d}]}{d\mathrm{t}} = k_{\mathrm{nr2}}[\mathrm{c}] + 2k_{\mathrm{nr3}}[\mathrm{e}] + k_{\mathrm{r}}[\mathrm{e}] - k_{\mathrm{f}}[\mathrm{c}][\mathrm{d}]$$

$$\frac{d[\mathrm{e}]}{d\mathrm{t}} = k_{\mathrm{f}}[\mathrm{c}][\mathrm{d}] - k_{\mathrm{r}}[\mathrm{e}] - k_{\mathrm{nr3}}[\mathrm{e}] - k_{\mathrm{ET}}[\mathrm{e}]$$

$$\frac{d[\mathrm{f}]}{d\mathrm{t}} = k_{\mathrm{ET}}[\mathrm{e}]$$

was solved numerically at different initial concentrations of Ni and the resulting kinetics for the observable decay of **c** and **e** after 1 ns were fit with a single exponential decay, in a manor analogous to experimental data analysis, to generate a k_{obs} versus concentration plot.

The following is the algorithm and corresponding *Mathematica* code were used to carry out simulations:

1. Measured concentrations, corresponding k_{obs} from global analysis, and bootstrap confidence intervals were loaded into *Mathematica*. The concentration versus k_{obs} data was then interpolated to generate additional concentrations to aid in the visualization of simulation results.

```
experimental={{0.0006271186440677966`,0.000240732`},{0.001305084745762712`,0.000256
383`},{0.001983050847457627`,0.000265136`},{0.002661016949152542`,0.000266315`}};

fitintervals={{{0.0006271186440677966`,0.000239918`},{0.001305084745762712`,0.0002552
5`},{0.001983050847457627`,0.000263757`},{0.002661016949152542`,0.000264235`}},{{0.00
06271186440677966`,0.000241646`},{0.001305084745762712`,0.000257529`},{0.001983050
847457627`,0.000266637`},{0.002661016949152542`,0.000268114`}}};

low=fitintervals[[1]];
high=fitintervals[[2]];

experimentalinterpolation=Table[{t,Interpolation[experimental][t]},{t,0.000627118644067796
6`,0.002661016949152542`,0.0006271186440677966`/20}];

concentrations=Transpose[experimentalinterpolation][[1]];
```

2. The initial conditions and parameters for differential equations were then defined. Both k_{nr1} and k_{ISC} were approximated from the experimental data (rate constants are in units of ps^{-1}). Note that by experimental design both corresponding components (a and b) are

no longer present at the pump-probe delay in which data analysis begins (after 1 ns). The initial population (in units of molarity) was approximated from the amplitude of the bleach after 1 ps pump-probe delay using a calibration curve and Beer's Law. The %population is then just the population divided by the measured total concentration of nickel. It was assumed that the %population was the same for each concentration. Note that all parameters were approximated from the data to best represent the observed kinetics though the exact values were not important for modeling and a fit could be found with different initial conditions.

```
knr1=5;
kISC=0.5;
population=2.06215*10^-5;
percentpopulation=population/0.0006271186440677966`;
```

3. Next a simulation function dependent on the rate constants was written. Note that this was done to enable a fit to be found by rapid screening of rate constant combinations. The simulation starts from a pump-probe delay of t=0 with the only species present being a and d with concentrations defined by the total concentration of Ni (taken from the interpolated concentrations in step 1) and %population. This function was solved from 0 to 7000 ps and gives a numerical solution to the system of differential equations defined by the specified rate constants (k_f, k_r, k_{nr2}, k_{nr3}, k_{ET}) and concentration point (n).

```
Clear[knr2,knr3,kET,kr,kf];

sim[kf_,kr_,knr2_,knr3_,kET_]:=
NDSolve[{
a'[t]==-knr1*a[t],
b'[t]==knr1*a[t]-kISC*b[t],
c'[t]==kISC*b[t]-knr2*c[t]-kf*c[t]*d[t]+kr*e[t],
d'[t]==knr2*c[t]+2knr3*e[t]+kr*e[t]-kf*c[t]*d[t],
e'[t]==kf*c[t]*d[t]-kr*e[t]-knr3*e[t]-kET*e[t],
f'[t]==kET*e[t],
a[0]==concentrations[[n]]*percentpopulation,
b[0]==0,
c[0]==0,
d[0]==concentrations[[n]]-concentrations[[n]]*percentpopulation,
e[0]==0,
f[0]==0
},{a,b,c,d,e,f},{t,0,7000}];
```

4. Rate constants were then selected, and a simulation was carried out with the first concentration point (n=1) to illustrate the results. Note that experimentally, the observable which is fit with global analysis is taken to be the total concentration of c and e. The kinetic scheme reproduces the observed saturation curve when a quasi-steady-state condition ($k_f[c][d] \approx (k_r + k_r + k_{nr3})[e]$) is met. If this condition is satisfied, there are numerous sets of rate constants which reproduce the observed kinetics. Accordingly, the fitted rate constants should not be considered to represent to true values. Rather the important fact to consider is whether the saturation scheme can reproduce the observed kinetics. This section of code gives the plots shown in figure S140.

```
kf=1.4;
kr=0.0006;
knr2=0.00019;
knr3=0.00027;
kET=0.000011;

values={kf,kr,knr2,knr3,kET};

n=1;
ss=sim[values[[1]],values[[2]],values[[3]],values[[4]],values[[5]]];

Show[
Plot[
{Evaluate[10^6*a[t]/.ss],10^6*Evaluate[b[t]/.ss],10^6*Evaluate[c[t]/.ss],10^6*Evaluate[e[t]/.ss
],10^6*Evaluate[c[t]/.ss]+10^6*Evaluate[e[t]/.ss],10^6*Evaluate[f[t]/.ss]},
{t,0,7000},
PlotLegends->{"a","b","c","e","c + e","f"},
Frame->True,
ImageSize->500,
PlotRange->Full,
GridLines->Automatic,
FrameStyle->Directive[Black,18],
AspectRatio->1,
FrameLabel->{"t (ps)","[Ni] (\[Mu]M)"}
],
Plot[
{(10^6*Evaluate[c[t]/.ss]+10^6*Evaluate[e[t]/.ss])-
0.25,(10^6*Evaluate[c[t]/.ss]+10^6*Evaluate[e[t]/.ss])+0.25},
{t,0,7000},
PlotStyle->Directive[ColorData[97,5],Opacity[0.1]],
Filling->{1->{2}}
]
]

Plot[
{Evaluate[10^6*a[t]/.ss],10^6*Evaluate[b[t]/.ss],10^6*Evaluate[c[t]/.ss],10^6*Evaluate[e[t]/.ss
],10^6*Evaluate[c[t]/.ss]+10^6*Evaluate[e[t]/.ss],10^6*Evaluate[f[t]/.ss]},
{t,0,10},
PlotLegends->{"a","b","c","e","c + e","f"},
Frame->True,
ImageSize->500,
PlotRange->Full,
GridLines->Automatic,
FrameStyle->Directive[Black,18],
AspectRatio->1,
FrameLabel->{"t (ps)","[Ni] (\[Mu]M)"}
]
```

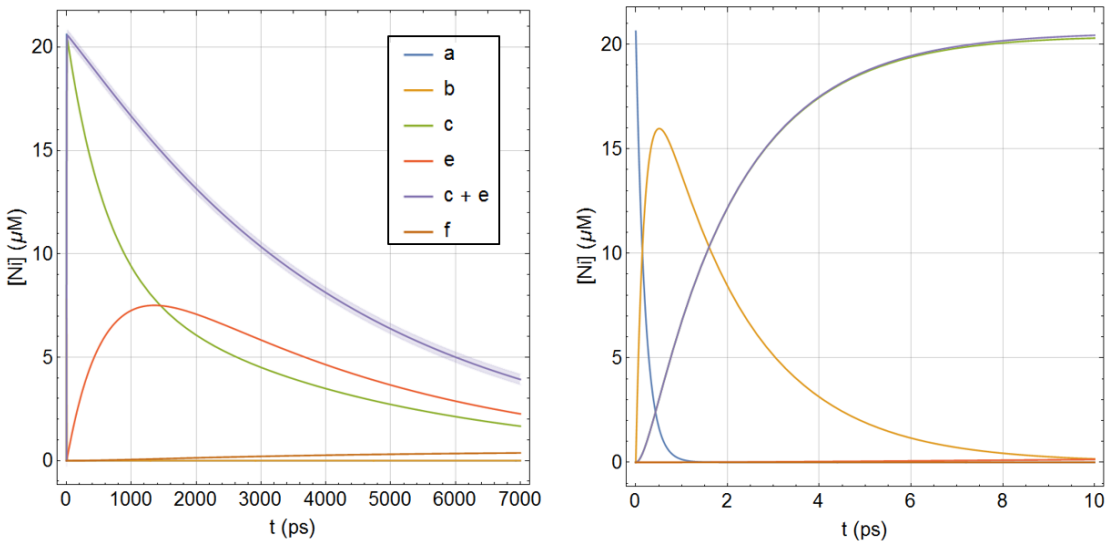

Fig. S140. Simulated kinetics for photoinduced disproportionation pathway. Initial conditions: $[a]_{t=0} = [Ni] \times$ %population, $[b]_{t=0} = 0$, $[c]_{t=0} = 0$, $[d]_{t=0} = [Ni] \times (1 -$ %population), $[e]_{t=0} = 0$, $[f]_{t=0} = 0$. Full time course (left) an initial dynamics (right).

5. Next the numerical solution for the concentration of c and e (an interpolation function highlighted in purple in figure S140) was converted to a set of pump-probe delay (*t*) versus concentration (*c* + *e*) data points, the natural log of the concentration was taken, a linear regression of the *t* versus *ln*(c + e) was carried out, and the initial concentration of nickel was paired with the resulting slope of the line. This process was carried out for each initial concentration of nickel (taken from the interpolated concentrations in step 1). Algorithmically, this was done in parallel by first generating a time versus concentration matrix for all initial concentration values and then carrying out the above analysis on each set.

```
simkin=
ParallelTable[
Module[{},
n=k;
ss=sim[values[[1]],values[[2]],values[[3]],values[[4]],values[[5]]];
Map[Flatten,Table[{t,(Evaluate[c[t]/.ss]+Evaluate[e[t]/.ss])},{t,1000,7000,100}]]
],
{k,1,Count[experimentalinterpolation,x_],1}
];

logger[{x_,y_}]:={x,Log[y]};
abs[{x_,y_}]:={x,Abs[y]};
simkinln=Table[Map[logger,Map[abs,simkin[[m]]]],{m,1,Count[simkin,x_],1}];
points=Thread[{concentrations,ParallelTable[Abs[LinearModelFit[simkinln[[m]],t,t]["BestFitPar
ameters"][[2]]],{m,1,Count[simkin,x_],1}]}];
```

6. The raw output can then be visualized to qualitatively check for a fit with the interpolated experimental data. Finally, the simulated data can be plotted together with

the experimental data and bootstrap confidence intervals. The raw simulation output and processed plot can be seen in figure S141.

```
ListPlot[{points,experimentalinterpolation},
Frame->True,
GridLines->Automatic,
ImageSize->500,
FrameStyle->Directive[Black,18],
PlotStyle->{ColorData[97,2],ColorData[97,1]},
AspectRatio->1,
FrameLabel->{"[Ni] (M)","Subscript[k, obs] (ps^-1)"}]

Show[
ListPlot[
{1000*experimental,Null},
Frame->True,
GridLines->Automatic,
ImageSize->500,
FrameStyle->Directive[Black,18],
PlotStyle->{ColorData[97,2],ColorData[97,1]},
AspectRatio->1,
FrameLabel->{"[Ni] (mM)","Subscript[k, obs] (ns^-1)"},
PlotRange->{{0.6,2.7},{0.237,0.27}}
],
ListLinePlot[
{1000*low,1000*high},
PlotStyle->Directive[ColorData[97,2],Opacity[0.1]],
Filling->{1->{2}}
],
ListLinePlot[
{1000*points,Null},
PlotStyle->{Directive[Dashed,Thick],Directive[Thick]},
PlotLegends->{Style["Numerical Simulation",18],Style["Experimental and 95% Subscript[CI, Fit]",18]}
]
]
```

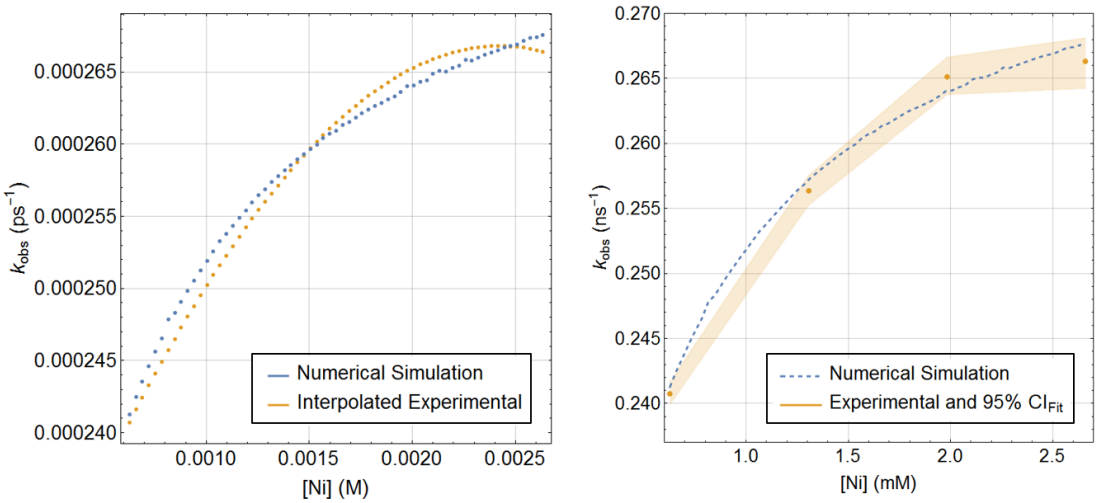

Fig. S141. Comparison of simulated and experimental concentration versus k_{obs} plots. Unprocessed simulation output (left) is plotted together with interpolated experimental data. Numerical simulation output (shown as an interpolated line rather than as individual points) is plotted against experimental data with 95% confidence intervals (right).

X. C–O Coupling Experiments

Representative Procedure. A ½-dram vial (Fisher part number: 03-338AA) equipped with a PTFE-coated stir bar was brought into a N_2-filled glove box and charged with K_3PO_4 (21.2 mg, 0.1 mmol, 2 equiv.). To the reaction vial the following were added successively: a clear stock solution of 4-bromoacetophenone (10.0 mg, 0.05 mmol, 1 equiv) in THF (0.5 mL), and a dark purple solution of $Ni(cod)_2$ (1.4 mg, 5 μmol, 0.1 equiv.) and 4,4′-di-*tert*-butyl-2,2′-bipyridine (1.4 mg, 5 μmol, 0.1 equiv.) in THF (0.5 mL). The vial was capped with a Teflon septum cap and sealed with electrical tape. The reaction vial was removed from the glove box, set to stir (800 rpm) and irradiated with a blue LED array (Figure S142, cooled with both a fan above and pressurized air that was directed through tygon tubing mounted next to the reaction array) for 15 hours. The crude reaction was analyzed by GC-FID relative to 1-fluoronaphthalene as an external standard. Note: the authentic products 4'-butoxyacetophenone and 4,4'-diacetylbiphenyl were purchased from Sigma Aldrich and used to determine a response factors and retention times for GC-FID quantification.

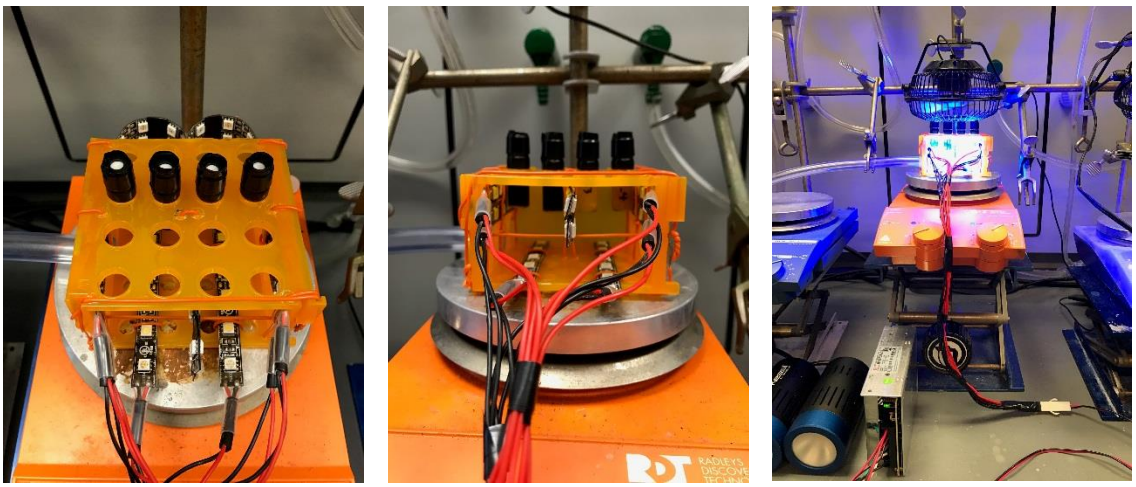

Figure S142. Example of a blue LED array used for small scale screening.

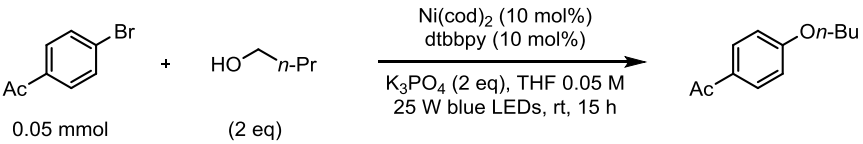

Entry	Control	Ar-Br Conversion	Ar-O*n*-Bu Yield
1[a]	None	47%	**41%**
2[a]	Dark	24%	**18%**
3	No Ni/dtbbpy	11%	**0%**
4	No K_3PO_4	13%	**3%**

Fig. S143. Initial discovery and controls for C–O coupling reaction. Yield and conversion determined by GC-FID using 1-fluoronaphthalene as an external standard. (a) Reactions ran for 19 h.

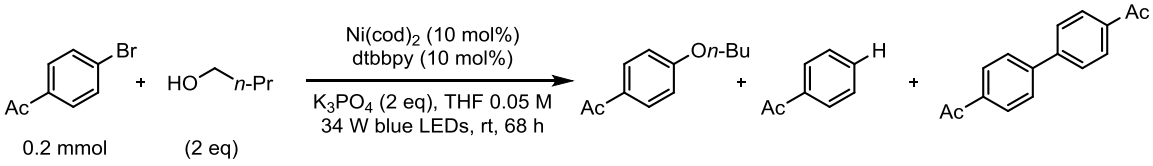

Entry	Control	Ar-Br Conversion	Ar-O*n*-Bu Yield	Ar-H Yield	Ar-Ar Yield
1	None	100%	**79%**	5%	4%
2	Dark	40%	**26%**	0%	0%

Fig. S144. Experiments with temperature control. Yield and conversion determined by GC-FID using 1-fluoronaphthalene as an external standard. The dark entry was taped with electrical tape, covered with foil, and placed in front of the 34 W blue LED lamp alongside the reaction. The temperature of both solutions was measured to be 27°C after 68 h of irradiation.

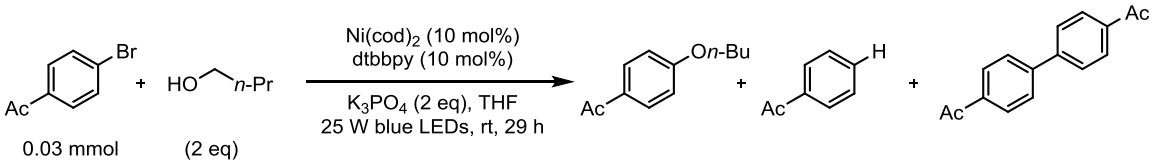

Entry	[Ar-Br] (M)	Ar-Br Conversion	Ar-O*n*-Bu Yield	Ar-H Yield	Ar-Ar Yield
1	0.025	49%	**27%**	1%	2%
2	0.05	67%	**49%**	1%	3%
3	0.10	75%	**57%**	0%	3%

Fig. S145. Concentration dependence. Yield and conversion determined by GC-FID using 1-fluoronaphthalene as an external standard. The reaction showed a significant concentration dependence, consistent with photoinduced disproportionation hypothesis.

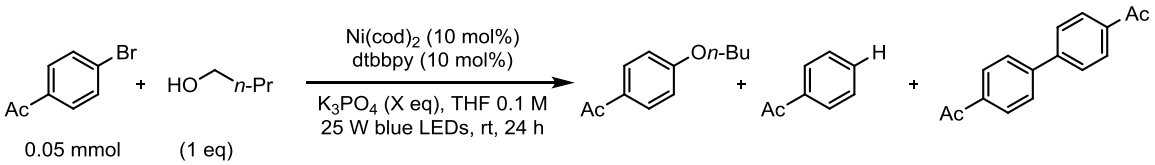

Entry	K_3PO_4	Ar-Br Conversion	Ar-O*n*-Bu Yield	Ar-H Yield	Ar-Ar Yield
1	1 eq	52%	**32%**	1%	3%
2	2 eq	76%	**56%**	1%	4%
3	3 eq	88%	**67%**	1%	7%

Fig. S146. Base equivalents screen. Yield and conversion determined by GC-FID using 1-fluoronaphthalene as an external standard.

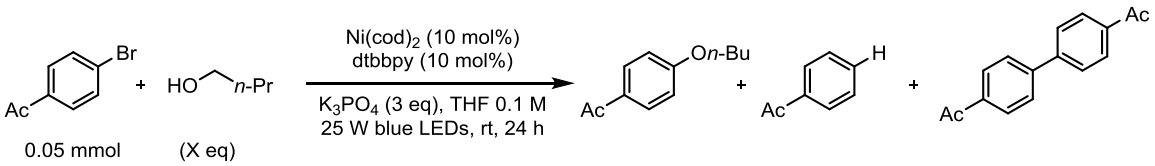

Entry	*n*-BuOH	Ar-Br Conversion	Ar-O*n*-Bu Yield	Ar-H Yield	Ar-Ar Yield
1	1 eq	88%	**67%**	1%	7%
2	1.5 eq	91%	**74%**	1%	5%
3	2 eq	92%	**75%**	1%	4%

Fig. S147. Alcohol equivalents screen. Yield and conversion determined by GC-FID using 1-fluoronaphthalene as an external standard.

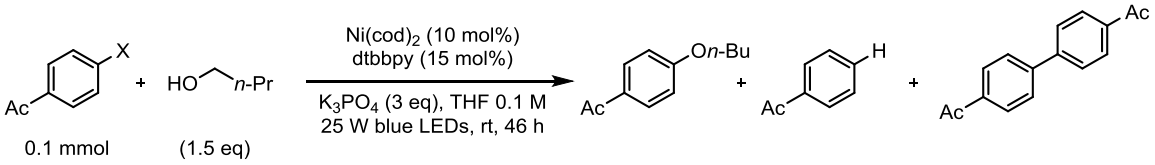

Entry	X	Ar-X Conversion	Ar-O*n*-Bu Yield	Ar-H Yield	Ar-Ar Yield
1	Cl	38%	**4%**	0%	10%
2[a]	Br	100%	**80%**	1%	14%
3	I	100%	**79%**	0%	6%

Fig. S148. Halide screen. Yield and conversion determined by GC-FID using 1-fluoronaphthalene as an external standard. The observed reactivity correlates with the expected ability of Ni(I)(dtbbpy)(O*n*-Bu) to undergo oxidative addition. (a) Reaction was run for 44 h.

Discussion. We considered possible mechanisms for the observed C–O coupling reaction with emphasis on mechanisms that could explain both the observed thermal and photochemical outcomes (Figure S138). Preliminary data collected from computational and optimization studies is most consistent with the mechanism outlined in figure S149. Computational studies suggest that reductive elimination from a Ni(II) aryl alkoxide complex is not thermodynamically feasible with a computed free energy change of +45 kcal mol^{-1} (Figure S34). In contrast, reductive elimination from a Ni(III) aryl alkoxide complex **I** to give the observed C–O coupling product and Ni(I) species **G** was computed to be exergonic with a free energy change of -39 kcal mol^{-1} (Figure S33). Subsequent ligand exchange would result in the generation of Ni(I) alkoxide complex **H** which could then undergo oxidative addition to regenerate **I** (approximately thermoneutral: ΔG = +4 kcal mol^{-1}, Figure S35) to turn over the catalytic cycle.

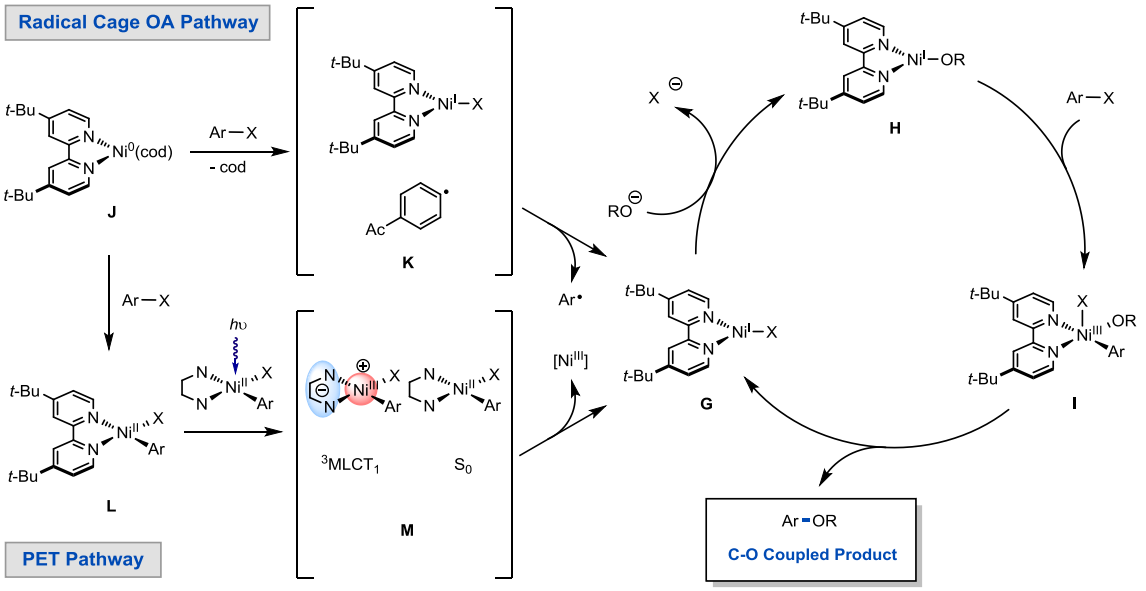

Fig. S149. Proposed catalytic cycle.

It is well known that oxidative addition of aryl halides to Ni(0) proceeds via a radical cage pathway, either undergoing cage collapse to generate Ni(II) aryl halide complexes or cage escape to generate Ni(I) and an aryl radical.[42] Starting from Ni(0) precatalyst **J**, oxidative addition via the radical cage escape mechanism could account for the observed product formation in the absence of light by generation of on cycle Ni(I) species **G**. However, only a fraction of oxidative addition steps would result in the generation of Ni(I) while the remainder would result in the generation of Ni(II) aryl halide complex **L**. By analogy to the photophysics Ni(II)(*o*-tolyl) halide complexes studied in this manuscript, irradiation of **L** should generate ^{3}MLCT Ni(II) which could then engage in bimolecular electron transfer with ground state Ni(II) to give a Ni(III) complex and on cycle Ni(I) complex **G**. Note that the Ni(III) Aryl halide complex generated in this way could undergo reductive elimination of Ar–X, providing an additional equivalent of on cycle Ni(I) without actually consuming aryl halide. Therefore, photoinitiation of a thermal Ni(I)/Ni(III) C–O catalytic cycle could account for the significant increase reaction efficiency observed upon irradiation. It is

noteworthy that preliminary optimization studies are consistent with this proposal: (1) increased reaction efficiency was observed with increasing concentration (Figure S145) and (2) 4-iodoacetophenone and 4-bromoacetophenone efficiently provided aryl alkoxide product while 4-chloroacetophenone performed poorly (the expected rate of Ni(I) oxidative addition is Ar–I > Ar–Br > Ar–Cl).[42]

XI. LED Emission Spectrum

Emission spectra were measured on a digital spectrometer with optical fiber (Ocean Optics USB4000).

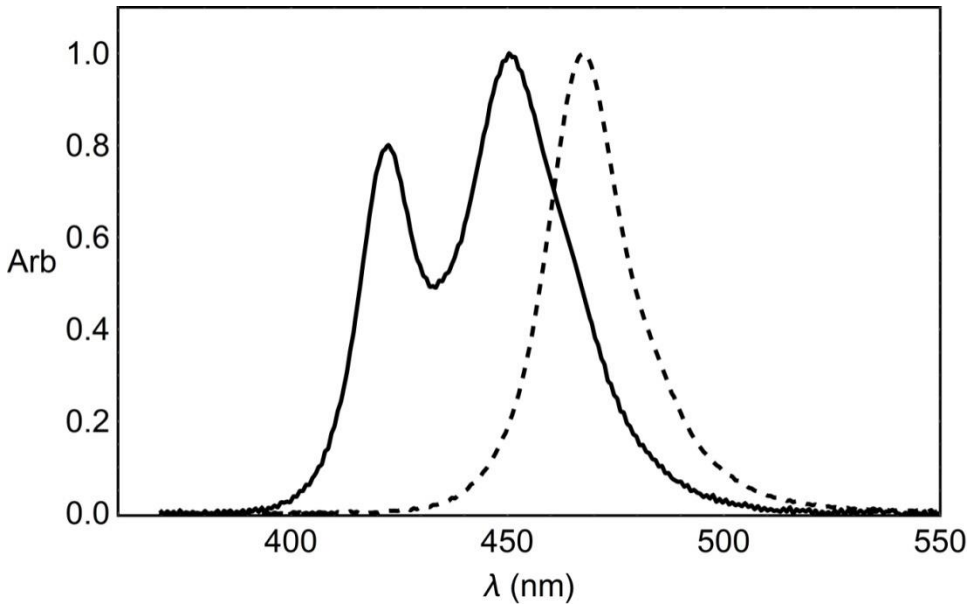

Fig. S150. Normalized emission spectra for light sources. Emission spectrum from a 25W blue LED array shown as dashed line with emission maximum at λ_{max} = 467 nm. Emission spectrum from a 34 W blue Kessil Lamp shown as solid line with emission maximum at λ_{max} = 450 nm flanked by a second peak at λ = 422 nm.

XII. Electrochemical MLCT Assignment

Computational studies of Ni(dtbbpy)(*o*-tolyl)Cl (**1–Cl**) led to the assignment of the first singlet transition at 634 nm to a MLCT. Electronic structure calculations suggest that the HOMO and LUMO of **1–Cl** are Ni-centered (dz^2 parentage) and dtbbpy-π*-centered respectively. Therefore, according to the square scheme presented in figure S151 the band gap between the first reduction and oxidation of **1–Cl** provides a good approximation of the expected $^1MLCT_1$ transition energy. Electrochemical peak potentials for Ni(dtbbpy)(*o*-tolyl)Cl (**1–Cl**) were measured via cyclic voltammetry in a previous study.[22]

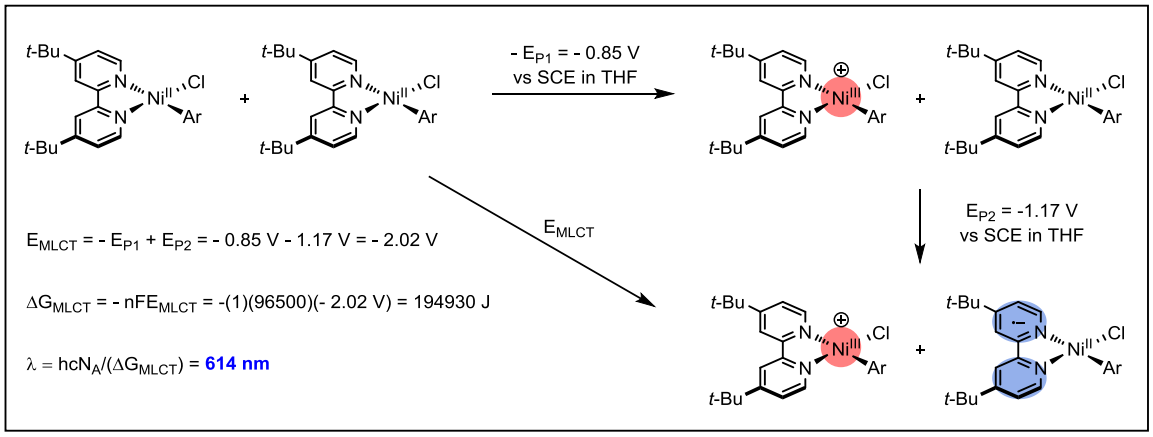

Fig. S151. Thermodynamic cycle for calculation of $^1MLCT_1$ transition energy via electrochemical peak potentials.

XIII. References

1. Nozik, A. J.; Miller, J. *Chem. Rev.* **2010**, *110*, 6443.
2. Grätzel, M. *Inorg Chem* **2005**, *44*, 6841.
3. Morris, A. J.; Meyer, G. J.; Fujita, E. *Acc. Chem. Res.* **2009**, *42*, 1983.
4. Esswein, A. J.; Nocera, D. G. *Chem. Rev.* **2007**, *107*, 4022.
5. Willkomm, J.; Orchard, K. L.; Reynal, A.; Pastor, E.; Durrant, J. R.; Reisner, E. *Chem. Soc. Rev.* **2016**, *45*, 9.
6. Romero, N. A.; Nicewicz, D. A. *Chem. Rev.* **2016**, *116*, 10075.
7. Prier, C. K.; Rankic, D. A.; MacMillan, D. W. *Chem. Rev.* **2013**, *113*, 5322.
8. Tucker, J. W.; Stephenson, C. R. *J. Org. Chem.* **2012**, *77*, 1617.
9. Schultz, D. M.; Yoon, T. P. *Science* **2014**, *343*, 1239176.
10. Kavarnos, G. J.; Turro, N. J. *Chem. Rev.* **1986**, *86*, 401.
11. Arias-Rotondo, D. M.; McCusker, J. K. *Chem. Soc. Rev.* **2016**, *45*, 5803.
12. Kalyanasundaram, K. *Coord. Chem. Rev.* **1982**, *46*, 159.
13. Liu, Y.; Persson, P.; Sundstrom, V.; Warnmark, K. *Acc. Chem. Res.* **2016**, *49*, 1477.
14. Scaltrito, D. V.; Thompson, D. W.; O'Callaghan, J. A.; Meyer, G. J. *Coord. Chem. Rev.* **2000**, *208*, 243.
15. Higgins, R. F.; Fatur, S. M.; Shepard, S. G.; Stevenson, S. M.; Boston, D. J.; Ferreira, E. M.; Damrauer, N. H.; Rappe, A. K.; Shores, M. P. *J. Am. Chem. Soc.* **2016**, *138*, 5451.
16. Creutz, S. E.; Lotito, K. J.; Fu, G. C.; Peters, J. C. *Science* **2012**, *338*, 647.
17. Balzani, V.; Bergamini, G.; Campagna, S.; Puntoriero, F. *Top. Curr. Chem*. **2007**, *280*, 1.
18. Caspar, J. V.; Meyer, T. J. *J. Am. Chem. Soc.* **1983**, *105*, 5583.
19. Cannizzo, A.; Milne, C. J.; Consani, C.; Gawelda, W.; Bressler, C.; van Mourik, F.; Chergui, M. *Coord. Chem. Rev.* **2010**, *254*, 2677.
20. Zuo, Z.; Ahneman, D. T.; Chu, L.; Terrett, J. A.; Doyle, A. G.; MacMillan, D. W. C. *Science* **2014**, *345*, 437.
21. Tellis, J. C.; Primer, D. N.; Molander, G. A. *Science* **2014**, *345*, 433.
22. Shields, B. J.; Doyle, A. G. *J. Am. Chem. Soc.* **2016**, *138*, 12719.
23. Heitz, D. R.; Tellis, J. C.; Molander, G. A. *J. Am. Chem. Soc.* **2016**, *138*, 12715.
24. Chergui, M. *Acc. Chem. Res.* **2015**, *48*, 801.
25. Powers, D. C.; Anderson, B. L.; Nocera, D. G. *J. Am. Chem. Soc.* **2013**, *135*, 18876.
26. Lockwood, G.; McGarvey, J. J.; Devonshire, R. *Chem. Phys. Lett.* **1982**, *86*, 127.
27. Hwang, S. J.; Powers, D. C.; Maher, A. G.; Anderson, B. L.; Hadt, R. G.; Zheng, S. L.; Chen, Y. S.; Nocera, D. G. *J. Am. Chem. Soc.* **2015**, *137*, 6472.
28. Klein, A.; Kaiser, A.; Wielandt, W.; Belaj, F.; Wendel, E.; Bertagnolli, H.; Zalis, S. *Inorg. Chem.* **2008**, *47*, 11324.
29. Biswas, S.; Weix, D. J. *J. Am. Chem. Soc.* **2013**, *135*, 16192.
30. Frei, F.; Rondi, A.; Espa, D.; Mercuri, M. L.; Pilia, L.; Serpe, A.; Odeh, A.; Van Mourik, F.; Chergui, M.; Feurer, T.; Deplano, P.; Vlcek, A.; Cannizzo, A. *Dalton Trans.* **2014**, *43*, 17666.
31. Noviandri, I.; Brown, K. N.; Fleming, D. S.; Gulyas, P. T.; Lay, P. A.; Masters, A. F.; Phillips, L. *J. Phys. Chem. B.* **1999**, *103*, 6713.
32. Brown, K. E.; Salamant, W. A.; Shoer, L. E.; Young, R. M.; Wasielewski, M. R. *J.*

Phys. Chem. Lett. **2014**, *5*, 2588.
33. Ishida, N.; Masuda, Y.; Ishikawa, N.; Murakami, M. *Asian J. Org. Chem.* **2017**, *6*, 669.
34. Welin, E. R.; Le, C.; Arias-Rotondo, D. M.; McCusker, J. K.; MacMillan, D. W. C. *Science* **2017**, *355*, 380.
35. Frisch, M. J.; Trucks, G. W.; Schlegel, H. B.; Scuseria, G. E.; Robb, M. A.; Cheeseman, J. R.; Scalmani, G.; Barone, V.; Mennucci, B.; Petersson, G. A.; Nakatsuji, H.; Caricato, M.; Li, X.; Hratchian, H. P.; Izmaylov, A. F.; Bloino, J.; Zheng, G.; Sonnenberg, J. L.; Hada, M.; Ehara, M.; Toyota, K.; Fukuda, R.; Hasegawa, J.; Ishida, M.; Nakajima, T.; Honda, Y.; Kitao, O.; Nakai, H.; Vreven, T.; Montgomery, J. A., Jr.; Peralta, J. E.; Ogliaro, F.; Bearpark, M.; Heyd, J. J.; Brothers, E.; Kudin, K. N.; Staroverov, V. N.; Keith, T.; Kobayashi, R.; Normand, J.; Raghavachari, K.; Rendell, A.; Burant, J. C.; Iyengar, S. S.; Tomasi, J.; Cossi, M.; Rega, N.; Millam, J. M.; Klene, M.; Knox, J. E.; Cross, J. B.; Bakken, V.; Adamo, C.; Jaramillo, J.; Gomperts, R.; Stratmann, R. E.; Yazyev, O.; Austin, A. J.; Cammi, R.; Pomelli, C.; Ochterski, J. W.; Martin, R. L.; Morokuma, K.; Zakrzewski, V. G.; Voth, G. A.; Salvador, P.; Dannenberg, J. J.; Dapprich, S.; Daniels, A. D.; Farkas, O.; Foresman, J. B.; Ortiz, J. V.; Cioslowski, J.; Fox, D. J. Gaussian 09, revision D.01; Gaussian, Inc.: Wallingford, CT, 2009.
36. Frisch, M. J.; Trucks, G. W.; Schlegel, H. B.; Scuseria, G. E.; Robb, M. A.; Cheeseman, J. R.; Scalmani, G.; Barone, V.; Petersson, G. A.; Nakatsuji, H.; Li, X.; Caricato, M.; Marenich, A. V.; Bloino, J.; Janesko, B. G.; Gomperts, R.; Mennucci, B.; Hratchian, H. P.; Ortiz, J. V.; Izmaylov, A. F.; Sonnenberg, J. L.; Williams-Young, D.; Ding, F.; Lipparini, F.; Egidi, F.; Goings, J.; Peng, B.; Petrone, A.; Henderson, T.; Ranasinghe, D.; Zakrzewski, V. G.; Gao, J.; Rega, N.; Zheng, G.; Liang, W.; Hada, M.; Ehara, M.; Toyota, K.; Fukuda, R.; Hasegawa, J.; Ishida, M.; Nakajima, T.; Honda, Y.; Kitao, O.; Nakai, H.; Vreven, T.; Throssell, K.; Montgomery, J. A., Jr.; Peralta, J. E.; Ogliaro, F.; Bearpark, M. J.; Heyd, J. J.; Brothers, E. N.; Kudin, K. N.; Staroverov, V. N.; Keith, T. A.; Kobayashi, R.; Normand, J.; Raghavachari, K.; Rendell, A. P.; Burant, J. C.; Iyengar, S. S.; Tomasi, J.; Cossi, M.; Millam, J. M.; Klene, M.; Adamo, C.; Cammi, R.; Ochterski, J. W.; Martin, R. L.; Morokuma, K.; Farkas, O.; Foresman, J. B.; Fox, D. J. Gaussian 16, Revision A.03; Gaussian, Inc., Wallingford CT, 2016.
37. Niehaus, T. A.; Hofbeck, T.; Yersin, H. *RSC Adv.* **2015**, *5*, 63318.
38. Nguyen, K. A.; Kennel, J. *J. Chem. Phys.* **2002**, *117*, 7128.
39. Lakowicz, J. R. Principles of Fluorescence Spectroscopy; Kluwer Academic/ Plenum Publishers: New York, 1999.
40. Mullen, K. M.; van Stokkum, I. H. M. *J. Stat. Software* **2007**, *18*, 3.
41. Snellenburg, J. J.; Laptenok, S.; Seger, R.; Mullen, K. M.; van Stokkum, I. H. M. *J. Stat. Software* **2012**, *49*, 3.
42. Tsou, T. T.; Kochi, J. K. *J. Am. Chem. Soc.* **1979**, *101*, 6319.

XIV. NMR Spectra

NMR data. Chemical shifts for protons are reported in parts per million downfield from tetramethylsilane and are referenced to residual protium in the NMR solvent (DCM = δ 5.32 ppm, THF = δ 1.73 and 3.58 ppm). Chemical shifts for carbon are reported in parts per million downfield from tetramethylsilane and are referenced to the carbon resonances of the solvent residual peak (DCM-d_2 = δ 54.0 ppm, THF = δ 25.4 and 67.6 ppm). NMR data are represented as follows: chemical shift (δ ppm), multiplicity (s = singlet, d = doublet, t = triplet, q = quartet, p = pentet, m = multiplet), coupling constant in Hertz (Hz), integration.

^{1}H NMR (501 MHz, DCM-d2): Ni(dtbbpy)(*o*-tolyl)Cl (1–Cl)

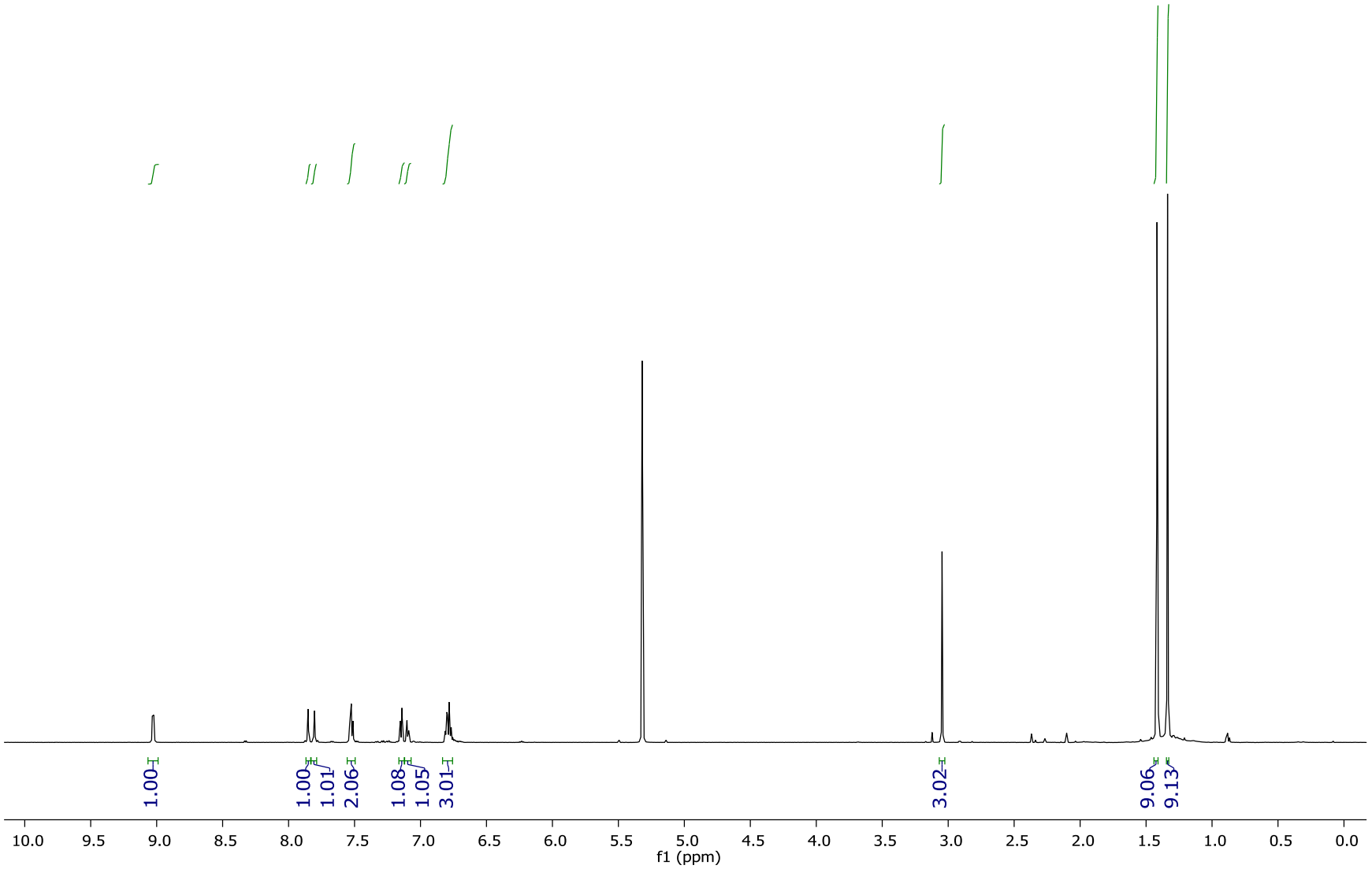

^{13}C NMR (126 MHz, DCM-d2, APT): Ni(dtbbpy)(*o*-tolyl)Cl (1–Cl)

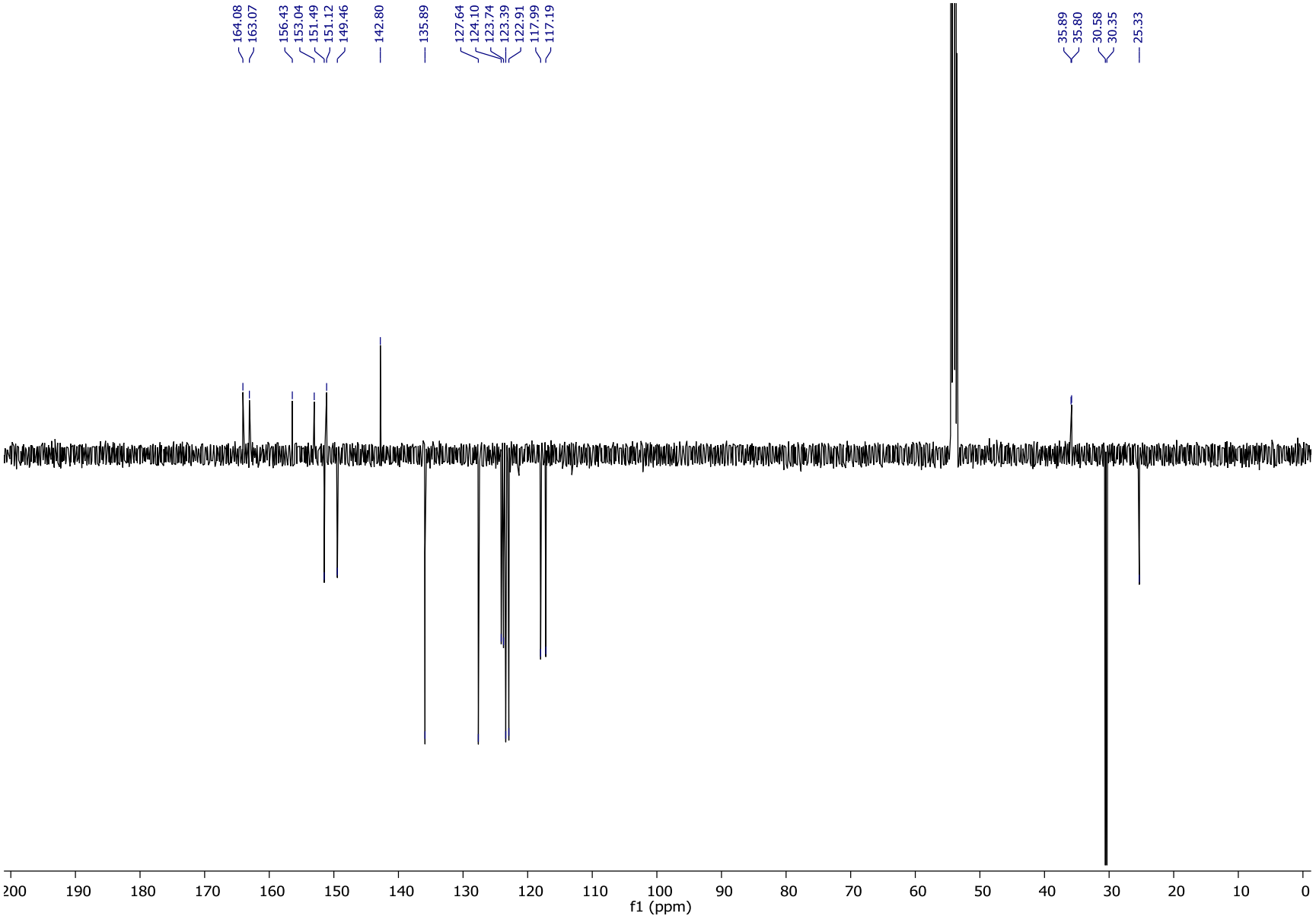

^{1}H NMR (501 MHz, DCM-d2): Ni(dtbbpy)(*o*-tolyl)Br (1–Br)

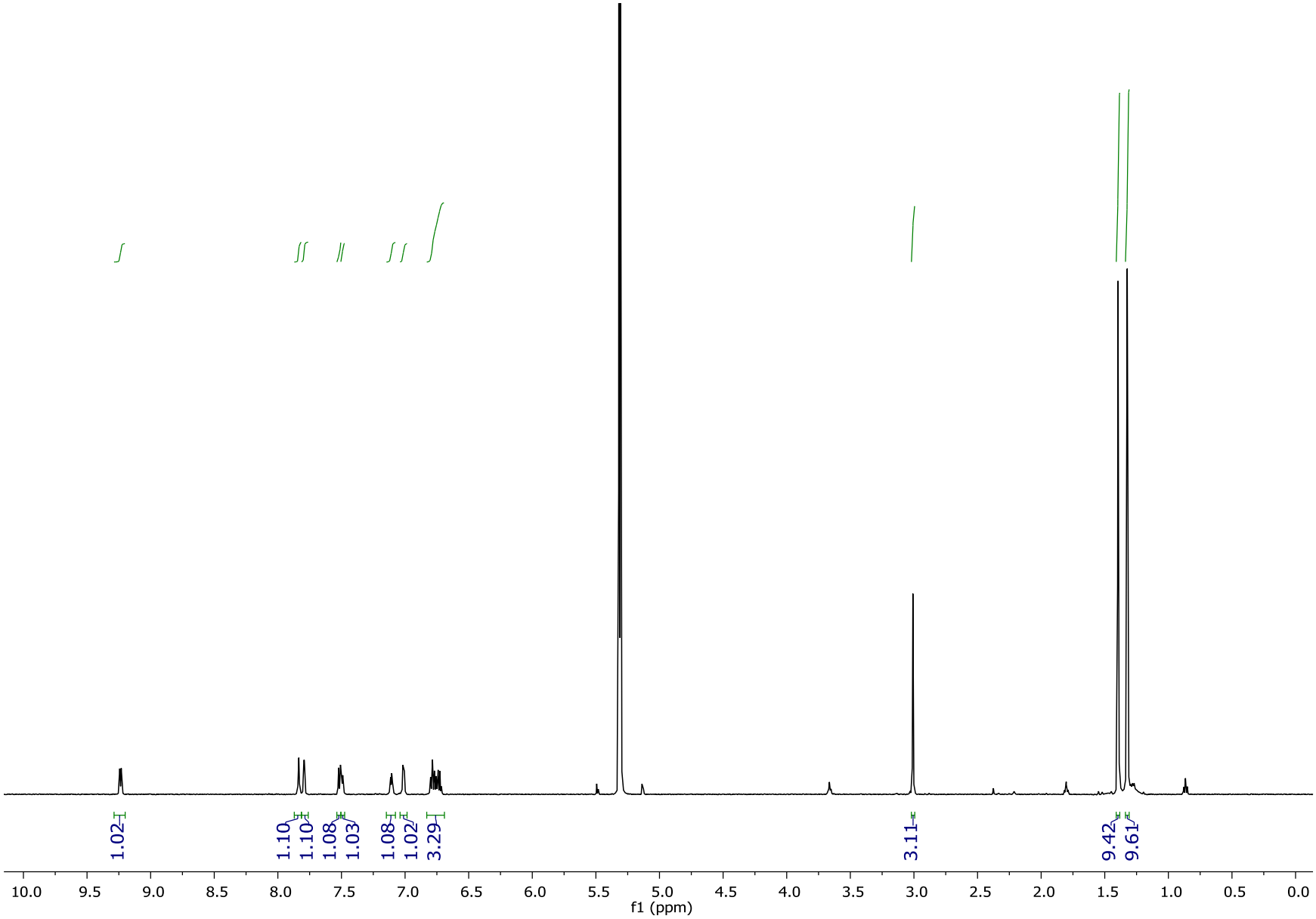

^{13}C NMR (126 MHz, DCM-d2): Ni(dtbbpy)(*o*-tolyl)Br (1–Br)

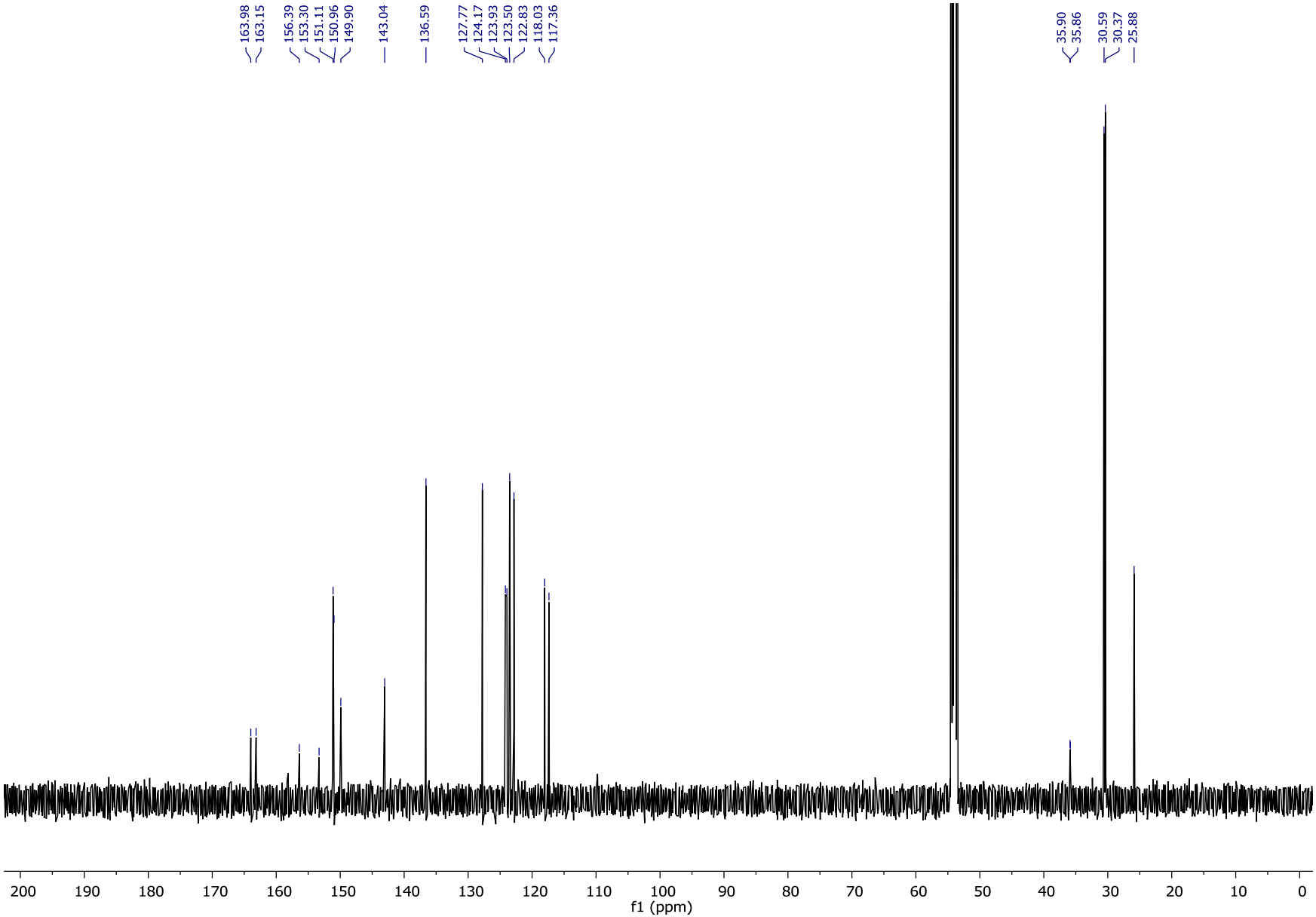

^{1}H NMR (501 MHz, DCM-d2): Ni(dtbbpy)(*o*-tolyl)I (1–I)

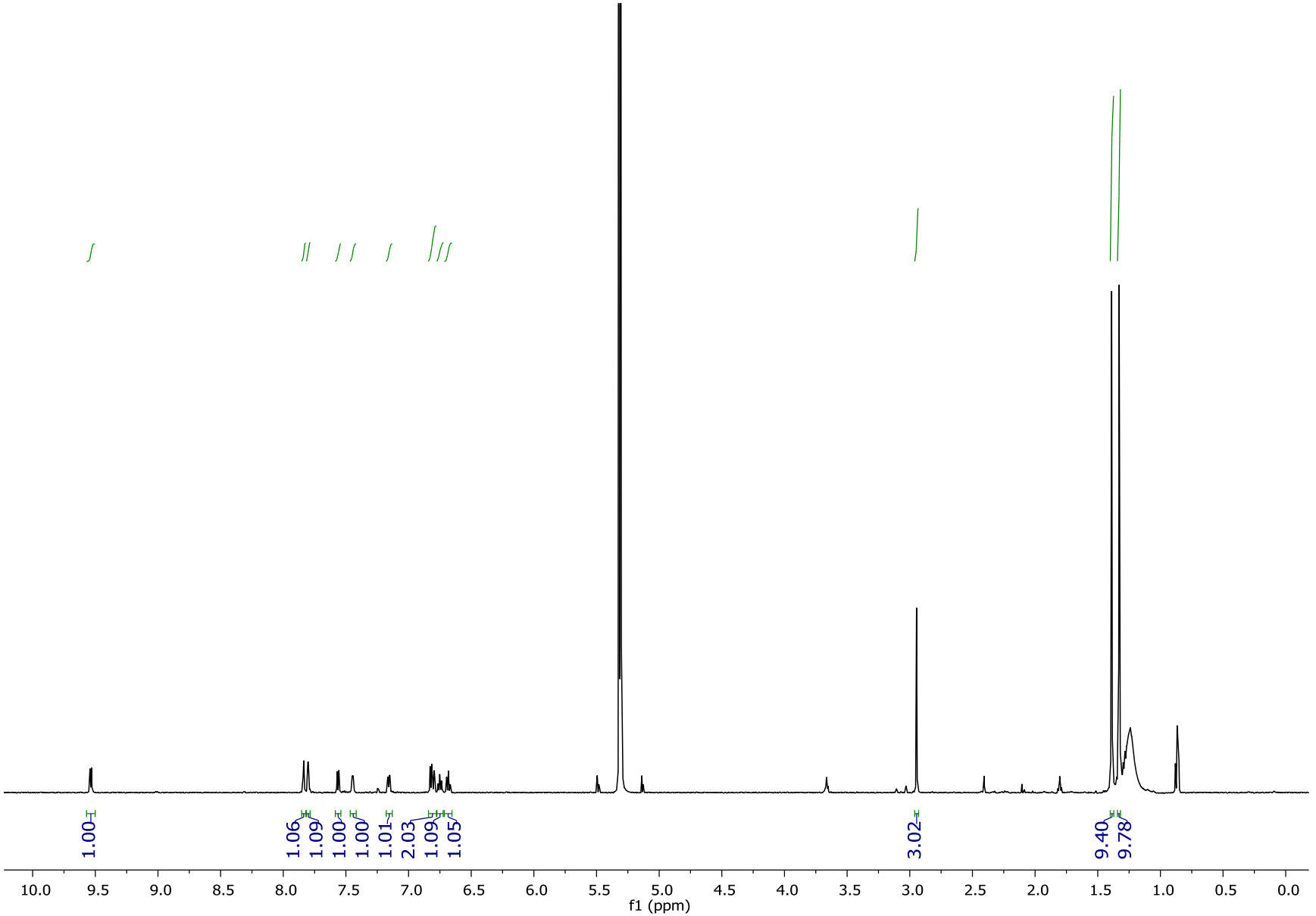

^{13}C NMR (126 MHz, DCM-d2): Ni(dtbbpy)(*o*-tolyl)I (1–I)

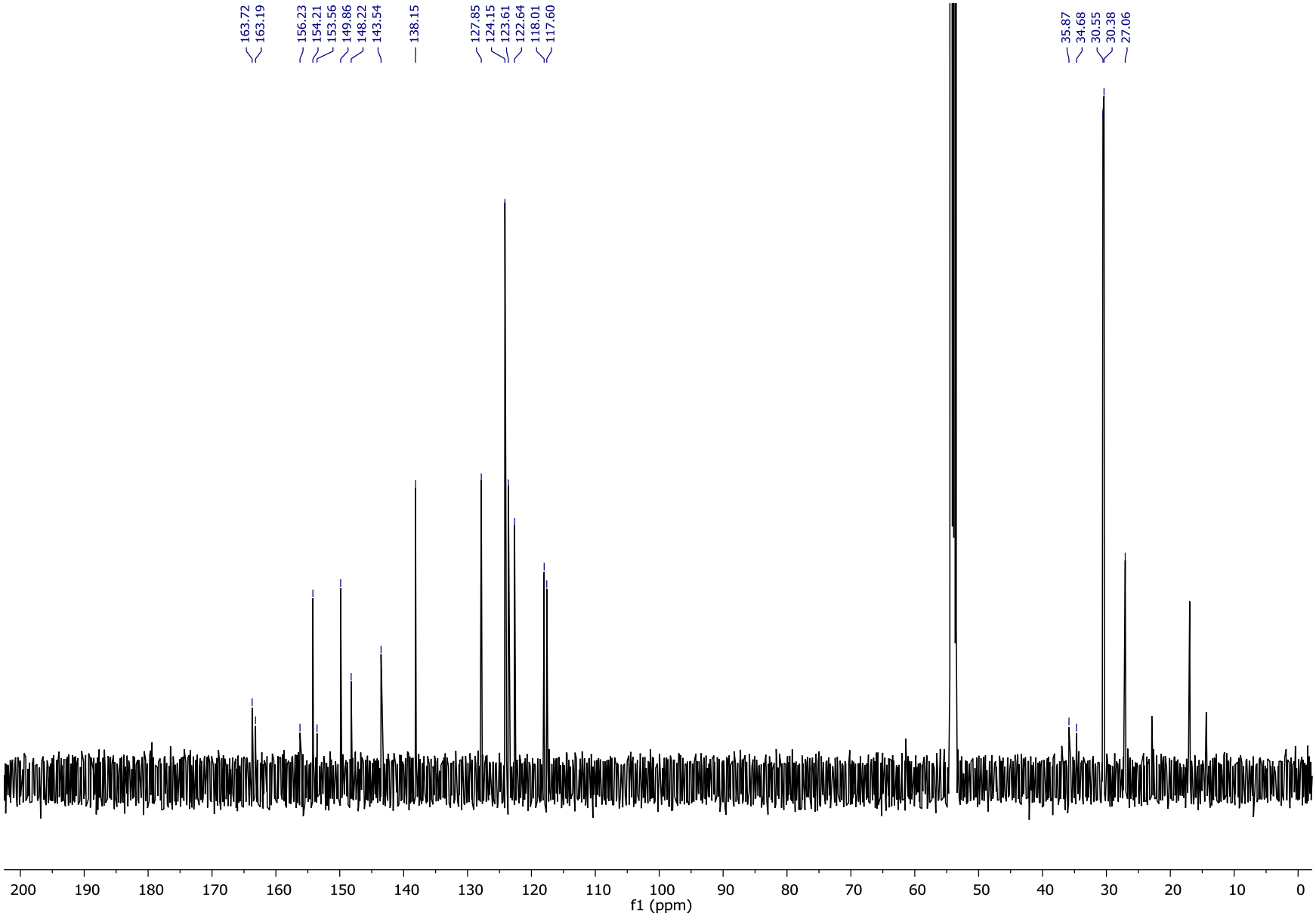

XV. Tabulated Computational Data

Table S16. Cartesian coordinates for gas phase geometry-optimized Ni(II)(dtbbpy)(*o*-tolyl)Cl S_0 (**1–Cl**).

Atom	X	Y	Z
Ni	0.026205	0.744235	0
C	1.85428	2.895347	0.047731
C	-0.31658	3.675248	-0.00289
C	2.338074	4.195833	0.086685
C	0.112292	4.993499	0.0344
H	-1.36778	3.430824	-0.04295
C	1.472677	5.292394	0.082809
H	3.405754	4.35391	0.123753
H	-0.63803	5.769929	0.026443
C	2.71663	1.698584	0.054137
C	4.105476	1.726345	0.061677
C	4.843681	0.538969	0.071197
H	4.617334	2.677442	0.05899
C	2.719709	-0.60706	0.060359
C	4.107531	-0.64523	0.071015
H	2.112631	-1.50457	0.058361
H	4.591617	-1.6102	0.077902
C	-1.84656	1.079621	-0.109
C	-2.65212	1.226073	1.033907
C	-2.42686	1.251531	-1.36772
C	-4.00008	1.566875	0.879856
C	-3.77338	1.587846	-1.51038
C	-4.56329	1.753612	-0.37939
H	-4.62081	1.677942	1.763637
H	-4.19987	1.711579	-2.49984
Cl	-0.38935	-1.40947	0.042886
N	0.522204	2.631139	0.004669
N	2.032991	0.535656	0.051796
H	-1.82829	1.11061	-2.26182
H	-5.61157	2.012497	-0.47307
C	2.024433	6.721113	0.134352
C	6.376783	0.578016	0.079017
C	2.844173	6.902155	1.430889
H	2.224755	6.732105	2.313832
H	3.692095	6.216895	1.479236
H	3.237568	7.919736	1.483884
C	2.93535	6.960932	-1.08951
H	3.784394	6.275556	-1.10957

H	2.381235	6.836294	-2.02204
H	3.332254	7.978242	-1.06483
C	0.904121	7.772662	0.118285
H	0.302149	7.713005	-0.79067
H	0.239383	7.673488	0.978742
H	1.34242	8.771459	0.156153
C	6.860254	1.331421	1.337481
H	6.500556	2.361373	1.360846
H	6.517632	0.835445	2.247844
H	7.951892	1.361596	1.358322
C	6.873046	1.313441	-1.18511
H	6.540442	0.803827	-2.09163
H	6.512706	2.342522	-1.22742
H	7.964845	1.344178	-1.19484
C	6.991033	-0.83087	0.092185
H	6.698032	-1.39532	0.979697
H	6.708615	-1.40746	-0.79093
H	8.079525	-0.75156	0.097993
C	-2.08769	1.00116	2.416182
H	-1.68859	-0.01173	2.504301
H	-1.26299	1.687682	2.631701
H	-2.84987	1.14194	3.185342

Table S17. Cartesian coordinates for gas phase geometry-optimized Ni(II)(dtbbpy)(*o*-tolyl)Cl T_1 (**1–Cl**).

Atom	X	Y	Z
Ni	-0.23585	0.492662	0
C	1.596224	2.617456	0.05809
C	-0.62224	3.437084	0.008217
C	2.054057	3.949783	0.092257
C	-0.19544	4.7339	0.037672
H	-1.67631	3.208273	-0.03016
C	1.202093	5.030258	0.085896
H	3.122887	4.108667	0.129377
H	-0.93965	5.514743	0.022023
C	2.428563	1.466958	0.061445
C	3.840702	1.467737	0.07352
C	4.567555	0.295356	0.075278
H	4.352974	2.419406	0.079575
C	2.453098	-0.87503	0.046827
C	3.829128	-0.91509	0.061446
H	1.864628	-1.78353	0.040969
H	4.315825	-1.8776	0.063915
C	-2.14675	0.81708	-0.10181
C	-2.91365	1.039722	1.042718
C	-2.69234	0.876589	-1.37505
C	-4.26174	1.367228	0.85576
C	-4.03903	1.205223	-1.53495
C	-4.82177	1.453372	-0.41476
H	-4.87971	1.550085	1.728288
H	-4.4658	1.257412	-2.52939
Cl	-0.73858	-1.61262	0.2061
N	0.214553	2.366464	0.017344
N	1.74999	0.26641	0.046918
H	-2.08837	0.668357	-2.25102
H	-5.86942	1.704966	-0.52644
C	1.746234	6.464341	0.136574
C	6.103857	0.327766	0.086852
C	2.551798	6.663865	1.439472
H	1.92457	6.490669	2.316469
H	3.40272	5.983377	1.498473
H	2.937343	7.685384	1.493528
C	2.668654	6.713416	-1.07677
H	3.521672	6.032936	-1.08548
H	2.125237	6.579747	-2.01449
H	3.058148	7.734525	-1.05221

C	0.620647	7.51136	0.104401
H	0.026676	7.441583	-0.80917
H	-0.05178	7.412586	0.958976
H	1.052895	8.513401	0.14021
C	6.594923	1.082402	1.341216
H	6.242153	2.114667	1.358195
H	6.244344	0.594389	2.253024
H	7.687425	1.103661	1.365628
C	6.611581	1.05242	-1.17871
H	6.275091	0.541057	-2.08301
H	6.255881	2.082739	-1.22586
H	7.70434	1.075696	-1.18826
C	6.713602	-1.08382	0.108215
H	6.411974	-1.64371	0.99578
H	6.432547	-1.66249	-0.774
H	7.802813	-1.0092	0.119552
C	-2.33393	0.938175	2.430526
H	-1.93132	-0.06116	2.609897
H	-1.51785	1.65137	2.576409
H	-3.09282	1.140117	3.187094

Table S18. Cartesian coordinates for gas phase geometry-optimized Ni(II)(dtbbpy)(*o*-tolyl)Br S_0 (**1–Br**).

Atom	X	Y	Z
Ni	-0.3826	0.566038	0
C	1.762865	2.410986	0.066365
C	-0.25913	3.52085	0.042828
C	2.444909	3.620347	0.079006
C	0.370732	4.756089	0.058222
H	-1.33617	3.444289	0.023875
C	1.761542	4.83887	0.075275
H	3.524767	3.610913	0.090027
H	-0.24966	5.639609	0.054869
C	2.427985	1.094219	0.07196
C	3.804448	0.911568	0.118052
C	4.357129	-0.37244	0.113944
H	4.452689	1.774337	0.160122
C	2.086575	-1.1837	0.023002
C	3.45199	-1.43137	0.063048
H	1.355757	-1.98288	-0.0131
H	3.783965	-2.45864	0.055441
C	-2.17675	1.207471	-0.03549
C	-2.8943	1.480515	1.142757
C	-2.76601	1.506539	-1.26643
C	-4.16085	2.067137	1.050012
C	-4.0306	2.089743	-1.34713
C	-4.73012	2.377889	-0.18153
H	-4.71336	2.275673	1.960997
H	-4.46599	2.308218	-2.31605
N	0.406208	2.358738	0.044665
N	1.575658	0.048256	0.027324
H	-2.24082	1.272229	-2.18645
H	-5.71554	2.826711	-0.22735
C	2.530118	6.16465	0.086223
C	5.877522	-0.56355	0.167681
C	3.406704	6.23416	1.355917
H	2.795572	6.17942	2.259061
H	4.134917	5.422401	1.393395
H	3.958999	7.176208	1.376826
C	3.431039	6.239516	-1.16614
H	4.160306	5.428313	-1.19264
H	2.837322	6.187649	-2.08098
H	3.982918	7.182024	-1.17298
C	1.586311	7.37768	0.079659

H	0.956723	7.399116	-0.81216
H	0.938694	7.394735	0.958593
H	2.174787	8.296774	0.087939
C	6.420734	0.060303	1.472114
H	6.215024	1.130423	1.529393
H	5.97658	-0.41458	2.349244
H	7.503503	-0.07298	1.526234
C	6.523475	0.138898	-1.04672
H	6.148872	-0.27487	-1.98513
H	6.327154	1.212339	-1.05074
H	7.606744	0.000881	-1.02403
C	6.274669	-2.04785	0.136897
H	5.871473	-2.59608	0.990671
H	5.938565	-2.54039	-0.77773
H	7.362009	-2.13421	0.175923
C	-2.32837	1.131666	2.498434
H	-2.14494	0.057159	2.571172
H	-1.37033	1.629586	2.676803
H	-3.01055	1.420247	3.300712
Br	-1.22021	-1.61318	-0.06181

Table S19. Cartesian coordinates for gas phase geometry-optimized Ni(II)(dtbbpy)(*o*-tolyl)I S_0 (**1–I**).

Atom	X	Y	Z
Ni	-1.29647	-0.39583	-0.08424
C	1.211175	0.926419	-0.04604
C	-0.50673	2.4635	-0.07642
C	2.148971	1.950756	-0.04913
C	0.385475	3.524985	-0.07698
H	-1.57288	2.633132	-0.09231
C	1.758996	3.291912	-0.06334
H	3.198883	1.698904	-0.04093
H	-0.0198	4.525522	-0.08907
C	1.564804	-0.50551	-0.02835
C	2.869653	-0.98143	0.012323
C	3.134791	-2.35338	0.025299
H	3.688512	-0.27795	0.0352
C	0.742761	-2.65481	-0.04196
C	2.021995	-3.19141	-0.00361
H	-0.13541	-3.28766	-0.06434
H	2.122248	-4.26639	0.003496
C	-2.8905	0.649542	-0.11147
C	-3.47723	1.138598	1.069831
C	-3.40265	1.072906	-1.34096
C	-4.54314	2.040261	0.980145
C	-4.46501	1.97293	-1.41809
C	-5.03512	2.465574	-0.25025
H	-4.99799	2.410924	1.893539
H	-4.84617	2.279464	-2.38595
N	-0.12145	1.181131	-0.06099
N	0.503334	-1.34169	-0.05462
H	-2.98252	0.682754	-2.26182
H	-5.86455	3.161744	-0.29325
C	2.807587	4.409457	-0.06617
C	4.578575	-2.86652	0.070387
C	3.683138	4.288492	1.200456
H	3.079095	4.377922	2.105596
H	4.211887	3.334854	1.24254
H	4.432226	5.083247	1.213051
C	3.695849	4.269493	-1.32197
H	4.224585	3.315177	-1.34446
H	3.100918	4.345387	-2.23433
H	4.445235	5.063901	-1.3389
C	2.163055	5.804558	-0.07977

H	1.55086	5.962026	-0.97
H	1.540312	5.974347	0.800855
H	2.944674	6.566254	-0.08048
C	5.264756	-2.34165	1.350632
H	5.297647	-1.25129	1.379399
H	4.742164	-2.68563	2.245447
H	6.293543	-2.70541	1.398053
C	5.339932	-2.3517	-1.17087
H	4.871755	-2.70324	-2.09247
H	5.374269	-1.26158	-1.20644
H	6.369785	-2.71517	-1.15383
C	4.644941	-4.40193	0.078479
H	4.145073	-4.82683	0.951195
H	4.19748	-4.83397	-0.81883
H	5.688284	-4.72059	0.11065
C	-2.99235	0.688247	2.426824
H	-3.09596	-0.39429	2.531538
H	-1.93362	0.921437	2.576173
H	-3.55704	1.166563	3.2296
I	-2.77562	-2.47589	-0.16028

Table S20. Cartesian coordinates for gas phase geometry-optimized Ni(II)(dtbbpy)Cl_2 T_0 (**2**).

Atom	X	Y	Z
C	-1.64046	-0.40881	0
C	-3.53522	0.911406	0.001382
C	-2.4201	-1.55879	-0.00043
C	-4.36717	-0.19889	0.001137
H	-3.93903	1.915868	0.002038
C	-3.81633	-1.48018	0.000175
H	-1.9384	-2.52521	-0.00131
H	-5.43498	-0.042	0.001641
C	-0.1557	-0.40892	-0.00052
C	0.623801	-1.55898	0.000001
C	2.020056	-1.48051	-0.00065
H	0.142018	-2.52535	0.000992
C	1.739199	0.911097	-0.0021
C	2.571033	-0.19931	-0.00179
H	2.143122	1.915513	-0.00288
H	3.63886	-0.04253	-0.00237
N	-2.20933	0.812132	0.000822
N	0.41332	0.811959	-0.00146
C	-4.66359	-2.75818	-0.00027
C	2.867158	-2.75863	-1.6E-05
C	-4.3338	-3.58475	-1.26269
H	-4.5505	-3.01906	-2.171
H	-3.28441	-3.8821	-1.29482
H	-4.93638	-4.49543	-1.27848
C	-4.33289	-3.58621	1.260951
H	-3.28348	-3.8836	1.291968
H	-4.54894	-3.02158	2.17007
H	-4.93546	-4.49692	1.276117
C	-6.1698	-2.45278	0.000439
H	-6.4718	-1.89115	0.886752
H	-6.47242	-1.89013	-0.88501
H	-6.72986	-3.38936	0.000099
C	2.536147	-3.58698	-1.26094
H	1.486695	-3.88425	-1.2917
H	2.752113	-3.02264	-2.17026
H	3.138598	-4.49776	-1.27595
C	2.537489	-3.5848	1.262699
H	2.754401	-3.01887	2.170807
H	1.488075	-3.88202	1.295082
H	3.139973	-4.49554	1.278649

C	4.373402	-2.45341	-0.00108
H	4.675306	-1.89206	-0.88761
H	4.676247	-1.89053	0.884147
H	4.933353	-3.39005	-0.00057
Ni	-0.89791	2.37074	-4.8E-05
Cl	-0.89925	3.145104	-2.09615
Cl	-0.89616	3.143876	2.09661

Table S21. Cartesian coordinates for gas phase geometry-optimized Ni(II)(dtbbpy)Cl_2 S_1 (**2**).

Atom	X	Y	Z
Ni	0.662002	-0.65124	0
C	-0.07389	-3.37362	-0.0003
C	-1.95361	-2.03339	0.000481
C	-0.86031	-4.51655	-0.00043
C	-2.78802	-3.14187	0.000511
H	-2.33253	-1.01958	0.000653
C	-2.25544	-4.42956	-0.00004
H	-0.38008	-5.48384	-0.00095
H	-3.85393	-2.97121	0.000896
C	1.396726	-3.37394	0.000035
C	2.182755	-4.51716	0.000033
C	3.577891	-4.43062	-0.00022
H	1.702262	-5.4843	0.00037
C	3.277021	-2.03431	-0.00041
C	4.110958	-3.14312	-0.00052
H	3.656237	-1.02064	-0.00046
H	5.176952	-2.97298	-0.00081
Cl	2.225762	0.88675	0.000519
N	-0.62142	-2.13526	0.000108
N	1.944719	-2.13581	-0.00017
C	-3.11375	-5.69906	-0.00014
C	4.435754	-5.70042	-0.00016
C	-2.79107	-6.5295	-1.26188
H	-3.00327	-5.96258	-2.17052
H	-1.74419	-6.83585	-1.2937
H	-3.40145	-7.435	-1.27721
C	-2.79056	-6.52992	1.261205
H	-1.74364	-6.83616	1.292511
H	-3.00246	-5.96331	2.17011
H	-3.40087	-7.43546	1.276468
C	-4.6169	-5.37915	0.00019
H	-4.91326	-4.81384	0.885983
H	-4.91349	-4.81321	-0.88513
H	-5.18631	-6.31013	-4.5E-05
C	4.112173	-6.53132	-1.26139
H	3.065163	-6.83727	-1.29257
H	4.324168	-5.96488	-2.17038
H	4.72221	-7.43705	-1.2766
C	4.112904	-6.53066	1.261692
H	4.325416	-5.96375	2.170263

H	3.065913	-6.8366	1.293635
H	4.722956	-7.43638	1.277025
C	5.939031	-5.38108	-0.00068
H	6.235459	-4.81577	-0.88645
H	6.235994	-4.81538	0.88466
H	6.508075	-6.31228	-0.00065
Cl	-0.90081	0.88716	-0.00106

Table S22. Cartesian coordinates for gas phase geometry-optimized Ni(III)(dtbbpy)(*p*-AcPh)(OMe)Br (**A**).

Atom	X	Y	Z
Ni	-0.44549	0.136268	0
C	-2.36171	2.285055	-0.17395
C	-0.23207	3.148674	0.029432
C	-2.90262	3.561504	-0.10767
C	-0.7156	4.446998	0.095964
H	0.827479	2.947197	0.092244
C	-2.0865	4.687214	0.032244
H	-3.97521	3.677904	-0.15417
H	-0.00366	5.250909	0.205299
C	-3.1732	1.057181	-0.31372
C	-4.55568	1.026753	-0.4401
C	-5.23221	-0.19211	-0.56188
H	-5.11229	1.952203	-0.44034
C	-3.06894	-1.24786	-0.42617
C	-4.44813	-1.34586	-0.55594
H	-2.40799	-2.1065	-0.41268
H	-4.88861	-2.32746	-0.64407
C	1.433037	0.498218	-0.12587
C	1.93897	0.595412	-1.42285
C	2.281497	0.717337	0.958966
C	3.273305	0.929896	-1.63538
C	3.613439	1.05212	0.742489
C	4.128691	1.167555	-0.55382
H	3.639893	0.997907	-2.65206
H	4.278266	1.227409	1.579096
N	-1.02429	2.084852	-0.10535
N	-2.45405	-0.07751	-0.31104
H	1.899532	0.62705	1.967074
H	1.304602	0.393552	-2.27868
C	-2.7026	6.087629	0.120789
C	-6.7603	-0.2147	-0.68979
C	-3.54349	6.357263	-1.14633
H	-2.92827	6.300511	-2.04674
H	-4.36355	5.645532	-1.25385
H	-3.97953	7.357343	-1.09705
C	-3.61121	6.157493	1.368169
H	-4.42538	5.43268	1.319999
H	-3.04298	5.962528	2.279566
H	-4.05496	7.152118	1.449796
C	-1.63155	7.183842	0.234218

H	-1.02604	7.071286	1.135611
H	-0.96497	7.193255	-0.63069
H	-2.11588	8.160451	0.285931
C	-7.17748	0.582057	-1.94545
H	-6.86317	1.625698	-1.89142
H	-6.74424	0.147101	-2.84853
H	-8.26446	0.569244	-2.05092
C	-7.38256	0.435782	0.565418
H	-7.09574	-0.10364	1.470106
H	-7.07274	1.475332	0.683491
H	-8.47218	0.420473	0.491269
C	-7.3094	-1.64436	-0.81827
H	-6.92434	-2.15026	-1.70601
H	-7.07121	-2.25274	0.056415
H	-8.39668	-1.60934	-0.90653
O	-0.18911	-1.58817	-0.50962
C	0.831643	-2.45445	-0.08508
H	0.939256	-2.45435	1.005635
H	0.562227	-3.47113	-0.39845
H	1.805536	-2.21295	-0.52763
Br	-0.78612	0.115597	2.500965
C	5.566791	1.534636	-0.7294
O	6.273338	1.785602	0.229927
C	6.142156	1.58943	-2.13364
H	6.045419	0.623378	-2.63481
H	5.617504	2.328255	-2.74438
H	7.193894	1.858879	-2.06857

Table S23. Cartesian coordinates for gas phase geometry-optimized Ni(I)(dtbbpy)Br (**B**).

Atom	X	Y	Z
Ni	-1.326	0.545073	0
C	-4.0682	1.283377	0.000077
C	-2.73664	3.169768	0.000087
C	-5.21342	2.070456	0.000105
C	-3.84179	4.006156	0.000098
H	-1.73045	3.570308	0.0001
C	-5.13021	3.465008	0.000106
H	-6.18144	1.590478	0.000114
H	-3.67833	5.073404	0.000099
C	-4.06796	-0.19431	0.000012
C	-5.2129	-0.98179	0.000107
C	-5.12921	-2.37632	0.000035
H	-6.1811	-0.50217	0.000225
C	-2.73574	-2.08023	-0.00027
C	-3.84061	-2.91701	-0.00019
H	-1.72941	-2.48043	-0.00041
H	-3.67672	-3.98419	-0.00031
N	-2.83124	1.835521	0.000073
N	-2.83082	-0.74603	-0.00015
C	-6.40395	4.318864	0.000146
C	-6.40265	-3.23066	0.00023
C	-7.23482	3.99453	-1.2607
H	-6.66825	4.207636	-2.16941
H	-7.53636	2.946258	-1.29201
H	-8.1431	4.601249	-1.27706
C	-7.23469	3.994563	1.261083
H	-7.53623	2.94629	1.292445
H	-6.66803	4.207691	2.169731
H	-8.14297	4.601282	1.277519
C	-6.09143	5.823927	0.000109
H	-5.52715	6.12349	0.885662
H	-5.5273	6.123475	-0.88554
H	-7.02534	6.388854	0.00018
C	-7.23393	-2.90648	-1.26038
H	-7.5357	-1.85827	-1.29162
H	-6.66759	-3.11949	-2.16925
H	-8.14208	-3.5134	-1.27646
C	-7.23327	-2.90681	1.261389
H	-6.66639	-3.11998	2.169891
H	-7.53508	-1.85863	1.292998
H	-8.14136	-3.5138	1.277825

C	-6.08963	-4.7356	-3.5E-05
H	-5.52556	-5.03487	-0.88582
H	-5.52511	-5.03509	0.885383
H	-7.02336	-5.30082	0.000137
Br	0.976569	0.545192	0.000309

Table S24. Cartesian coordinates for gas phase geometry-optimized 4-methoxyacetophenone (**C**).

Atom	X	Y	Z
C	-1.52516	-0.05241	0
C	-2.89591	-0.22865	0.000058
C	-3.74574	0.883183	0.000034
C	-3.20017	2.171506	-0.00029
C	-1.82258	2.330889	-0.00037
C	-0.96013	1.231702	-0.00018
H	-0.89026	-0.92874	-1.1E-05
H	-3.33599	-1.21729	0.000085
H	-3.8359	3.045318	-0.00051
H	-1.38912	3.322674	-0.00053
O	-5.0757	0.610643	0.000316
C	0.511949	1.473086	0.000121
O	0.961866	2.605106	0.000605
C	1.447811	0.278257	-3.9E-05
H	1.285248	-0.34669	0.881459
H	1.284086	-0.34798	-0.88035
H	2.473802	0.638921	-0.00088
C	-6.00038	1.692916	0.000243
H	-5.88826	2.313433	-0.89332
H	-6.98763	1.237387	0.000695
H	-5.88773	2.314033	0.893363

Table S25. Cartesian coordinates for gas phase geometry-optimized Ni(II)(dtbbpy)(*p*-AcPh)(OMe) (**D**).

Atom	X	Y	Z
Ni	-0.77044	0.691824	0
C	1.100421	2.810269	0.027791
C	-1.05501	3.633862	0.014036
C	1.611267	4.100987	0.037708
C	-0.59883	4.942644	0.024167
H	-2.11219	3.415272	0.00256
C	0.76906	5.214802	0.035775
H	2.683142	4.235465	0.046325
H	-1.33285	5.734531	0.021329
C	1.933517	1.594815	0.030986
C	3.32315	1.568055	0.047845
C	4.008823	0.349396	0.051201
H	3.873098	2.497942	0.059201
C	1.840945	-0.71416	0.019063
C	3.225933	-0.80716	0.035575
H	1.171968	-1.56842	0.006823
H	3.673969	-1.78944	0.036536
C	-2.64385	1.018711	-0.00756
C	-3.38143	1.075488	1.183701
C	-3.34851	1.248312	-1.20177
C	-4.74459	1.354409	1.188664
C	-4.7074	1.530844	-1.20711
C	-5.43099	1.591291	-0.0088
H	-5.27086	1.386049	2.135304
H	-5.2368	1.706287	-2.13574
N	-0.23944	2.570331	0.014916
N	1.211752	0.458767	0.017087
H	-2.82663	1.201018	-2.15224
H	-2.88859	0.890901	2.132678
C	1.350051	6.632894	0.045905
C	5.542649	0.325387	0.071462
C	2.21063	6.821713	1.314389
H	1.61385	6.681516	2.217973
H	3.045447	6.119787	1.351742
H	2.626071	7.8317	1.336184
C	2.229391	6.832051	-1.20804
H	3.064324	6.129936	-1.23901
H	1.646027	6.700029	-2.12152
H	2.645625	7.841927	-1.21501
C	0.250692	7.706682	0.042025

H	-0.37801	7.643524	-0.8484
H	-0.39115	7.636531	0.922536
H	0.709669	8.696906	0.049317
C	6.046472	1.043509	1.342547
H	5.731807	2.087806	1.373605
H	5.67314	0.553499	2.244046
H	7.138243	1.025517	1.374249
C	6.080465	1.054119	-1.17944
H	5.733045	0.570869	-2.09482
H	5.765314	2.098256	-1.21093
H	7.17272	1.037593	-1.18093
C	6.099546	-1.10723	0.073116
H	5.777198	-1.66884	0.952172
H	5.800277	-1.66216	-0.81825
H	7.190314	-1.07207	0.087424
O	-0.92302	-1.12354	-0.01276
C	-2.07623	-1.91176	-0.05096
H	-2.69628	-1.73224	-0.94079
H	-1.77337	-2.96862	-0.07159
H	-2.72488	-1.77575	0.82637
C	-6.88705	1.900546	-0.05855
O	-7.44731	2.155038	-1.11165
C	-7.68192	1.892636	1.237009
H	-7.62303	0.91803	1.72703
H	-7.29454	2.634622	1.939443
H	-8.7208	2.121173	1.009403

Table S26. Cartesian coordinates for gas phase geometry-optimized Ni(0)(dtbbpy) (**E**).

Atom	X	Y	Z
Ni	1.198565	0.828092	0.062814
C	0.477162	-1.71557	-0.06486
C	-1.38454	-0.41724	-0.56377
C	-0.33966	-2.82076	0.134541
C	-2.23664	-1.48241	-0.34675
H	-1.774	0.54038	-0.88589
C	-1.72715	-2.74542	-0.00984
H	0.123787	-3.7457	0.452055
H	-3.29679	-1.3214	-0.47964
C	1.921937	-1.71543	0.188232
C	2.739059	-2.82047	-0.01076
C	4.126458	-2.74487	0.134243
H	2.275907	-3.74553	-0.32834
C	3.783222	-0.41669	0.687651
C	4.6356	-1.48177	0.47128
H	4.172273	0.541204	1.009468
H	5.69565	-1.32058	0.604721
N	-0.03788	-0.49923	-0.46231
N	2.436685	-0.49894	0.58564
C	-2.60689	-3.98009	0.220543
C	5.006504	-3.9794	-0.09569
C	-2.18116	-5.10448	-0.74878
H	-2.29374	-4.78715	-1.78763
H	-1.13994	-5.39483	-0.59921
H	-2.79897	-5.9931	-0.59527
C	-2.43798	-4.47132	1.675284
H	-1.40453	-4.74663	1.891889
H	-2.73246	-3.69581	2.385427
H	-3.06196	-5.35106	1.853444
C	-4.0957	-3.67971	-0.01622
H	-4.47027	-2.9161	0.668714
H	-4.28445	-3.34519	-1.03857
H	-4.6833	-4.58528	0.14824
C	4.838467	-4.47063	-1.55054
H	3.80522	-4.74623	-1.76768
H	5.133103	-3.695	-2.2605
H	5.462802	-5.35017	-1.72839
C	4.580376	-5.10389	0.873354
H	4.692345	-4.7866	1.912283
H	3.53927	-5.39434	0.723186
H	5.198383	-5.99243	0.72014

C	6.49516	-3.67888	0.141886
H	6.869947	-2.91502	-0.54265
H	6.683362	-3.34461	1.164419
H	7.082958	-4.58432	-0.02253

Table S27. Cartesian coordinates for gas phase geometry-optimized Ni(I)(dtbbpy)(OMe) (**F**).

Atom	X	Y	Z
Ni	-1.62002	0.40366	0
C	-0.87834	-2.3386	0.126159
C	1.004058	-1.0023	-0.04809
C	-0.07654	-3.47269	0.236614
C	1.84579	-2.09377	0.045318
H	1.399928	0.000146	-0.15517
C	1.313108	-3.38306	0.200056
H	-0.55024	-4.43765	0.350368
H	2.911475	-1.92552	0.0018
C	-2.34403	-2.34379	0.126547
C	-3.13782	-3.48363	0.236211
C	-4.52807	-3.4036	0.20034
H	-2.65734	-4.4454	0.348483
C	-4.23569	-1.02053	-0.04556
C	-5.06983	-2.11791	0.047508
H	-4.6385	-0.02075	-0.15171
H	-6.13669	-1.95702	0.004878
N	-0.33445	-1.09793	-0.00739
N	-2.89668	-1.10702	-0.00597
C	2.179637	-4.64321	0.321313
C	-5.38582	-4.66993	0.319575
C	1.874167	-5.35063	1.659762
H	2.08498	-4.69464	2.506814
H	0.830022	-5.65995	1.72806
H	2.49262	-6.2457	1.760707
C	1.857632	-5.59898	-0.84839
H	0.808824	-5.90016	-0.84958
H	2.071224	-5.12682	-1.80957
H	2.464037	-6.50483	-0.77272
C	3.681532	-4.31837	0.279827
H	3.970274	-3.84647	-0.66157
H	3.978281	-3.66063	1.099396
H	4.25702	-5.24124	0.373908
C	-5.07478	-5.3781	1.656348
H	-4.02872	-5.68128	1.723103
H	-5.28877	-4.72508	2.504894
H	-5.68769	-6.2771	1.756098
C	-5.05782	-5.62097	-0.85232
H	-5.27565	-5.14844	-1.81237
H	-4.00684	-5.91443	-0.85495

H	-5.65756	-6.53136	-0.77798
C	-6.88996	-4.35539	0.279412
H	-7.19114	-3.7019	1.100774
H	-7.18219	-3.88305	-0.66068
H	-7.45892	-5.28253	0.371104
O	-1.63107	2.196161	0.147851
C	-1.65002	3.154839	1.150759
H	-1.61433	4.169053	0.721995
H	-2.56063	3.104778	1.771475
H	-0.79228	3.07104	1.839374

Table S28. Cartesian coordinates for gas phase geometry-optimized 4-bromoacetophenone (**F**).

Atom	X	Y	Z
C	-0.02621	-0.37736	0
C	-1.4157	-0.41632	0.000048
C	-2.12299	0.778604	-0.00012
C	-1.46799	2.006367	-0.00032
C	-0.08213	2.028938	-0.00035
C	0.657867	0.841513	-0.0002
H	0.516808	-1.3132	0.000134
H	-1.93921	-1.36234	0.000212
H	-2.03407	2.927694	-0.00045
H	0.451753	2.970225	-0.00049
C	2.155141	0.931869	-0.00022
O	2.707478	2.014798	-6.5E-05
C	2.965523	-0.34851	-0.00013
H	2.741215	-0.95419	0.881301
H	2.740693	-0.95479	-0.88099
H	4.022351	-0.09237	-0.00049
Br	-4.038	0.735657	-7.8E-05

Calculated Orbital Contribution Data for TD-DFT Transitions. The significance of Kohn-Sham orbital contributions to a transition were evaluated (frontier orbital diagrams presented in section IV) using the fractional sum of squares of the transition coefficient ($C_i^2/\Sigma C_i^2$).

Table S29. TD-DFT calculated transition Kohn-Sham orbital contributions for [Ni(dtbbpy)(*o*-tolyl)Cl] S_0 (**x**).

Excited State	KS Orbital Transition			C_i	$C_i^2/\Sigma C_i^2$
1	117A	->	124A	-0.13591	2%
	118A	->	124A	0.14928	2%
	120A	->	124A	0.69600	43%
	117B	->	124B	0.13591	2%
	118B	->	124B	-0.14928	2%
	120B	->	124B	-0.69600	43%
	120A	<-	124A	0.20717	4%
	120B	<-	124B	-0.20717	4%
2	113A	->	124A	-0.24706	6%
	115A	->	124A	-0.19881	4%
	119A	->	124A	0.63372	38%
	113B	->	124B	0.24706	6%
	115B	->	124B	0.19881	4%
	119B	->	124B	-0.63372	38%
	119A	<-	124A	0.14492	2%
	119B	<-	124B	-0.14492	2%
3	115A	->	124A	0.67885	45%
	119A	->	124A	0.17158	3%
	115B	->	124B	-0.67885	45%
	119B	->	124B	-0.17158	3%
	115A	<-	124A	0.14169	2%
	115B	<-	124B	-0.14169	2%
4	110A	->	124A	0.25484	7%
	111A	->	124A	-0.23668	6%
	116A	->	124A	-0.22050	5%
	117A	->	124A	0.42040	19%
	118A	->	124A	0.19551	4%
	119A	->	121A	0.27249	8%
	120A	->	121A	-0.13308	2%
	110B	->	124B	-0.25484	7%
	111B	->	124B	0.23668	6%
	116B	->	124B	0.22050	5%
	117B	->	124B	-0.42040	19%
	118B	->	124B	-0.19551	4%
	119B	->	121B	-0.27249	8%

	120B	->	121B	0.13308	2%
5	117A	->	124A	0.10312	1%
	118A	->	121A	0.10827	1%
	120A	->	121A	0.66191	46%
	120A	->	122A	0.11996	2%
	117B	->	124B	-0.10312	1%
	118B	->	121B	-0.10827	1%
	120B	->	121B	-0.66191	46%
	120B	->	122B	-0.11996	2%
6	110A	->	124A	-0.12147	2%
	117A	->	124A	-0.16201	3%
	118A	->	124A	-0.11192	1%
	119A	->	121A	0.61097	42%
	119A	->	122A	0.12253	2%
	110B	->	124B	0.12147	2%
	117B	->	124B	0.16201	3%
	118B	->	124B	0.11192	1%
	119B	->	121B	-0.61097	42%
	119B	->	122B	-0.12253	2%
7	118A	->	121A	0.11574	1%
	120A	->	121A	0.68013	49%
	118B	->	121B	0.11574	1%
	120B	->	121B	0.68013	49%
8	115A	->	121A	-0.18447	4%
	119A	->	121A	0.47707	25%
	120A	->	124A	-0.44810	22%
	115B	->	121B	-0.18447	4%
	119B	->	121B	0.47707	25%
	120B	->	124B	-0.44810	22%
9	113A	->	124A	-0.19129	4%
	115A	->	124A	-0.13836	2%
	118A	->	121A	0.20990	5%
	119A	->	124A	0.60032	38%
	120A	->	121A	-0.10072	1%
	113B	->	124B	-0.19129	4%
	115B	->	124B	-0.13836	2%
	118B	->	121B	0.20990	5%
	119B	->	124B	0.60032	38%
	120B	->	121B	-0.10072	1%
10	114A	->	124A	-0.11755	1%
	118A	->	124A	0.15073	2%
	119A	->	121A	0.46574	23%
	120A	->	124A	0.47667	24%
	114B	->	124B	-0.11755	1%
	118B	->	124B	0.15073	2%

	119B	->	121B	0.46574	23%
	120B	->	124B	0.47667	24%
11	115A	->	121A	0.59956	38%
	115A	->	122A	0.11914	2%
	118A	->	121A	0.31378	10%
	115B	->	121B	-0.59956	38%
	115B	->	122B	-0.11914	2%
	118B	->	121B	-0.31378	10%
12	115A	->	121A	-0.29964	9%
	116A	->	121A	-0.11600	1%
	117A	->	121A	0.12853	2%
	118A	->	121A	0.59406	37%
	115B	->	121B	0.29964	9%
	116B	->	121B	0.11600	1%
	117B	->	121B	-0.12853	2%
	118B	->	121B	-0.59406	37%
13	118A	->	121A	0.63298	43%
	119A	->	124A	-0.24930	7%
	118B	->	121B	0.63298	43%
	119B	->	124B	-0.24930	7%
14	115A	->	124A	0.51832	29%
	116A	->	121A	0.13541	2%
	117A	->	121A	-0.37325	15%
	118A	->	121A	0.17783	3%
	119A	->	124A	0.10158	1%
	115B	->	124B	0.51832	29%
	116B	->	121B	0.13541	2%
	117B	->	121B	-0.37325	15%
	118B	->	121B	0.17783	3%
	119B	->	124B	0.10158	1%
15	116A	->	121A	-0.20983	5%
	117A	->	121A	0.63617	43%
	118A	->	121A	-0.11995	2%
	120A	->	121A	0.10854	1%
	116B	->	121B	0.20983	5%
	117B	->	121B	-0.63617	43%
	118B	->	121B	0.11995	2%
	120B	->	121B	-0.10854	1%
16	110A	->	124A	0.25621	7%
	111A	->	124A	-0.21434	5%
	114A	->	124A	-0.11868	1%
	115A	->	124A	0.12346	2%
	116A	->	124A	-0.23658	6%
	117A	->	124A	0.45200	22%
	118A	->	124A	0.26268	7%

	110B	->	124B	0.25621	7%
	111B	->	124B	-0.21434	5%
	114B	->	124B	-0.11868	1%
	115B	->	124B	0.12346	2%
	116B	->	124B	-0.23658	6%
	117B	->	124B	0.45200	22%
	118B	->	124B	0.26268	7%
17	115A	->	121A	0.10492	1%
	115A	->	124A	0.39696	17%
	116A	->	121A	-0.15515	3%
	117A	->	121A	0.52811	30%
	115B	->	121B	0.10492	1%
	115B	->	124B	0.39696	17%
	116B	->	121B	-0.15515	3%
	117B	->	121B	0.52811	30%
18	115A	->	121A	0.63636	45%
	119A	->	121A	0.17410	3%
	119A	->	122A	-0.11706	2%
	115B	->	121B	0.63636	45%
	119B	->	121B	0.17410	3%
	119B	->	122B	-0.11706	2%
19	114A	->	124A	0.40306	18%
	117A	->	124A	0.23774	6%
	118A	->	124A	-0.28345	9%
	119A	->	121A	-0.12626	2%
	119A	->	122A	0.32474	12%
	120A	->	124A	0.15146	3%
	114B	->	124B	-0.40306	18%
	117B	->	124B	-0.23774	6%
	118B	->	124B	0.28345	9%
	119B	->	121B	0.12626	2%
	119B	->	122B	-0.32474	12%
	120B	->	124B	-0.15146	3%
20	120A	->	121A	0.12036	2%
	120A	->	122A	-0.68211	48%
	120B	->	121B	-0.12036	2%
	120B	->	122B	0.68211	48%
21	120A	->	122A	0.68442	50%
	120B	->	122B	0.68442	50%
22	114A	->	124A	0.23976	6%
	117A	->	124A	0.14794	2%
	118A	->	124A	-0.17552	3%
	119A	->	121A	0.10349	1%
	119A	->	122A	-0.57916	37%
	114B	->	124B	-0.23976	6%

	117B	->	124B	-0.14794	2%
	118B	->	124B	0.17552	3%
	119B	->	121B	-0.10349	1%
	119B	->	122B	0.57916	37%
23	116A	->	121A	-0.65438	44%
	117A	->	121A	-0.23771	6%
	116B	->	121B	0.65438	44%
	117B	->	121B	0.23771	6%
24	116A	->	121A	0.66185	45%
	117A	->	121A	0.22479	5%
	116B	->	121B	0.66185	45%
	117B	->	121B	0.22479	5%
25	115A	->	121A	0.11514	1%
	119A	->	122A	0.67255	47%
	119A	->	123A	-0.13723	2%
	115B	->	121B	0.11514	1%
	119B	->	122B	0.67255	47%
	119B	->	123B	-0.13723	2%
26	112A	->	121A	-0.38703	18%
	112A	->	122A	0.19076	4%
	119A	->	122A	-0.10399	1%
	119A	->	123A	0.47617	27%
	112B	->	121B	0.38703	18%
	112B	->	122B	-0.19076	4%
	119B	->	122B	0.10399	1%
	119B	->	123B	-0.47617	27%
27	118A	->	122A	0.67544	50%
	118B	->	122B	-0.67544	50%
28	118A	->	122A	0.68449	50%
	118B	->	122B	0.68449	50%
29	118A	->	123A	0.11736	1%
	120A	->	123A	0.68765	49%
	118B	->	123B	-0.11736	1%
	120B	->	123B	-0.68765	49%
30	118A	->	123A	0.11047	1%
	120A	->	123A	0.69275	49%
	118B	->	123B	0.11047	1%
	120B	->	123B	0.69275	49%
31	112A	->	121A	0.46057	23%
	112A	->	122A	-0.12133	2%
	119A	->	123A	0.47997	25%
	112B	->	121B	-0.46057	23%
	112B	->	122B	0.12133	2%
	119B	->	123B	-0.47997	25%
32	119A	->	122A	0.10682	1%

	119A	->	123A	0.66970	49%
	119B	->	122B	0.10682	1%
	119B	->	123B	0.66970	49%
33	115A	->	121A	0.13210	2%
	115A	->	122A	-0.62634	42%
	116A	->	122A	-0.13985	2%
	117A	->	122A	0.20246	4%
	115B	->	121B	-0.13210	2%
	115B	->	122B	0.62634	42%
	116B	->	122B	0.13985	2%
	117B	->	122B	-0.20246	4%
34	115A	->	122A	-0.23247	6%
	116A	->	122A	0.15358	3%
	117A	->	122A	-0.61851	42%
	115B	->	122B	0.23247	6%
	116B	->	122B	-0.15358	3%
	117B	->	122B	0.61851	42%
35	116A	->	122A	-0.20812	5%
	117A	->	122A	0.64914	45%
	116B	->	122B	-0.20812	5%
	117B	->	122B	0.64914	45%
36	115A	->	122A	0.67220	48%
	115A	->	123A	0.10252	1%
	117A	->	122A	0.10891	1%
	115B	->	122B	0.67220	48%
	115B	->	123B	0.10252	1%
	117B	->	122B	0.10891	1%
37	114A	->	121A	0.67421	48%
	118A	->	123A	0.12280	2%
	114B	->	121B	-0.67421	48%
	118B	->	123B	-0.12280	2%
38	114A	->	121A	-0.13270	2%
	115A	->	123A	0.12400	2%
	117A	->	122A	-0.10657	1%
	118A	->	122A	-0.10072	1%
	118A	->	123A	0.64845	44%
	114B	->	121B	0.13270	2%
	115B	->	123B	-0.12400	2%
	117B	->	122B	0.10657	1%
	118B	->	122B	0.10072	1%
	118B	->	123B	-0.64845	44%
39	114A	->	121A	0.53301	30%
	118A	->	123A	0.43179	20%
	114B	->	121B	0.53301	30%
	118B	->	123B	0.43179	20%

40	114A	->	121A	-0.44230	21%
	118A	->	123A	0.51973	29%
	114B	->	121B	-0.44230	21%
	118B	->	123B	0.51973	29%
41	116A	->	122A	-0.59391	38%
	116A	->	123A	-0.11135	1%
	116A	->	128A	0.18425	4%
	117A	->	122A	-0.17735	3%
	118A	->	129A	0.18782	4%
	116B	->	122B	0.59391	38%
	116B	->	123B	0.11135	1%
	116B	->	128B	-0.18425	4%
	117B	->	122B	0.17735	3%
	118B	->	129B	-0.18782	4%
42	116A	->	122A	0.65609	46%
	117A	->	122A	0.19828	4%
	116B	->	122B	0.65609	46%
	117B	->	122B	0.19828	4%
43	112A	->	121A	0.20071	4%
	113A	->	121A	-0.14044	2%
	115A	->	122A	0.10059	1%
	115A	->	123A	0.61350	41%
	118A	->	123A	-0.12630	2%
	112B	->	121B	-0.20071	4%
	113B	->	121B	0.14044	2%
	115B	->	122B	-0.10059	1%
	115B	->	123B	-0.61350	41%
	118B	->	123B	0.12630	2%
44	113A	->	121A	-0.65941	48%
	115A	->	123A	-0.14661	2%
	113B	->	121B	0.65941	48%
	115B	->	123B	0.14661	2%
45	115A	->	123A	0.10347	1%
	116A	->	123A	-0.20433	4%
	117A	->	123A	0.65138	44%
	115B	->	123B	-0.10347	1%
	116B	->	123B	0.20433	4%
	117B	->	123B	-0.65138	44%
46	116A	->	122A	0.27287	8%
	116A	->	128A	0.33693	13%
	117A	->	128A	0.12707	2%
	118A	->	124A	-0.17042	3%
	118A	->	129A	0.45571	24%
	116B	->	122B	-0.27287	8%
	116B	->	128B	-0.33693	13%

	117B	->	128B	-0.12707	2%
	118B	->	124B	0.17042	3%
	118B	->	129B	-0.45571	24%
47	113A	->	121A	0.45378	21%
	115A	->	123A	-0.11906	1%
	116A	->	123A	-0.17229	3%
	117A	->	123A	0.47996	24%
	113B	->	121B	0.45378	21%
	115B	->	123B	-0.11906	1%
	116B	->	123B	-0.17229	3%
	117B	->	123B	0.47996	24%
48	113A	->	121A	0.48567	25%
	115A	->	123A	-0.11879	1%
	116A	->	123A	0.12840	2%
	117A	->	123A	-0.45530	22%
	113B	->	121B	0.48567	25%
	115B	->	123B	-0.11879	1%
	116B	->	123B	0.12840	2%
	117B	->	123B	-0.45530	22%
49	112A	->	121A	-0.10300	1%
	113A	->	121A	0.12471	2%
	115A	->	123A	0.63872	44%
	118A	->	124A	-0.15722	3%
	112B	->	121B	-0.10300	1%
	113B	->	121B	0.12471	2%
	115B	->	123B	0.63872	44%
	118B	->	124B	-0.15722	3%
50	114A	->	124A	0.41226	19%
	116A	->	128A	0.12231	2%
	118A	->	124A	0.49045	27%
	118A	->	129A	0.13302	2%
	114B	->	124B	-0.41226	19%
	116B	->	128B	-0.12231	2%
	118B	->	124B	-0.49045	27%
	118B	->	129B	-0.13302	2%
51	113A	->	121A	0.15352	3%
	114A	->	124A	0.11923	2%
	115A	->	123A	0.13982	2%
	117A	->	124A	-0.24094	6%
	118A	->	124A	0.56037	34%
	120A	->	124A	-0.17001	3%
	113B	->	121B	0.15352	3%
	114B	->	124B	0.11923	2%
	115B	->	123B	0.13982	2%
	117B	->	124B	-0.24094	6%

	118B	->	124B	0.56037	34%
	120B	->	124B	-0.17001	3%
52	112A	->	121A	0.12073	2%
	112A	->	122A	0.30768	10%
	115A	->	123A	-0.10792	1%
	116A	->	122A	-0.11207	1%
	116A	->	123A	0.54611	32%
	117A	->	123A	0.17667	3%
	112B	->	121B	-0.12073	2%
	112B	->	122B	-0.30768	10%
	115B	->	123B	0.10792	1%
	116B	->	122B	0.11207	1%
	116B	->	123B	-0.54611	32%
	117B	->	123B	-0.17667	3%
53	116A	->	122A	-0.10073	1%
	116A	->	123A	0.65995	44%
	117A	->	123A	0.21036	5%
	116B	->	122B	-0.10073	1%
	116B	->	123B	0.65995	44%
	117B	->	123B	0.21036	5%
54	106A	->	123A	0.11364	1%
	107A	->	123A	-0.10602	1%
	112A	->	121A	-0.19960	4%
	112A	->	122A	-0.51540	28%
	116A	->	123A	0.35319	13%
	117A	->	123A	0.11384	1%
	106B	->	123B	-0.11364	1%
	107B	->	123B	0.10602	1%
	112B	->	121B	0.19960	4%
	112B	->	122B	0.51540	28%
	116B	->	123B	-0.35319	13%
	117B	->	123B	-0.11384	1%
55	106A	->	121A	0.29973	10%
	106A	->	122A	-0.15181	3%
	107A	->	122A	0.27003	8%
	108A	->	123A	-0.15306	3%
	109A	->	123A	0.16664	3%
	112A	->	123A	0.31159	11%
	112A	->	125A	-0.23113	6%
	113A	->	123A	-0.10364	1%
	115A	->	123A	0.13082	2%
	119A	->	125A	0.13552	2%
	106B	->	121B	-0.29973	10%
	106B	->	122B	0.15181	3%
	107B	->	122B	-0.27003	8%

	108B	->	123B	0.15306	3%
	109B	->	123B	-0.16664	3%
	112B	->	123B	-0.31159	11%
	112B	->	125B	0.23113	6%
	113B	->	123B	0.10364	1%
	115B	->	123B	-0.13082	2%
	119B	->	125B	-0.13552	2%
56	110A	->	121A	-0.22133	5%
	111A	->	121A	0.53623	31%
	114A	->	122A	0.36046	14%
	110B	->	121B	0.22133	5%
	111B	->	121B	-0.53623	31%
	114B	->	122B	-0.36046	14%
57	111A	->	121A	-0.36780	14%
	114A	->	122A	0.58007	36%
	111B	->	121B	0.36780	14%
	114B	->	122B	-0.58007	36%
58	110A	->	121A	-0.12092	2%
	111A	->	121A	0.20117	4%
	114A	->	122A	0.64946	44%
	110B	->	121B	-0.12092	2%
	111B	->	121B	0.20117	4%
	114B	->	122B	0.64946	44%
59	110A	->	121A	-0.23786	6%
	111A	->	121A	0.60790	38%
	114A	->	122A	-0.24141	6%
	110B	->	121B	-0.23786	6%
	111B	->	121B	0.60790	38%
	114B	->	122B	-0.24141	6%
60	116A	->	124A	0.50170	27%
	116A	->	129A	-0.12863	2%
	117A	->	124A	0.24979	7%
	118A	->	125A	-0.11742	1%
	118A	->	128A	-0.34288	13%
	116B	->	124B	-0.50170	27%
	116B	->	129B	0.12863	2%
	117B	->	124B	-0.24979	7%
	118B	->	125B	0.11742	1%
	118B	->	128B	0.34288	13%
61	112A	->	121A	0.57119	36%
	112A	->	122A	0.14938	2%
	113A	->	122A	0.30557	10%
	115A	->	123A	0.10396	1%
	112B	->	121B	0.57119	36%
	112B	->	122B	0.14938	2%

	113B	->	122B	0.30557	10%
	115B	->	123B	0.10396	1%
62	107A	->	121A	-0.11986	2%
	107A	->	123A	-0.15379	3%
	108A	->	121A	0.32556	13%
	109A	->	121A	-0.36938	17%
	112A	->	123A	0.11849	2%
	113A	->	121A	-0.10028	1%
	113A	->	122A	0.23278	7%
	119A	->	125A	-0.18623	4%
	107B	->	121B	0.11986	2%
	107B	->	123B	0.15379	3%
	108B	->	121B	-0.32556	13%
	109B	->	121B	0.36938	17%
	112B	->	123B	-0.11849	2%
	113B	->	121B	0.10028	1%
	113B	->	122B	-0.23278	7%
	119B	->	125B	0.18623	4%
63	106A	->	121A	0.11055	1%
	112A	->	123A	-0.17770	4%
	113A	->	122A	0.10899	1%
	116A	->	124A	-0.30975	11%
	117A	->	124A	-0.15087	3%
	118A	->	125A	-0.14566	2%
	118A	->	128A	-0.43033	22%
	118A	->	129A	0.10269	1%
	119A	->	125A	0.19539	4%
	106B	->	121B	-0.11055	1%
	112B	->	123B	0.17770	4%
	113B	->	122B	-0.10899	1%
	116B	->	124B	0.30975	11%
	117B	->	124B	0.15087	3%
	118B	->	125B	0.14566	2%
	118B	->	128B	0.43033	22%
	118B	->	129B	-0.10269	1%
	119B	->	125B	-0.19539	4%
64	116A	->	124A	0.60525	39%
	117A	->	124A	0.33003	11%
	116B	->	124B	0.60525	39%
	117B	->	124B	0.33003	11%
65	106A	->	121A	-0.21735	6%
	112A	->	123A	0.35296	15%
	113A	->	122A	-0.33842	14%
	116A	->	124A	-0.12596	2%
	118A	->	125A	-0.10163	1%

	118A	->	128A	-0.20864	5%
	119A	->	125A	-0.25969	8%
	106B	->	121B	0.21735	6%
	112B	->	123B	-0.35296	15%
	113B	->	122B	0.33842	14%
	116B	->	124B	0.12596	2%
	118B	->	125B	0.10163	1%
	118B	->	128B	0.20864	5%
	119B	->	125B	0.25969	8%
66	110A	->	121A	0.60606	40%
	111A	->	121A	0.19720	4%
	114A	->	123A	-0.10998	1%
	120A	->	125A	-0.18915	4%
	110B	->	121B	-0.60606	40%
	111B	->	121B	-0.19720	4%
	114B	->	123B	0.10998	1%
	120B	->	125B	0.18915	4%
67	106A	->	121A	0.16822	3%
	108A	->	121A	0.17146	3%
	109A	->	121A	-0.20860	5%
	112A	->	123A	-0.29714	10%
	113A	->	122A	-0.49280	27%
	120A	->	125A	0.12261	2%
	106B	->	121B	-0.16822	3%
	108B	->	121B	-0.17146	3%
	109B	->	121B	0.20860	5%
	112B	->	123B	0.29714	10%
	113B	->	122B	0.49280	27%
	120B	->	125B	-0.12261	2%
68	110A	->	121A	-0.16258	3%
	113A	->	122A	-0.10395	1%
	118A	->	125A	-0.10820	1%
	120A	->	125A	-0.63533	43%
	120A	->	126A	0.12369	2%
	110B	->	121B	0.16258	3%
	113B	->	122B	0.10395	1%
	118B	->	125B	0.10820	1%
	120B	->	125B	0.63533	43%
	120B	->	126B	-0.12369	2%
69	110A	->	121A	-0.12081	2%
	120A	->	125A	0.67095	47%
	120A	->	126A	-0.13009	2%
	110B	->	121B	-0.12081	2%
	120B	->	125B	0.67095	47%
	120B	->	126B	-0.13009	2%

70	112A	->	121A	-0.29222	9%
	113A	->	122A	0.56177	33%
	113A	->	123A	-0.10289	1%
	119A	->	125A	0.24716	6%
	112B	->	121B	-0.29222	9%
	113B	->	122B	0.56177	33%
	113B	->	123B	-0.10289	1%
	119B	->	125B	0.24716	6%
71	110A	->	121A	0.62638	41%
	111A	->	121A	0.28085	8%
	120A	->	125A	0.11096	1%
	110B	->	121B	0.62638	41%
	111B	->	121B	0.28085	8%
	120B	->	125B	0.11096	1%
72	116A	->	125A	-0.12713	2%
	116A	->	128A	-0.47191	26%
	117A	->	128A	-0.16537	3%
	118A	->	129A	0.40229	19%
	116B	->	125B	0.12713	2%
	116B	->	128B	0.47191	26%
	117B	->	128B	0.16537	3%
	118B	->	129B	-0.40229	19%
73	107A	->	121A	0.10693	1%
	113A	->	122A	0.11685	2%
	113A	->	124A	-0.46694	27%
	116A	->	128A	-0.10113	1%
	119A	->	124A	-0.19657	5%
	119A	->	125A	-0.32770	13%
	107B	->	121B	-0.10693	1%
	113B	->	122B	-0.11685	2%
	113B	->	124B	0.46694	27%
	116B	->	128B	0.10113	1%
	119B	->	124B	0.19657	5%
	119B	->	125B	0.32770	13%
74	106A	->	121A	0.13810	2%
	107A	->	121A	0.10580	1%
	112A	->	123A	-0.11638	2%
	113A	->	122A	0.14725	3%
	113A	->	124A	0.39715	18%
	119A	->	124A	0.15435	3%
	119A	->	125A	-0.42434	21%
	106B	->	121B	-0.13810	2%
	107B	->	121B	-0.10580	1%
	112B	->	123B	0.11638	2%
	113B	->	122B	-0.14725	3%

	113B	->	124B	-0.39715	18%
	119B	->	124B	-0.15435	3%
	119B	->	125B	0.42434	21%
75	113A	->	122A	-0.24642	6%
	119A	->	125A	0.62744	42%
	119A	->	126A	-0.12032	2%
	113B	->	122B	-0.24642	6%
	119B	->	125B	0.62744	42%
	119B	->	126B	-0.12032	2%
76	106A	->	121A	0.25927	8%
	107A	->	121A	-0.47096	25%
	109A	->	121A	0.10094	1%
	112A	->	125A	-0.16708	3%
	113A	->	123A	0.11994	2%
	114A	->	123A	-0.31251	11%
	106B	->	121B	-0.25927	8%
	107B	->	121B	0.47096	25%
	109B	->	121B	-0.10094	1%
	112B	->	125B	0.16708	3%
	113B	->	123B	-0.11994	2%
	114B	->	123B	0.31251	11%
77	107A	->	121A	-0.25705	7%
	110A	->	121A	0.12296	2%
	113A	->	123A	0.15730	3%
	114A	->	123A	0.58684	38%
	107B	->	121B	0.25705	7%
	110B	->	121B	-0.12296	2%
	113B	->	123B	-0.15730	3%
	114B	->	123B	-0.58684	38%
78	114A	->	123A	0.69438	50%
	114B	->	123B	0.69438	50%
79	118A	->	125A	0.67086	48%
	118A	->	126A	-0.13038	2%
	118B	->	125B	0.67086	48%
	118B	->	126B	-0.13038	2%
80	120A	->	125A	-0.13425	2%
	120A	->	126A	-0.67373	48%
	120B	->	125B	0.13425	2%
	120B	->	126B	0.67373	48%
81	113A	->	123A	-0.10937	1%
	120A	->	125A	0.12725	2%
	120A	->	126A	0.67720	47%
	113B	->	123B	-0.10937	1%
	120B	->	125B	0.12725	2%
	120B	->	126B	0.67720	47%

82	107A	->	121A	-0.18080	4%
	113A	->	123A	-0.45420	23%
	118A	->	125A	0.43373	21%
	118A	->	128A	-0.13698	2%
	107B	->	121B	0.18080	4%
	113B	->	123B	0.45420	23%
	118B	->	125B	-0.43373	21%
	118B	->	128B	0.13698	2%
83	107A	->	121A	0.16968	3%
	113A	->	123A	0.44479	22%
	118A	->	125A	0.45432	23%
	118A	->	128A	-0.14246	2%
	107B	->	121B	-0.16968	3%
	113B	->	123B	-0.44479	22%
	118B	->	125B	-0.45432	23%
	118B	->	128B	0.14246	2%
84	113A	->	123A	0.46736	23%
	113A	->	124A	-0.41518	18%
	114A	->	124A	0.19614	4%
	119A	->	124A	-0.15468	3%
	119A	->	126A	0.12243	2%
	113B	->	123B	0.46736	23%
	113B	->	124B	-0.41518	18%
	114B	->	124B	0.19614	4%
	119B	->	124B	-0.15468	3%
	119B	->	126B	0.12243	2%
85	113A	->	123A	0.48153	25%
	113A	->	124A	0.41102	18%
	119A	->	124A	0.14484	2%
	119A	->	126A	-0.19773	4%
	113B	->	123B	0.48153	25%
	113B	->	124B	0.41102	18%
	119B	->	124B	0.14484	2%
	119B	->	126B	-0.19773	4%
86	111A	->	124A	0.11226	1%
	119A	->	125A	-0.13252	2%
	119A	->	126A	-0.66675	47%
	111B	->	124B	-0.11226	1%
	119B	->	125B	0.13252	2%
	119B	->	126B	0.66675	47%
87	110A	->	124A	-0.24832	7%
	111A	->	124A	0.49080	27%
	116A	->	124A	-0.20502	5%
	117A	->	124A	0.26977	8%
	119A	->	126A	0.15185	3%

	110B	->	124B	0.24832	7%
	111B	->	124B	-0.49080	27%
	116B	->	124B	0.20502	5%
	117B	->	124B	-0.26977	8%
	119B	->	126B	-0.15185	3%
88	113A	->	124A	0.21819	5%
	119A	->	125A	0.11905	1%
	119A	->	126A	0.64590	44%
	113B	->	124B	0.21819	5%
	119B	->	125B	0.11905	1%
	119B	->	126B	0.64590	44%
89	108A	->	121A	-0.17653	4%
	109A	->	121A	0.22716	6%
	112A	->	121A	-0.16355	3%
	112A	->	122A	0.53611	33%
	115A	->	125A	0.19952	5%
	108B	->	121B	-0.17653	4%
	109B	->	121B	0.22716	6%
	112B	->	121B	-0.16355	3%
	112B	->	122B	0.53611	33%
	115B	->	125B	0.19952	5%
90	116A	->	129A	-0.21642	5%
	117A	->	129A	-0.10478	1%
	118A	->	126A	0.60516	41%
	120A	->	129A	-0.15922	3%
	116B	->	129B	0.21642	5%
	117B	->	129B	0.10478	1%
	118B	->	126B	-0.60516	41%
	120B	->	129B	0.15922	3%
91	118A	->	125A	0.12501	2%
	118A	->	126A	0.68188	48%
	118B	->	125B	0.12501	2%
	118B	->	126B	0.68188	48%
92	115A	->	125A	-0.20132	4%
	116A	->	125A	-0.12751	2%
	116A	->	129A	-0.33525	12%
	117A	->	125A	0.31137	11%
	117A	->	129A	-0.15035	2%
	118A	->	126A	-0.30700	10%
	118A	->	128A	0.12443	2%
	120A	->	129A	-0.24478	7%
	115B	->	125B	0.20132	4%
	116B	->	125B	0.12751	2%
	116B	->	129B	0.33525	12%
	117B	->	125B	-0.31137	11%

	117B	->	129B	0.15035	2%
	118B	->	126B	0.30700	10%
	118B	->	128B	-0.12443	2%
	120B	->	129B	0.24478	7%
93	115A	->	125A	-0.26171	8%
	116A	->	125A	-0.14930	2%
	116A	->	129A	0.34847	14%
	117A	->	125A	0.42226	20%
	117A	->	129A	0.13946	2%
	118A	->	128A	-0.14081	2%
	120A	->	129A	0.14043	2%
	115B	->	125B	0.26171	8%
	116B	->	125B	0.14930	2%
	116B	->	129B	-0.34847	14%
	117B	->	125B	-0.42226	20%
	117B	->	129B	-0.13946	2%
	118B	->	128B	0.14081	2%
	120B	->	129B	-0.14043	2%
94	116A	->	125A	-0.19761	4%
	117A	->	125A	0.64037	44%
	117A	->	126A	-0.13012	2%
	116B	->	125B	-0.19761	4%
	117B	->	125B	0.64037	44%
	117B	->	126B	-0.13012	2%
95	108A	->	122A	-0.10357	1%
	109A	->	122A	0.12452	2%
	115A	->	125A	-0.53074	32%
	115A	->	126A	0.10558	1%
	117A	->	125A	-0.34194	13%
	108B	->	122B	0.10357	1%
	109B	->	122B	-0.12452	2%
	115B	->	125B	0.53074	32%
	115B	->	126B	-0.10558	1%
	117B	->	125B	0.34194	13%
96	111A	->	124A	-0.12065	2%
	116A	->	129A	0.29858	10%
	117A	->	125A	-0.11143	1%
	120A	->	128A	0.26273	8%
	120A	->	129A	-0.51525	29%
	111B	->	124B	0.12065	2%
	116B	->	129B	-0.29858	10%
	117B	->	125B	0.11143	1%
	120B	->	128B	-0.26273	8%
	120B	->	129B	0.51525	29%
97	107A	->	121A	-0.10294	1%

	110A	->	124A	-0.26842	8%
	111A	->	124A	0.29694	10%
	112A	->	121A	0.10641	1%
	112A	->	122A	-0.24417	7%
	113A	->	124A	0.15054	3%
	114A	->	124A	0.19919	5%
	115A	->	125A	0.20131	5%
	116A	->	124A	-0.16558	3%
	117A	->	124A	0.22382	6%
	118A	->	124A	0.10852	1%
	107B	->	121B	-0.10294	1%
	110B	->	124B	-0.26842	8%
	111B	->	124B	0.29694	10%
	112B	->	121B	0.10641	1%
	112B	->	122B	-0.24417	7%
	113B	->	124B	0.15054	3%
	114B	->	124B	0.19919	5%
	115B	->	125B	0.20131	5%
	116B	->	124B	-0.16558	3%
	117B	->	124B	0.22382	6%
	118B	->	124B	0.10852	1%
98	107A	->	121A	-0.14086	2%
	110A	->	124A	0.13893	2%
	111A	->	124A	-0.17661	3%
	112A	->	122A	-0.11715	1%
	112A	->	123A	-0.21010	5%
	115A	->	125A	0.54495	32%
	115A	->	126A	-0.10565	1%
	117A	->	124A	-0.11643	1%
	117A	->	125A	0.11166	1%
	107B	->	121B	-0.14086	2%
	110B	->	124B	0.13893	2%
	111B	->	124B	-0.17661	3%
	112B	->	122B	-0.11715	1%
	112B	->	123B	-0.21010	5%
	115B	->	125B	0.54495	32%
	115B	->	126B	-0.10565	1%
	117B	->	124B	-0.11643	1%
	117B	->	125B	0.11166	1%
99	107A	->	123A	-0.20102	5%
	108A	->	121A	-0.14014	2%
	108A	->	122A	0.29395	10%
	108A	->	123A	-0.13124	2%
	109A	->	121A	0.18489	4%
	109A	->	122A	-0.33255	13%

	109A	->	123A	0.15741	3%
	111A	->	122A	0.19025	4%
	112A	->	122A	0.10829	1%
	115A	->	125A	-0.23614	6%
	107B	->	123B	0.20102	5%
	108B	->	121B	0.14014	2%
	108B	->	122B	-0.29395	10%
	108B	->	123B	0.13124	2%
	109B	->	121B	-0.18489	4%
	109B	->	122B	0.33255	13%
	109B	->	123B	-0.15741	3%
	111B	->	122B	-0.19025	4%
	112B	->	122B	-0.10829	1%
	115B	->	125B	0.23614	6%
100	120A	->	128A	0.53809	31%
	120A	->	129A	-0.42189	19%
	120B	->	128B	0.53809	31%
	120B	->	129B	-0.42189	19%

Table S30. TD-DFT calculated transition Kohn-Sham orbital contributions for [Ni(dtbbpy)(*o*-tolyl)Br] S_0 (**x**).

Excited State	KS Orbital Transition			C_i	$C_i^2/\Sigma C_i^2$
1	126A	->	133A	0.16035	2%
	127A	->	133A	-0.51440	23%
	128A	->	133A	-0.45497	18%
	129A	->	133A	-0.18095	3%
	126B	->	133B	-0.16035	2%
	127B	->	133B	0.51440	23%
	128B	->	133B	0.45497	18%
	129B	->	133B	0.18095	3%
	127A	<-	133A	-0.15122	2%
	128A	<-	133A	-0.14123	2%
	127B	<-	133B	0.15122	2%
	128B	<-	133B	0.14123	2%
2	123A	->	133A	-0.33299	11%
	124A	->	133A	0.19307	4%
	128A	->	133A	0.26761	7%
	129A	->	133A	-0.53696	28%
	123B	->	133B	0.33299	11%
	124B	->	133B	-0.19307	4%
	128B	->	133B	-0.26761	7%
	129B	->	133B	0.53696	28%
	129A	<-	133A	-0.12140	1%
	129B	<-	133B	0.12140	1%
3	123A	->	133A	-0.11205	1%
	124A	->	133A	-0.67539	44%
	125A	->	133A	-0.10896	1%
	129A	->	133A	-0.14862	2%
	123B	->	133B	0.11205	1%
	124B	->	133B	0.67539	44%
	125B	->	133B	0.10896	1%
	129B	->	133B	0.14862	2%
	124A	<-	133A	-0.14258	2%
	124B	<-	133B	0.14258	2%
4	119A	->	133A	-0.37821	15%
	121A	->	133A	0.18695	4%
	125A	->	133A	0.15549	3%
	126A	->	133A	-0.50759	27%
	129A	->	130A	-0.13778	2%
	119B	->	133B	0.37821	15%
	121B	->	133B	-0.18695	4%
	125B	->	133B	-0.15549	3%

	126B	->	133B	0.50759	27%
	129B	->	130B	0.13778	2%
5	123A	->	130A	-0.14402	2%
	126A	->	133A	0.11105	1%
	128A	->	130A	0.22448	5%
	129A	->	130A	-0.60628	40%
	129A	->	131A	-0.11020	1%
	123B	->	130B	0.14402	2%
	126B	->	133B	-0.11105	1%
	128B	->	130B	-0.22448	5%
	129B	->	130B	0.60628	40%
	129B	->	131B	0.11020	1%
6	126A	->	130A	0.10742	1%
	127A	->	130A	-0.44432	21%
	128A	->	130A	-0.50432	26%
	129A	->	130A	-0.12918	2%
	126B	->	130B	-0.10742	1%
	127B	->	130B	0.44432	21%
	128B	->	130B	0.50432	26%
	129B	->	130B	0.12918	2%
7	127A	->	130A	0.44864	21%
	128A	->	130A	0.48032	24%
	129A	->	130A	0.19845	4%
	127B	->	130B	0.44864	21%
	128B	->	130B	0.48032	24%
	129B	->	130B	0.19845	4%
8	124A	->	130A	-0.16006	3%
	126A	->	133A	0.11274	1%
	127A	->	133A	-0.36031	13%
	128A	->	130A	-0.20230	4%
	128A	->	133A	-0.29870	9%
	129A	->	130A	0.40883	17%
	129A	->	133A	-0.12890	2%
	124B	->	130B	-0.16006	3%
	126B	->	133B	0.11274	1%
	127B	->	133B	-0.36031	13%
	128B	->	130B	-0.20230	4%
	128B	->	133B	-0.29870	9%
	129B	->	130B	0.40883	17%
	129B	->	133B	-0.12890	2%
9	123A	->	133A	0.26815	8%
	124A	->	133A	-0.12519	2%
	128A	->	130A	-0.15049	2%
	128A	->	133A	-0.27678	8%
	129A	->	133A	0.52344	30%

	123B	->	133B	0.26815	8%
	124B	->	133B	-0.12519	2%
	128B	->	130B	-0.15049	2%
	128B	->	133B	-0.27678	8%
	129B	->	133B	0.52344	30%
10	127A	->	133A	0.36462	14%
	128A	->	130A	-0.19675	4%
	128A	->	133A	0.27216	8%
	129A	->	130A	0.45831	22%
	129A	->	133A	0.14186	2%
	127B	->	133B	0.36462	14%
	128B	->	130B	-0.19675	4%
	128B	->	133B	0.27216	8%
	129B	->	130B	0.45831	22%
	129B	->	133B	0.14186	2%
11	126A	->	130A	-0.12897	2%
	127A	->	130A	0.50007	25%
	128A	->	130A	-0.41344	17%
	129A	->	130A	-0.23505	6%
	126B	->	130B	0.12897	2%
	127B	->	130B	-0.50007	25%
	128B	->	130B	0.41344	17%
	129B	->	130B	0.23505	6%
12	124A	->	133A	0.14076	2%
	126A	->	130A	-0.19340	4%
	127A	->	130A	0.48702	24%
	128A	->	130A	-0.38136	15%
	129A	->	130A	-0.19366	4%
	129A	->	133A	-0.10368	1%
	124B	->	133B	0.14076	2%
	126B	->	130B	-0.19340	4%
	127B	->	130B	0.48702	24%
	128B	->	130B	-0.38136	15%
	129B	->	130B	-0.19366	4%
	129B	->	133B	-0.10368	1%
13	122A	->	133A	0.10465	1%
	124A	->	130A	0.65487	45%
	124A	->	131A	0.12811	2%
	125A	->	130A	0.12813	2%
	122B	->	133B	-0.10465	1%
	124B	->	130B	-0.65487	45%
	124B	->	131B	-0.12811	2%
	125B	->	130B	-0.12813	2%
14	124A	->	133A	0.47722	25%
	126A	->	130A	-0.40352	18%

	127A	->	130A	-0.17209	3%
	129A	->	133A	0.17321	3%
	124B	->	133B	0.47722	25%
	126B	->	130B	-0.40352	18%
	127B	->	130B	-0.17209	3%
	129B	->	133B	0.17321	3%
15	125A	->	130A	-0.11574	1%
	126A	->	130A	0.66387	46%
	127A	->	130A	0.16614	3%
	125B	->	130B	0.11574	1%
	126B	->	130B	-0.66387	46%
	127B	->	130B	-0.16614	3%
16	119A	->	133A	0.34506	13%
	121A	->	133A	-0.15651	3%
	125A	->	133A	-0.16752	3%
	126A	->	133A	0.54050	31%
	119B	->	133B	0.34506	13%
	121B	->	133B	-0.15651	3%
	125B	->	133B	-0.16752	3%
	126B	->	133B	0.54050	31%
17	124A	->	133A	0.45551	22%
	126A	->	130A	0.50945	27%
	127A	->	130A	0.11312	1%
	124B	->	133B	0.45551	22%
	126B	->	130B	0.50945	27%
	127B	->	130B	0.11312	1%
18	122A	->	133A	-0.45945	23%
	124A	->	130A	0.14833	2%
	127A	->	133A	0.27113	8%
	128A	->	133A	-0.32922	12%
	129A	->	133A	-0.17434	3%
	122B	->	133B	0.45945	23%
	124B	->	130B	-0.14833	2%
	127B	->	133B	-0.27113	8%
	128B	->	133B	0.32922	12%
	129B	->	133B	0.17434	3%
	122A	<-	133A	-0.11938	2%
	122B	<-	133B	0.11938	2%
19	124A	->	130A	0.63971	44%
	125A	->	130A	0.15316	3%
	129A	->	130A	0.13526	2%
	129A	->	131A	-0.11253	1%
	124B	->	130B	0.63971	44%
	125B	->	130B	0.15316	3%
	129B	->	130B	0.13526	2%

	129B	->	131B	-0.11253	1%
20	123A	->	131A	-0.10321	1%
	128A	->	131A	0.23468	6%
	129A	->	130A	0.12870	2%
	129A	->	131A	-0.61200	41%
	123B	->	131B	0.10321	1%
	128B	->	131B	-0.23468	6%
	129B	->	130B	-0.12870	2%
	129B	->	131B	0.61200	41%
21	127A	->	131A	-0.40086	17%
	128A	->	131A	-0.53426	30%
	129A	->	131A	-0.17065	3%
	127B	->	131B	0.40086	17%
	128B	->	131B	0.53426	30%
	129B	->	131B	0.17065	3%
22	127A	->	131A	0.40255	17%
	128A	->	131A	0.51482	28%
	129A	->	131A	0.23145	6%
	127B	->	131B	0.40255	17%
	128B	->	131B	0.51482	28%
	129B	->	131B	0.23145	6%
23	124A	->	130A	0.11790	1%
	128A	->	131A	-0.28345	8%
	129A	->	131A	0.61505	39%
	129A	->	132A	-0.12049	1%
	124B	->	130B	0.11790	1%
	128B	->	131B	-0.28345	8%
	129B	->	131B	0.61505	39%
	129B	->	132B	-0.12049	1%
24	124A	->	130A	-0.14884	2%
	125A	->	130A	0.66807	46%
	126A	->	130A	0.11288	1%
	124B	->	130B	0.14884	2%
	125B	->	130B	-0.66807	46%
	126B	->	130B	-0.11288	1%
25	124A	->	130A	-0.16619	3%
	125A	->	130A	0.67740	47%
	124B	->	130B	-0.16619	3%
	125B	->	130B	0.67740	47%
26	127A	->	131A	-0.55735	32%
	128A	->	131A	0.36826	14%
	129A	->	131A	0.19214	4%
	127B	->	131B	0.55735	32%
	128B	->	131B	-0.36826	14%
	129B	->	131B	-0.19214	4%

27	120A	->	130A	0.31034	11%
	120A	->	131A	-0.16331	3%
	123A	->	130A	-0.19221	4%
	125A	->	130A	-0.11066	1%
	128A	->	132A	0.18704	4%
	129A	->	131A	0.11767	2%
	129A	->	132A	-0.47532	25%
	120B	->	130B	-0.31034	11%
	120B	->	131B	0.16331	3%
	123B	->	130B	0.19221	4%
	125B	->	130B	0.11066	1%
	128B	->	132B	-0.18704	4%
	129B	->	131B	-0.11767	2%
	129B	->	132B	0.47532	25%
28	127A	->	131A	0.56363	33%
	128A	->	131A	-0.36923	14%
	129A	->	131A	-0.18205	3%
	127B	->	131B	0.56363	33%
	128B	->	131B	-0.36923	14%
	129B	->	131B	-0.18205	3%
29	127A	->	132A	-0.39355	16%
	128A	->	132A	-0.53420	30%
	129A	->	132A	-0.19649	4%
	127B	->	132B	0.39355	16%
	128B	->	132B	0.53420	30%
	129B	->	132B	0.19649	4%
30	127A	->	132A	0.41035	17%
	128A	->	132A	0.51524	27%
	129A	->	132A	0.22630	5%
	127B	->	132B	0.41035	17%
	128B	->	132B	0.51524	27%
	129B	->	132B	0.22630	5%
31	120A	->	130A	0.45269	22%
	120A	->	131A	-0.12437	2%
	123A	->	130A	-0.19506	4%
	128A	->	132A	-0.18773	4%
	129A	->	132A	0.40841	18%
	120B	->	130B	-0.45269	22%
	120B	->	131B	0.12437	2%
	123B	->	130B	0.19506	4%
	128B	->	132B	0.18773	4%
	129B	->	132B	-0.40841	18%
32	126A	->	131A	0.64396	44%
	127A	->	132A	0.23863	6%
	126B	->	131B	-0.64396	44%

	127B	->	132B	-0.23863	6%
33	126A	->	131A	-0.34499	13%
	128A	->	132A	-0.21173	5%
	129A	->	132A	0.54264	32%
	126B	->	131B	-0.34499	13%
	128B	->	132B	-0.21173	5%
	129B	->	132B	0.54264	32%
34	126A	->	131A	0.55916	33%
	127A	->	132A	0.18534	4%
	128A	->	132A	-0.20324	4%
	129A	->	132A	0.29417	9%
	126B	->	131B	0.55916	33%
	127B	->	132B	0.18534	4%
	128B	->	132B	-0.20324	4%
	129B	->	132B	0.29417	9%
35	120A	->	130A	-0.26692	8%
	123A	->	130A	-0.61356	42%
	120B	->	130B	0.26692	8%
	123B	->	130B	0.61356	42%
36	124A	->	130A	-0.13234	2%
	124A	->	131A	0.65404	45%
	125A	->	131A	0.16236	3%
	124B	->	130B	0.13234	2%
	124B	->	131B	-0.65404	45%
	125B	->	131B	-0.16236	3%
37	123A	->	130A	0.66194	47%
	124A	->	131A	-0.17942	3%
	123B	->	130B	0.66194	47%
	124B	->	131B	-0.17942	3%
38	122A	->	130A	-0.12386	2%
	126A	->	131A	0.22348	5%
	126A	->	132A	0.17245	3%
	127A	->	132A	-0.48429	24%
	128A	->	132A	0.35593	13%
	129A	->	132A	0.18485	3%
	122B	->	130B	0.12386	2%
	126B	->	131B	-0.22348	5%
	126B	->	132B	-0.17245	3%
	127B	->	132B	0.48429	24%
	128B	->	132B	-0.35593	13%
	129B	->	132B	-0.18485	3%
39	123A	->	130A	0.14803	2%
	124A	->	131A	0.58630	37%
	125A	->	131A	0.17017	3%
	127A	->	132A	-0.20359	4%

	128A	->	132A	0.13047	2%
	129A	->	132A	0.11272	1%
	123B	->	130B	0.14803	2%
	124B	->	131B	0.58630	37%
	125B	->	131B	0.17017	3%
	127B	->	132B	-0.20359	4%
	128B	->	132B	0.13047	2%
	129B	->	132B	0.11272	1%
40	124A	->	131A	0.25629	7%
	126A	->	131A	-0.18418	4%
	126A	->	132A	-0.13273	2%
	127A	->	132A	0.46456	23%
	128A	->	132A	-0.34668	13%
	129A	->	132A	-0.15588	3%
	124B	->	131B	0.25629	7%
	126B	->	131B	-0.18418	4%
	126B	->	132B	-0.13273	2%
	127B	->	132B	0.46456	23%
	128B	->	132B	-0.34668	13%
	129B	->	132B	-0.15588	3%
41	122A	->	130A	-0.68123	49%
	127A	->	132A	0.10177	1%
	122B	->	130B	0.68123	49%
	127B	->	132B	-0.10177	1%
42	122A	->	130A	0.69622	50%
	122B	->	130B	0.69622	50%
43	124A	->	131A	-0.13835	2%
	125A	->	131A	0.56059	35%
	125A	->	132A	0.11513	1%
	125A	->	137A	-0.22542	6%
	126A	->	138A	-0.12029	2%
	127A	->	138A	-0.16374	3%
	128A	->	138A	0.11750	2%
	124B	->	131B	0.13835	2%
	125B	->	131B	-0.56059	35%
	125B	->	132B	-0.11513	1%
	125B	->	137B	0.22542	6%
	126B	->	138B	0.12029	2%
	127B	->	138B	0.16374	3%
	128B	->	138B	-0.11750	2%
44	124A	->	132A	-0.27562	8%
	126A	->	132A	-0.60095	39%
	127A	->	132A	-0.16272	3%
	124B	->	132B	0.27562	8%
	126B	->	132B	0.60095	39%

	127B	->	132B	0.16272	3%
45	120A	->	130A	-0.16047	3%
	124A	->	131A	-0.10079	1%
	124A	->	132A	-0.57785	36%
	125A	->	132A	-0.15884	3%
	126A	->	132A	0.27152	8%
	120B	->	130B	0.16047	3%
	124B	->	131B	0.10079	1%
	124B	->	132B	0.57785	36%
	125B	->	132B	0.15884	3%
	126B	->	132B	-0.27152	8%
46	124A	->	131A	-0.17712	3%
	125A	->	131A	0.61556	40%
	126A	->	132A	0.25741	7%
	124B	->	131B	-0.17712	3%
	125B	->	131B	0.61556	40%
	126B	->	132B	0.25741	7%
47	125A	->	131A	-0.24314	6%
	125A	->	132A	-0.11358	1%
	126A	->	132A	0.62302	40%
	127A	->	132A	0.14219	2%
	125B	->	131B	-0.24314	6%
	125B	->	132B	-0.11358	1%
	126B	->	132B	0.62302	40%
	127B	->	132B	0.14219	2%
48	122A	->	133A	-0.21107	5%
	125A	->	131A	0.33795	12%
	125A	->	137A	0.27060	8%
	126A	->	138A	0.19300	4%
	127A	->	133A	-0.20351	4%
	127A	->	138A	0.26317	7%
	128A	->	133A	0.15380	3%
	128A	->	138A	-0.18498	4%
	129A	->	133A	0.11612	1%
	129A	->	138A	-0.11460	1%
	122B	->	133B	0.21107	5%
	125B	->	131B	-0.33795	12%
	125B	->	137B	-0.27060	8%
	126B	->	138B	-0.19300	4%
	127B	->	133B	0.20351	4%
	127B	->	138B	-0.26317	7%
	128B	->	133B	-0.15380	3%
	128B	->	138B	0.18498	4%
	129B	->	133B	-0.11612	1%
	129B	->	138B	0.11460	1%

49	124A	->	132A	0.27742	8%
	127A	->	133A	-0.38803	16%
	128A	->	133A	0.41699	19%
	129A	->	133A	0.24558	7%
	124B	->	132B	0.27742	8%
	127B	->	133B	-0.38803	16%
	128B	->	133B	0.41699	19%
	129B	->	133B	0.24558	7%
50	122A	->	133A	-0.39113	16%
	123A	->	133A	-0.13500	2%
	125A	->	131A	-0.10709	1%
	125A	->	137A	-0.20814	5%
	126A	->	138A	-0.11225	1%
	127A	->	133A	-0.30539	10%
	127A	->	138A	-0.17609	3%
	128A	->	133A	0.21340	5%
	128A	->	138A	0.14855	2%
	129A	->	133A	0.19347	4%
	122B	->	133B	0.39113	16%
	123B	->	133B	0.13500	2%
	125B	->	131B	0.10709	1%
	125B	->	137B	0.20814	5%
	126B	->	138B	0.11225	1%
	127B	->	133B	0.30539	10%
	127B	->	138B	0.17609	3%
	128B	->	133B	-0.21340	5%
	128B	->	138B	-0.14855	2%
	129B	->	133B	-0.19347	4%
51	120A	->	130A	-0.10802	1%
	124A	->	132A	0.59808	40%
	125A	->	132A	0.14032	2%
	127A	->	133A	0.18515	4%
	128A	->	133A	-0.14880	2%
	120B	->	130B	-0.10802	1%
	124B	->	132B	0.59808	40%
	125B	->	132B	0.14032	2%
	127B	->	133B	0.18515	4%
	128B	->	133B	-0.14880	2%
52	119A	->	130A	0.19441	4%
	121A	->	130A	-0.65929	46%
	119B	->	130B	-0.19441	4%
	121B	->	130B	0.65929	46%
53	115A	->	132A	-0.10128	1%
	116A	->	131A	0.11218	1%
	116A	->	132A	0.12418	2%

	120A	->	130A	0.20227	5%
	120A	->	131A	0.48245	26%
	123A	->	131A	0.32031	11%
	124A	->	132A	-0.13056	2%
	125A	->	132A	0.14822	2%
	115B	->	132B	0.10128	1%
	116B	->	131B	-0.11218	1%
	116B	->	132B	-0.12418	2%
	120B	->	130B	-0.20227	5%
	120B	->	131B	-0.48245	26%
	123B	->	131B	-0.32031	11%
	124B	->	132B	0.13056	2%
	125B	->	132B	-0.14822	2%
54	119A	->	130A	-0.20431	4%
	121A	->	130A	0.66825	46%
	119B	->	130B	-0.20431	4%
	121B	->	130B	0.66825	46%
55	120A	->	131A	-0.20336	5%
	125A	->	132A	0.63977	45%
	120B	->	131B	0.20336	5%
	125B	->	132B	-0.63977	45%
56	124A	->	132A	-0.15238	2%
	125A	->	131A	-0.10447	1%
	125A	->	132A	0.66797	46%
	124B	->	132B	-0.15238	2%
	125B	->	131B	-0.10447	1%
	125B	->	132B	0.66797	46%
57	120A	->	131A	0.28902	9%
	123A	->	131A	-0.57914	37%
	123A	->	133A	-0.10268	1%
	125A	->	132A	0.14037	2%
	120B	->	131B	-0.28902	9%
	123B	->	131B	0.57914	37%
	123B	->	133B	0.10268	1%
	125B	->	132B	-0.14037	2%
58	122A	->	133A	0.13263	2%
	123A	->	131A	0.11501	1%
	123A	->	133A	-0.54964	32%
	125A	->	133A	0.16934	3%
	128A	->	133A	-0.17550	3%
	129A	->	133A	0.27281	8%
	122B	->	133B	-0.13263	2%
	123B	->	131B	-0.11501	1%
	123B	->	133B	0.54964	32%
	125B	->	133B	-0.16934	3%

	128B	->	133B	0.17550	3%
	129B	->	133B	-0.27281	8%
59	123A	->	131A	0.67420	50%
	123B	->	131B	0.67420	50%
60	115A	->	130A	-0.28682	9%
	115A	->	131A	0.13487	2%
	116A	->	130A	-0.11334	1%
	116A	->	131A	-0.24749	7%
	117A	->	132A	0.11462	1%
	118A	->	132A	-0.18011	4%
	120A	->	132A	-0.25869	7%
	120A	->	134A	-0.21699	5%
	123A	->	131A	0.12010	2%
	123A	->	132A	-0.25317	7%
	124A	->	132A	-0.13270	2%
	129A	->	134A	0.15981	3%
	115B	->	130B	0.28682	9%
	115B	->	131B	-0.13487	2%
	116B	->	130B	0.11334	1%
	116B	->	131B	0.24749	7%
	117B	->	132B	-0.11462	1%
	118B	->	132B	0.18011	4%
	120B	->	132B	0.25869	7%
	120B	->	134B	0.21699	5%
	123B	->	131B	-0.12010	2%
	123B	->	132B	0.25317	7%
	124B	->	132B	0.13270	2%
	129B	->	134B	-0.15981	3%
61	119A	->	130A	0.63045	43%
	121A	->	130A	0.20564	5%
	122A	->	131A	-0.13734	2%
	119B	->	130B	-0.63045	43%
	121B	->	130B	-0.20564	5%
	122B	->	131B	0.13734	2%
62	119A	->	133A	0.12122	2%
	122A	->	133A	0.10385	1%
	123A	->	133A	-0.13468	2%
	124A	->	133A	0.10527	1%
	125A	->	133A	-0.54450	33%
	126A	->	133A	-0.28371	9%
	127A	->	137A	0.10764	1%
	119B	->	133B	-0.12122	2%
	122B	->	133B	-0.10385	1%
	123B	->	133B	0.13468	2%
	124B	->	133B	-0.10527	1%

	125B	->	133B	0.54450	33%
	126B	->	133B	0.28371	9%
	127B	->	137B	-0.10764	1%
63	119A	->	130A	-0.40675	17%
	121A	->	130A	-0.13477	2%
	122A	->	131A	0.17925	3%
	123A	->	133A	-0.23878	6%
	125A	->	133A	0.40749	18%
	126A	->	133A	0.13908	2%
	129A	->	133A	0.12587	2%
	119B	->	130B	-0.40675	17%
	121B	->	130B	-0.13477	2%
	122B	->	131B	0.17925	3%
	123B	->	133B	-0.23878	6%
	125B	->	133B	0.40749	18%
	126B	->	133B	0.13908	2%
	129B	->	133B	0.12587	2%
64	119A	->	130A	0.43286	20%
	121A	->	130A	0.14218	2%
	122A	->	131A	-0.16050	3%
	125A	->	133A	0.46080	22%
	126A	->	133A	0.17680	3%
	119B	->	130B	0.43286	20%
	121B	->	130B	0.14218	2%
	122B	->	131B	-0.16050	3%
	125B	->	133B	0.46080	22%
	126B	->	133B	0.17680	3%
65	119A	->	130A	-0.13029	2%
	122A	->	131A	-0.67592	48%
	119B	->	130B	0.13029	2%
	122B	->	131B	0.67592	48%
66	119A	->	130A	0.24940	6%
	122A	->	131A	0.64591	44%
	119B	->	130B	0.24940	6%
	122B	->	131B	0.64591	44%
67	117A	->	130A	0.11724	2%
	118A	->	130A	-0.19174	5%
	120A	->	132A	0.18889	4%
	123A	->	132A	-0.12315	2%
	125A	->	138A	0.11707	2%
	126A	->	137A	0.20609	5%
	127A	->	137A	0.31243	12%
	128A	->	137A	-0.24063	7%
	129A	->	134A	0.25888	8%
	129A	->	137A	-0.14869	3%

	117B	->	130B	-0.11724	2%
	118B	->	130B	0.19174	5%
	120B	->	132B	-0.18889	4%
	123B	->	132B	0.12315	2%
	125B	->	138B	-0.11707	2%
	126B	->	137B	-0.20609	5%
	127B	->	137B	-0.31243	12%
	128B	->	137B	0.24063	7%
	129B	->	134B	-0.25888	8%
	129B	->	137B	0.14869	3%
68	115A	->	131A	0.10004	1%
	116A	->	132A	0.10052	1%
	117A	->	130A	-0.16179	3%
	118A	->	130A	0.26446	9%
	120A	->	132A	-0.24870	8%
	123A	->	132A	0.16484	3%
	126A	->	137A	0.15769	3%
	127A	->	137A	0.24303	7%
	128A	->	134A	0.20840	5%
	128A	->	137A	-0.18860	4%
	129A	->	134A	-0.16061	3%
	129A	->	137A	-0.11873	2%
	115B	->	131B	-0.10004	1%
	116B	->	132B	-0.10052	1%
	117B	->	130B	0.16179	3%
	118B	->	130B	-0.26446	9%
	120B	->	132B	0.24870	8%
	123B	->	132B	-0.16484	3%
	126B	->	137B	-0.15769	3%
	127B	->	137B	-0.24303	7%
	128B	->	134B	-0.20840	5%
	128B	->	137B	0.18860	4%
	129B	->	134B	0.16061	3%
	129B	->	137B	0.11873	2%
69	119A	->	130A	-0.13793	2%
	120A	->	130A	-0.17929	3%
	123A	->	133A	0.56026	34%
	125A	->	133A	0.15850	3%
	126A	->	133A	0.12129	2%
	128A	->	133A	0.13558	2%
	129A	->	133A	-0.20966	5%
	119B	->	130B	-0.13793	2%
	120B	->	130B	-0.17929	3%
	123B	->	133B	0.56026	34%
	125B	->	133B	0.15850	3%

	126B	->	133B	0.12129	2%
	128B	->	133B	0.13558	2%
	129B	->	133B	-0.20966	5%
70	120A	->	130A	0.57085	37%
	120A	->	131A	0.13294	2%
	123A	->	132A	-0.27159	8%
	123A	->	133A	0.15732	3%
	120B	->	130B	0.57085	37%
	120B	->	131B	0.13294	2%
	123B	->	132B	-0.27159	8%
	123B	->	133B	0.15732	3%
71	115A	->	130A	-0.16631	3%
	115A	->	131A	-0.10857	1%
	117A	->	130A	-0.21360	5%
	118A	->	130A	0.36905	16%
	120A	->	132A	0.39880	18%
	123A	->	132A	-0.22430	6%
	115B	->	130B	0.16631	3%
	115B	->	131B	0.10857	1%
	117B	->	130B	0.21360	5%
	118B	->	130B	-0.36905	16%
	120B	->	132B	-0.39880	18%
	123B	->	132B	0.22430	6%
72	115A	->	130A	0.19423	4%
	120A	->	134A	0.10435	1%
	123A	->	132A	-0.48842	26%
	128A	->	134A	0.13755	2%
	129A	->	134A	-0.38088	16%
	115B	->	130B	-0.19423	4%
	120B	->	134B	-0.10435	1%
	123B	->	132B	0.48842	26%
	128B	->	134B	-0.13755	2%
	129B	->	134B	0.38088	16%
73	127A	->	134A	-0.41351	18%
	128A	->	134A	-0.50907	28%
	129A	->	134A	-0.18748	4%
	127B	->	134B	0.41351	18%
	128B	->	134B	0.50907	28%
	129B	->	134B	0.18748	4%
74	127A	->	134A	0.39677	16%
	128A	->	134A	0.50853	26%
	129A	->	134A	0.26973	7%
	127B	->	134B	0.39677	16%
	128B	->	134B	0.50853	26%
	129B	->	134B	0.26973	7%

75	119A	->	133A	0.28880	9%
	121A	->	133A	-0.44848	23%
	125A	->	133A	0.28972	9%
	126A	->	133A	-0.27845	9%
	119B	->	133B	-0.28880	9%
	121B	->	133B	0.44848	23%
	125B	->	133B	-0.28972	9%
	126B	->	133B	0.27845	9%
76	120A	->	130A	0.22983	6%
	123A	->	132A	0.62020	42%
	129A	->	134A	0.14306	2%
	120B	->	130B	0.22983	6%
	123B	->	132B	0.62020	42%
	129B	->	134B	0.14306	2%
77	123A	->	132A	-0.12925	2%
	128A	->	134A	-0.31340	11%
	129A	->	134A	0.59326	38%
	123B	->	132B	-0.12925	2%
	128B	->	134B	-0.31340	11%
	129B	->	134B	0.59326	38%
78	115A	->	130A	-0.20192	5%
	118A	->	130A	-0.10089	1%
	120A	->	132A	0.11972	2%
	123A	->	132A	0.12953	2%
	125A	->	134A	-0.11815	2%
	125A	->	137A	0.39848	18%
	126A	->	138A	-0.14014	2%
	127A	->	138A	-0.21885	5%
	128A	->	134A	0.12860	2%
	128A	->	138A	0.19046	4%
	129A	->	134A	-0.23360	6%
	129A	->	138A	0.11391	1%
	115B	->	130B	0.20192	5%
	118B	->	130B	0.10089	1%
	120B	->	132B	-0.11972	2%
	123B	->	132B	-0.12953	2%
	125B	->	134B	0.11815	2%
	125B	->	137B	-0.39848	18%
	126B	->	138B	0.14014	2%
	127B	->	138B	0.21885	5%
	128B	->	134B	-0.12860	2%
	128B	->	138B	-0.19046	4%
	129B	->	134B	0.23360	6%
	129B	->	138B	-0.11391	1%
79	115A	->	130A	-0.27454	9%

	118A	->	130A	-0.13626	2%
	120A	->	132A	0.18555	4%
	120A	->	134A	-0.11271	1%
	123A	->	132A	0.15604	3%
	125A	->	137A	-0.30288	11%
	126A	->	138A	0.10691	1%
	127A	->	138A	0.16171	3%
	128A	->	134A	0.14586	2%
	128A	->	138A	-0.13616	2%
	129A	->	134A	-0.31661	12%
	115B	->	130B	0.27454	9%
	118B	->	130B	0.13626	2%
	120B	->	132B	-0.18555	4%
	120B	->	134B	0.11271	1%
	123B	->	132B	-0.15604	3%
	125B	->	137B	0.30288	11%
	126B	->	138B	-0.10691	1%
	127B	->	138B	-0.16171	3%
	128B	->	134B	-0.14586	2%
	128B	->	138B	0.13616	2%
	129B	->	134B	0.31661	12%
80	116A	->	130A	0.25019	7%
	122A	->	132A	-0.61193	43%
	116B	->	130B	-0.25019	7%
	122B	->	132B	0.61193	43%
81	115A	->	130A	-0.11685	2%
	116A	->	130A	0.54511	33%
	118A	->	132A	0.11541	1%
	120A	->	134A	-0.10399	1%
	122A	->	132A	0.28177	9%
	123A	->	132A	-0.19828	4%
	115B	->	130B	0.11685	2%
	116B	->	130B	-0.54511	33%
	118B	->	132B	-0.11541	1%
	120B	->	134B	0.10399	1%
	122B	->	132B	-0.28177	9%
	123B	->	132B	0.19828	4%
82	122A	->	132A	0.51141	27%
	127A	->	134A	0.37921	15%
	128A	->	134A	-0.23622	6%
	129A	->	134A	-0.12604	2%
	122B	->	132B	0.51141	27%
	127B	->	134B	0.37921	15%
	128B	->	134B	-0.23622	6%
	129B	->	134B	-0.12604	2%

83	122A	->	132A	0.46976	23%
	127A	->	134A	-0.42208	18%
	128A	->	134A	0.25866	7%
	129A	->	134A	0.13634	2%
	122B	->	132B	0.46976	23%
	127B	->	134B	-0.42208	18%
	128B	->	134B	0.25866	7%
	129B	->	134B	0.13634	2%
84	126A	->	134A	-0.15422	3%
	127A	->	134A	0.51036	28%
	127A	->	137A	0.12847	2%
	128A	->	134A	-0.33584	12%
	128A	->	137A	-0.11102	1%
	129A	->	134A	-0.17710	3%
	126B	->	134B	0.15422	3%
	127B	->	134B	-0.51036	28%
	127B	->	137B	-0.12847	2%
	128B	->	134B	0.33584	12%
	128B	->	137B	0.11102	1%
	129B	->	134B	0.17710	3%
85	128A	->	135A	-0.12150	2%
	129A	->	135A	0.68205	48%
	128B	->	135B	0.12150	2%
	129B	->	135B	-0.68205	48%
86	128A	->	135A	-0.17526	3%
	129A	->	135A	0.67525	47%
	128B	->	135B	-0.17526	3%
	129B	->	135B	0.67525	47%
87	127A	->	135A	0.29118	9%
	128A	->	135A	0.62317	41%
	127B	->	135B	-0.29118	9%
	128B	->	135B	-0.62317	41%
88	119A	->	133A	0.45343	22%
	121A	->	133A	-0.28039	9%
	122A	->	133A	-0.14073	2%
	125A	->	133A	0.20744	5%
	126A	->	133A	-0.31208	11%
	127A	->	133A	-0.12537	2%
	119B	->	133B	0.45343	22%
	121B	->	133B	-0.28039	9%
	122B	->	133B	-0.14073	2%
	125B	->	133B	0.20744	5%
	126B	->	133B	-0.31208	11%
	127B	->	133B	-0.12537	2%
89	119A	->	131A	0.11373	1%

	121A	->	131A	-0.68385	49%
	119B	->	131B	-0.11373	1%
	121B	->	131B	0.68385	49%
90	127A	->	135A	0.28112	8%
	128A	->	135A	0.62720	40%
	129A	->	135A	0.13637	2%
	127B	->	135B	0.28112	8%
	128B	->	135B	0.62720	40%
	129B	->	135B	0.13637	2%
91	119A	->	131A	-0.11978	1%
	121A	->	131A	0.68129	49%
	119B	->	131B	-0.11978	1%
	121B	->	131B	0.68129	49%
92	119A	->	133A	-0.42394	20%
	121A	->	133A	-0.43959	21%
	125A	->	133A	-0.10221	1%
	126A	->	133A	0.13793	2%
	127A	->	135A	0.11451	1%
	127A	->	138A	-0.13547	2%
	128A	->	138A	-0.12872	2%
	119B	->	133B	0.42394	20%
	121B	->	133B	0.43959	21%
	125B	->	133B	0.10221	1%
	126B	->	133B	-0.13793	2%
	127B	->	135B	-0.11451	1%
	127B	->	138B	0.13547	2%
	128B	->	138B	0.12872	2%
93	126A	->	134A	0.68540	50%
	126B	->	134B	0.68540	50%
94	125A	->	138A	0.12249	2%
	126A	->	134A	0.65043	47%
	127A	->	134A	0.12776	2%
	125B	->	138B	-0.12249	2%
	126B	->	134B	-0.65043	47%
	127B	->	134B	-0.12776	2%
95	127A	->	135A	0.60436	39%
	128A	->	135A	-0.28689	9%
	129A	->	135A	-0.14141	2%
	127B	->	135B	-0.60436	39%
	128B	->	135B	0.28689	9%
	129B	->	135B	0.14141	2%
96	127A	->	135A	0.63570	41%
	128A	->	135A	-0.26178	7%
	129A	->	135A	-0.12955	2%
	127B	->	135B	0.63570	41%

	128B	->	135B	-0.26178	7%
	129B	->	135B	-0.12955	2%
97	117A	->	130A	-0.13181	2%
	118A	->	130A	0.24640	7%
	120A	->	130A	-0.18950	4%
	120A	->	131A	0.56735	35%
	124A	->	134A	-0.17219	3%
	117B	->	130B	-0.13181	2%
	118B	->	130B	0.24640	7%
	120B	->	130B	-0.18950	4%
	120B	->	131B	0.56735	35%
	124B	->	134B	-0.17219	3%
98	125A	->	138A	0.53840	32%
	126A	->	134A	-0.10376	1%
	126A	->	138A	0.14149	2%
	127A	->	137A	-0.15824	3%
	127A	->	138A	0.16784	3%
	128A	->	138A	0.25147	7%
	129A	->	138A	0.11490	1%
	125B	->	138B	-0.53840	32%
	126B	->	134B	0.10376	1%
	126B	->	138B	-0.14149	2%
	127B	->	137B	0.15824	3%
	127B	->	138B	-0.16784	3%
	128B	->	138B	-0.25147	7%
	129B	->	138B	-0.11490	1%
99	117A	->	131A	-0.10315	1%
	118A	->	131A	0.18038	4%
	118A	->	132A	-0.12940	2%
	124A	->	134A	0.61470	41%
	125A	->	134A	0.13612	2%
	117B	->	131B	0.10315	1%
	118B	->	131B	-0.18038	4%
	118B	->	132B	0.12940	2%
	124B	->	134B	-0.61470	41%
	125B	->	134B	-0.13612	2%
100	119A	->	133A	0.13979	2%
	121A	->	133A	0.11194	1%
	125A	->	138A	0.29231	9%
	127A	->	137A	0.16775	3%
	127A	->	138A	-0.32307	11%
	128A	->	137A	0.28715	9%
	128A	->	138A	-0.33178	12%
	129A	->	137A	0.11017	1%
	129A	->	138A	-0.10786	1%

119B	->	133B	-0.13979	2%
121B	->	133B	-0.11194	1%
125B	->	138B	-0.29231	9%
127B	->	137B	-0.16775	3%
127B	->	138B	0.32307	11%
128B	->	137B	-0.28715	9%
128B	->	138B	0.33178	12%
129B	->	137B	-0.11017	1%
129B	->	138B	0.10786	1%

Table S31. TD-DFT calculated transition Kohn-Sham orbital contributions for [Ni(dtbbpy)(*o*-tolyl)I] S_0 (**x**).

Excited State	KS Orbital Transition			C_i	$C_i^2/\Sigma C_i^2$
1	107A	->	119A	-0.10341	1%
	112A	->	119A	-0.14658	2%
	113A	->	119A	0.69818	41%
	115A	->	119A	-0.16112	2%
	107B	->	119B	0.10341	1%
	112B	->	119B	0.14658	2%
	113B	->	119B	-0.69818	41%
	115B	->	119B	0.16112	2%
	113A	<-	119A	0.22356	4%
	113B	<-	119B	-0.22356	4%
2	109A	->	119A	0.44080	18%
	110A	->	119A	-0.16829	3%
	111A	->	119A	0.15679	2%
	114A	->	119A	0.50428	23%
	115A	->	119A	-0.12033	1%
	109B	->	119B	-0.44080	18%
	110B	->	119B	0.16829	3%
	111B	->	119B	-0.15679	2%
	114B	->	119B	-0.50428	23%
	115B	->	119B	0.12033	1%
	109A	<-	119A	0.11684	1%
	114A	<-	119A	0.11657	1%
	109B	<-	119B	-0.11684	1%
	114B	<-	119B	-0.11657	1%
3	109A	->	119A	0.16098	2%
	110A	->	119A	0.64277	39%
	111A	->	119A	-0.22182	5%
	114A	->	119A	0.13065	2%
	109B	->	119B	-0.16098	2%
	110B	->	119B	-0.64277	39%
	111B	->	119B	0.22182	5%
	114B	->	119B	-0.13065	2%
	110A	<-	119A	0.14078	2%
	110B	<-	119B	-0.14078	2%
4	105A	->	119A	0.42660	19%
	107A	->	119A	-0.14446	2%
	108A	->	119A	-0.14840	2%
	111A	->	119A	0.10779	1%
	112A	->	119A	0.48012	24%
	115A	->	119A	-0.12159	2%

	105B	->	119B	-0.42660	19%
	107B	->	119B	0.14446	2%
	108B	->	119B	0.14840	2%
	111B	->	119B	-0.10779	1%
	112B	->	119B	-0.48012	24%
	115B	->	119B	0.12159	2%
5	109A	->	116A	0.20473	5%
	114A	->	116A	0.61031	40%
	115A	->	116A	-0.21667	5%
	109B	->	116B	-0.20473	5%
	114B	->	116B	-0.61031	40%
	115B	->	116B	0.21667	5%
6	112A	->	116A	0.10506	1%
	113A	->	116A	-0.61697	39%
	113A	->	117A	-0.10992	1%
	114A	->	116A	0.14299	2%
	115A	->	116A	0.26195	7%
	112B	->	116B	-0.10506	1%
	113B	->	116B	0.61697	39%
	113B	->	117B	0.10992	1%
	114B	->	116B	-0.14299	2%
	115B	->	116B	-0.26195	7%
7	113A	->	116A	0.59664	38%
	115A	->	116A	-0.33327	12%
	113B	->	116B	0.59664	38%
	115B	->	116B	-0.33327	12%
8	110A	->	116A	0.12333	2%
	112A	->	119A	-0.10137	1%
	113A	->	119A	0.51795	28%
	114A	->	116A	-0.40032	17%
	115A	->	116A	0.10651	1%
	115A	->	119A	-0.10020	1%
	110B	->	116B	0.12333	2%
	112B	->	119B	-0.10137	1%
	113B	->	119B	0.51795	28%
	114B	->	116B	-0.40032	17%
	115B	->	116B	0.10651	1%
	115B	->	119B	-0.10020	1%
9	113A	->	116A	0.28220	8%
	114A	->	116A	0.18369	3%
	115A	->	116A	0.61073	38%
	113B	->	116B	-0.28220	8%
	114B	->	116B	-0.18369	3%
	115B	->	116B	-0.61073	38%
10	109A	->	119A	0.20518	4%

	113A	->	116A	0.25266	7%
	114A	->	116A	0.12922	2%
	114A	->	119A	0.27714	8%
	115A	->	116A	0.53631	30%
	109B	->	119B	0.20518	4%
	113B	->	116B	0.25266	7%
	114B	->	116B	0.12922	2%
	114B	->	119B	0.27714	8%
	115B	->	116B	0.53631	30%
11	109A	->	119A	0.30577	10%
	110A	->	119A	-0.13087	2%
	111A	->	119A	0.12211	2%
	112A	->	116A	0.16022	3%
	113A	->	116A	-0.22064	5%
	113A	->	119A	0.10194	1%
	114A	->	119A	0.43210	19%
	115A	->	116A	-0.27648	8%
	115A	->	119A	-0.13048	2%
	109B	->	119B	0.30577	10%
	110B	->	119B	-0.13087	2%
	111B	->	119B	0.12211	2%
	112B	->	116B	0.16022	3%
	113B	->	116B	-0.22064	5%
	113B	->	119B	0.10194	1%
	114B	->	119B	0.43210	19%
	115B	->	116B	-0.27648	8%
	115B	->	119B	-0.13048	2%
12	113A	->	119A	0.41032	18%
	114A	->	116A	0.53330	31%
	114A	->	119A	-0.11497	1%
	113B	->	119B	0.41032	18%
	114B	->	116B	0.53330	31%
	114B	->	119B	-0.11497	1%
13	107A	->	119A	-0.19338	4%
	108A	->	119A	0.40061	17%
	110A	->	116A	-0.20499	4%
	113A	->	119A	0.10911	1%
	114A	->	116A	0.11883	1%
	114A	->	119A	0.12035	1%
	115A	->	119A	0.43322	19%
	107B	->	119B	0.19338	4%
	108B	->	119B	-0.40061	17%
	110B	->	116B	0.20499	4%
	113B	->	119B	-0.10911	1%
	114B	->	116B	-0.11883	1%

	114B	->	119B	-0.12035	1%
	115B	->	119B	-0.43322	19%
	108A	<-	119A	0.12760	2%
	108B	<-	119B	-0.12760	2%
14	109A	->	119A	0.14172	2%
	110A	->	119A	0.57395	35%
	111A	->	119A	-0.20564	4%
	112A	->	116A	-0.23745	6%
	114A	->	119A	0.15406	3%
	109B	->	119B	0.14172	2%
	110B	->	119B	0.57395	35%
	111B	->	119B	-0.20564	4%
	112B	->	116B	-0.23745	6%
	114B	->	119B	0.15406	3%
15	108A	->	119A	-0.12488	2%
	110A	->	116A	-0.56422	33%
	110A	->	117A	-0.10333	1%
	111A	->	116A	0.27194	8%
	112A	->	116A	0.18602	4%
	115A	->	119A	-0.15186	2%
	108B	->	119B	0.12488	2%
	110B	->	116B	0.56422	33%
	110B	->	117B	0.10333	1%
	111B	->	116B	-0.27194	8%
	112B	->	116B	-0.18602	4%
	115B	->	119B	0.15186	2%
16	110A	->	116A	0.18981	4%
	112A	->	116A	0.65128	45%
	113A	->	116A	0.12688	2%
	110B	->	116B	-0.18981	4%
	112B	->	116B	-0.65128	45%
	113B	->	116B	-0.12688	2%
17	105A	->	119A	0.38010	16%
	107A	->	119A	-0.13984	2%
	108A	->	119A	-0.10787	1%
	112A	->	119A	0.52529	31%
	105B	->	119B	0.38010	16%
	107B	->	119B	-0.13984	2%
	108B	->	119B	-0.10787	1%
	112B	->	119B	0.52529	31%
18	110A	->	119A	0.24963	6%
	111A	->	119A	-0.11170	1%
	112A	->	116A	0.62543	40%
	113A	->	116A	0.13570	2%
	110B	->	119B	0.24963	6%

	111B	->	119B	-0.11170	1%
	112B	->	116B	0.62543	40%
	113B	->	116B	0.13570	2%
19	110A	->	116A	0.58606	37%
	111A	->	116A	-0.30185	10%
	114A	->	116A	0.12644	2%
	114A	->	117A	-0.12045	2%
	110B	->	116B	0.58606	37%
	111B	->	116B	-0.30185	10%
	114B	->	116B	0.12644	2%
	114B	->	117B	-0.12045	2%
20	109A	->	116A	0.22651	5%
	109A	->	117A	0.14826	2%
	114A	->	116A	-0.17465	3%
	114A	->	117A	0.55803	33%
	115A	->	117A	-0.23122	6%
	109B	->	116B	-0.22651	5%
	109B	->	117B	-0.14826	2%
	114B	->	116B	0.17465	3%
	114B	->	117B	-0.55803	33%
	115B	->	117B	0.23122	6%
21	113A	->	117A	-0.34764	13%
	114A	->	117A	0.20587	4%
	115A	->	117A	0.56147	33%
	113B	->	117B	0.34764	13%
	114B	->	117B	-0.20587	4%
	115B	->	117B	-0.56147	33%
22	113A	->	117A	-0.29917	9%
	115A	->	117A	0.62436	41%
	113B	->	117B	-0.29917	9%
	115B	->	117B	0.62436	41%
23	113A	->	117A	-0.13693	2%
	114A	->	117A	0.66603	47%
	114A	->	118A	-0.11571	1%
	113B	->	117B	-0.13693	2%
	114B	->	117B	0.66603	47%
	114B	->	118B	-0.11571	1%
24	106A	->	116A	0.13038	2%
	109A	->	116A	-0.47734	24%
	110A	->	116A	-0.13831	2%
	111A	->	116A	-0.26198	7%
	114A	->	116A	0.13377	2%
	114A	->	117A	0.29634	9%
	114A	->	118A	-0.16909	3%
	106B	->	116B	-0.13038	2%

	109B	->	116B	0.47734	24%
	110B	->	116B	0.13831	2%
	111B	->	116B	0.26198	7%
	114B	->	116B	-0.13377	2%
	114B	->	117B	-0.29634	9%
	114B	->	118B	0.16909	3%
25	113A	->	117A	-0.58533	36%
	114A	->	117A	-0.13547	2%
	115A	->	117A	-0.33099	12%
	113B	->	117B	0.58533	36%
	114B	->	117B	0.13547	2%
	115B	->	117B	0.33099	12%
26	113A	->	117A	0.60664	38%
	114A	->	117A	0.11479	1%
	115A	->	117A	0.31152	10%
	113B	->	117B	0.60664	38%
	114B	->	117B	0.11479	1%
	115B	->	117B	0.31152	10%
27	109A	->	116A	0.17838	3%
	110A	->	116A	0.33363	11%
	111A	->	116A	0.58674	35%
	109B	->	116B	0.17838	3%
	110B	->	116B	0.33363	11%
	111B	->	116B	0.58674	35%
28	109A	->	116A	0.25116	7%
	110A	->	116A	-0.23607	6%
	111A	->	116A	-0.57442	35%
	114A	->	118A	0.15122	2%
	109B	->	116B	-0.25116	7%
	110B	->	116B	0.23607	6%
	111B	->	116B	0.57442	35%
	114B	->	118B	-0.15122	2%
29	109A	->	116A	0.64891	45%
	111A	->	116A	-0.20753	5%
	109B	->	116B	0.64891	45%
	111B	->	116B	-0.20753	5%
30	106A	->	116A	-0.13758	2%
	106A	->	117A	0.10017	1%
	109A	->	116A	-0.30191	10%
	109A	->	118A	0.11588	1%
	114A	->	118A	0.52703	29%
	115A	->	118A	-0.25335	7%
	106B	->	116B	0.13758	2%
	106B	->	117B	-0.10017	1%
	109B	->	116B	0.30191	10%

	109B	->	118B	-0.11588	1%
	114B	->	118B	-0.52703	29%
	115B	->	118B	0.25335	7%
31	112A	->	117A	0.23004	6%
	113A	->	118A	-0.33703	12%
	114A	->	118A	0.24766	6%
	115A	->	118A	0.49734	26%
	112B	->	117B	-0.23004	6%
	113B	->	118B	0.33703	12%
	114B	->	118B	-0.24766	6%
	115B	->	118B	-0.49734	26%
32	112A	->	117A	0.20316	4%
	113A	->	118A	-0.33607	12%
	115A	->	118A	0.57354	34%
	112B	->	117B	0.20316	4%
	113B	->	118B	-0.33607	12%
	115B	->	118B	0.57354	34%
33	113A	->	118A	-0.11162	1%
	114A	->	117A	0.10235	1%
	114A	->	118A	0.65967	47%
	113B	->	118B	-0.11162	1%
	114B	->	117B	0.10235	1%
	114B	->	118B	0.65967	47%
34	112A	->	117A	-0.43651	20%
	113A	->	118A	-0.52669	29%
	115A	->	118A	-0.12585	2%
	112B	->	117B	0.43651	20%
	113B	->	118B	0.52669	29%
	115B	->	118B	0.12585	2%
35	112A	->	117A	0.45339	21%
	113A	->	118A	0.51069	27%
	115A	->	118A	0.13027	2%
	112B	->	117B	0.45339	21%
	113B	->	118B	0.51069	27%
	115B	->	118B	0.13027	2%
36	101A	->	120A	-0.10896	1%
	106A	->	116A	-0.58251	38%
	106A	->	117A	0.19402	4%
	114A	->	118A	-0.23329	6%
	101B	->	120B	0.10896	1%
	106B	->	116B	0.58251	38%
	106B	->	117B	-0.19402	4%
	114B	->	118B	0.23329	6%
37	112A	->	117A	0.47293	23%
	112A	->	118A	0.12081	2%

	113A	->	118A	-0.29562	9%
	114A	->	118A	-0.12616	2%
	115A	->	118A	-0.37712	15%
	112B	->	117B	-0.47293	23%
	112B	->	118B	-0.12081	2%
	113B	->	118B	0.29562	9%
	114B	->	118B	0.12616	2%
	115B	->	118B	0.37712	15%
38	112A	->	117A	0.47561	23%
	112A	->	118A	0.10763	1%
	113A	->	118A	-0.31255	10%
	114A	->	118A	-0.13628	2%
	115A	->	118A	-0.36496	14%
	112B	->	117B	0.47561	23%
	112B	->	118B	0.10763	1%
	113B	->	118B	-0.31255	10%
	114B	->	118B	-0.13628	2%
	115B	->	118B	-0.36496	14%
39	110A	->	116A	-0.12911	2%
	110A	->	117A	0.60663	39%
	111A	->	117A	-0.29769	9%
	110B	->	116B	0.12911	2%
	110B	->	117B	-0.60663	39%
	111B	->	117B	0.29769	9%
40	108A	->	116A	0.67861	50%
	108B	->	116B	-0.67861	50%
41	108A	->	119A	-0.10009	1%
	110A	->	117A	0.26377	7%
	111A	->	117A	-0.14769	2%
	113A	->	119A	0.11217	1%
	114A	->	119A	0.12489	2%
	115A	->	119A	0.58807	36%
	108B	->	119B	-0.10009	1%
	110B	->	117B	0.26377	7%
	111B	->	117B	-0.14769	2%
	113B	->	119B	0.11217	1%
	114B	->	119B	0.12489	2%
	115B	->	119B	0.58807	36%
42	108A	->	116A	-0.12998	2%
	110A	->	117A	0.53572	31%
	110A	->	118A	0.10032	1%
	111A	->	117A	-0.30442	10%
	115A	->	119A	-0.24984	7%
	108B	->	116B	-0.12998	2%
	110B	->	117B	0.53572	31%

	110B	->	118B	0.10032	1%
	111B	->	117B	-0.30442	10%
	115B	->	119B	-0.24984	7%
43	108A	->	116A	0.67746	50%
	108B	->	116B	0.67746	50%
44	107A	->	119A	0.15591	3%
	108A	->	119A	-0.37786	16%
	109A	->	119A	0.24810	7%
	113A	->	119A	0.10634	1%
	115A	->	119A	0.45733	23%
	107B	->	119B	-0.15591	3%
	108B	->	119B	0.37786	16%
	109B	->	119B	-0.24810	7%
	113B	->	119B	-0.10634	1%
	115B	->	119B	-0.45733	23%
45	109A	->	119A	-0.24259	7%
	110A	->	117A	-0.17822	4%
	111A	->	117A	-0.33511	12%
	111A	->	123A	0.16211	3%
	112A	->	118A	0.36341	15%
	112A	->	124A	-0.14940	2%
	114A	->	119A	0.23172	6%
	115A	->	124A	-0.12025	2%
	109B	->	119B	0.24259	7%
	110B	->	117B	0.17822	4%
	111B	->	117B	0.33511	12%
	111B	->	123B	-0.16211	3%
	112B	->	118B	-0.36341	15%
	112B	->	124B	0.14940	2%
	114B	->	119B	-0.23172	6%
	115B	->	124B	0.12025	2%
46	109A	->	119A	0.20261	5%
	111A	->	117A	0.13708	2%
	111A	->	118A	0.12133	2%
	112A	->	118A	0.55961	37%
	114A	->	119A	-0.20079	5%
	109B	->	119B	-0.20261	5%
	111B	->	117B	-0.13708	2%
	111B	->	118B	-0.12133	2%
	112B	->	118B	-0.55961	37%
	114B	->	119B	0.20079	5%
47	108A	->	119A	-0.21008	5%
	109A	->	119A	-0.29397	10%
	110A	->	117A	0.12879	2%
	110A	->	118A	-0.13838	2%

	111A	->	117A	0.35934	15%
	111A	->	118A	0.15869	3%
	111A	->	123A	-0.10467	1%
	114A	->	119A	0.31407	11%
	108B	->	119B	0.21008	5%
	109B	->	119B	0.29397	10%
	110B	->	117B	-0.12879	2%
	110B	->	118B	0.13838	2%
	111B	->	117B	-0.35934	15%
	111B	->	118B	-0.15869	3%
	111B	->	123B	0.10467	1%
	114B	->	119B	-0.31407	11%
48	112A	->	118A	0.68240	50%
	112B	->	118B	0.68240	50%
49	106A	->	116A	0.14812	3%
	110A	->	117A	0.15400	3%
	110A	->	118A	0.57431	38%
	111A	->	118A	-0.21790	5%
	112A	->	118A	0.11929	2%
	106B	->	116B	-0.14812	3%
	110B	->	117B	-0.15400	3%
	110B	->	118B	-0.57431	38%
	111B	->	118B	0.21790	5%
	112B	->	118B	-0.11929	2%
50	105A	->	116A	0.12964	2%
	107A	->	116A	-0.65845	47%
	108A	->	116A	-0.10173	1%
	105B	->	116B	-0.12964	2%
	107B	->	116B	0.65845	47%
	108B	->	116B	0.10173	1%
51	110A	->	117A	0.33177	12%
	110A	->	118A	0.11026	1%
	111A	->	117A	0.58878	37%
	110B	->	117B	0.33177	12%
	110B	->	118B	0.11026	1%
	111B	->	117B	0.58878	37%
52	105A	->	116A	-0.12551	2%
	107A	->	116A	0.67947	48%
	105B	->	116B	-0.12551	2%
	107B	->	116B	0.67947	48%
53	109A	->	117A	0.54559	34%
	111A	->	117A	0.13795	2%
	111A	->	123A	0.19139	4%
	112A	->	124A	-0.20053	5%
	114A	->	117A	-0.11246	1%

	115A	->	124A	-0.17171	3%
	109B	->	117B	-0.54559	34%
	111B	->	117B	-0.13795	2%
	111B	->	123B	-0.19139	4%
	112B	->	124B	0.20053	5%
	114B	->	117B	0.11246	1%
	115B	->	124B	0.17171	3%
54	109A	->	117A	0.36532	16%
	110A	->	117A	-0.16603	3%
	111A	->	117A	-0.30162	11%
	111A	->	123A	-0.22688	6%
	112A	->	124A	0.26620	8%
	115A	->	124A	0.22681	6%
	109B	->	117B	-0.36532	16%
	110B	->	117B	0.16603	3%
	111B	->	117B	0.30162	11%
	111B	->	123B	0.22688	6%
	112B	->	124B	-0.26620	8%
	115B	->	124B	-0.22681	6%
55	109A	->	117A	0.59211	37%
	110A	->	118A	0.28340	9%
	111A	->	118A	-0.19612	4%
	109B	->	117B	0.59211	37%
	110B	->	118B	0.28340	9%
	111B	->	118B	-0.19612	4%
56	109A	->	117A	-0.29767	10%
	109A	->	119A	0.27086	8%
	110A	->	118A	0.47850	25%
	111A	->	118A	-0.19125	4%
	114A	->	119A	-0.18008	4%
	109B	->	117B	-0.29767	10%
	109B	->	119B	0.27086	8%
	110B	->	118B	0.47850	25%
	111B	->	118B	-0.19125	4%
	114B	->	119B	-0.18008	4%
57	109A	->	117A	0.15873	3%
	109A	->	119A	0.47537	24%
	110A	->	118A	-0.25777	7%
	111A	->	119A	0.13544	2%
	114A	->	119A	-0.36005	14%
	109B	->	117B	0.15873	3%
	109B	->	119B	0.47537	24%
	110B	->	118B	-0.25777	7%
	111B	->	119B	0.13544	2%
	114B	->	119B	-0.36005	14%

58	106A	->	116A	0.16446	3%
	106A	->	117A	0.30886	11%
	109A	->	118A	0.49133	28%
	111A	->	118A	0.23021	6%
	114A	->	118A	-0.13781	2%
	106B	->	116B	-0.16446	3%
	106B	->	117B	-0.30886	11%
	109B	->	118B	-0.49133	28%
	111B	->	118B	-0.23021	6%
	114B	->	118B	0.13781	2%
59	105A	->	119A	-0.24228	6%
	107A	->	119A	0.38420	16%
	108A	->	119A	0.14069	2%
	111A	->	119A	-0.19670	4%
	112A	->	119A	0.41799	19%
	113A	->	119A	0.14680	2%
	105B	->	119B	0.24228	6%
	107B	->	119B	-0.38420	16%
	108B	->	119B	-0.14069	2%
	111B	->	119B	0.19670	4%
	112B	->	119B	-0.41799	19%
	113B	->	119B	-0.14680	2%
60	109A	->	118A	0.30571	10%
	110A	->	118A	0.21645	5%
	111A	->	118A	0.56912	35%
	109B	->	118B	0.30571	10%
	110B	->	118B	0.21645	5%
	111B	->	118B	0.56912	35%
61	101A	->	118A	-0.10013	1%
	106A	->	116A	0.14879	2%
	106A	->	117A	0.42140	20%
	109A	->	118A	-0.14434	2%
	110A	->	118A	-0.26288	8%
	111A	->	117A	0.10093	1%
	111A	->	118A	-0.37318	16%
	101B	->	118B	0.10013	1%
	106B	->	116B	-0.14879	2%
	106B	->	117B	-0.42140	20%
	109B	->	118B	0.14434	2%
	110B	->	118B	0.26288	8%
	111B	->	117B	-0.10093	1%
	111B	->	118B	0.37318	16%
62	105A	->	116A	-0.11125	2%
	106A	->	117A	0.29103	10%
	109A	->	118A	-0.36509	16%

	111A	->	118A	0.42606	22%
	105B	->	116B	0.11125	2%
	106B	->	117B	-0.29103	10%
	109B	->	118B	0.36509	16%
	111B	->	118B	-0.42606	22%
63	105A	->	116A	-0.65404	47%
	107A	->	116A	-0.12364	2%
	111A	->	118A	-0.10767	1%
	105B	->	116B	0.65404	47%
	107B	->	116B	0.12364	2%
	111B	->	118B	0.10767	1%
64	109A	->	118A	0.60062	39%
	110A	->	118A	-0.17720	3%
	111A	->	118A	-0.26990	8%
	109B	->	118B	0.60062	39%
	110B	->	118B	-0.17720	3%
	111B	->	118B	-0.26990	8%
65	105A	->	116A	0.66650	48%
	107A	->	116A	0.12384	2%
	105B	->	116B	0.66650	48%
	107B	->	116B	0.12384	2%
66	105A	->	119A	0.13390	2%
	109A	->	119A	-0.13883	2%
	110A	->	119A	0.22465	5%
	111A	->	119A	0.56145	33%
	112A	->	119A	-0.27029	8%
	105B	->	119B	0.13390	2%
	109B	->	119B	-0.13883	2%
	110B	->	119B	0.22465	5%
	111B	->	119B	0.56145	33%
	112B	->	119B	-0.27029	8%
67	107A	->	119A	0.30712	10%
	109A	->	119A	-0.12775	2%
	110A	->	119A	0.22528	5%
	111A	->	119A	0.56086	33%
	107B	->	119B	-0.30712	10%
	109B	->	119B	0.12775	2%
	110B	->	119B	-0.22528	5%
	111B	->	119B	-0.56086	33%
68	108A	->	117A	0.68462	50%
	108B	->	117B	-0.68462	50%
69	108A	->	117A	0.69041	50%
	108B	->	117B	0.69041	50%
70	101A	->	116A	0.25928	7%
	101A	->	117A	-0.17995	4%

	102A	->	117A	0.23907	6%
	104A	->	118A	0.16981	3%
	106A	->	118A	0.33960	13%
	106A	->	120A	0.22119	5%
	109A	->	118A	-0.24711	7%
	110A	->	118A	0.12878	2%
	114A	->	120A	-0.14904	2%
	101B	->	116B	-0.25928	7%
	101B	->	117B	0.17995	4%
	102B	->	117B	-0.23907	6%
	104B	->	118B	-0.16981	3%
	106B	->	118B	-0.33960	13%
	106B	->	120B	-0.22119	5%
	109B	->	118B	0.24711	7%
	110B	->	118B	-0.12878	2%
	114B	->	120B	0.14904	2%
71	111A	->	124A	-0.11861	2%
	112A	->	120A	-0.11627	1%
	112A	->	123A	0.35181	14%
	113A	->	123A	0.12996	2%
	115A	->	120A	-0.37270	15%
	115A	->	123A	0.38202	16%
	111B	->	124B	0.11861	2%
	112B	->	120B	0.11627	1%
	112B	->	123B	-0.35181	14%
	113B	->	123B	-0.12996	2%
	115B	->	120B	0.37270	15%
	115B	->	123B	-0.38202	16%
72	102A	->	118A	-0.10697	1%
	103A	->	116A	0.14925	3%
	104A	->	116A	-0.29818	10%
	106A	->	118A	0.19503	4%
	114A	->	120A	0.49941	29%
	115A	->	120A	-0.12408	2%
	102B	->	118B	0.10697	1%
	103B	->	116B	-0.14925	3%
	104B	->	116B	0.29818	10%
	106B	->	118B	-0.19503	4%
	114B	->	120B	-0.49941	29%
	115B	->	120B	0.12408	2%
73	105A	->	119A	0.11676	1%
	106A	->	116A	0.56868	35%
	106A	->	117A	0.12326	2%
	107A	->	119A	-0.13821	2%
	109A	->	118A	0.11726	1%

	111A	->	119A	-0.10018	1%
	112A	->	119A	-0.10110	1%
	114A	->	120A	0.17997	4%
	115A	->	120A	-0.15675	3%
	105B	->	119B	0.11676	1%
	106B	->	116B	0.56868	35%
	106B	->	117B	0.12326	2%
	107B	->	119B	-0.13821	2%
	109B	->	118B	0.11726	1%
	111B	->	119B	-0.10018	1%
	112B	->	119B	-0.10110	1%
	114B	->	120B	0.17997	4%
	115B	->	120B	-0.15675	3%
74	101A	->	116A	0.18390	4%
	102A	->	118A	-0.10487	1%
	103A	->	116A	0.20035	5%
	104A	->	116A	-0.42817	22%
	106A	->	118A	-0.32572	13%
	114A	->	120A	-0.21153	5%
	101B	->	116B	-0.18390	4%
	102B	->	118B	0.10487	1%
	103B	->	116B	-0.20035	5%
	104B	->	116B	0.42817	22%
	106B	->	118B	0.32572	13%
	114B	->	120B	0.21153	5%
75	106A	->	116A	0.17276	3%
	113A	->	120A	-0.21978	5%
	114A	->	120A	-0.22396	5%
	115A	->	120A	0.58594	36%
	106B	->	116B	0.17276	3%
	113B	->	120B	-0.21978	5%
	114B	->	120B	-0.22396	5%
	115B	->	120B	0.58594	36%
76	113A	->	120A	-0.17851	3%
	114A	->	120A	0.62515	42%
	115A	->	120A	0.21899	5%
	113B	->	120B	-0.17851	3%
	114B	->	120B	0.62515	42%
	115B	->	120B	0.21899	5%
77	112A	->	123A	0.19677	4%
	113A	->	120A	-0.37272	16%
	114A	->	120A	0.11042	1%
	115A	->	120A	0.46422	25%
	115A	->	123A	0.17686	4%
	112B	->	123B	-0.19677	4%

	113B	->	120B	0.37272	16%
	114B	->	120B	-0.11042	1%
	115B	->	120B	-0.46422	25%
	115B	->	123B	-0.17686	4%
78	107A	->	117A	-0.67462	48%
	108A	->	118A	0.12947	2%
	107B	->	117B	0.67462	48%
	108B	->	118B	-0.12947	2%
79	107A	->	117A	0.66754	47%
	108A	->	118A	-0.17648	3%
	107B	->	117B	0.66754	47%
	108B	->	118B	-0.17648	3%
80	101A	->	116A	0.34707	14%
	102A	->	116A	0.13813	2%
	104A	->	116A	0.16670	3%
	106A	->	118A	-0.32433	13%
	106A	->	120A	0.12085	2%
	114A	->	120A	0.36170	16%
	101B	->	116B	-0.34707	14%
	102B	->	116B	-0.13813	2%
	104B	->	116B	-0.16670	3%
	106B	->	118B	0.32433	13%
	106B	->	120B	-0.12085	2%
	114B	->	120B	-0.36170	16%
81	105A	->	119A	-0.10390	1%
	110A	->	123A	0.15557	3%
	111A	->	120A	-0.12287	2%
	111A	->	123A	0.43718	23%
	112A	->	124A	0.22373	6%
	113A	->	120A	-0.20251	5%
	115A	->	124A	0.29058	10%
	105B	->	119B	0.10390	1%
	110B	->	123B	-0.15557	3%
	111B	->	120B	0.12287	2%
	111B	->	123B	-0.43718	23%
	112B	->	124B	-0.22373	6%
	113B	->	120B	0.20251	5%
	115B	->	124B	-0.29058	10%
82	105A	->	119A	0.43235	21%
	106A	->	116A	-0.21865	5%
	107A	->	119A	-0.19982	4%
	110A	->	119A	-0.10193	1%
	111A	->	119A	-0.23626	6%
	112A	->	119A	-0.32477	12%
	105B	->	119B	0.43235	21%

	106B	->	116B	-0.21865	5%
	107B	->	119B	-0.19982	4%
	110B	->	119B	-0.10193	1%
	111B	->	119B	-0.23626	6%
	112B	->	119B	-0.32477	12%
83	113A	->	120A	0.63478	42%
	115A	->	120A	0.27058	8%
	113B	->	120B	0.63478	42%
	115B	->	120B	0.27058	8%
84	107A	->	117A	0.10597	1%
	108A	->	118A	0.48772	27%
	111A	->	123A	-0.11356	1%
	113A	->	120A	-0.35817	15%
	115A	->	120A	-0.19424	4%
	115A	->	123A	-0.11265	1%
	107B	->	117B	-0.10597	1%
	108B	->	118B	-0.48772	27%
	111B	->	123B	0.11356	1%
	113B	->	120B	0.35817	15%
	115B	->	120B	0.19424	4%
	115B	->	123B	0.11265	1%
85	108A	->	118A	0.45032	23%
	113A	->	120A	0.40393	18%
	115A	->	120A	0.26935	8%
	115A	->	123A	0.10340	1%
	108B	->	118B	-0.45032	23%
	113B	->	120B	-0.40393	18%
	115B	->	120B	-0.26935	8%
	115B	->	123B	-0.10340	1%
86	105A	->	119A	0.45083	23%
	107A	->	119A	0.34988	14%
	108A	->	119A	0.20081	4%
	111A	->	119A	-0.16313	3%
	111A	->	123A	0.10722	1%
	112A	->	119A	-0.20997	5%
	105B	->	119B	-0.45083	23%
	107B	->	119B	-0.34988	14%
	108B	->	119B	-0.20081	4%
	111B	->	119B	0.16313	3%
	111B	->	123B	-0.10722	1%
	112B	->	119B	0.20997	5%
87	107A	->	117A	0.17403	3%
	108A	->	118A	0.67707	47%
	107B	->	117B	0.17403	3%
	108B	->	118B	0.67707	47%

88	101A	->	116A	0.21484	5%
	102A	->	116A	-0.60332	40%
	104A	->	118A	-0.13127	2%
	106A	->	120A	0.15372	3%
	101B	->	116B	-0.21484	5%
	102B	->	116B	0.60332	40%
	104B	->	118B	0.13127	2%
	106B	->	120B	-0.15372	3%
89	114A	->	121A	-0.31258	10%
	115A	->	121A	0.62068	40%
	114B	->	121B	0.31258	10%
	115B	->	121B	-0.62068	40%
90	114A	->	121A	-0.28985	9%
	115A	->	121A	0.63784	41%
	114B	->	121B	-0.28985	9%
	115B	->	121B	0.63784	41%
91	114A	->	121A	-0.62533	40%
	115A	->	121A	-0.30670	10%
	114B	->	121B	0.62533	40%
	115B	->	121B	0.30670	10%
92	114A	->	121A	0.63828	42%
	115A	->	121A	0.28865	8%
	114B	->	121B	0.63828	42%
	115B	->	121B	0.28865	8%
93	107A	->	118A	-0.66938	48%
	108A	->	118A	-0.12791	2%
	107B	->	118B	0.66938	48%
	108B	->	118B	0.12791	2%
94	107A	->	118A	0.68662	50%
	107B	->	118B	0.68662	50%
95	113A	->	121A	-0.67242	48%
	113A	->	124A	-0.10686	1%
	113A	->	126A	0.10030	1%
	113B	->	121B	0.67242	48%
	113B	->	124B	0.10686	1%
	113B	->	126B	-0.10030	1%
96	113A	->	121A	0.68979	50%
	113B	->	121B	0.68979	50%
97	112A	->	120A	0.67340	50%
	112B	->	120B	0.67340	50%
98	105A	->	117A	-0.12103	2%
	111A	->	124A	-0.10196	1%
	112A	->	120A	0.65021	45%
	115A	->	123A	0.14991	2%
	105B	->	117B	0.12103	2%

	111B	->	124B	0.10196	1%
	112B	->	120B	-0.65021	45%
	115B	->	123B	-0.14991	2%
99	105A	->	117A	-0.52747	32%
	111A	->	124A	0.28554	10%
	113A	->	124A	-0.17821	4%
	115A	->	124A	0.19279	4%
	105B	->	117B	0.52747	32%
	111B	->	124B	-0.28554	10%
	113B	->	124B	0.17821	4%
	115B	->	124B	-0.19279	4%
100	105A	->	117A	-0.41263	19%
	110A	->	124A	-0.11127	1%
	111A	->	124A	-0.32177	12%
	112A	->	120A	-0.14757	2%
	112A	->	124A	0.11837	2%
	113A	->	124A	0.25326	7%
	115A	->	124A	-0.22509	6%
	105B	->	117B	0.41263	19%
	110B	->	124B	0.11127	1%
	111B	->	124B	0.32177	12%
	112B	->	120B	0.14757	2%
	112B	->	124B	-0.11837	2%
	113B	->	124B	-0.25326	7%
	115B	->	124B	0.22509	6%

Table S32. TD-DFT calculated transition Kohn-Sham orbital contributions for [Ni(dtbbpy)Cl_2] T_0 (**x**).

Excited State	KS Orbital Transition			C_i	$C_i^2/\Sigma C_i^2$
1	91B	->	105B	0.28387	8%
	92B	->	105B	0.22667	5%
	93B	->	106B	-0.19999	4%
	94B	->	105B	0.29985	9%
	97B	->	106B	-0.27455	7%
	99B	->	105B	-0.32659	10%
	102B	->	106B	0.31741	10%
	103B	->	105B	0.68765	46%
	103B	<-	105B	0.10673	1%
2	91B	->	106B	0.22416	5%
	92B	->	106B	0.17882	3%
	93B	->	105B	-0.30503	9%
	94B	->	106B	0.24026	6%
	97B	->	105B	-0.41863	17%
	99B	->	106B	-0.23741	5%
	102B	->	105B	0.53176	27%
	103B	->	106B	0.52380	26%
	97B	<-	105B	-0.10139	1%
	102B	<-	105B	0.10048	1%
3	95B	->	106B	0.65500	42%
	96B	->	106B	0.69495	47%
	101B	->	106B	0.31241	9%
	95B	<-	106B	0.10261	1%
	96B	<-	106B	0.10871	1%
4	91B	->	106B	0.19802	4%
	92B	->	106B	0.15813	3%
	93B	->	105B	0.23962	6%
	94B	->	106B	0.20823	4%
	97B	->	105B	0.33612	11%
	99B	->	106B	-0.24860	6%
	102B	->	105B	-0.53303	29%
	103B	->	106B	0.60533	37%
5	91B	->	105B	-0.11782	1%
	93B	->	106B	-0.33188	11%
	94B	->	105B	-0.12805	2%
	97B	->	106B	-0.46510	22%
	99B	->	105B	0.12366	2%
	102B	->	106B	0.66965	46%
	103B	->	105B	-0.39915	16%
6	95B	->	105B	0.59955	37%

	96B	->	105B	0.67209	46%
	101B	->	105B	0.40905	17%
7	103B	->	104B	0.98441	100%
8	102B	->	104B	0.98969	100%
9	104A	->	106A	0.98409	99%
	99B	->	105B	-0.10230	1%
10	105A	->	106A	0.98888	99%
	103B	->	104B	-0.10111	1%
11	103A	->	106A	0.98999	100%
12	98A	->	106A	0.14737	2%
	102A	->	106A	0.98057	98%
13	95A	->	109A	0.13832	2%
	96A	->	108A	-0.12939	2%
	97A	->	106A	-0.13025	2%
	97A	->	107A	-0.12619	2%
	99A	->	106A	-0.59968	39%
	99A	->	107A	0.22270	5%
	103A	->	106A	-0.10246	1%
	92B	->	109B	0.10791	1%
	94B	->	108B	-0.10646	1%
	97B	->	107B	0.11948	2%
	98B	->	104B	0.60360	39%
	98B	->	107B	-0.20194	4%
14	100B	->	105B	0.99212	100%
15	101A	->	106A	0.10481	1%
	99B	->	104B	-0.15160	2%
	100B	->	106B	-0.11780	1%
	101B	->	105B	-0.21601	5%
	103B	->	107B	0.92650	90%
16	91B	->	106B	-0.12439	2%
	94B	->	106B	-0.11255	1%
	97B	->	105B	0.12748	2%
	99B	->	106B	0.81451	68%
	102B	->	105B	0.16876	3%
	103B	->	106B	0.48662	24%
17	95B	->	105B	-0.12981	2%
	96B	->	105B	-0.25248	6%
	99B	->	104B	0.18377	3%
	100B	->	106B	0.68131	47%
	101B	->	105B	0.57589	33%
	103B	->	107B	0.28289	8%
18	104A	->	106A	0.12222	2%
	104A	->	107A	-0.13532	2%
	91B	->	105B	-0.14948	2%
	92B	->	105B	-0.11862	1%

	94B	->	105B	-0.16029	3%
	97B	->	106B	-0.16115	3%
	99B	->	105B	0.73068	55%
	101B	->	104B	0.31299	10%
	102B	->	106B	-0.10151	1%
	103B	->	105B	0.46392	22%
19	96B	->	106B	-0.33326	11%
	101B	->	106B	0.91990	86%
	102B	->	107B	-0.17870	3%
20	99B	->	105B	-0.25100	6%
	101B	->	104B	0.94508	91%
	103B	->	105B	-0.16231	3%
21	93B	->	105B	-0.16474	3%
	97B	->	105B	-0.27454	8%
	99B	->	106B	0.16434	3%
	100B	->	104B	0.88547	79%
	102B	->	105B	-0.27216	7%
22	101A	->	106A	-0.29717	10%
	99B	->	104B	0.86789	82%
	100B	->	106B	-0.20535	5%
	101B	->	105B	-0.10837	1%
	103B	->	107B	0.16782	3%
23	101B	->	106B	0.16992	3%
	102B	->	107B	0.97646	97%
24	93B	->	105B	0.32587	11%
	97B	->	105B	0.54883	30%
	98B	->	105B	0.10612	1%
	99B	->	106B	-0.18874	4%
	100B	->	104B	0.45383	21%
	102B	->	105B	0.57823	34%
25	104A	->	107A	0.96379	97%
	97B	->	106B	-0.13097	2%
	102B	->	106B	-0.12110	2%
26	105A	->	107A	0.91265	86%
	100B	->	106B	-0.29673	9%
	101B	->	105B	0.22664	5%
27	105A	->	107A	-0.37490	15%
	95B	->	105B	-0.31933	11%
	99B	->	104B	-0.10880	1%
	100B	->	106B	-0.58711	36%
	101B	->	105B	0.59701	37%
	102B	->	108B	-0.11537	1%
28	99A	->	106A	-0.14275	2%
	103B	->	108B	0.97490	98%
29	104A	->	107A	0.16573	3%

	91B	->	105B	-0.12271	2%
	93B	->	106B	0.33080	11%
	94B	->	105B	-0.18917	4%
	97B	->	106B	0.57237	34%
	98B	->	106B	0.11385	1%
	102B	->	106B	0.63126	41%
	103B	->	105B	0.22446	5%
30	103A	->	107A	0.99269	100%
	101A	->	106A	0.85631	80%
	99B	->	104B	0.36742	15%
	99B	->	107B	-0.13400	2%
	102B	->	108B	0.16764	3%
32	101A	->	106A	-0.12450	2%
	102B	->	108B	0.97294	98%
33	98A	->	107A	0.12544	2%
	102A	->	106A	-0.10392	1%
	102A	->	107A	0.83003	70%
	104A	->	108A	-0.51350	27%
34	100A	->	106A	0.97326	98%
	102A	->	108A	0.12647	2%
35	102A	->	107A	0.53792	29%
	104A	->	108A	0.83384	71%
36	99A	->	106A	-0.12630	2%
	99A	->	107A	-0.16470	3%
	105A	->	108A	0.91546	89%
	98B	->	104B	0.14922	2%
	98B	->	107B	0.16387	3%
	103B	->	108B	-0.10007	1%
37	95A	->	106A	-0.14011	2%
	95A	->	107A	0.14370	2%
	96A	->	107A	-0.21441	5%
	97A	->	108A	-0.21612	5%
	99A	->	108A	0.21606	5%
	99A	->	109A	0.14780	2%
	101A	->	106A	0.34482	13%
	101A	->	107A	-0.27748	8%
	103A	->	108A	-0.19364	4%
	91B	->	104B	0.10775	1%
	92B	->	104B	-0.10287	1%
	92B	->	107B	0.18694	4%
	93B	->	108B	-0.11797	1%
	94B	->	107B	-0.17758	3%
	97B	->	108B	0.19442	4%
	98B	->	108B	-0.21143	5%
	98B	->	109B	-0.15175	2%

	99B	->	107B	0.54536	32%
38	95A	->	108A	0.14880	2%
	96A	->	108A	-0.13851	2%
	97A	->	106A	-0.11522	1%
	97A	->	107A	-0.13822	2%
	99A	->	106A	0.32599	11%
	99A	->	107A	0.47926	23%
	101A	->	108A	-0.13165	2%
	105A	->	108A	0.38989	16%
	92B	->	108B	0.16456	3%
	94B	->	108B	-0.11299	1%
	97B	->	104B	0.11362	1%
	97B	->	107B	0.16547	3%
	98B	->	104B	-0.22093	5%
	98B	->	107B	-0.45362	21%
	99B	->	108B	0.20988	5%
	103B	->	108B	0.14524	2%
39	103A	->	108A	0.97475	97%
	99B	->	107B	0.17385	3%
40	94B	->	105B	-0.10591	1%
	101B	->	107B	0.98074	99%
41	100B	->	107B	0.99730	100%
42	91B	->	105B	0.36587	14%
	92B	->	105B	0.29469	9%
	94B	->	105B	0.59968	37%
	97B	->	106B	0.16874	3%
	99B	->	105B	0.48387	24%
	101B	->	107B	0.17536	3%
	102B	->	106B	0.14471	2%
	103B	->	105B	-0.26487	7%
43	96A	->	108A	-0.12578	2%
43	97A	->	106A	-0.49714	27%
43	99A	->	106A	0.10389	1%
	99A	->	107A	-0.33304	12%
	101A	->	108A	-0.12652	2%
	93B	->	104B	-0.20895	5%
	94B	->	108B	-0.10637	1%
	97B	->	104B	0.54927	33%
	97B	->	107B	0.10157	1%
	98B	->	107B	0.33455	12%
	99B	->	108B	0.20835	5%
44	98A	->	108A	0.12265	2%
	100A	->	106A	-0.14784	2%
	102A	->	108A	0.97113	96%
45	98A	->	106A	-0.30180	9%

	91B	->	106B	0.38306	15%
	92B	->	106B	0.30654	10%
	94B	->	106B	0.63468	41%
	99B	->	106B	0.36654	14%
	103B	->	106B	-0.32883	11%
46	95A	->	106A	0.21497	5%
	95A	->	107A	-0.12203	2%
	96A	->	107A	0.11893	1%
	97A	->	108A	0.12507	2%
	99A	->	108A	-0.14896	2%
	99A	->	109A	-0.16257	3%
	101A	->	107A	0.25282	7%
	91B	->	104B	-0.14234	2%
	92B	->	104B	0.10548	1%
	92B	->	107B	-0.16680	3%
	97B	->	108B	-0.12978	2%
	98B	->	108B	0.19036	4%
	98B	->	109B	0.14808	2%
	99B	->	107B	0.77808	64%
47	98A	->	106A	0.90427	85%
	102A	->	106A	-0.13474	2%
	104A	->	108A	0.15310	2%
	91B	->	106B	0.14333	2%
	92B	->	106B	0.11728	1%
	94B	->	106B	0.20275	4%
	99B	->	106B	0.11139	1%
	103B	->	106B	-0.10645	1%
48	99A	->	106A	0.54570	31%
	99A	->	107A	0.10050	1%
	101A	->	108A	0.12823	2%
	95B	->	106B	-0.22093	5%
	96B	->	106B	0.18262	4%
	97B	->	104B	-0.18863	4%
	98B	->	104B	0.60012	38%
	98B	->	107B	0.22667	5%
	99B	->	108B	0.30635	10%
49	95A	->	106A	0.28798	9%
	95A	->	107A	0.14768	2%
	96A	->	106A	0.27035	8%
	97A	->	108A	0.12909	2%
	99A	->	108A	0.52428	30%
	101A	->	106A	-0.10842	1%
	91B	->	104B	-0.26019	7%
	91B	->	107B	-0.10523	1%
	92B	->	104B	0.13302	2%

	92B	->	107B	0.11051	1%
	94B	->	104B	0.25256	7%
	98B	->	108B	-0.52377	30%
50	101B	->	108B	0.99843	100%
51	100B	->	108B	0.99822	100%
52	95A	->	106A	-0.17366	3%
	95A	->	107A	0.13381	2%
	99A	->	108A	0.20486	4%
	99A	->	109A	0.13287	2%
	101A	->	107A	0.88291	80%
	91B	->	104B	0.12624	2%
	92B	->	104B	-0.17503	3%
	98B	->	108B	-0.13739	2%
	98B	->	109B	-0.15101	2%
53	95B	->	106B	0.68193	48%
	96B	->	106B	-0.57932	35%
	97B	->	104B	-0.18644	4%
	98B	->	107B	0.10058	1%
	99B	->	108B	0.31780	10%
	101B	->	106B	-0.14546	2%
54	97A	->	106A	0.21906	5%
	97A	->	107A	-0.18055	3%
	99A	->	106A	-0.26877	8%
	99A	->	107A	-0.19985	4%
	101A	->	108A	-0.20754	4%
	95B	->	106B	-0.21881	5%
	96B	->	106B	0.18697	4%
	97B	->	104B	-0.30499	10%
	98B	->	104B	-0.26700	7%
	99B	->	108B	0.69131	50%
55	95A	->	106A	-0.38536	16%
	96A	->	106A	0.51564	29%
	97A	->	108A	0.14537	2%
	99A	->	108A	-0.12111	2%
	99A	->	109A	0.17844	3%
	101A	->	107A	-0.14545	2%
	92B	->	104B	-0.45231	22%
	94B	->	104B	0.40444	18%
	97B	->	108B	-0.12868	2%
	98B	->	109B	-0.17717	3%
56	100A	->	107A	-0.38209	15%
	95B	->	104B	0.33299	11%
	96B	->	104B	0.84628	73%
	96B	->	107B	0.10295	1%
57	100A	->	107A	0.90623	85%

	95B	->	104B	0.18949	4%
	96B	->	104B	0.33777	12%
58	97B	->	105B	-0.10841	1%
	98B	->	105B	0.98891	99%
59	90B	->	106B	0.16002	3%
	94B	->	104B	-0.23620	6%
	95B	->	105B	0.66139	47%
	96B	->	105B	-0.62085	41%
	100B	->	106B	-0.16426	3%
60	96A	->	108A	0.11056	1%
	97A	->	106A	0.24646	6%
	97A	->	107A	0.14376	2%
	99A	->	107A	-0.14468	2%
	101A	->	108A	0.48982	25%
	93B	->	107B	0.14853	2%
	94B	->	108B	0.11508	1%
	97B	->	104B	0.50641	26%
	97B	->	107B	-0.21974	5%
	98B	->	107B	-0.34881	13%
	99B	->	108B	0.39156	16%
61	97B	->	106B	-0.10812	1%
	98B	->	106B	0.98631	99%
62	97A	->	106A	-0.51608	27%
	97A	->	107A	0.11167	1%
	99A	->	106A	-0.17401	3%
	99A	->	107A	0.30225	9%
	101A	->	108A	0.54134	30%
	93B	->	104B	-0.23793	6%
	97B	->	104B	-0.31031	10%
	97B	->	107B	-0.19353	4%
	98B	->	104B	-0.21187	5%
	98B	->	107B	0.14536	2%
	99B	->	108B	0.15366	2%
63	95B	->	104B	0.89648	85%
	96B	->	104B	-0.37365	15%
64	101A	->	108A	-0.15578	3%
	97B	->	107B	-0.12324	2%
	98B	->	107B	-0.11288	1%
	103B	->	109B	0.94895	95%
65	98A	->	106A	-0.13301	2%
	98A	->	107A	0.37823	15%
	100A	->	108A	0.89437	83%
66	96A	->	108A	-0.22272	5%
	97A	->	106A	0.15680	3%
	97A	->	107A	-0.42578	19%

	99A	->	107A	-0.19860	4%
	101A	->	108A	0.57140	34%
	91B	->	108B	0.11150	1%
	93B	->	107B	-0.18700	4%
	94B	->	108B	-0.17208	3%
	97B	->	107B	0.43618	20%
	99B	->	108B	-0.17281	3%
	103B	->	109B	0.21495	5%
67	95A	->	106A	0.16445	3%
	96A	->	107A	-0.28395	9%
	97A	->	108A	-0.26796	8%
	99A	->	109A	-0.10082	1%
	101A	->	107A	0.13179	2%
	91B	->	104B	-0.13951	2%
	91B	->	107B	0.22994	6%
	93B	->	108B	-0.16513	3%
	94B	->	104B	0.51363	29%
	94B	->	107B	-0.33275	12%
	97B	->	108B	0.33041	12%
	98B	->	108B	0.34232	13%
	99B	->	107B	-0.11695	1%
68	97A	->	106A	0.10965	1%
	99A	->	106A	-0.17154	3%
	99A	->	107A	0.47871	24%
	93B	->	104B	0.52719	29%
	97B	->	104B	0.30721	10%
	97B	->	107B	0.12818	2%
	98B	->	104B	-0.14325	2%
	98B	->	107B	0.49337	25%
	103B	->	109B	0.21202	5%
69	96A	->	106A	-0.12499	2%
	99A	->	108A	0.10382	1%
	94B	->	104B	0.12601	2%
	102B	->	109B	0.96891	96%
70	95A	->	107A	-0.10470	1%
	96A	->	106A	0.52193	29%
	96A	->	107A	-0.29662	9%
	97A	->	108A	-0.22210	5%
	99A	->	108A	-0.47902	25%
	101A	->	107A	0.12635	2%
	92B	->	104B	0.11811	2%
	94B	->	104B	-0.25917	7%
	98B	->	108B	-0.37085	15%
	102B	->	109B	0.21007	5%
71	98A	->	107A	0.82001	70%

	100A	->	108A	-0.41252	18%
	104A	->	109A	-0.34819	13%
72	98A	->	107A	0.32146	11%
	100A	->	108A	-0.10086	1%
	104A	->	109A	0.92803	88%
73	105A	->	109A	0.99720	100%
74	92A	->	106A	-0.12485	2%
	94A	->	106A	-0.16272	3%
	98A	->	108A	0.85518	83%
	102A	->	108A	-0.13320	2%
	89B	->	104B	0.10377	1%
	90B	->	108B	-0.13091	2%
	95B	->	104B	-0.13024	2%
	96B	->	107B	-0.11708	2%
	103B	->	110B	0.18024	4%
75	103A	->	109A	0.99274	100%
76	98A	->	108A	-0.15919	3%
	103B	->	110B	0.97846	97%
77	95B	->	107B	0.31896	10%
	96B	->	104B	-0.10157	1%
	96B	->	107B	0.93308	89%
78	98A	->	107A	0.16660	3%
	84B	->	104B	-0.11284	1%
	87B	->	104B	-0.13436	2%
	89B	->	108B	-0.10031	1%
	90B	->	104B	0.93023	90%
	90B	->	107B	0.10506	1%
	95B	->	108B	-0.11340	1%
79	96A	->	106A	-0.10198	1%
	99A	->	108A	-0.23069	6%
	90B	->	106B	0.18048	4%
	91B	->	104B	0.56163	34%
	92B	->	104B	0.45702	22%
	94B	->	104B	0.46738	24%
	94B	->	107B	0.17420	3%
	98B	->	108B	-0.24420	6%
80	102B	->	110B	0.99498	100%
81	98A	->	108A	0.12268	2%
	98A	->	109A	0.11354	1%
	102A	->	109A	0.97716	97%
82	93A	->	106A	-0.24225	6%
	95A	->	108A	0.13281	2%
	97A	->	106A	-0.46287	23%
	99A	->	107A	-0.28694	9%
	90B	->	105B	-0.20446	5%

	93B	->	104B	0.60339	39%
	97B	->	104B	-0.13555	2%
	97B	->	107B	0.22507	5%
	98B	->	107B	-0.27945	8%
83	96A	->	108A	0.10601	1%
	97A	->	107A	0.40573	17%
	93B	->	104B	-0.30544	10%
	93B	->	107B	0.34630	13%
	94B	->	108B	0.18156	3%
	97B	->	107B	0.72248	55%
84	105A	->	110A	0.97272	96%
	105A	->	113A	0.10374	1%
	95B	->	107B	-0.17953	3%
85	104A	->	110A	0.99088	100%
86	98A	->	108A	-0.16993	3%
	105A	->	110A	0.19487	4%
	90B	->	108B	-0.11184	1%
	95B	->	107B	0.89827	83%
	96B	->	107B	-0.29804	9%
87	93B	->	105B	0.80981	68%
	94B	->	106B	0.11258	1%
	97B	->	105B	-0.54247	31%
88	95A	->	106A	0.51710	28%
	95A	->	107A	0.34404	13%
	96A	->	106A	-0.22653	5%
	97A	->	108A	0.19672	4%
	99A	->	108A	-0.40873	18%
	99A	->	109A	0.24266	6%
	92B	->	104B	-0.36945	15%
	94B	->	104B	0.12547	2%
	97B	->	108B	0.25467	7%
	98B	->	108B	-0.14077	2%
89	94A	->	106A	0.95471	95%
	98A	->	108A	0.20851	5%
90	103A	->	110A	0.99224	99%
	103A	->	113A	0.10665	1%
91	98A	->	108A	0.10899	1%
	92B	->	105B	-0.15590	3%
	93B	->	106B	0.78786	65%
	94B	->	105B	0.17354	3%
	97B	->	106B	-0.52010	28%
92	96B	->	108B	-0.10695	1%
	101B	->	109B	0.99253	99%
93	95A	->	106A	0.11220	1%
	95A	->	107A	0.25980	7%

	96A	->	106A	0.27074	8%
	99A	->	109A	0.20634	5%
	91B	->	107B	-0.27333	8%
	92B	->	104B	0.42714	20%
	92B	->	107B	0.39851	17%
	93B	->	108B	0.13800	2%
	94B	->	104B	-0.10651	1%
	98B	->	108B	0.42801	20%
	98B	->	109B	-0.32846	12%
94	95B	->	108B	0.34212	12%
	96B	->	108B	0.92898	87%
	101B	->	109B	0.11088	1%
95	100B	->	109B	0.99772	100%
96	93A	->	106A	-0.18669	4%
	95A	->	108A	0.10005	1%
	101A	->	109A	-0.10491	1%
	90B	->	105B	0.32946	11%
	99B	->	109B	0.88463	83%
97	93A	->	106A	-0.24285	6%
	84B	->	105B	-0.20644	4%
	87B	->	105B	-0.16814	3%
	90B	->	105B	0.81512	70%
	99B	->	109B	-0.39174	16%
98	95A	->	107A	-0.14050	2%
	96A	->	106A	0.10948	1%
	96A	->	107A	0.13572	2%
	99A	->	108A	0.12368	2%
	90B	->	106B	-0.11729	1%
	93B	->	108B	0.15974	3%
	94B	->	107B	0.55388	32%
	97B	->	108B	0.73973	57%
99	95A	->	106A	0.39898	17%
	95A	->	107A	-0.18418	4%
	96A	->	106A	0.33026	12%
	96A	->	107A	0.33686	12%
	99A	->	108A	0.19079	4%
	91B	->	104B	0.59186	37%
	92B	->	104B	-0.17775	3%
	94B	->	104B	-0.17249	3%
	94B	->	107B	-0.25349	7%
	98B	->	108B	0.10715	1%
100	91B	->	105B	0.33334	11%
	92B	->	105B	0.64471	43%
	93B	->	106B	0.22421	5%
	94B	->	105B	-0.61057	38%

97B	->	106B	-0.1409	2%